An energy based method for coupled vibro-acoustic systems

Rainer Stelzer

Numéro d'ordre: Année 2012

THESE

UNE MÉTHODE ÉNERGÉTIQUE POUR LES SYSTÈMES VIBRO-ACOUSTIQUES COUPLÉS

Présentée devant
l'Institut National des Sciences Appliquées de Lyon

Pour obtenir
le GRADE DE DOCTEUR

Ecole doctorale:
Mécanique, Energétique, Génie Civil, Acoustique

Spécialité:
Acoustique

Par
Rainer STELZER

Thèse soutenue le 28 septembre 2012 devant la Commission d'examen

Jury

Ennes Sarradj (Professeur)	TU Cottbus	Rapporteur
Robin Langley (Professeur)	University of Cambridge	Rapporteur
Herve Riou (Maître de Conférences)	LMT Cachan	Examinateur
Michaël Thivant	Vibratec	Examinateur
Goran Pavic (Professeur)	INSA de Lyon	Directeur de thèse
Nicolas Totaro (Maître de Conférences)	INSA de Lyon	Co-Directeur de thèse

Thèse préparée au Laboratoire Vibrations Acoustique de l'INSA de Lyon

INSA Direction de la Recherche - Ecoles Doctorales – Quinquennal 2011-2015

SIGLE	ECOLE DOCTORALE	NOM ET COORDONNEES DU RESPONSABLE
CHIMIE	**CHIMIE DE LYON** **http://www.edchimie-lyon.fr** Insa : R. GOURDON	M. Jean Marc LANCELIN Université de Lyon – Collège Doctoral Bât ESCPE 43 bd du 11 novembre 1918 69622 VILLEURBANNE Cedex Tél : 04.72.43 13 95 directeur@edchimie-lyon.fr
E.E.A.	**ELECTRONIQUE, ELECTROTECHNIQUE, AUTOMATIQUE** **http://edeea.ec-lyon.fr** Secrétariat : M.C. HAVGOUDOUKIAN eea@ ec-lyon.fr	M. Gérard SCORLETTI Ecole Centrale de Lyon 36 avenue Guy de Collongue 69134 ECULLY Tél : 04.72.18 60 97 Fax : 04 78 43 37 17 Gerard.scorletti@ec-lyon.fr
E2M2	**EVOLUTION, ECOSYSTEME, MICROBIOLOGIE, MODELISATION** **http://e2m2.universite-lyon.fr** Insa : H. CHARLES	Mme Gudrun BORNETTE CNRS UMR 5023 LEHNA Université Claude Bernard Lyon 1 Bât Forel 43 bd du 11 novembre 1918 69622 VILLEURBANNE Cédex Tél : 04.72.43.12.94 e2m2@biomserv.univ-lyon1.fr
EDISS	**INTERDISCIPLINAIRE SCIENCES-SANTE** **http://ww2.ibcp.fr/ediss** Sec : Safia AIT CHALAL Insa : M. LAGARDE	M. Didier REVEL Hôpital Louis Pradel Bâtiment Central 28 Avenue Doyen Lépine 69677 BRON Tél : 04.72.68 49 09 Fax :04 72 35 49 16 Didier.revel@creatis.uni-lyon1.fr
INFOMATHS	**INFORMATIQUE ET MATHEMATIQUES** http://infomaths.univ-lyon1.fr	M. Johannes KELLENDONK Université Claude Bernard Lyon 1 INFOMATHS Bâtiment Braconnier 43 bd du 11 novembre 1918 69622 VILLEURBANNE Cedex Tél : 04.72. 44.82.94 Fax 04 72 43 16 87 infomaths@univ-lyon1.fr
Matériaux	**MATERIAUX DE LYON** Secrétariat : M. LABOUNE PM : 71.70 -Fax : 87.12 Bat. Saint Exupéry Ed.materiaux@ insa-lyon.fr	M. Jean-Yves BUFFIERE INSA de Lyon MATEIS Bâtiment Saint Exupéry 7 avenue Jean Capelle 69621 VILLEURBANNE Cédex Tél : 04.72.43 83 18 Fax 04 72 43 85 28 Jean-yves.buffiere@insa-lyon.fr
MEGA	**MECANIQUE, ENERGETIQUE, GENIE CIVIL, ACOUSTIQUE** Secrétariat : M. LABOUNE PM : 71.70 -Fax : 87.12 Bat. Saint Exupéry mega@insa-lyon.fr	M. Philippe BOISSE INSA de Lyon Laboratoire LAMCOS Bâtiment Jacquard 25 bis avenue Jean Capelle 69621 VILLEURBANNE Cedex Tél :04.72.43.71.70 Fax : 04 72 43 72 37 Philippe.boisse@insa-lyon.fr
ScSo	**ScSo*** M. OBADIA Lionel Sec : Viviane POLSINELLI Insa : J.Y. TOUSSAINT	M. OBADIA Lionel Université Lyon 2 86 rue Pasteur 69365 LYON Cedex 07 Tél : 04.78.69.72.76 Fax : 04.37.28.04.48 Lionel.Obadia@univ-lyon2.fr

*ScSo : Histoire, Geographie, Aménagement, Urbanisme, Archéologie, Science politique, Sociologie, Anthropologie

Une méthode énergétique pour les systèmes vibro-acoustiques couplés

Résumé

Ce mémoire de thèse présente le développement de la méthode “statistical modal energy distribution analysis (SmEdA)” pour des systèmes vibro-acoustiques couplés. Cette méthode de calcul est basée sur le bilan énergétique dans des sous-systèmes fermés couplés, comme une structure ou une cavité. L’interaction entre de tels systèmes est décrite par des couplages entre les modes. La version initiale de SmEdA prend en compte seulement les modes qui ont une fréquence propre dans le bande d’excitation. Le travail présenté ici étudie l’effet des modes non résonants sur la réponse et identifie les cas dans lesquels un tel effet devient important. L’introduction des modes non résonants permet d’utiliser la méthode SmEdA dans des cas d’applications plus larges.
En outre, une nouvelle méthode de post-traitement a été développée pour calculer des distributions d’énergie dans les sous-systèmes. Finalement, une nouvelle méthode d’approximation pour la prise en compte des modes de systèmes de grandes dimensions ou mal définis a été formulée. Toutes ces méthodes ont été comparées avec d’autres méthodes de calcul via des exemples académiques et industriels. Ainsi, la nouvelle version de SmEdA incluant le post-traitement pour obtenir des distributions d’énergie a été validé et les avantages et possibilités d’applications sont montrés.

Mots-clés: SmEdA, méthode énergétique, systèmes vibro-acoustiques couplés, distribution d’énergie, systèmes mal définies, méthode modal

An energy based method for coupled vibro-acoustic systems

Abstract

This dissertation presents the further development of the statistical modal energy distribution analysis (SmEdA) for vibro-acoustic coupled problems. This prediction method is based on the energy balance in bounded coupled subsystems, like a structure or a cavity. The interaction between such subsystems is described by mode-to-mode coupling. The original SmEdA formulation takes into account only the modes having the eigenfrequencies within the excitation band. The present work investigates the effect of non resonant modes to the response and identifies cases in which such an effect becomes important. The inclusion of non resonant modes has thus resulted in a new SmEdA formulation which can be used in extended applications.
Furthermore, a new post-processing method has been developed to predict energy distribution within subsystems. Finally a novel approximation method for handling modes of huge or ill-defined systems has been formulated. All these methods have been compared to other prediction methods via academic and industrial examples. In this way, the extended SmEdA approach including the post-processing for energy distribution has been validated and its advantages and application possibilities have been demonstrated.

Keywords: SmEdA, energy based method, coupled vibro-acoustic systems, energy distribution, ill-defined system, modal approach

Contents

Part I.

Exuctive Summary and Discussion

1. Introduction and scientific context

The importance of the prediction of the vibro-acoustic behaviour of industrial products is increasing. One reason for this is that more and more producers want to get products sounding well and to reduce disturbing noises for the users of their products. To reach this aim without spending a lot of time for tests on real products, which costs also a lot, the sound design at an early stage of development becomes more and more important. Thus, methods have been developed to study the contribution of different sound sources and the influence of different transmission paths on the global synthesized sound of a product. Examples for such methods are the virtual noise synthesis [1] and the virtual acoustic prototype [2]. Another reason for the increasing of the need of predictive methods is the problem that strong vibrations and high noise levels can damage structures or electronic equipment like in aerospace applications [3]. Therefore, it is necessary to take into account these aspects already in the design stage. To reach all these aims effective calculations methods are needed to predict for example transfer functions characterising transmission paths. The frequency range of interest, for which vibro-acoustic calculations should be executed, is normally quite huge for example 20Hz to 2000Hz for aerospace applications [3]. Thus, the biggest wavelength at the lowest frequency of interest can be 100 times bigger or even more than the smallest wavelength at the highest frequency of interest. That means that the wavelength can be very big and very small in comparison to the dimensions of a product or a room and so different phenomena are important for the different wavelengths. Because of that the frequency range can be divided for example in three ranges, the low, the mid and the high frequency range. In the case of a low damped system the low frequency range is characterised by the single responses of single modes, because the modal density is here quite small [4]. Thus, single maxima which belong to the eigenfrequencies can be seen separately in the frequency response. For this frequency range the finite element method (FEM) (see chapter 1.1.2) is the most popular calculation method. But the computational cost of FEM is increasing with the frequency because as explained before the wavelength becomes smaller and so more discrete points are necessary to describe these vibrations. Also, in the high frequency range the modal density becomes high and so the response at one frequency is here an average response of a high number of modes. These modes are in addition very sensitive to small changes of characteristics of the respective systems as explained in [5]. Thus, the responses of nominally identical industrial products excited at high frequencies can be very different. Because of these reasons it makes no sense to calculate detailed response for each point with a deterministic method like FEM [5]. The most well known method to calculate such averaged frequency responses in the high frequency range is the statistical energy analysis (SEA), which is presented more detailed in chapter 1.1.1. All in all, there are well established calculation methods for the low frequency range and for the high frequency range. But in between in the mid frequency range the modal densities are too low to use SEA and the computational cost is still quite high using FEM. To solve this problem many different methods have been developed in the last 10 years. So there are for example the hybrid FEM/SEA method, the wave based method, the variational theory of complex rays (VTCR) and the complex envelope vectorization (CEV), which are presented shortly in chapter 1.1.3. One of these is also the statistical modal energy distribution analysis (SmEdA), which is the topic of this

dissertation. The development of SmEdA has been started by Maxit and Guyader [6]. Their aim was to get an energy based method like SEA, which can be used at lower frequencies, too. In the last three years SmEdA has been further developed in the framework of ITN Marie Curie project GA-214909 “MID-FREQUENCY - CAE Methodologies for Mid-Frequency Analysis in Vibration and Acoustics”. The main subjects of this research discussed in thesis are:

- a new original method to take into non resonant modes in SmEdA
- a new postprocessing method to predict energy distributions of coherent sound fields with the modal information and the results of SmEdA
- a novel method to handle ill defined systems
- the discussion of methods for systems with high modal densities to reduce the computational cost of SmEdA

All the results of the research are summarised, discussed and commented in part I of this thesis following chapters about the scientific context and the detailed presentation of the subject. The details of the research like derivations of formulae can be found in the publications of part II. In this context, it has to be mentioned that some errors in the publications have been corrected and the appearance of the publications have been adapted to that of this thesis. Thus, the publications in part II look not exactly like the original ones. Furthermore, some errors in the publications have been corrected and the appearance of the publications have been adapted to that of this thesis. Thus, the publications in part II look not exactly like the original ones.

1.1. Calculation methods in vibro-acoustics

1.1.1. Statistical Energy Analysis

The statistical energy analysis is the most popular energy based method. The development of it started in the early 1960s with the works over coupled oscillators from Lyon and Smith [7]. At first, simple coupled oscillators and the relation between their energies and the power input were investigated and discussed in lot of publications like [8], [9] or [10]. These oscillators are described by two coupled differential equations, which are given in the case of a gyroscopic coupling by

$$\begin{aligned} \ddot{y}_1(t) + \Delta_1 \dot{y}_1(t) + \omega_1^2 y_1(t) - \sqrt{M_1^{-1} M_2}\,\gamma \dot{y}_2(t) &= F_1(t) \\ \ddot{y}_2(t) + \Delta_2 \dot{y}_2(t) + \omega_2^2 y_2(t) + \sqrt{M_2^{-1} M_1}\,\gamma \dot{y}_1(t) &= F_2(t) \end{aligned} \tag{1.1}$$

where $\Delta_i = \omega_i \eta_i$ is the damping coefficient, γ is the gyroscopic coupling factor and M_1, M_2, y_1 and y_2 are the masses and the displacement of the oscillators one and two. As shown under the condition of a white noise excitation [8], the time-averaged power flow P_{ij}^{ex} between resonant excited oscillators is direct proportional to the difference of their time-averaged energies E_i and E_j.

$$P_{ij}^{ex} = \eta_{ij}(E_i - E_j) \tag{1.2}$$

where η_{ij} is the coupling factor. From equation (1.1) and (1.2) it follows for the coupling factor that

$$\eta_{ij} = \frac{\gamma^2 \left(\eta_i \omega_i \omega_j^2 + \eta_j \omega_j \omega_i^2 \right)}{(\omega_i^2 - \omega_j^2)^2 + (\eta_i \omega_i + \eta_j \omega_j)(\eta_i \omega_i \omega_j^2 + \eta_j \omega_j \omega_i^2)} \tag{1.3}$$

A detailed description of the derivation of η_{ij} can be found in chapter 11. This so defined exchanged power is used in a power balance equation for the oscillators as follows:

$$\Pi_i = \Pi_i^{dis} + P_{ij}^{ex} = \omega_c \eta_i E_i + \omega_c \eta_{ij}(E_i - E_j) \tag{1.4}$$

where ω_c is the central frequency of the excited frequency band and Π_i and Π_i^{dis} are the input power and the dissipated power of the oscillator i. This principle to describe coupled oscillators with power balance equations has been extended to a lot of other coupled system like coupled structures. A derivation of SEA for general coupled subsystems can be found in [11] and some application possibilities are shown for example in [12] or in [13]. To predict the coupling factors for other systems, there are the modal approach, the wave approach and experimental and numerical methods [7]. The first, the modal approach, splits the coupling of two subsystems into couplings of modes, what is comparable with the coupling between oscillator. The same procedure is used for the statistical modal energy distribution analysis (SmEdA) (see chapter 1.1.4.1), and thus SmEdA can be regarded also as a kind of modal approach to calculate SEA coupling factors (see chapter 1.1.4.5). The wave approach is discussed in detail for different types of subsystems by Lyon and DeJong [7]. Here, the coupling factors are defined by describing the transmission of waves from one semi-infinite subsystem to another. The so predicted coupling factors for a cavity-plate-cavity system from Lyon and DeJong are explained in detail in chapters 6 and 11. As this approach is very common, there can be found coupling factors predicted in this way also in other publications like for the cavity-plate-cavity coupling in [14]. Using the experimental method, the energies in the subsystems are measured for a known power input. In this way, the coupling factors are determined by equation (1.2). More information about the experimental method can be found for example in [15]. Instead of making measurements, the energies of subsystems can be also calculated for a given power input with numerical methods like the finite element method FEM [16]. Another possibility to get SEA coupling factors is to combine measurements with mobilities as described in [5].
The big advantage of the SEA method is that there is only a linear system of equations with one equation for each subsystem, which has to be solved to get results for the energies of these subsystems. But SEA is in general only a method for high frequencies, because the modal density in an excited frequency band has to be high so that the statistical assumption of the equipartition of the total energy on the modes is valid. A detailed discussion of the validity of SEA can be found for example in [17]. Because of this equipartition assumption it is principally not possible in SEA to take into account non resonant modes relating to an excited frequency band. This problem is solved for example for the sound transmission through a structure using non physical direct coupling factors between two rooms [7]. Moreover, this assumption is also the reason why SEA can not be used for narrow band excitations without additional statistics [5]. But it can be considered that the energy is ergodic so that a energy averaged over a frequency band is equal to the average energy of an ensemble of systems with random properties, which is excited at a single frequency [18]. In this way, a variance of this mean energy of an ensemble of random structures can be also calculated. Because of that SEA is a good method for taking into account uncertainties. A last problem of SEA mentioned here is that only global energies are output and there is so no information about the distribution of these energies [5].

1.1.2. FEM for fluid-structure problems

For FEM calculations, like in the commercial program Nastran [19], the following coupled differential equation formulation is used to describe the coupled fluid-structure problem:

$$\begin{bmatrix} M_s & 0 \\ -C^T & M_f \end{bmatrix} \begin{bmatrix} \ddot{U} \\ \ddot{P} \end{bmatrix} + \begin{bmatrix} D_s & 0 \\ 0 & D_f \end{bmatrix} \begin{bmatrix} \dot{U} \\ \dot{P} \end{bmatrix} + \begin{bmatrix} K_s & C \\ 0 & K_f \end{bmatrix} \begin{bmatrix} U \\ P \end{bmatrix} = \begin{bmatrix} L_s \\ L_f \end{bmatrix} \tag{1.5}$$

where U is the vector of the displacements of the FEM-nodes of the structure, C is the coupling matrix describing the coupling between two systems, P is the vector of the pressures at the FEM-nodes in the fluid and M_s, M_f, D_s, D_f, K_s, K_f, L_s and L_f are respectively the mass, the damping and the stiffness matrices and the external force vectors of the structure and the fluid. Here, it is assumed that a vibrating structure at the boundary of a cavity can be represented as a source on a rigid wall of the cavity, whose boundaries are all rigid [20]. Equation 1.5 can be symetrisized and also written as a function of the modes of the structure and the cavity instead of physical degrees of freedom. This procedure is called modal reduction [19] and hence equation 1.5 reads:

$$\begin{bmatrix} m_s & 0 \\ 0 & -m_f \end{bmatrix} \begin{bmatrix} \ddot{\xi}_s \\ \ddot{\xi}_f \end{bmatrix} + \begin{bmatrix} d_s & \zeta^T \\ \zeta & -d_f \end{bmatrix} \begin{bmatrix} \dot{\xi}_s \\ \dot{\xi}_f \end{bmatrix} + \begin{bmatrix} k_s & 0 \\ 0 & -k_f \end{bmatrix} \begin{bmatrix} \xi_s \\ \xi_f \end{bmatrix} = \begin{bmatrix} f_s \\ -g_f \end{bmatrix} \tag{1.6}$$

where

$$\begin{aligned} U = \Phi_s \xi_s \,, P = \Phi_f \xi_f \,, \\ m_s = \Phi_s^T M_s \Phi_s \,, m_f = \Phi_f^T M_f \Phi_f \,, \\ d_s = \Phi_s^T D_s \Phi_s \,, d_f = \Phi_f^T D_f \Phi_f \,, \\ k_s = \Phi_s^T K_s \Phi_s \,, k_f = \Phi_f^T K_f \Phi_f \,, \\ f_s = \Phi_s^T L \,, g_f = \Phi_f^T G_f = \Phi_f^T \int_0^t L_f \end{aligned} \tag{1.7}$$

and Φ_s, Φ_f, ξ_s and ξ_f are the mode shapes and the modal amplitudes of the structure respectively of the cavity. This modal equation is similar to the system of equations of two coupled gyroscopic oscillators (equation (1.1)), which is used in SEA and also for SmEdA (see chapter 1.1.4.1). One problem of FEM is that the mesh of nodes for FEM has to become finer and finer to describe well the displacement if the frequency of excitation grows, because the wavelength of the modes become smaller in this case. Thus, the computational cost of FEM increases then and so FEM is in general only a method for low frequencies. Another problem specially of equations (1.5) and (1.6) for the fluid-structure interaction is that the boundary condition of the equality of the normal velocities, are not fully respected as discussed in chapters 9 and 11. This could be especially important if more than two subsystems are coupled.

1.1.3. Mid-frequency methods

1.1.3.1. Hybrid FEM-SEA method

A first example for a mid-frequency method is the hybrid FEM-SEA method [21, 22]. Here, one system is divided into subsystems like in SEA, but only the subsystems which cannot be treated as SEA subsystems are handled with FEM. Thus, the first step of the hybrid FEM-SEA is to define for which subsystems FEM is necessary. This can be decided for example using the expected wavelengths of the result [23]. If the wavelengths are big in comparison to the dimension of a subsystem, it should be tackled with FEM. Next, finite element models are created for these chosen subsystems. To describe the interaction between the SEA and the FEM

subsystems the sound field of a SEA subsystem is split in a direct field and a reverberant field. This direct field at the boundary is represented by a direct field dynamic matrix, which is a function of the degrees of freedom at the boundaries of the FEM subsystems. The matrix can be calculated using the boundary element method or analytic approaches [23]. The influence of the reverberant field is described by a force exciting the FEM subsystems. After that the variables which are necessary for the SEA equations like the power input are calculated using the direct field dynamic matrix and the force representing the reverberant sound field. Finally, the energies of the SEA subsystems are calculated first from the SEA equations and then the FEM equations are solved using these energies of the SEA subsystem to get the response in the FEM subsystems. One advantage of that method is that the computational cost can be reduced dramatically in this way, because the much more time consuming FEM is used only for limited parts of a system in which it is an indispensable necessity. Also, the results are ensemble averaged ones and so uncertainties are directly taken into account in this method [23].

1.1.3.2. Trefftz methods

The wave based method (WBM) [24] and the variational theory of complex rays (VTCR) [25, 26] are examples for Trefftz methods. The differences between WBM and VTCR are that they use different wave functions and different variational formulations [27]. Therefore, the procedure of calculation and advantages and disadvantages of a Trefftz method are discussed in the following only on the example of WBM. This is a method to calculate time independent dynamic problems, which can be bounded or unbounded. First, the volume of a cavity or the area of a structure are split in so called “subdomains”. These parts have to be convex and non overlapping. The variables of the subdomains like pressure or displacement are described then in this method as a sum over a weighted set of functions. The special feature of such a Trefftz method herein is that these functions are exact solutions of the respective differential equation and not just arbitrary functions like polynomial functions. To calculate the weighting factors of these functions a variational formulation of the problem is used. In this way, a linear system of equations is build which have to be solved to calculate the weighting factors of the wave functions and so the results for the field variables. One problem of WBM is that it can be difficult to describe complex geometries with convex subdomains. This can be solved using a hybrid FEM/WBM method, because in this way small regions with complex geometries can be described with a FEM mesh and the huge rest with WBM subdomains [28]. Another problem of WBM is that complex numerical integrations are necessary to obtain the system matrix of the linear system of equations. This leads to problems with the accuracy of the values of the matrices and thus to ill-conditioned matrices. Also, the system matrices are fully populated. On the one hand, these two drawbacks make the WBM calculation more complex than a FEM calculation. On the other hand, the system matrices are much smaller in WBM than in FEM because of the smaller numbers of degrees of freedom and the convergence rate is also higher in WBM than in FEM. But all in all the computational cost of WBM is much smaller than that of FEM and thus it is possible to handle problems at higher frequencies with WBM than with FEM. Furthermore, WBM can be combined like FEM with SEA (see previous chapter) to reduce the computational cost again if one or more parts of a systems can be described statistically [29].

1.1.3.3. Complex Envelope vectorization

The complex envelope vectorization (CEV) [30] is a further development of the complex envelope displacement analysis (CEDA) [31]. In CEDA a complex envelope displacement is used for the calculation instead of the direct use of the physical displacement. This complex envelope

displacement is here defined via a Hilbert transform from the physical displacement. In a more practical sense this Hilbert transformation can be better understood by a look at the example of a fast oscillating signal in the time domain. The signal is transformed in the frequency domain using a Fourier Transform. After that the frequency spectrum is filtered and shift to a lower frequency range. The inverse Fourier transform of this frequency spectrum leads finally to a much slower oscillating signal in the time domain which is the complex envelope displacement of the original signal. This CEDA principle used successfully for one dimensional systems was extended in CEV to three dimensional discrete systems. A field variable is defined in CEV then as a complex envelope vector. The advantage of this method is that the mesh can be much coarser than normally in FEM because the frequency spectrum of the complex envelope vector consists of lower frequencies than the real physical field variable as explained above. Thus, less discrete points are necessary to describe the longer wavelengths of the complex envelop vector. Because of that the computational cost is reduced by CEV and calculations of problems in which higher frequencies play a role become possible. But the disadvantage of this method is that it can be only really successfully applied if the role of single modes can be neglected. Otherwise the CEV results show correctly only the principle trend. Therefore, the ideal conditions for the use of CEV are principally highly damped systems, external acoustic problems or high frequencies.

1.1.4. Statistical modal Energy distribution analysis

1.1.4.1. Basic principle

Maxit and Guyader [32, 6] have started to develop the statistical modal energy distribution analysis (SmEdA) to get an energy based method like SEA, which can be used also at lower frequencies. For this purpose it is necessary to overcome the SEA condition of equipartition of modal energies in an excited frequency band, because that is only true at high frequencies, where the number of modes is high. To reach this aim a coupling between modes of different subsystems is used to determine the interaction between subsystems instead of a coupling between whole subsystems like in SEA. Maxit and Guyader used the analogy that the coupling between modes is equal to a gyroscopic coupling between oscillators (see Figure 1.1) as discussed for example in [33]. This principle is valid if one subsystem can be handled uncoupled as blocked and the connected one uncoupled as free on the coupling area. This is the principle of the dual modal formulation first introduced by Karnopp. It can be applied for example for the case of a structure-cavity system (see Figure 1.2), at which vibrations of the structure can be described with in vacuo modes and vibrations in the cavity with modes predicted under the assumption of rigid walls. These modes can be calculated analytically for simple geometries like in [34] and [35] or otherwise with FEM. The gyroscopic coupling factor for such modes is defined as, [6],

$$\gamma_{pq}^{12} = \frac{1}{\sqrt{(\omega_p^1)^2 M_p^1 M_q^2}} \int_S p_p^1 W_q^2 n^2 \, dS = \frac{W_{pq}^{12}}{\sqrt{(\omega_p^1)^2 M_p^1 M_q^2}} \tag{1.8}$$

where W_{pq}^{12}, the integral over the coupling area S of the product of the mode shapes, is the interaction modal work, n^2 is the normal vector of the structure and M_p^1 and M_q^2 are the modal masses of the p-th and q-th mode of the subsystems one and two. In such a case, the coupling factor β_{pq}^{12} between two modes is given similar to the coupling factor between two oscillator, equation (1.3), by, [6]:

$$\beta_{pq}^{12} = \frac{(W_{pq}^{12})^2}{M_p^1 M_q^2 (\omega_q^2)^2} \left[\frac{\eta_p^1 \omega_p^1 (\omega_q^2)^2 + \eta_q^2 \omega_q^2 (\omega_p^1)^2}{((\omega_p^1)^2 - (\omega_q^2)^2)^2 + (\eta_p^1 \omega_p^1 + \eta_q^2 \omega_q^2)(\eta_p^1 \omega_p^1 (\omega_q^2)^2 + \eta_q^2 \omega_q^2 (\omega_p^1)^2)} \right] \tag{1.9}$$

where M_p^1, M_q^2, ω_p^1 and ω_q^2 are the modal masses and the eigenfrequencies of the p-th and the q-th mode of the subsystems one and two. In this way, an analogous mechanical model is created in which every oscillator represents one mode. The masses and the damping factors of these oscillators are the modal masses and the modal damping factors of the respective modes. Due to that the modal energies can be calculated with SEA-like power balance equations for each mode respectively oscillator as follows:

$$\Pi_p^1 = \eta_p^1 \omega_p^1 E_p^1 + \sum_{q=1}^{q_{max}} \beta_{pq}^{12} (E_p^1 - E_q^2) \tag{1.10}$$

where Π_p^1 is the power input in the p-th mode of subsystem one. Thus the coupling between two subsystems is described in SmEdA by modal power balance equations instead of power balance equations for each subsystem only like in SEA. The whole energy E^i of a subsystem i is the sum of all the energies E_n^i of resonant modes of this subsystem [36, 37].

$$E^i = \sum_n E_n^i \tag{1.11}$$

But in this original formulation of SmEdA only resonant modes can be taken into account due to the assumption of a white noise excitation for the derivation of the modal coupling loss factor, equation (1.9). Therefore, this total energy is only equal to the real total energy if approximately all the energy is stored in resonant modes.

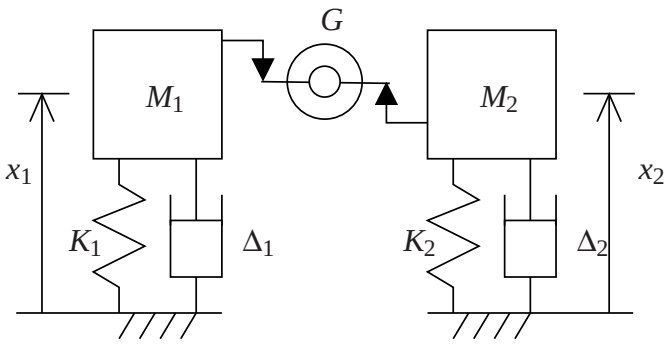

Figure 1.1.: Analogous mechanical model: Two gyroscopic coupled oscillators

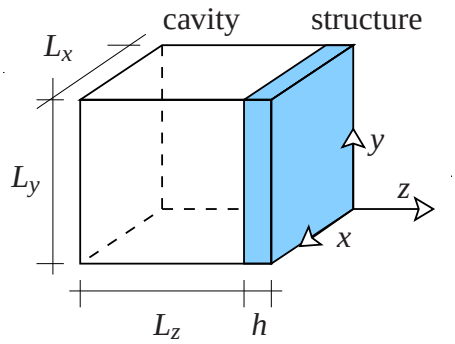

Figure 1.2.: System in reality: A cavity coupled to a structure

1.1.4.2. Limits of SmEdA

SmEdA describes all the processes with undamped modes, like it is described in the previous chapter, and so it is necessary to pay attention what can be characterised by them. In principle every vibration can be described as a sum of these modes, because they are an orthogonal complete set of function [38]. But one problem in this context is the damping at the boundary, because systems with damped boundaries are not really "closed". This cause that the orthogonality relation between the modes which would describe exactly the problem is not valid any more [38]. Thus, there would be also an interaction between the modes which cannot be described with the SmEdA method. Especially for fluids in cavities this can be a problem, because the damping is normally given only through absorbing materials at the walls. In the case of high damped boundaries the direct field is dominating in a cavity and not the reverberant sound field. Therefore, to be sure that the influence of the direct sound field is small, the critical distance d, which is used in room acoustics for diffuse sound fields, can give a rough indication. The critical distance d is the distance, at which the sound pressure level of the direct and the reverberant sound field are equal, and is given in [39] by

$$d = \sqrt{\frac{\gamma A_S}{16\pi} e^{\frac{A_S}{S}}} \tag{1.12}$$

where γ is the source directivity and S is the interior surface area of the cavity. The equivalent absorption area A_s can be connected to the damping factor, which is used in SmEdA, for example with equation (1.30). If this critical distance d is small compared to the dimensions of the cavity, the sound field is dominated by the reverberant one and the direct field is negligible. Another limitation in SmEdA is that the external excitations of different subsystems have to be uncorrelated, because as explained in chapter 11 this is assumed for the derivation of the coupling loss factor, equation (1.9). Furthermore, SmEdA is a method for stationary problems, because the used energy balance, equation (1.10), is time independent. To sum up, SmEdA can be applied only for stationary problems of more or less closed coupled subsystems, whose external excitations are uncorrelated.

1.1.4.3. Power input of a mode

Besides the coupling loss factors, the damping factors and the eigensystems, the external power input is one quantity that has to be known in advance for power balance equation systems, equation (1.10). For this purpose analytic solutions in modal description of the uncoupled subsystems are used as described in [40] (see chapter 9). In this way, the frequency averaged input power of a mode m can be written for example for a structure, which is excited between the frequencies ω_1 and ω_2, as

$$\Pi_m = \frac{1}{\Delta\omega} \int_{\omega_1}^{\omega_2} \frac{1}{2} \int_A \Re[p_{ex}(A) v_m^*(A)]\, dA\, d\omega \tag{1.13}$$

with the uncoupled velocity [38]

$$v_m(A) = \frac{\Phi_m(A)}{M_m\left(\omega_m^2 - \omega^2 + i\eta_s\omega_m\omega\right)} \int_A i\omega p_{ex}(A)\Phi_m(A)\, dA \tag{1.14}$$

where ω_m and M_m are the eigenfrequency and the modal mass of a mode m, $p_{ex}(A)$ is an external pressure acting on an area A of a structure, $\Phi_m(A)$ is the mode shape of a mode m at the excitation area A, ω is the excitation frequency, η_s is the modal damping factor and * denotes the

complex conjugate. In the case of a structure excited with a broadband point force F ($|F| = 1N$), it follows analytically that the power input of a resonant mode is given by, [41],

$$\Pi_m = \frac{\pi \left(\Phi_m(\varepsilon)\right)^2}{4M_m \Delta\omega} \tag{1.15}$$

where M_m is the modal mass of the mode m, $\Phi_m(\varepsilon)$ is the mode shape at the point of excitation ε and $\Delta\omega$ is the band width of the excited frequency band. Similar to this equation the power input Π_{in} of a whole subsystem is determinate in SEA as follows [7]:

$$\Pi_{in} = \frac{S_f \Delta\omega n(\omega)}{4M} \tag{1.16}$$

where $n(\omega)$ is the modal density in the excited frequency band, M is the mass of the subsystem and S_f is the power spectrum of the excitation force. To get the exact power input for all modes, resonant and non resonant ones, the integral over the excited frequency range in equation (1.13) has to be predicted numerically as done for the SmEdA calculations in [42], [34], [35],[43] and [40] (chapters 6 to 11). In the same way the power input in cavity subsystems are obtained for excitations with monopole sources and for excitations via vibrating structures. For the first kind of excitation, the monopole excitation, the power input is given by, [44],

$$\Pi_m = \frac{1}{\Delta\omega} \int_{\omega_1}^{\omega_2} \frac{1}{2} \Re[p_m(x_q) Q^*] \, d\omega \tag{1.17}$$

with the modal pressure $p_m(x_q)$ at the location x_q of the monopole

$$p_m(x_q) = i\omega\rho_f Q \frac{\Psi_m^2(x_q)}{N_m(k^2 - k_m^2)} \tag{1.18}$$

where Q is the the volume source strength of a point monopole [44], $\Psi_m(x_q)$ is the mode shape of the cavity mode m at the excitation point x_q, ρ_f is the density of the fluid and N_m is the norm of a mode m. The wavenumbers k_m and k are defined as

$$k_m = \frac{\omega_m}{c_f} \tag{1.19}$$

and

$$k = \frac{\omega}{c_f(1 + i\eta_f)} \tag{1.20}$$

where c_f is the sound velocity of the fluid. The relation between the damping factor η_f of the fluid and the damping η used in equation (2.1) of SmEdA is approximately given by, [40],

$$\eta_f = \frac{\eta}{2} \tag{1.21}$$

For the excitation via a vibrating structure, the power input can be written as

$$\Pi_m = \frac{1}{\Delta\omega} \int_{\omega_1}^{\omega_2} \frac{1}{2} \int_A \Re \left(\frac{p_m(A) p_m^*(A)}{Z} \right) dA \, d\omega \tag{1.22}$$

with the modal pressure $p_m(A)$ at the excitation area A, [41],

$$p_m(A) = -\rho_f \omega^2 \Phi_m \sum_s \frac{a_s W_{ms}}{N_m(k^2 - k_m^2)} \tag{1.23}$$

where Z is the impedance of the fluid, W_{ms} is the interaction modal work, equation (1.8), and a_s is the modal amplitude of the s-th mode of a structure, which is equal to the amplitude of the velocity $v_m(A)$ from equation (1.14). Finally, for all the different excitation possibilities it is important to pay attention to the correlation between different sources. One example for that is the excitation of a subsystem with more than one point force. The resulting power input of each force alone can be only added if the forces are fully uncorrelated. Otherwise, the power input in a mode have to be calculated for completely correlated forces with equation (1.13) as follows using the sum of the scalar products (denoted by: $\circ$) between the forces and the modal shape vectors:

$$\Pi_m = \frac{1}{\Delta\omega}\int_{\omega_1}^{\omega_2} \Re\left[\frac{\left(\sum_i F_i \circ \Phi_m(\varepsilon_i)\right)^2}{M_n\left(\omega_m^2 - \omega^2 + i\eta_s\omega_m\omega\right)}\right] d\omega \tag{1.24}$$

where ε_i is the point on a structure, at which a force F_i excites the structure. This formula was used for example for the calculations in [43] and chapter 8. A part of a double deck train is there excited by eight correlated point forces at the bottom of the structure.

1.1.4.4. Damping in SmEdA

For both the power balance equation system of SmEdA, equation (2.1), and the power input it is necessary to define in advance the damping, which is characterized by a modal damping factor η_i. The modal damping factors are all equal if the damping is distributed uniformly in a subsystem. But in the case of a localised damping each modal damping factor has a unique value. For structures this characterisation of the damping is not problematic, because here the damping is normally described with the quantity η_i using a complex elasticity modulus $B = \hat{B}(1+i\eta)$ [38]. Moreover, as explained in chapter 9 there are also methods for structures, like the strain energy method [45, 46] or the complex eigenvalue method [46, 47, 48], to predict one damping factor for each mode. The strain energy method is used for multi-layered structures or structures with added damping materials in some areas. Here, it is assumed that the damping factor η_d of the damping material is much bigger than those of the other component. The modal damping factor for a mode n is then given by

$$\eta_n = \frac{\eta_d E_{d,n}^s}{E_n^s} \tag{1.25}$$

where E_n^s is the total modal strain energy of mode n and $E_{d,n}^s$ is the modal strain energy of a mode n contained within the area of the damping material. The other method, the complex eigenvalue method, is applied to arbitrary structures like vehicle components [47]. To get a damping factor for each real mode used for example in SmEdA, the complex eigenvalue problem of a damped system, which is described by the following equation, is solved first in this method.

$$M\ddot{y} + D\dot{y} + Ky = F \tag{1.26}$$

where y is the displacement, F is the excitation force vector and M, K and D are the mass, the stiffness and the damping matrix. The modal damping factors η_m can be calculated from the real and the imaginary part of the complex eigenvalues λ_m as follows [47]:

$$\eta_m = \frac{|\Re(\lambda_m)|}{|\Im(\lambda_m)|} \tag{1.27}$$

In cavities the damping is caused in contrast normally by absorbent materials at the boundaries and not by a damping in the material as for structures. The absorption of these materials at

the boundary is described by an absorption coefficient α or a boundary impedance Z_B. Thus, formulae are needed to calculate equivalent damping factors from these quantities. The relation between α and Z_B is given in [49] by

$$\alpha = 1 - \left| \frac{\frac{Z_B}{\rho_f c_f} - 1}{\frac{Z_B}{\rho_f c_f} + 1} \right|^2 \tag{1.28}$$

where ρ_f and c_f are the density and the speed of sound of the fluid. Under the assumptions of a uniformly distributed damping and a diffuse sound field in a cavity, one global damping factor η_f, which is equal for every mode, can be calculated from α as follows, [14]:

$$\eta_f = \frac{A_f c_f}{4\omega V_f} \tag{1.29}$$

with the equivalent absorption area A_f

$$A_f = \sum_n S_n \alpha_n \tag{1.30}$$

where ω is the frequency of excitation, V_f is the volume of the fluid , S_n are areas of the boundary surface and α_n are the absorption coefficients of these areas. To our knowledge this is the only relation, which could be found in the literature, between α and a damping factor η_i and there are no special methods to predict damping factors for the cavities in the case of a localised damping as for structures. But maybe the complex eigenvalue method, equation (1.27), can be also used for cavities to get damping factors for each mode. For all the calculations presented in this dissertation it was assumed to simplify the problem that the damping is described for structures and for cavities with one global damping factor.

1.1.4.5. Relation between SmEdA and SEA

As shown and discussed in [50] and [37] it is possible to get good SEA coupling factors using results of SmEdA . The SEA coupling loss factors η_{ij} can be namely written as a function of the modal coupling factors β_{pq}^{ij}, equation (1.9), on condition of modal equipartition of energy as follows:

$$\eta_{12} = \frac{1}{p_{max}\omega_c} \sum_{p=1}^{p_{max}} \sum_{q=1}^{q_{max}} \beta_{pq}^{12} \tag{1.31}$$

$$\eta_{21} = \frac{1}{q_{max}\omega_c} \sum_{p=1}^{p_{max}} \sum_{q=1}^{q_{max}} \beta_{pq}^{12} \tag{1.32}$$

where p_{max} and q_{max} are the number of resonant modes relating to an excited frequency band of the subsystems one and two and ω_c is the central frequency. Only resonant modes can be taken into account for these formulae, because only for them the assumption of modal equipartition of energy is so far valid. These SEA coupling factors predicted in this way can be used for a normal SEA calculation as described in chapter 1.1.1 or in a hybrid SEA/SmEdA technique. Such a technique was first used in [50] in connection with structure-structure coupling. Here, some subsystems are described with SEA-like equations and others with equations for each

mode. Thus, for example a mixed power balance equation system for two connected subsystems reads, [50]:

$$\begin{aligned} P^1 &= \omega_c \left(\eta^1 + \eta_{12}\right) E^1 - E_m^2 \sum_n \beta_{nm}^{12} \\ P_m^2 &= \left(\eta_m^2 \omega_m^2 + \sum_n \beta_{nm}^{12}\right) E_m^2 - \frac{E^1}{n} \sum_n \beta_{nm} \end{aligned} \tag{1.33}$$

where ω_m^2, η_m^2, P_m^2 and E_m^2 are the eigenfrequency, the damping factor, the input power and the modal energy of the mode m of subsystem two, ω_c is the central frequency of the excited frequency band, n is the number of modes of subsystem one in the excited frequency band and η^1, P^1, and E^1 are the damping factor, the input power and the energy of the whole subsystem one.

1.1.4.6. Postprocessing for energy distributions

The idea in [36], [51] and [52] was to predict with a postprocessing method energy distributions of subsystems using the modal information and the outputs of SmEdA. In these articles it is approximated that the modes are uncorrelated. Under such an assumption, an energy distribution e^i of a subsystem i can be written as a function of total, kinetic or potential modal energy distributions e_n^i as

$$e^i = \sum_n e_n^i \tag{1.34}$$

The total modal energy density distribution e_n^t is given in these articles by

$$e_n^i = \frac{E_n}{N_n} \Phi_n^2 \tag{1.35}$$

where E_n and N_n are the total energy and the norm of a mode n. The kinetic and the potential modal energy distributions, e_n^k and e_n^p, are defined as, [37],

$$e_n^p = E_n^p \frac{\left(\Phi_n^Q\right)^T K \Phi_n}{K_n} = \frac{E_n \left(\Phi_n^Q\right)^T K \Phi_n}{2K_n} \tag{1.36}$$

$$e_n^k = E_n^k \frac{\left(\Phi_n^Q\right)^T M \Phi_n}{M_n} = \frac{E_n \left(\Phi_n^Q\right)^T M \Phi_n}{2M_n} \tag{1.37}$$

This formulation for energy distributions works so far if the damping of the subsystem is small, as demonstrated in [36]. But in the case of high damping the energy distribution predicted with this method shows no concentration of energy around the point of excitation as the result of an analytical approach [36].

1.2. Transmission Loss

1.2.1. Definition

The transmission loss characterises the physical process of the transmission of the acoustical power through a partition with the transmission factor τ. This factor τ is the ratio between the transmitted power P_t and the incident power P_i.

$$\tau = \frac{P_t}{P_i} \tag{1.38}$$

And the transmission loss R is defined with that as follows [53]:

$$R = 10\lg\left(\frac{1}{\tau}\right) = 10\lg\left(\frac{P_i}{P_t}\right) \tag{1.39}$$

If there are on both sides of a partition closed rooms, like it is the case normally for transmission loss measurements, an averaged pressure for each room is calculated from the measured or predicted pressures. To determine for this case the transmission loss the incident power P_i can be expressed under the assumption of a diffuse sound field in the sending room as follows, [49]:

$$P_i = \frac{\tilde{p}_i^2 S}{4\rho c} \tag{1.40}$$

Moreover, the transmitted power P_t is equal to the dissipated power in the receiving room and this power is thus given under the same assumption as for P_i by , [49],

$$P_t = \frac{\tilde{p}_t^2 A_r}{4\rho c} \tag{1.41}$$

Here, $\tilde{p}_t^2$ and $\tilde{p}_i^2$ are the effective values of the space averaged quadratic pressures in the sending and the receiving room, S is the area of the partition and ρ and c are the density and the speed of sound of the fluid in the rooms. The equivalent absorption area A_r can be described as a function of the damping factor η_r normally used in SEA under the assumption of equipartition of the damping in the receiving room as follows, [14]:

$$\eta_r = \frac{A_r c}{4\omega V_r} \tag{1.42}$$

where ω is the excitation frequency and V_r is the volume of the receiving room. From the equations (1.40) and (1.41) it follows for the transmission loss:

$$R = 10\lg\left(\frac{\tilde{p}_i^2}{\tilde{p}_t^2}\right) - 10\lg\left(\frac{A_r}{S}\right) \tag{1.43}$$

The output of energy based methods like SEA and SmEdA is the energy of subsystems. The transmission loss, equation (1.43), can be written in terms of energies because of the proportionality between the energy and the respective quadratic pressures as:

$$R = 10\lg\left(\frac{E_i}{E_t}\right) - 10\lg\left(\frac{A_r}{S}\right) \tag{1.44}$$

where E_i and E_t are the total energies in the sending and the receiving room. The problem of these definitions of the transmission loss, equations (1.43) and (1.44), is that they are only valid under the assumption of diffuse sound fields. In this case the kinetic and the potential energies are equal, because the space averaged energy density e_d is given as twice the potential energy [44].

$$e_d = \frac{\tilde{p}^2}{2\rho c^2} \tag{1.45}$$

But the sound fields of small cavities are not diffuse especially at low frequencies and thus equations (1.43) and (1.44) are not valid anymore. Because of that it would be necessary to find another definition of the transmission loss. Another definition for the transmission loss was

found in [54], The transmission loss is there given under the assumption of equal rooms on both sides of the partition by

$$R_N = 10\lg\left(\frac{\tilde{p}_i^2}{\tilde{p}_t^2}\right) - 10\lg\left(\frac{A_r}{S}\right) - 10\lg\left(\frac{A_r + A_s}{2S}\right) - 6 \tag{1.46}$$

But this definition of the transmission loss by Nilsson seems also not accurate enough. One reason is that, R_N has to converge to R for a frequency, which goes to infinity, because the number of modes in an arbitrary small frequency band goes then to infinity for a cavity and so the sound field becomes diffuse. But that is in general not the case for R_N. Because of these problems to find a correct definition of the transmission loss, equations (1.43) and (1.44) are used for the result presented in this work, like it is done for example in [55] or [56]. Therefore, the values for the transmission loss are maybe not fully correct, but in this way the different calculation methods can be compared together. Also, the effects, which appear in finite small cavity-structure-cavity systems (see chapter 2.2), can be so investigated.

1.2.2. Transmission Loss of infinite plates

To predict the transmission loss many ways have been developed using different calculation methods. An overview over these different possibilities is given in chapters 6 and 11. In the following only the excerpt of these chapters about the simple transmission loss models, the mass law and the formula of Cremer for infinite plates, are presented. For the mass law Newton's third law, action is equal to reaction, is used and it is assumed that the plate in between two free sound fields is rigid [53]. In this way, the transmission loss is given by

$$R_M = 10\lg\left[1 + \left(\frac{\omega m \cos\vartheta}{2\rho c}\right)^2\right] \tag{1.47}$$

The mass law shows that the transmission loss depends on the mass of a partition (m: mass per area), the angular frequency ω, the density ρ and the speed of sound c of the fluid and the angle of incidence ϑ. The theoretical background of this law was first formulated by Rayleigh [57] and experimentally verified amongst others by Berger [58]. The further development was made by Cremer. He used instead of the assumption of a rigid structure the plate equation of Kirchhoff to describe the deformation of the plate. Under the assumption of an infinite plate he got the following equation for the transmission loss [53], which depends additionally to the mass law also on the bending stiffness B:

$$R_C = 10\lg\left[1 + \left(\omega m - B\omega^3\frac{\sin^4\vartheta}{c^4}\right)^2\left(\frac{\cos\vartheta}{2\rho c}\right)^2\right] \tag{1.48}$$

This additional dependency characterises the so called coincidence effect. This is a resonance effect which appears for the case that the fluid wave length projected on the plate and the wave length of the excited free plate bending wave are equal. The minimal frequency where it can occur is the critical frequency

$$f_c = \frac{c^2}{2\pi}\sqrt{\frac{m}{B}}\,. \tag{1.49}$$

Due to the simplicity of this formula and the correct tendency it provides, especially above the critical frequency, it is still often used.

1.3. Presentation of the subject

As shown in the previous chapters there are already well developed calculation methods for vibro-acoustic problems even for the mid-frequency range. Nevertheless, it is interesting to further develop the statistical modal energy distribution analysis especially for coupled vibro-acoustic problems. The beauty of this method is that it is even for complex coupled systems possible to calculate quite easy an averaged energy like in SEA. But in contrast to SEA energy distributions for areas of interest of the subsystems can be also predicted and it is not necessary that the sound fields are diffuse. As shown in chapter 1.1.4.5 another good feature of SmEdA is that it can be simply combined with SEA to extend the range of application to higher frequencies. Furthermore, the energies can be directly calculated as averages over whole frequencies band with different bandwidths and not only for excitation with single frequencies like in FEM. To get a well developed SmEdA, which can be used for a width range of applications, this method has been further developed in some points through the research of the last years presented in this thesis. As explained in chapter 1.1.4.1 the original formulation can take into account only resonant modes relating to an excited frequency. But non resonant modes are for example important for highly damped or narrow band excited systems. Because of that the theory of SmEdA has been extended so that also non resonant modes can be respected in the calculation. Moreover, a new post-processing method has been developed using the modal information and the modal results of SmEdA to predict energy distributions also of coherent sound fields and not only of incoherent ones like in previous works (see chapter 1.1.4.6).
Another important topic of the research of the last years was the development of a method which can approximate mode shapes and eigenfrequencies for ill defined systems. This method can be also used to reduce the computational cost, because in the case of a high modal density the calculation of modes is quite time consuming using for example FEM. In this context, also different mixed SEA/SmEdA formulations have been tested for cavity-structure-cavity using the relation of chapter 1.1.4.5, because the number of equations can be reduced dramatically in this way.
All the new developed methods are presented in the following chapters. To demonstrate herein their application possibilities and to validate them in comparison to other methods the results for simple academic and industrial cases are shown. But it was not the aim of this research to make an extensively comparison to other methods concerning for example the computational time, because the aim of this research was more to further develop the necessary theories.

2. Non resonant modes and SmEdA

2.1. Non resonant contribution in SmEdA

2.1.1. Principle

In chapter 11 the analogous mechanical model used of the original SmEdA (see 1.1.4.1 and Table 2.1) has been extended for the structure-cavity coupling so that all the modes, resonant and non resonant ones, can be taken into account and not only resonant modes. To reach this aim the formula of Cremer, equation (1.48), was used as a reference and in contrast to the original formulation it was payed attention to respect the boundary conditions on the coupling surface between a cavity and a structure, like the equality of normal velocities. Herein, the transmission through an infinite plate is described with couplings between modes, resonant and non resonant ones. In this way, it has been shown that this formula for the transmission loss of an infinite plate can be derived analytically using the SmEdA formulation. In consequence of this it follows that the boundary conditions on the coupling surface correspond in the analogous mechanical model to responses of the oscillators frequency averaged from zero to infinity. The kinetic and potential energies of the oscillators become equal in this way and thus there are no differences in the analogous mechanical model between the oscillators, which represent resonant modes, and those, which represent non resonant modes. But that moreover means that for the non resonant modes only the total energies are equal to those of the respective oscillators and the respective potential and kinetic energies are in contrast unequal. Furthermore, because of the averaged responses of the oscillators the coupling factors for the coupling between the oscillators are for every possible coupling between resonant and non resonant modes equal to the modal coupling loss factor of the original formulation, equation (1.9). Because of these reasons the total energies of these oscillators, which are equal to the respective total modal energies, can be calculated with a similar power balance equation as for the original formulation (equation (1.10)).

$$\Pi^1_{o,p} = \eta^1_p \omega^1_p E^1_p + \sum_{q=1}^{q_{max}} \beta^{12}_{pq}(E^1_p - E^2_q) \tag{2.1}$$

The investigation using the formula Cremer but do not show the connection between the power input of a oscillator $\Pi^1_{o,p}$ of the analogous mechanical model and the power input of a mode, because the transmission loss is independent from the size of the power input. Thus, the next section shows how this power input $\Pi^1_{o,p}$ results from the power input of a mode. The total energies of the subsystems are calculated with equation (1.11) like in the original formulation. All in all, the described extension summarized in Table 2.1 allows SmEdA to be used in all situations where also non resonant modes are indispensable for correct modelling. Examples for such cases are highly damped systems or systems excited at a single frequency. The limits of the extended SmEdA approach are the same as for the original one discussed in chapter 1.1.4.2. But after the integration of the non resonant modes in the approach the only remaining statistical aspect is that the excitations of different subsystems has to be uncorrelated.

problem in reality		**analogous mechanical model**
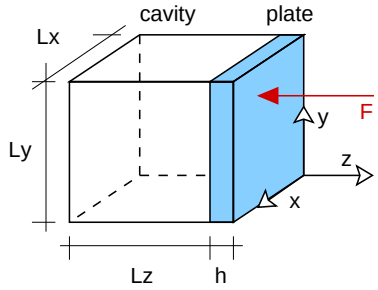		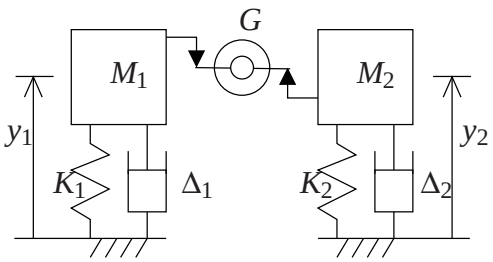
Original SmEdA formulation for resonant modes (see chapter 1.1.4.1)		
eigenmode	$\rightarrow$	oscillator
interaction between the pressure p_{cavity} and the velocity $v_{structure}$	$\rightarrow$	gyroscopic coupling described with the coupling factor β_{pq}^{12} (equation (1.9))
$E_{tot,m}$	$=$	$E_{tot,o}$
$E_{kin,m} = E_{pot,m}$	$\rightarrow$	$E_{kin,o} = E_{pot,o}$
η_m	$=$	η_o
Π_m	$=$	Π_o
Extensions for resonant and non resonant modes		
boundary conditions	$\rightarrow$	frequency averaged response from 0 to ∞ Hz ($\Rightarrow E_{kin,o} = E_{pot,o}$)
interaction between the pressure p_{cavity} and the velocity $v_{structure}$	$\rightarrow$	gyroscopic coupling described with the coupling factor β_{pq}^{12}, equation (1.9), for all the coupling possibilities between resonant and non resonant modes
for non resonant modes:		
$E_{kin,m}$	$\neq$	$E_{kin,o}$
$E_{pot,m}$	$\neq$	$E_{pot,o}$
Π_m	$\neq$	Π_o

Table 2.1.: Representation of coupled structure-cavity problems in the analogous mechanical model of SmEdA ($\rightarrow$: correspond to; $E_{tot,i}$, $E_{kin,i}$, $E_{pot,i}$: total, kinetic and potential energy; Π_i: power input; η_i: damping factor; m: mode of the real system; o: oscillator)

2.1.2. Power input of a SmEdA-oscillator

As explained in chapter 2.1, the modes are represented in the analogous model by oscillators, for which the kinetic and potential energies are equal. That means that the velocity or the pressure of a given non resonant mode and those of the respective oscillator are not equal and thus also the power inputs of them are different. But the relation between the two velocities is determined by the equality of the total energies, for example of a structure, as follows

$$\begin{aligned} E_o &= E_m \\ \frac{1}{2} M_m v_o^2 &= \frac{1}{4}\left(M_m v_m^2 + K_m u_m^2\right) \end{aligned} \tag{2.2}$$

where E_o, v_o are the total energy and the absolute value of the velocity of an oscillator, E_m, v_m and u_m are the total energy, the absolute value of the velocity and the absolute value of the

displacement of a mode and M and K are the modal mass and the modal stiffness. Thus, through division by M_m and using $\omega u_m = v_m$ and $K_m/M_m = \omega_m^2$ the relation between the velocities reads:

$$v_o^2 = \frac{v_m^2}{2}\left(1+\frac{\omega_m^2}{\omega^2}\right) \tag{2.3}$$

Moreover, the oscillators can be considered as uncoupled for the calculation of the power input like it is done also for the power input in modes. Thus, the power input Π_o as a function of the excitation frequency ω of an uncoupled oscillator is equal to the dissipated power Π_{dis}, which is under the assumption of a viscous damping proportional to the kinetic energy E_o^k:

$$\Pi_o = \Pi_{dis} = 2\eta\omega E_o^k = \frac{\eta\omega}{2} M v_o^2 \tag{2.4}$$

where η is the damping factor of the oscillator respectively of the mode. Insertion of equation (2.3) in this equation yields a relation between the power input Π_m of a mode and the power input Π_o of an oscillator.

$$\Pi_o = \frac{\eta\omega}{2} M \frac{v_m^2}{2}\left(1+\frac{\omega_m^2}{\omega^2}\right) = \frac{1}{2}\left(1+\frac{\omega_m^2}{\omega^2}\right)\Pi_m \tag{2.5}$$

This relation between the power input is valid in general also for cavities and not only for structures. This can be demonstrated using the same procedure but in connection with the formulae for the energies of cavities. Equation (2.5) shows that the power input of a mode and of a SmEdA-oscillator are equal for resonant modes as assumed in the original SmEdA formulation (see 1.1.4.1 and Table 2.1) and unequal for non resonant modes. Through insertion of equation (2.5) in equation (2.1) the power balance equations of an external excited subsystem can be written for a single frequency excitation also as

$$\Pi_p^1 = \frac{2\eta_p^1\omega_p^1}{\left(1+\frac{\omega_p^2}{\omega^2}\right)} E_p^1 + \frac{2}{\left(1+\frac{\omega_p^2}{\omega^2}\right)} \sum_{q=1}^{q_{max}} \beta_{pq}^{12}(E_p^1 - E_q^2) \tag{2.6}$$

It has to be noted that this additional factor has not been taken into account in the calculations in the publications of part II. Instead, it was considered that the both input of a mode and of an oscillator are equal. But that is in general not a problem, because the factor plays only an important role in special situations in which there are no modes in the excited frequency area like for excitations below the first resonance frequency.

2.1.3. Heavy fluids

One special case in which non resonant modes play an important role is the coupling between heavy fluids and structures as explained in [59]. In chapter 11 it is demonstrated that the formula of Cremer, equation (1.48), can be derived with SmEdA. This formula is not only applicable to light fluids but to heavy fluids too [60]. The question is if SmEdA can be used also for heavy fluids or only for light fluids as it was done in all the calculations before. One important point herein is if the vibrations of the subsystems can also be described in the case of a heavy fluid as a function of the uncoupled modes. This is investigated by a look at the following well established differential equation for structures under the influence of fluids [61, 62, 63, 64]

$$M\ddot{y} + Ky = P - \dot{y}Z \tag{2.7}$$

where P is the excitation force, y is the structural displacement and M and K are the mass and the stiffness matrix of a structure. The impedance Z, which describes the influence of the fluid and the radiation into the fluid, is in general a complex quantity. The real part of Z act as a damping term and the imaginary part of Z is an added mass term. Thus, because of this added mass effect a heavy fluid changes the eigensystems of a structure in the general case. But if a plane wave radiation in a free field is given, like in the formula of Cremer, Z is only real and reads:

$$Z = \rho_f c_f \tag{2.8}$$

where ρ_f and c_f are the density and the sound velocity of the fluid. Therefore, there is no added mass effect in this case and so also no change of the eigensystem of a structure. In the case of a closed finite cavity equation (2.7) can be expressed as a function of the uncoupled modes of the structure and the cavity as follows, [20]:

$$a_p m_p \left(\omega_p^2 - \omega^2\right) - 2\omega^2 \rho_f a_p \sum_n \mu_{pn} = \int_S f \Phi_p(S)\, dS + 2\omega^2 \rho_f \sum_{q \neq p} \sum_n a_q \mu_{pqn} \tag{2.9}$$

where

$$\mu_{pn} = \frac{\left[\int_S \Psi_n(S)\Phi_p(S)\, dS\right]^2}{m_n\left(k_n^2 - k^2\right)}, \tag{2.10}$$

$$\mu_{pqn} = \frac{\left[\int_S \Psi_n(S)\Phi_p(S)\, dS\right]\left[\int_S \Psi_n(S)\Phi_q(S)\, dS\right]}{m_n\left(k_n^2 - k^2\right)}, \tag{2.11}$$

S is the surface of the structure, k_n and k are wavenumbers as defined in equations (1.19) and (1.20), Ψ_n are the modal shapes of the fluid filled cavity and a_p, a_q, m_p and m_q are the modal amplitudes and modal masses of the structural modes Φ_p and Φ_q. The real part of the term μ_{pn} acts here as an added mass and thus, the modes of fluid loaded structures are indeed different to the in vacuo ones, but the vibrations can be expressed as a function of the in vacuo modes as mentioned in [20]. The reason for that is that the uncoupled modes are mathematically just a complete set of orthogonal functions and therefore, a sum of all these functions weighted with different amplitudes can represent other functions [38] like vibrations under fluid loading. Thus, it seems that SmEdA is also valid for modelling of heavy fluids using uncoupled modes, because as shown in chapter 1.1.4.1 the total energies are calculated by summing up the energies of the functions “uncoupled modes”. But it has to be clarified in the future for SmEdA calculations if the assumption, that the coupling has no influence to the power input, is still valid for the equations of the power input (see chapter 2.1.2) in the case of a heavy fluid. Otherwise, a new formulation for the power input has to be found.

2.2. Transmission Loss and non resonant modes

In chapter 11 it is demonstrated that the transmission loss predicted with SmEdA is equal to that of the formula of Cremer (see Figure 2.1), if the same assumptions are made, i.e. an infinite plate and a free field (infinite cavity). The transmission loss illustrated in Figure 2.1 is herein averaged over all possible angles of incidence (diffuse field). In this case of the infinite plate the transmission is fully described via non resonant modes of the infinite plate below the critical frequency and via resonant modes above the critical frequency. Thus, this comparison demonstrates that the extended version of SmEdA can in principle respect non resonant modes in a correct way and that the whole SmEdA approach is valid for the case of the infinite plate.

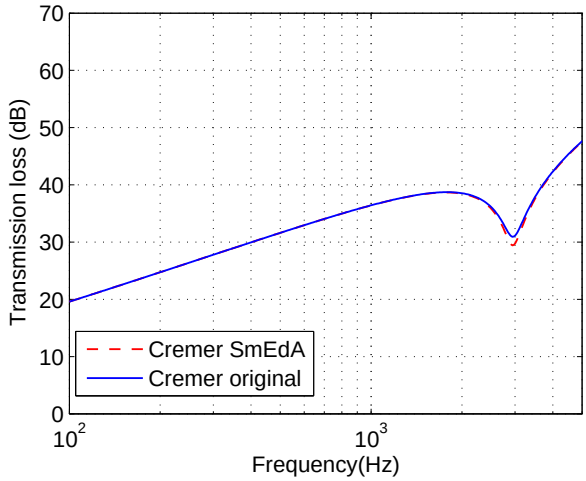

Figure 2.1.: Transmission loss of an infinite steel plate calculated with SmEdA ("Cremer SmEdA") and the formula of Cremer ("Cremer original") (plate damping $\eta_p = 0.1$)

To verify the transmission losses predicted with SmEdA for finite systems, in which the sound fields in cavities are not necessarily diffuse, the results of a small cavity-plate-cavity system are compared to those calculated with classical SEA and with FEM in chapters 6, 9 and 11. But for the SEA coupling loss factors as defined in [7] a diffuse sound field and the mass law are particularly assumed. The assumption of the diffuse sound field may lead to the huge differences in some cases in comparison to SmEdA which are shown in Figures 2.2 to 2.4, because there are for example only 11, 55 and 125 modes in the receiving room in the first three excited frequency bands. The results of FEM and of SmEdA are quite different, too (see Figure 2.5). One problem here could be that the used FEM formulation (see chapter 1.1.2) is in general only valid for structure-cavity systems but not for cavity-structure-cavity system as discussed in chapters 9 and 11. Because of this reason that no method without limitation was found for the investigated case and the problem with the definition of the transmission loss in connection with non diffuse sound fields (see chapter 1.2), the transmission losses predicted with SmEdA are here only qualitatively compared to some measurements and calculations for finite plates from the literature. In this way, the effects which appear for the transmission loss can be analysed and compared.

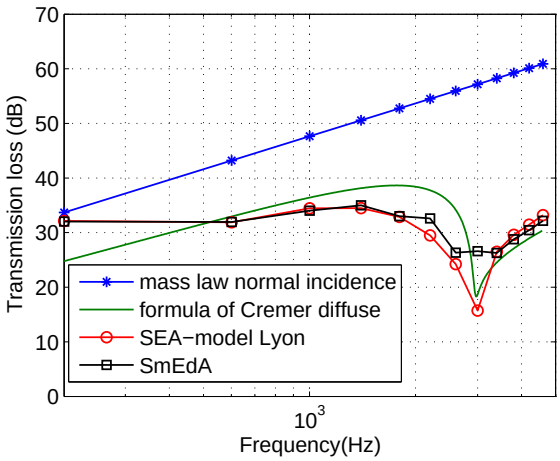

Figure 2.2.: Transmission loss calculated with different methods (plate damping $\eta_p = 0.001$)

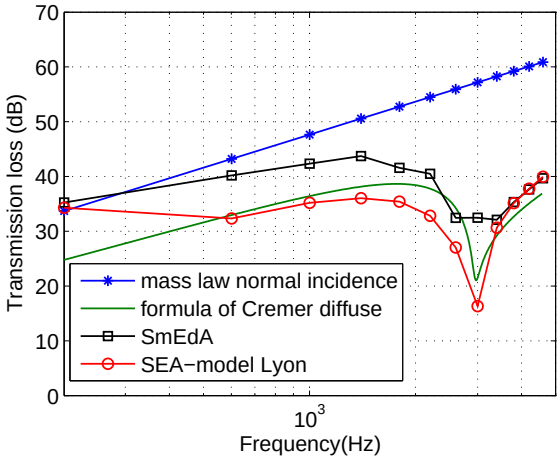

Figure 2.3.: Transmission loss calculated with different methods (plate damping $\eta_p = 0.01$)

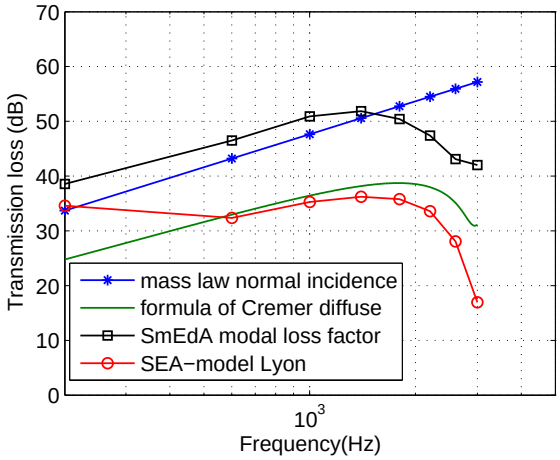

Figure 2.4.: Transmission loss calculated with different methods (plate damping $\eta_p = 0.1$)

One effect demonstrated by SmEdA is that it depends on the the boundary condition of a plate if the transmission is dominated below the critical frequency by the resonant modes or the

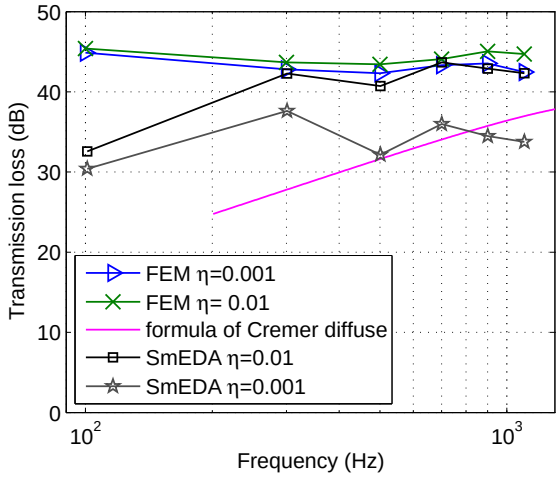

Figure 2.5.: Comparison of the transmission loss for different plate damping factors η calculated with SmEdA and FEM (frequency band width: 200 Hz)

non resonant modes. So, only the resonant modes are necessary in general for the calculation of the transmission loss of a simply supported plate (see Figures 2.6 to 2.8). Only for special cases, like a high damping, also non resonant modes have to be taken into account. In contrast, the transmission in the case of free plate is given only through the non resonant modes below the critical frequency (see Figure 2.9), because the result for the transmission loss is infinite if only resonant modes are used (see chapter 6). Here, it has to be noted that the modes of the free plate are not exact but only roughly estimated as

$$W_{mn}^{s} = \cos\left(\frac{m\pi x}{L_x}\right)\cos\left(\frac{n\pi y}{L_y}\right) \tag{2.12}$$

where m and n are positives integers and L_x and L_y are the dimension of the plate in the directions of x and y. The eigenfrequencies are predicted using the formulae of Warburton [65] in the form of Dickinson [66]. The eigensystems are thus only approximately defined but convenient to show the effect of a free boundary condition.

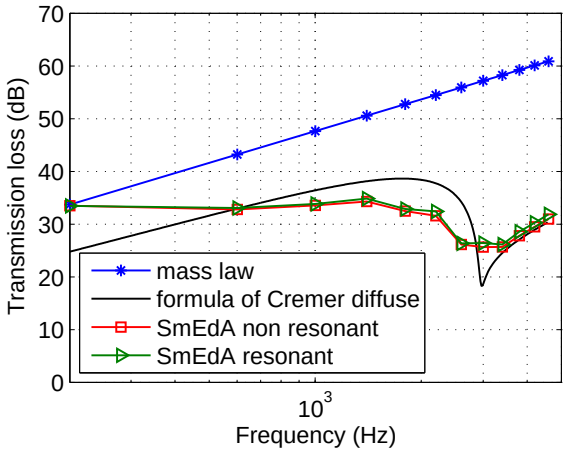

Figure 2.6.: Transmission loss of a simply supported steel plate (plate damping $\eta_p = 0.001$; frequency band width: 400 Hz)

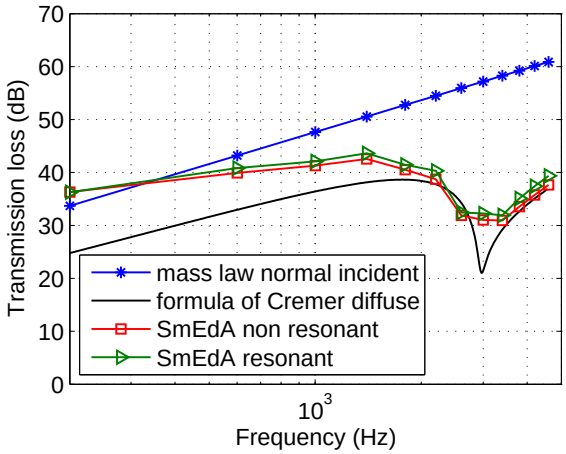

Figure 2.7.: Transmission loss of a simply supported steel plate (plate damping $\eta_p = 0.01$)

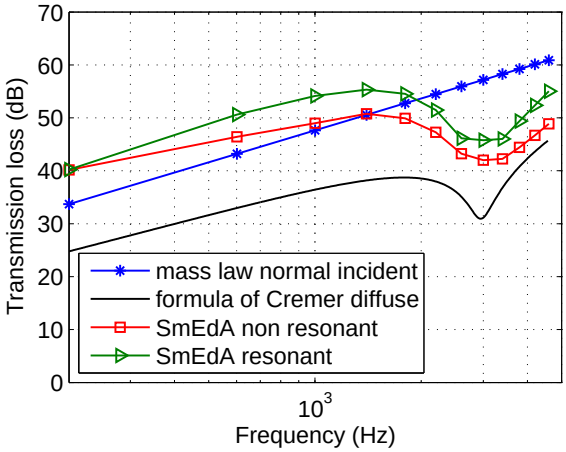

Figure 2.8.: Transmission loss of a simply supported steel plate (plate damping $\eta_p = 0.1$)

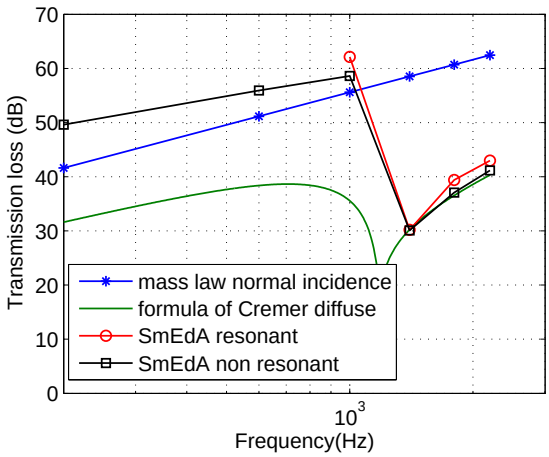

Figure 2.9.: Transmission loss of a free steel plate (plate damping $\eta_p = 0.01$)

To prove if this effect for different boundary conditions appears also in the case of a finite plate between free sound fields, results for the transmission loss, Figures 2.10 and 2.11, predicted with the method from Woodcock and Nicolas [63] are used. This calculation method is based on a variational formulation and uses a basis of polynomials. Furthermore, a free sound field is assumed there on both sides of the plate. Figure 2.10 demonstrates that the transmission through a simply supported small steel plate is dominated by resonant modes, because the transmission loss has minima always at the resonance frequencies of the plate. Contrary to that, the transmission loss of a free plate has only a few small minima at a very large angles of incidence (see Figure 2.11). Hence, the resonant modes are more or less not excited and so most of the sound is transmitted for a free boundary condition through the non resonant modes like in the calculations with SmEdA.

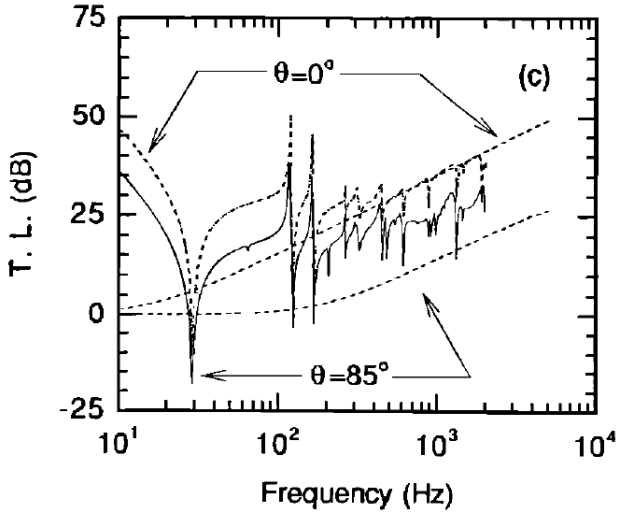

Figure 2.10.: Transmission loss of a simply supported steel plate under different angles of incidence Θ [63]

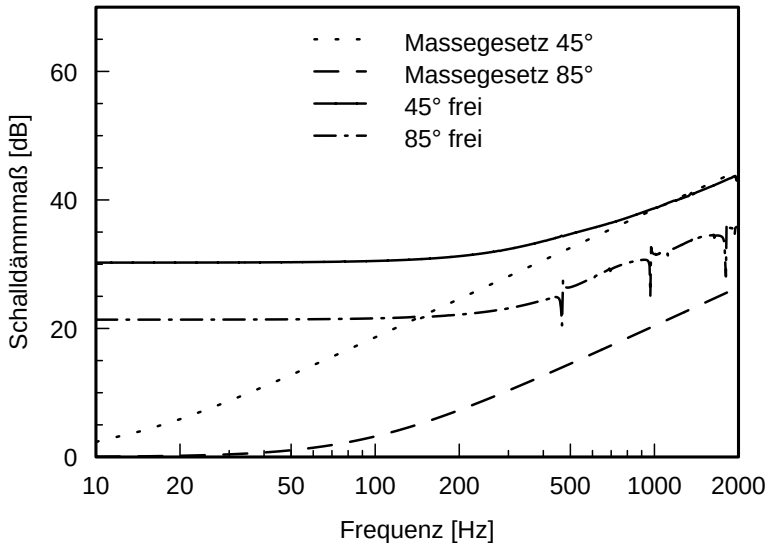

Figure 2.11.: Transmission loss (“Schalldämmmaß”) of a free plate under different angles of incidence Θ [42] (“Massegesetz”: mass law; “frei”: TL of a free plate calculated with the method of Woodcock and Nicolas)

Furthermore, it attracts attention that the minima due to the coincidence effect are not so distinctive in the transmission losses calculated with SmEdA, Figures 2.6 to 2.9, as for infinite plates. This phenomena was also noticed by Möser [49] in some measurements of the transmission loss (see Figures 2.12 and 2.13). He demonstrates that the coincidence effect is not so strong if the critical coincidence frequency is low. To explain this, it is first necessary to define what the coincidence is in the case of a finite plate. Bhattacharya, Guy and Crocker explained that the coincidence for a plate is a resonance effect between a cavity mode and a structure mode and is thus influenced by the interaction of the modes [67]. But in contrast to other resonance effects the wave length of the trace on the plate of the cavity mode is approximately equal to the wave length of the resonant plate mode. From this result it follows that it is necessary to have pairs of modes, which couple well, to get a good visible coincidence effect. But if the mode density is small, this is not necessarily the case. Thus, it can happen that the coincidence is not so visible as shown in Figure 2.14. Here, the transmission loss of a small glass plate was again calculated with the method of Woodcock and Nicolas.

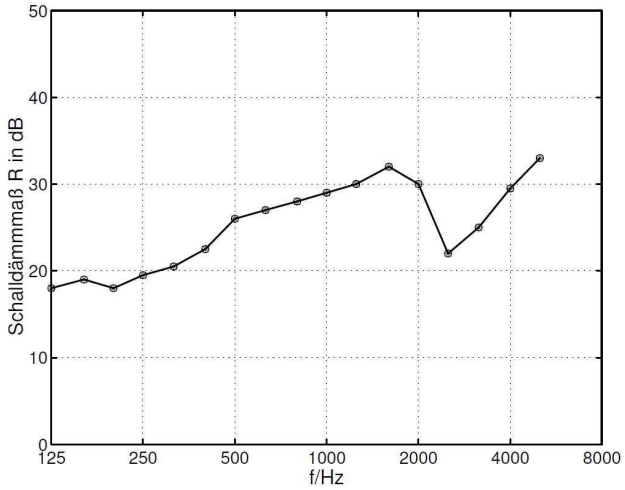

Figure 2.12.: Measured transmission loss (“Schalldämmmaß R”) of a glass plate [49] (critical coincidence frequency: 2500 Hz)

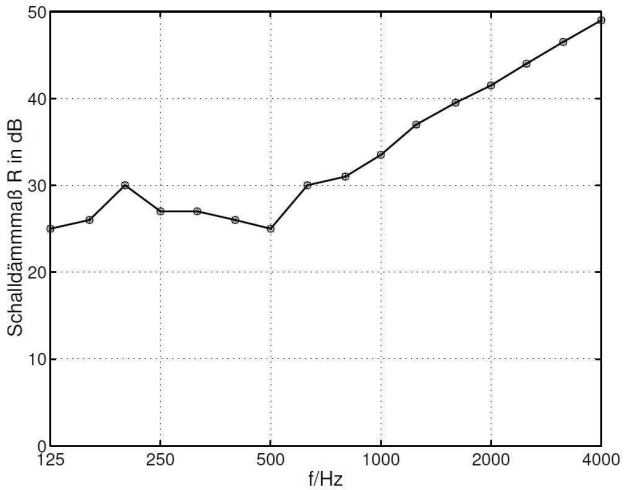

Figure 2.13.: Measured transmission loss (“Schalldämmmaß R”) of a plaster plate [49] (critical coincidence frequency: 350 Hz)

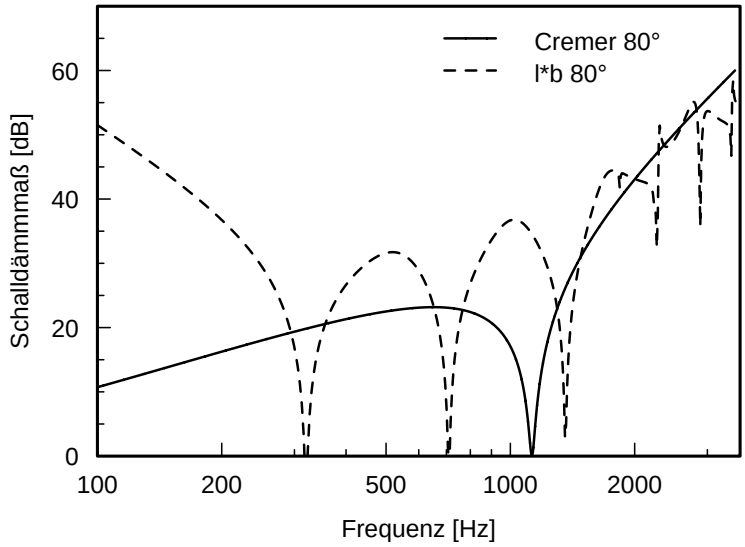

Figure 2.14.: Transmission loss of a small simply supported glass plate [42] (angle of incidence $\Theta = 80°$; "l^*b 80°": TL calculated with the method of Woodcock and Nicolas)

Finally, the transmission loss shown in Figure 2.14 converges after the the coincidence frequency against the result of the formula of Cremer. This is also the case for all here presented transmission losses predicted with SmEdA. All in all, most of the effects, which appear in the SmEdA results, can be found also in measurements and in obtained results for finite plates between free sound fields. Only the reason for the huge differences in the transmission losses for different plate damping factors, Figures 2.6 to 2.8, could not be investigated very well through a comparison with results from the literature. It is clear that there is an influence of the plate damping if resonant modes are important for the transmission like in the case of a simply supported plate. But the author of this theses could not find a clear answer in the literature how big this influence is. In [68] it is demonstrated on calculations of the transmission loss using

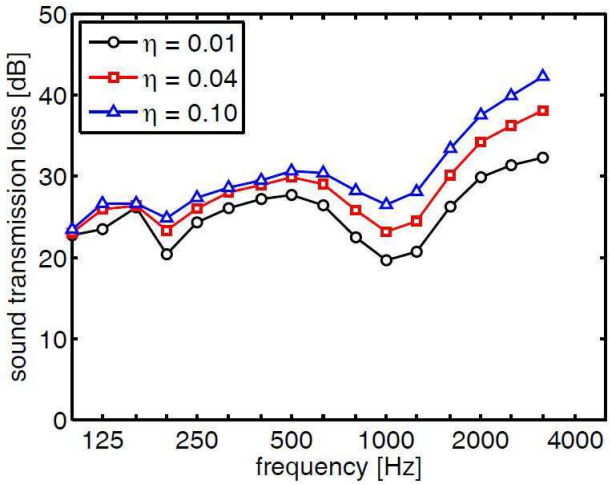

Figure 2.15.: Transmission loss of 25mm thick fiberboard panel calculated with the Wave Based Method (η: damping factor of the panel)

the wave based method (see 1.1.3.2) that as shown in figure 2.15 the influence of the damping can be similar to the one appearing in Figures 2.7 and 2.8. But this is not for all examples like that in [68]. One reason for the strong dependency on the damping could be the influence of the

small modal densities in the cavities on the transmission. Also, the problem with the definition of the transmission loss as described in chapter 1.2 could play a role here. But as demonstrated in Figures 2.10 and 2.11 it is possible to get a transmission loss which is higher than that of the formula of Cremer. The reason for that is in this case that the sound is radiated as non plane waves [63] and not as plane waves like in the formula of Cremer (see chapter 2.1.3). Moreover, it was shown for example by Bhattacharya and Guy [69] that the geometry of a room, which is one reason for different sound fields with high or low modal densities, has a significant influence on the transmission loss. They found this out by comparing transmission losses of plates, which were measured in different measurement facilities and in different geometric arrangements.

2.3. In which cases non resonant modes are necessary in general?

As shown in chapter 2.2 the boundary condition of a structure is one factor of influence if non resonant modes play a role in cavity-structure problems. So is for example the sound transmission through a simply supported plate in general dominated by resonant modes and through a free plate by non resonant modes below the critical frequency. But it is also demonstrated on these examples that the influence of non resonant modes increases with a rising damping of the plate. Thus, it depends on the damping if a calculation with resonant modes only is sufficient. Furthermore, in the case of a high structural damping it is necessary to take into account non resonant modes not only for the structure but also for the non external excited cavity. This effect is demonstrated in [40] and chapter 9 on an example of a plate-cavity system (Figures 2.16 and 2.17), which is excited by a point force on the structure. The importance of non resonant modes for the total energies of the subsystems increases here with the damping of the plate. The damping of the cavity is kept herein constant at 0.01. Figures 2.16 and 2.17 demonstrate that the results with non resonant modes agree well with those predicted by an usual FEM calculation (see chapter 1.1.2), which is used as reference.

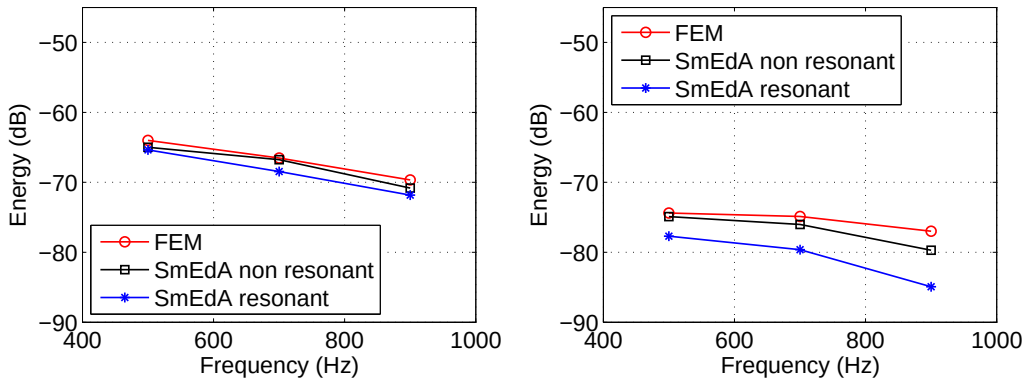

2.16.1: $\eta_p = 0.01$ 2.16.2: $\eta_p = 0.1$

Figure 2.16.: Energy ($10\lg[\text{energy}/1J]\ dB$) in the cavity at different plate damping factors η_p ("SmEdA non resonant": calculation with resonant and non resonant modes; frequency band width: 200 Hz)

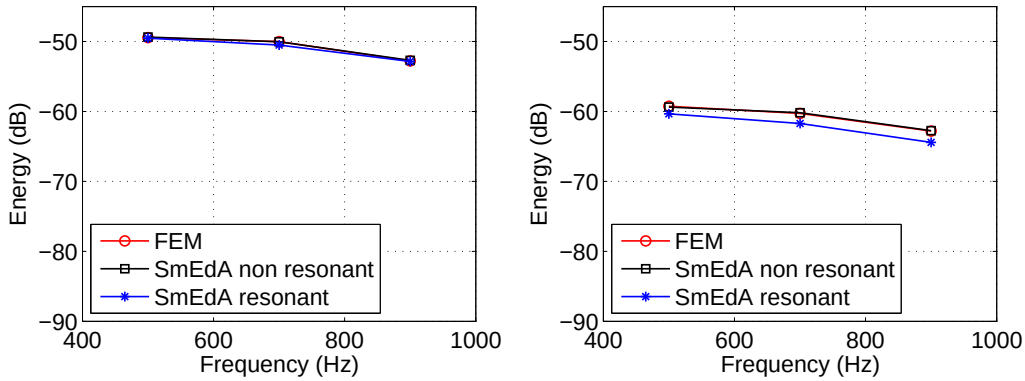

2.17.1: $\eta_p = 0.01$ 2.17.2: $\eta_p = 0.1$

Figure 2.17.: Energy ($10\lg[\text{energy}/1J]\ dB$) of the plate at different plate damping factors η_p ("SmEdA non resonant": calculation with resonant and non resonant modes; frequency band width: 200 Hz)

Moreover, it seems that the characteristics of the subsystems, like geometry and material, and the resultant particular modal interaction have an influence if non resonant modes are necessary for the calculation. That appears for example in the case of a part of a double deck train ([43] and [40]: chapters 8 and 9), which is excited at the bottom with eight point forces. Here, the damping is not very high, structural damping $\eta_s = 0.03$ and the cavity damping $\eta_c = 0.02$, and the boundary condition of the structure is simply supported. But nevertheless non resonant modes are important especially for the upper cavity as shown in Figure 2.18 on the ratios between the respective modal energies and the total energy of the respective subsystem. These modal distributions of the total energies do not look as it could be expected in the case of a high damping, because the energy is concentrated only to few modes outside the excited frequency band and is not flat like in the case of high damping.

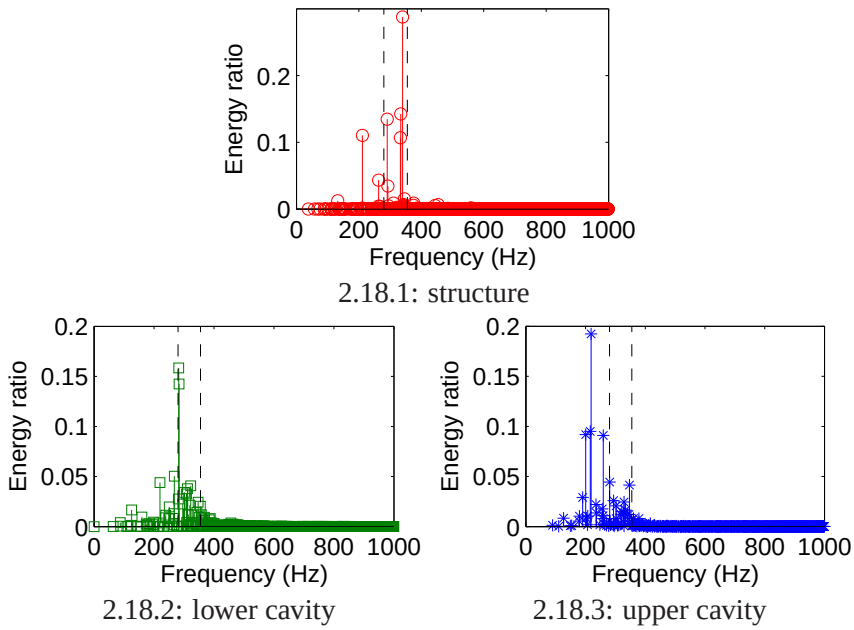

2.18.1: structure

2.18.2: lower cavity 2.18.3: upper cavity

Figure 2.18.: Energy ratios of the modes (frequency area between the dashed lines: excited frequency band between 280 and 355 Hz)

Furthermore, even if the part of the total energy, which is stored in the non resonant modes, is small like in Figure 2.16.1 for a cavity, these modal energies can have a big influence on the distribution of the energy in the cavity as demonstrated in Figure 2.19. How energy distributions are predicted using the modal outputs of SmEdA is explained in the chapter 3. All in all, because of these reasons it is difficult to say in advance if a calculation with resonant modes only is sufficient or not. Another question is how many non resonant modes have to be taken into account to reach an acceptable enough result. In the examples presented in this work this problem is solved by repeating the calculations several times with an increasing number of modes until the change of the result is smaller than an a priori specified value, for example 0.3 dB for total energies.

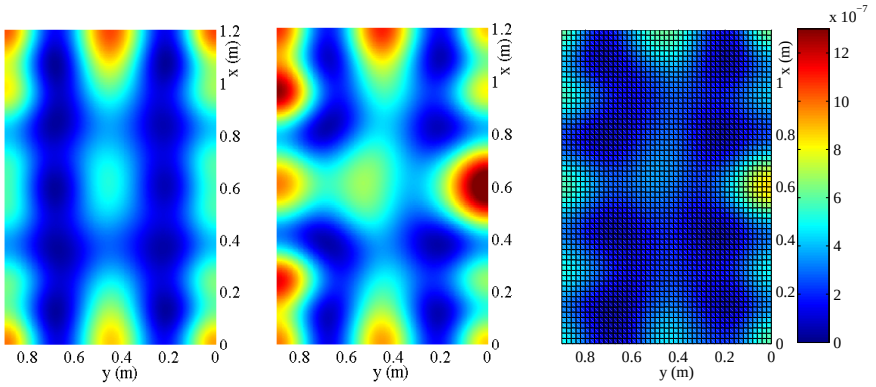

2.19.1: SmEdA resonant

2.19.2: SmEdA non resonant

2.19.3: FEM

Figure 2.19.: Energy density distribution in the cavity at $z = -0.3624$ (frequency band: 600-800 Hz; plate damping: $\eta_p = 0.01$; "SmEdA non resonant": calculation with resonant and non resonant modes)

3. Energy distributions in modal description

3.1. Postprocessing method

As explained in chapter 1.1.4.6 the existing postprocessing using modal information cannot predict in a satisfactory manner coherent energy distributions with for example concentrations around the area of excitation. Therefore, it was necessary to search for a new extended postprocessing method for energy distribution, which takes into account also the interaction between the modes of a subsystem. In [35] and chapter 7 the derivation of such a new method is described. The resultant equation is globally equal to the equation (1.34) of chapter 1.1.4.6 but modified with a term describing the correlation between the modes:

$$e^i(\Delta\omega) = \sum_m e^i_m(\Delta\omega) + 2\sum_m \sum_{n=m+1} C_{mn}\sqrt{e^i_m(\Delta\omega)e^i_n(\Delta\omega)} \tag{3.1}$$

A correlation factor C_{mn} is needed in this equation, because there is no information about the algebraic sign of the displacement of a modal response using an energy based method [35]. This information is necessary to characterise the spatial and the frequency correlation of modes. One possibility to approximate C_{mn} is given in [35] using the power input $\Pi_m(\omega)$ of the modes:

$$C_{mn} = \frac{\int_{\Delta\omega} S_{mn}\sqrt{\Pi_m(\omega)\Pi_n(\omega)}\,d\omega}{\sqrt{\int_{\Delta\omega}\Pi_m(\omega)\,d\omega\int_{\Delta\omega}\Pi_n(\omega)\,d\omega}} \tag{3.2}$$

Here, it is assumed that the subsystems can be considered as uncoupled for the postprocessing calculation of the energy distributions. Thus, the equations for the power input in uncoupled systems of chapter 2.1.2 can be used. The factor S_{mn} depends on the given excitation and can be approximated using analytic solutions from chapter 2.1.2 for the modal amplitudes of the velocities $\hat{v}$ or of the pressures $\hat{p}$ as follows [35]:

$$S_{mn} = sign(\hat{p}_m\hat{p}^*_n + \hat{p}^*_m\hat{p}_n) = sign(\hat{v}_m\hat{v}^*_n + \hat{v}^*_m\hat{v}_n) \tag{3.3}$$

where * denotes the conjugate complex of a variable. In the publications of part II this equation is misleadingly written without the terms "$+\hat{p}^*_m\hat{p}_n$" and "$+\hat{v}^*_m\hat{v}_n$" in the sign function. The other needed functions, the modal energy distributions appearing in equation (3.1), are discussed for structures and cavities in the following chapters.

3.2. Energy distributions of structures

The new postprocessing given by equation (3.1) was first used for the computation of total energy density distributions in [35] and chapter 7. The total modal energy density distributions, which are necessary for equation (3.1), are defined in this case as

$$e_n^i = \frac{E_n}{N_n}\Phi_n^2 \tag{3.4}$$

where N_n, Φ_n and E_n are the norm, the shape and the total energy of a mode n. Such energy density distributions of a simple cavity-plate system are compared in Figures 3.1 to 3.4 to those calculated with FEM, which is used as a reference. This comparison shows that the interaction between modes have to be respected using equation (3.1) (Figures "SmEdA") to get good results. Otherwise, if the equation without a correlation term, equation (1.34), is used like for the Figures entitled with "SmEdA diagonal", the differences with FEM are larger. The figures demonstrate also that the results predicted with equation (1.34) become better for small plate damping factors η_p and if a broadband excitation (Figures 3.3 and 3.4) is used instead of a single frequency excitation (Figures 3.1 and 3.2). The reason for this is that the correlation between the modes decline in these cases and so the sound field becomes more incoherent [35].

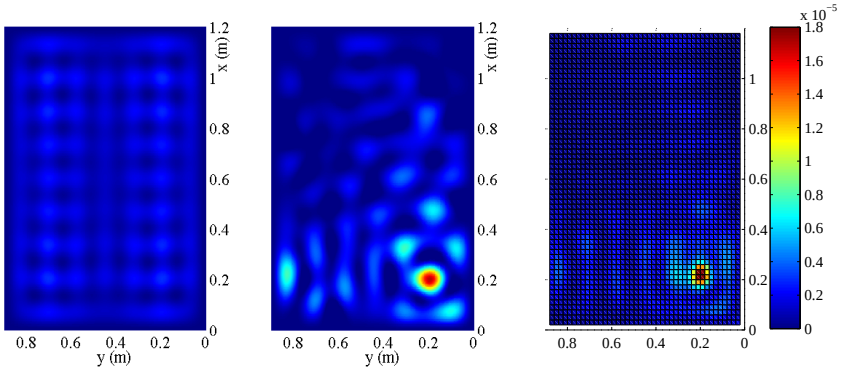

3.1.1: SmEdA diagonal 3.1.2: SmEdA 3.1.3: FEM

Figure 3.1.: Energy density distribution of a plate (excitation: 600Hz; damping $\eta_p = 0.1$)

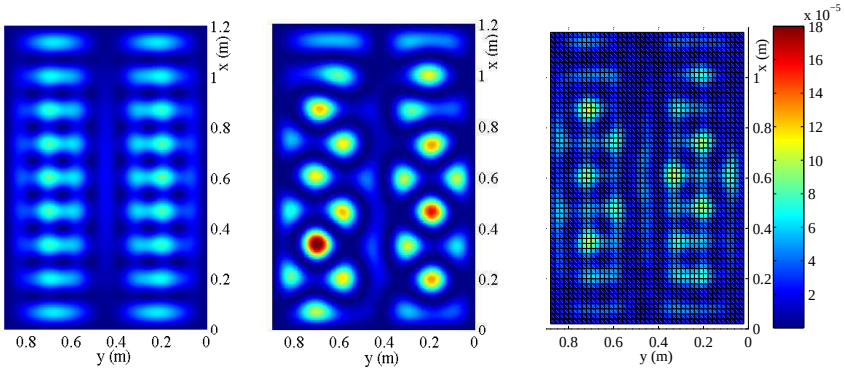

3.2.1: SmEdA diagonal 3.2.2: SmEdA 3.2.3: FEM

Figure 3.2.: Energy density distribution of a plate (excitation: 600Hz; damping $\eta_p = 0.01$)

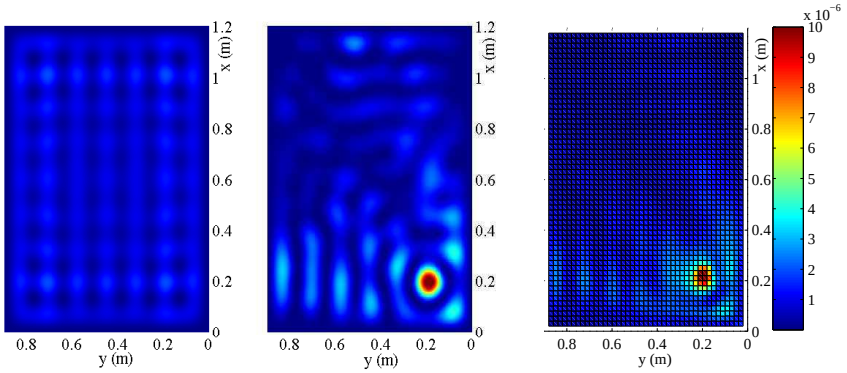

3.3.1: SmEdA diagonal 3.3.2: SmEdA 3.3.3: FEM

Figure 3.3.: Energy density distribution of a plate (excitation: 600-800 Hz; damping $\eta_p = 0.1$)

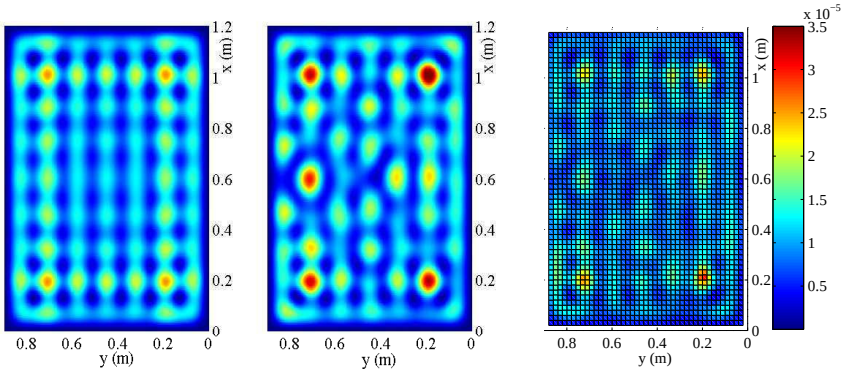

3.4.1: SmEdA diagonal 3.4.2: SmEdA 3.4.3: FEM

Figure 3.4.: Energy density distribution of a plate (excitation: 600-800 Hz; damping $\eta_p = 0.01$)

Still, the differences between the results of FEM and of SmEdA plus postprocessing are noticeable. On the one hand, SmEdA calculations are made using analytic mode shapes and can thus slightly differ from those obtained with FEM. On the other hand, it was assumed that the total energy density distributions are two times the kinetic or the potential energy density distributions. This is approximately correct for the total potential and kinetic energies under the given excitation but the differences in the density distributions of these energies can locally be large as shown for example in [70]. Because of that in [43], chapter 8, the equations (1.36) and (1.37) from Totaro and Guyader [52] for the modal kinetic and the modal potential energy distributions of structures, e_n^k and e_n^p, were used and extended for non resonant modes. The modal energy distributions then read:

$$e_n^p = E_n^p \frac{\left(\Phi_n^Q\right)^T K \Phi_n}{K_n} = \frac{E_n \left(\Phi_n^Q\right)^T K \Phi_n}{\left(1 + \frac{\omega^2}{\omega_n^2}\right) K_n} \tag{3.5}$$

$$e_n^k = E_n^k \frac{\left(\Phi_n^Q\right)^T M \Phi_n}{M_n} = \frac{E_n \left(\Phi_n^Q\right)^T M \Phi_n}{\left(1 + \frac{\omega_n^2}{\omega^2}\right) M_n} \tag{3.6}$$

where $(\Phi_n^Q)^T$ is the transpose of the shape function vector of the mode n at a point Q, Φ_n is here the complete shape function vector for all points Q, E_n^k and E_n^p are the kinetic and the potential energy of a mode n, K and M are the stiffness and the mass matrix predicted with FEM and K_n, M_n and ω_n are the modal stiffness, the modal mass and the eigenfrequency of a mode n. For a broadband excitation ω is approximately the central frequency of the excited band and the output of equations (3.5) and (3.6) is an energy for each single point and not an energy density like in equation (3.4). In [43] and chapter 8 it was found out that it is necessary that for these formulae the factor S_{mn}, equation (3.3), should be multiplied by a factor S_{mn}^d to describe the influence of the angle between two modal vectors Φ_m^Q at a point Q, because this angle is not always zero for a three dimensional structure like a double deck train. In particular, two modes are fully uncorrelated if the angle between two modal shape vectors at Q is 90°. Thus, S_{mn}^d is equal to the cosine of the angle α between two modal shape vectors at Q and S_{mn} is in this case written as

$$S_{mn} = S_{mn}^d \, sign(\hat{v}_m \hat{v}_n^*) = \frac{\Phi_m^Q \Phi_n^Q}{\left|\Phi_m^Q\right| \left|\Phi_n^Q\right|} \, sign(\hat{v}_m \hat{v}_n^*) \tag{3.7}$$

Using equation (3.6) a good result for the kinetic energy distribution of a part of a double-deck train was reached in comparison to FEM (see Figure 3.5) On the contrary, using equation (3.6)

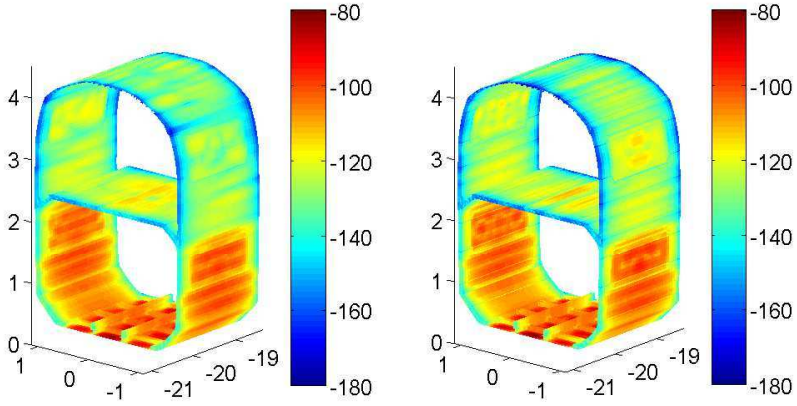

3.5.1: SmEdA (using all modes from 0 to 600 Hz)

3.5.2: FEM

Figure 3.5.: Kinetic energy distribution ($10\lg[\text{energy}/1J]\ dB$) of the train structure calculated with SmEdA and FEM (excited frequency band: 280-355 Hz)

the potential energy distribution for this example, Figure 3.6.1, is equal to the kinetic energy distribution but not to the potential energy distribution calculated with FEM, Figure 3.6.3. As explained in [40] the problem of this equation is that the potential energy can be not defined in single points but only within areas, like the elements of FEM (see chapter 9). Therefore, equation (3.6) has been rewritten for potential energy distributions of elements as follows:

$$e_n^p = E_n^p \frac{\left(\Phi_n^R\right)^T K_e \Phi_n^R}{K_n} = \frac{E_n E_{n,R}^s}{\left(1 + \dfrac{\omega_n^2}{\omega^2}\right) E_n^s} \tag{3.8}$$

where Φ_n^R is the modal vector of an element R of the mode n. Instead of calculating directly with the element stiffness matrix K_e the element modal strain energies $E_{m,R}^s$ and the total modal strain energy E_n^s, which can be calculated with some commercial FEM programs, can be used as

shown in equation (3.8). Using this equation (3.8) the results for the potential energy distribution (Figure 3.6.2) agree well with that of a FEM calculation. Furthermore, equations (3.5) and (3.8) have been applied successfully in [40] to a cavity-plate example as demonstrated on the kinetic and the potential energy distributions of the plate, Figures 3.7 to 3.10. The eigenmodes and eigenfrequencies were calculated for these results with FEM and not analytically like it was the case for the results presented in Figures 3.1 and 3.4.

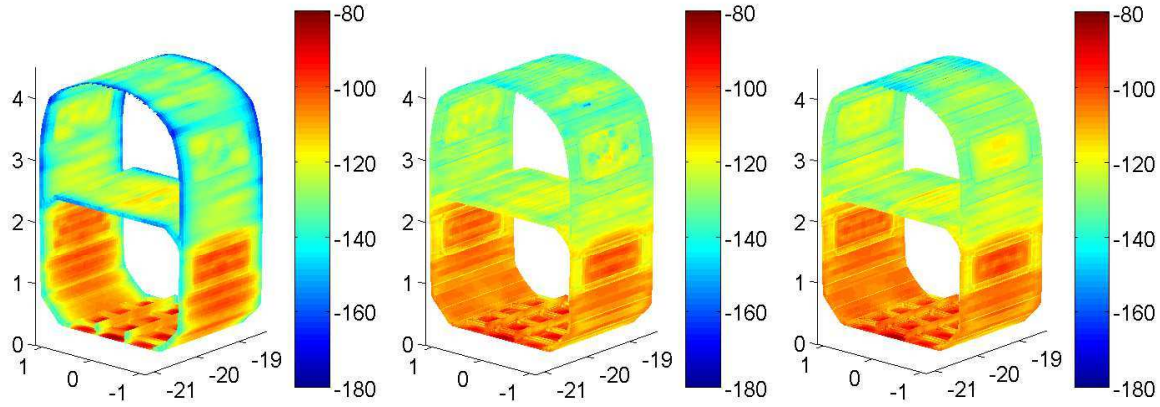

3.6.1: SmEdA using equation (3.5) 3.6.2: SmEdA using equation (3.8) 3.6.3: FEM

Figure 3.6.: Potential energy distribution ($10\lg[\text{energy}/1J]\ dB$) of the train structure calculated with SmEdA and FEM (excited frequency band: 280-355 Hz)

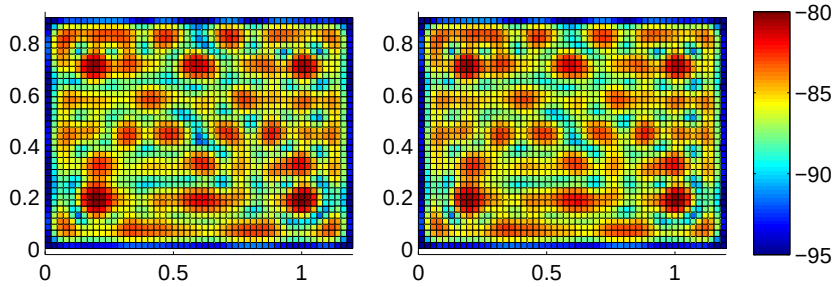

3.7.1: SmEdA 3.7.2: FEM

Figure 3.7.: Kinetic energy distribution ($10\lg[\text{energy}/1J]\ dB$) of a plate (excitation: 600-800 Hz; damping $\eta_p = 0.01$)

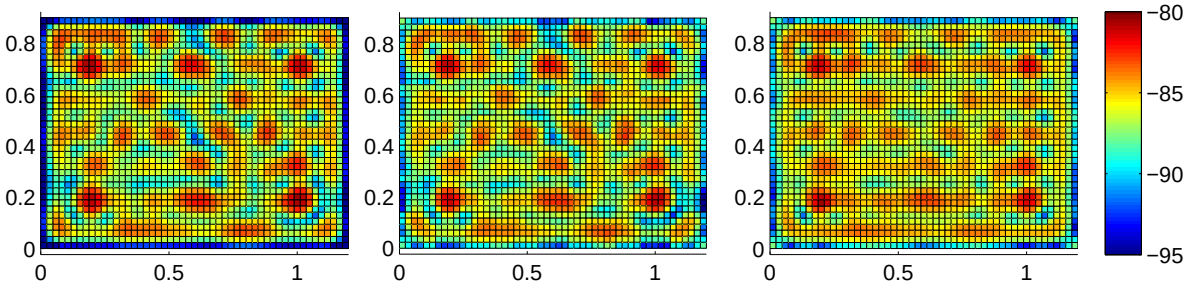

3.8.1: SmEdA using equation (3.5) 3.8.2: SmEdA using equation (3.8) 3.8.3: FEM

Figure 3.8.: Potential energy distribution ($10\lg[\text{energy}/1J]\ dB$) of a plate (excitation: 600-800 Hz; damping $\eta_p = 0.01$)

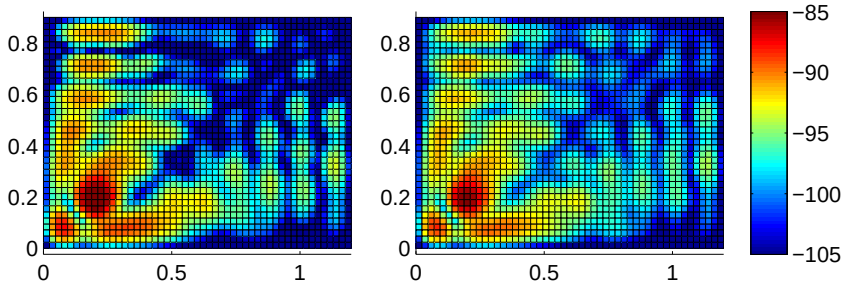

3.9.1: SmEdA 3.9.2: FEM

Figure 3.9.: Kinetic energy distribution ($10\lg[\text{energy}/1J]\ dB$) of a plate (excitation: 600-800 Hz; damping $\eta_p = 0.1$)

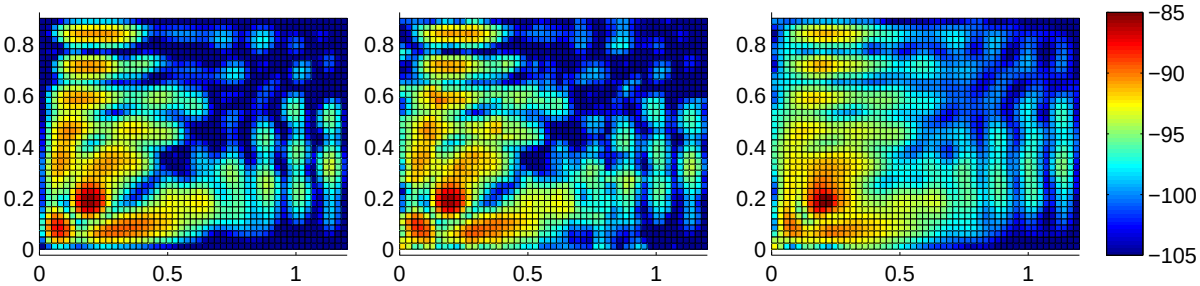

3.10.1: SmEdA using equation (3.5) 3.10.2: SmEdA using equation (3.8) 3.10.3: FEM

Figure 3.10.: Potential energy distribution ($10\lg[\text{energy}/1J]\ dB$) of a plate (excitation: 600-800 Hz; damping $\eta_p = 0.1$)

3.3. Energy distributions of cavities

For the modal energy density distributions in the cavities the following equation, which is equal to equation (3.4), has been used in all the publications, chapters 7 to 9:

$$e_n = \frac{E_n}{N_n}\Phi_n^2 \tag{3.9}$$

where N_n, Φ_n and E_n are the norm, the shape and the total energy of a mode n. The distributions of total energy densities predicted with the postprocessing method in combination with this equation have been compared to twice the potential energy density distributions calculated with FEM. This procedure is only correct for resonant modes, but it has been found that this error is negligible for the results presented in this thesis. The exact way is to predict only the potential energy density distributions e_n^p using the following equation and to compare these with the pressures respectively potential energies from FEM.

$$e_n^p = \frac{E_n^p}{N_n}\Phi_n^2 = \frac{E_n}{N_n\left(1+\frac{\omega_n^2}{\omega^2}\right)}\Phi_n^2 \tag{3.10}$$

where E_n^p and ω_n are the total potential energy and the eigenfrequency of the cavity mode n and ω is the frequency of excitation. The relation between E_n^p and E_n used here follows from the time and space averaged kinetic and potential energies, which are given in [44] by

$$E_n^p = \frac{\tilde{p}_n^2 V_f}{32\rho_f c_f^2} \tag{3.11}$$

$$E_n^k = \frac{\tilde{p}_n^2 V_f \omega_n^2}{32 \rho_f c_f^2 \omega^2} \tag{3.12}$$

where E_n^k and $\tilde{p}_n$ are the total kinetic energy and the modal pressure amplitude of a cavity mode n and V_f, ρ_f and c_f are the volume, the density and the speed of sound of the fluid. Thus, it follows for the relation between E_n^p and E_n^k that

$$\frac{E_n^k}{E_n^p} = \frac{\omega_n^2}{\omega^2} \tag{3.13}$$

Finally, the total energy of a mode n can be written with this equation as

$$E_n = E_n^k + E_n^p = E_n^p \left(1 + \frac{\omega_n^2}{\omega^2}\right) \tag{3.14}$$

Nevertheless, the energy density distribution in the mid of a cavity (Figure 3.11) is quite good in comparison to that of FEM as demonstrated in [40] and chapter 9 on the example of a point-excited plate coupled to a cavity. Furthermore, it is necessary also for the cavity to respect the correlation of the modes, because otherwise the differences to FEM are quite huge (see Figure 3.12) [35].

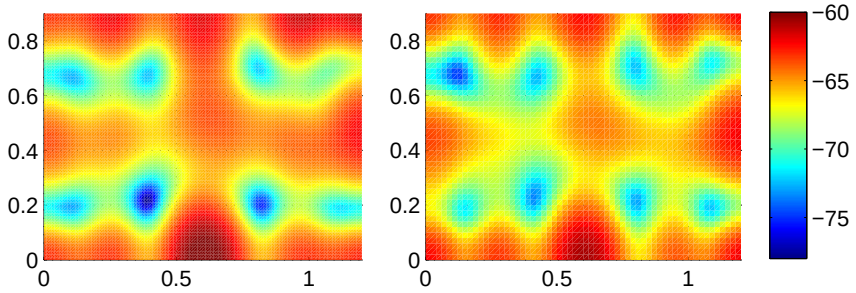

3.11.1: SmEdA 3.11.2: FEM

Figure 3.11.: Energy density distribution ($10\lg[\text{energy}/1J]\ dB$) in the cavity at $z = -0.3624$ (excitation: 600-800 Hz; damping $\eta_p = 0.01$)

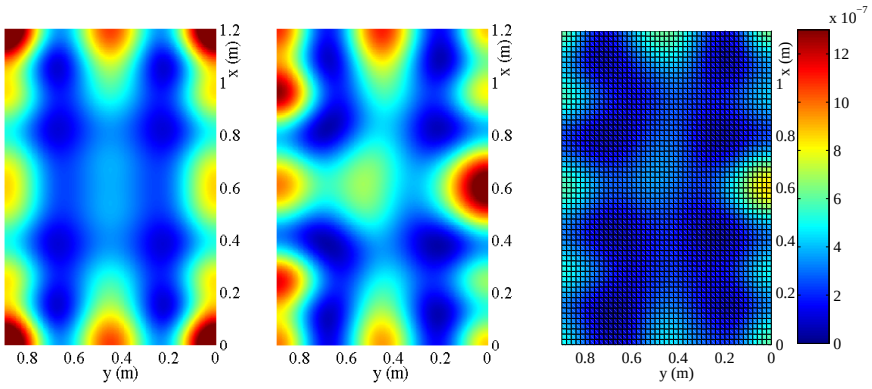

3.12.1: SmEdA diagonal 3.12.2: SmEdA 3.12.3: FEM

Figure 3.12.: Energy density distribution in the cavity at $z = -0.3624$ (excitation: 600-800 Hz; damping $\eta_p = 0.01$)

In the case of the example of the double deck train (see chapter 8) the energy density distributions in the mid of the cavities predicted with SmEdA plus the postprocessing are quite different in comparison to those calculated with FEM (see Figures 3.13 and 3.14). The reason for that is that also the total energies calculated with SmEdA and with FEM are quite different as shown in Table 3.1. The problem could be that the used FEM formulation is valid for cavity-structure systems but not for cavity-structure-cavity systems [40]. Another problem, which appears for these energy density distributions and is still unexplained, is the convergence of these energy density distributions, because they change if more modes are taken into account although these additional modes play no role for the total energies [40].

total energy [**dB**]	**SmEdA**	**FEM**	**difference** [**dB**]
structure	-56.8	-56.2	0.6
lower cavity	-67.4	-65.7	1.7
upper cavity	-81.1	-86.7	5.6

Table 3.1.: Comparison of the total energies ($10\,\mathrm{lg}[\mathrm{energy}/1J]\ dB$) of the subsystems calculated with SmEdA and FEM

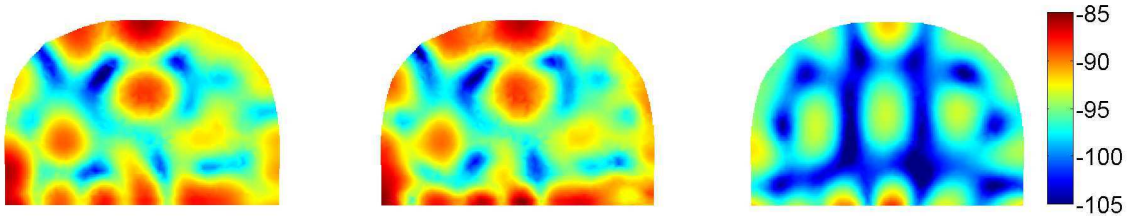

3.13.1: SmEdA (using all modes from 0 to 600 Hz)

3.13.2: SmEdA (using all modes from 0 to 1000 Hz)

3.13.3: FEM

Figure 3.13.: Energy distribution ($10\,\mathrm{lg}[\mathrm{energy}/1J]\ dB$) of the central section of the upper cavity calculated with SmEdA and FEM (excited frequency band: 280-355 Hz)

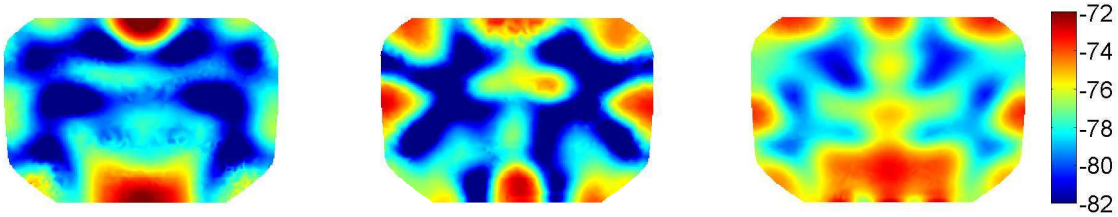

3.14.1: SmEdA (using all modes from 0 to 600 Hz)

3.14.2: SmEdA (using all modes from 0 to 1000 Hz)

3.14.3: FEM

Figure 3.14.: Energy distribution ($10\,\mathrm{lg}[\mathrm{energy}/1J]\ dB$) of the central section of the lower cavity calculated with SmEdA and FEM (excited frequency band: 280-355 Hz)

4. Methods for ill defined systems and systems with high mode densities

4.1. Hybrid SEA/SmEdA methods

One problem of SmEdA is that the computational cost is increasing with a rising number of modes, because the number of power balance equations is increasing in this case. As a solution for that the relation between SmEdA and SEA described in chapter 1.1.4.5 can be used to get SEA coupling factors. If only resonant modes are necessary to get a result with a sufficient accuracy, a normal SEA can be executed then with them. The advantage of this procedure is, that the computational cost can be reduced dramatically in this way compared to SmEdA, because the linear system of equations consists of only one equation per subsystem.

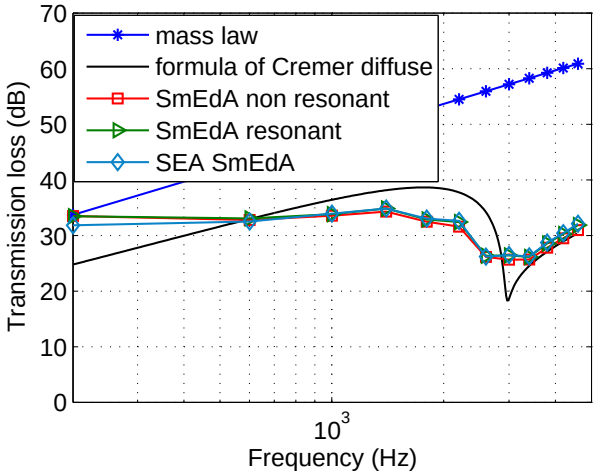

Figure 4.1.: Transmission loss for a plate damping $\eta_p = 0.001$ (frequency band width: 400 Hz; “SmEdA non resonant”: resonant and non resonant modes are used for the calculation)

Such a SEA method using these couplings factors predicted with SmEdA has been successfully tested on two different examples in [34] and [35] (see chapters 6 and 7). In [34] the transmission loss calculated with SEA is compared to that calculated with SmEdA. The plate damping factor is here 0.001 and the damping factors of both cavities are 0.01. The results of the two methods agree well with each other (see Figure 4.1). There is only a small difference between them at very low frequencies because of the very small mode density. The second example shown in [35] is the result for the energies of two cavities (cavity damping factor $\eta_c = 0.01$) which are excited by a point force excited plate (plate damping factor $\eta_p = 0.01$) in between of them. As demonstrated in Figure 4.2 the energies predicted with SEA are quite similar to those calculated with FEM.

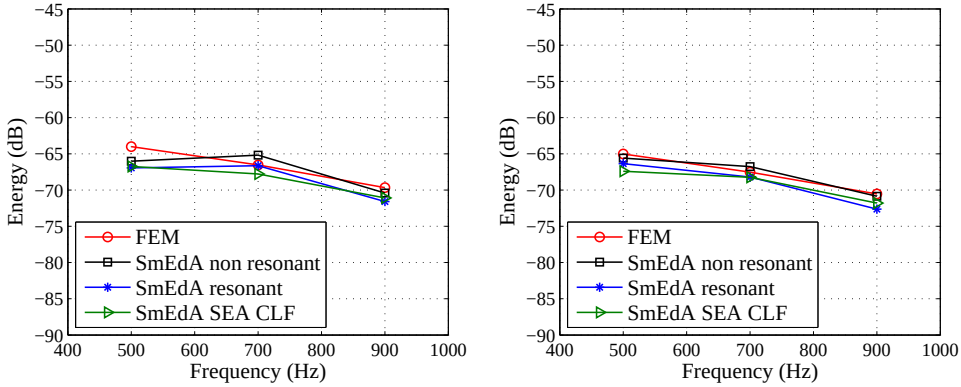

4.2.1: Energy in cavity 1 4.2.2: Energy in cavity 2

Figure 4.2.: Energies ($10\lg[\text{energy}/1J]\ dB$) in two cavities calculated with different methods (frequency band width: 200 Hz)

To reduce the computational cost at least also for problems, in which non resonant modes are additionally needed, the hybrid SEA/SmEdA technique explained in chapter 1.1.4.5 can be applied. Here, some subsystems are considered as SEA subsystems and some as SmEdA subsystems. This method was used in [71] for a cavity-structure-cavity example (see chapter 10). First, only the sending cavity was described by a SEA-like equation (line "SEA/SmEdA 1 cavity" in Figure 4.3). In this case the transmission loss of the chosen system predicted with a hybrid SEA/SmEdA method agrees well with that calculated with a full SmEdA method. In a second step a SEA-like equation was also used for the receiving cavity (line "SEA/SmEdA 2 cavities"). But here the differences between the results of SmEdA and of the hybrid SEA/SmEdA method are quite large as shown in Figure 4.3. The reason is that non resonant modes have to be taken into account also for the receiving cavity to calculate the transmission loss in the case of a plate damping $\eta_p = 0.1$ (see chapter 6). This is however not possible for a SEA-like equation as mentioned before.

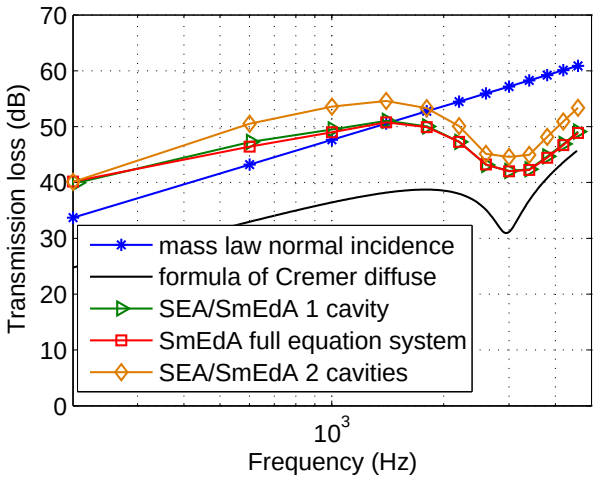

Figure 4.3.: Transmission loss calculated with mixed power balance equation systems (plate damping $\eta_p = 0.1$; frequency band width: 400 Hz)

4.2. Approximation of eigensystems

Amongst the problem mentioned in the previous chapter that the computational cost is increasing with a rising number of modes, the calculation of such a huge number of modes, which have to be known in advance for SmEdA, can be quite time consuming if FEM is used. This is especially a problem in the cases of big cavities or of high frequencies. Also, the exact geometry, which has to be known for such calculations, is sometimes unknown. Hence, it has been started to develop a method with which the mode shapes of a cavity on the coupling surface and the cavity eigenfrequencies can be approximated. The eigenfrequencies ω_m are given in [71] and chapter 10 approximately by

$$\omega_m = \sqrt[3]{\frac{6\pi^2 c_f^3 m}{V_f}} \tag{4.1}$$

where m is a positive integer and c_f and V_f are the speed of sound and the volume of the fluid in the cavity. To get also an approximation of the mode shapes on a coupling surface, it is assumed that the pressure distributions of modes on a surface are equal to these of incident waves. Every eigenfrequency is attributed to such a wave. The minimal trace wavelength λ_{min}^m on a surface of each of these waves is reached for an incidence parallel to this surface (angle of incidence $\vartheta = 90°$). Thus, this minimal wave length is given by

$$\lambda_{min}^m = \frac{2\pi c}{\omega_m \sin 90°} = \frac{2\pi c}{\omega_m} \tag{4.2}$$

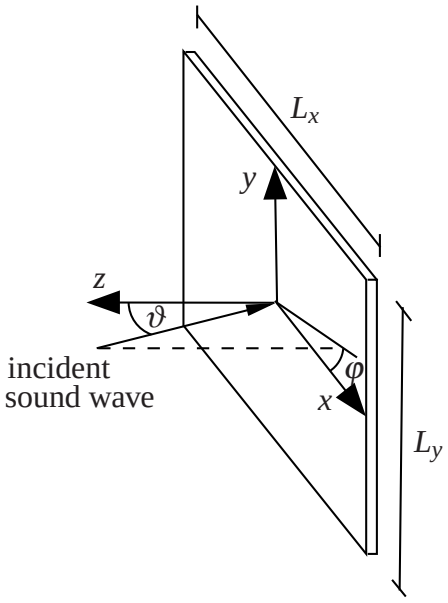

Figure 4.4.: Sound incident on a boundary surface

Additionally to the angle of incidence ϑ, the direction of incidence with an angle φ (see Figure 4.4) and the phase shift δ have to be defined to get a full description of an incident wave. In this way, the mode shapes Φ_m^s on the surface of for example a plane structure can be approximated as

$$\Phi_m^s = \cos\left(\frac{2\pi x}{\lambda_{m,x}^s} + \delta\right)\cos\left(\frac{2\pi y}{\lambda_{m,y}^s} + \delta\right) = \cos\left(k_f x \sin\vartheta\cos\varphi + \delta\right)\cos\left(k_f y \sin\vartheta\sin\varphi + \delta\right) \tag{4.3}$$

where k_f is the wavenumber of the fluid and $\lambda^s_{m,x}$ and $\lambda^s_{m,x}$ are the approximate wavelengths in the directions of x and y. The parameters φ, δ and ϑ are assumed to be uniformly distributed random numbers between zero and 2π respectively $\pi/2$ for ϑ like it would be the case in a semi-infinite cavity, in which the number of modes between two frequencies is infinite. These mode shapes and eigenfrequencies predicted in this way are used in SmEdA to calculate first the modal coupling factors, equation (1.9), and then the modal energies. All in all, this procedure can be understood also as a combination between a modal and wave approach in the sense of the prediction of SEA coupling factors (see chapter 1.1.1), because on the one hand waves in a semi-infinite space are considered, but on the other hand their coupling is described with the modal coupling factor. This approximation method was used in [71] for the calculation of the transmission loss of a small cavity-plate-cavity system. Here, as shown in table 4.1 the numbers of modes in the excited frequency bands are quite small and the difference between the exact and the approximate number of modes is large especially at lower frequencies.

frequency band	**number of modes**			
	sending cavity		receiving cavity	
	exact	approximate	exact	approximate
10 - 410 Hz	11	5	15	7
410 - 810 Hz	55	37	74	54
810 - 1210 Hz	125	100	180	142
1210 - 1610 Hz	237	194	321	277
1610 - 2010 Hz	373	318	517	454
2010 - 2410 Hz	517	473	740	677
2410 - 2810 Hz	741	660	1038	942
2810 - 3210 Hz	951	877	1340	1254
3210 - 3610 Hz	1213	1126	1724	1607
3610 - 4010 Hz	1514	1405	2133	2007
4010 - 4410 Hz	1810	1715	2589	2450
4410 - 4810 Hz	2183	2056	3079	2937

Table 4.1.: Exact and approximate number of modes in the different frequency bands

In spite of the differences mentioned above, the results for the transmission losses are good even for small systems. This is demonstrated in the Figures 4.5 and 4.6, where the approximate results are compared to those predicted with exact mode shapes and eigenfrequencies (line " SmEdA exact" in Figures 4.5 and 4.6). Two different phase shifts δ are tested, because the approximation of a uniformly random distributed δ is very incorrect in a small system. Another problem discussed in [71] is also the uniformly distribution of the angles φ and ϑ, which describe the direction of wave incidence, because in small systems some directions of incidence are dominant. Thus, it would be necessary to find convenient distributions for small systems. Furthermore, it is difficult to calculate the power input from an external source, because the modes are defined in this way only on the coupling area. One possible solution for this problem is to assume that the total power input can be equally split to all the resonant modes only, as it is done in SEA.

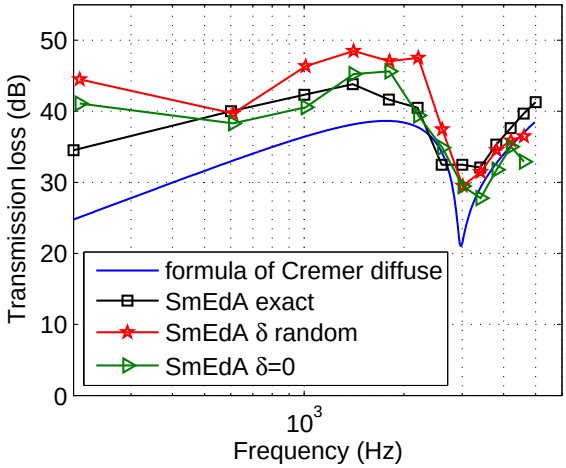

Figure 4.5.: Transmission loss for a plate damping factor $\eta_p = 0.01$ predicted with approximate modes

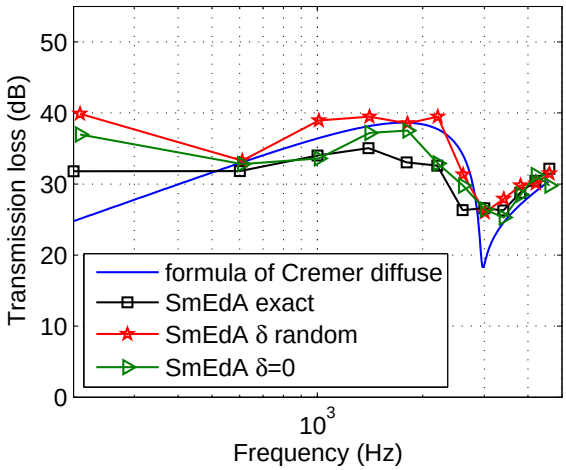

Figure 4.6.: Transmission loss for a plate damping factor $\eta_p = 0.001$ predicted with approximate modes

5. Conclusion and Perspective

One important research result presented in chapter 2 of this dissertation is the extension of SmEdA for structure-cavity problems so that non resonant modes can be taken into account. This extension allows SmEdA to be applied to a wider range of problems like narrow band excitations and highly damped systems. Also, SmEdA may be applied in the future to problems with heavy fluids as mentioned in chapters 2.1.3. In the context of the non resonant modes the transmission loss of finite systems has been also discussed. All the effects characterising the transmission loss in measurements and in calculations were found also in the transmission loss calculated with SmEdA. As the computation of the transmission loss in between closed cavities has been not well investigated, a more precise comparison between SmEdA and other methods was not possible. The important question which arose for all applications in connection with non resonant modes is: when is it necessary to take into account non resonant modes and how many of them. It has been found that many parameters influence the effect of non resonant modes, but no clear rule could be found. Thus, this could be investigated in more detail in the future research.
Another main topic, the energy distributions within subsystems, has been presented in the next chapter. With a new developed post-precessing it is now possible to predict energy distributions using the modal information and the modal energies of SmEdA even for very coherent sound fields, where the energy is concentrated in one region of a subsystem. Here, the convergence of the method, which is linked to the influence of non resonant modes mentioned before, should be investigated in the future. The main original idea of this new post-processing is the definition of a correlation factor, which describes the energy interaction between modes. This point could be further developed, because there may exist alternative ways to define this factor that are more convenient for some cases. One future application of this post-processing method is to predict transfer functions for local receiving points under given excitations. These functions can be used for example for the virtual noise synthesis.
Finally, a method to approximate eigensystems of cavities was developed. Such a method is important for ill defined systems and to reduce the computational cost of SmEdA as explained in chapter 4.2. As demonstrated on a transmission loss example the results using this methods are already relatively good even for small systems. But in the future it could be interesting to extend the method with statistical distributions, which can improve these results and which can provide good approximations even for low frequencies. Moreover, such methods could be used in the future to represent in SmEdA uncertainties that have an influence on the eigensystems. For the reduction of the computational cost also the existing relationship between SEA and SmEdA can be successfully applied as shown on a example of a cavity-structure-cavity case in chapter 4.1.
All in all, SmEdA has reached through the research discussed in this thesis a good level of theoretical development for coupled vibro-acoustic problems but of course SmEdA has still a big potential for development. One of the next step should be therefore the development of good SmEdA computer code, because except for the calculation of the eigensystems only simple and non efficient programs has been written and used for the theoretical further development of SmEdA . Because of that it was not possible and also not the aim to compare SmEdA extensively

to other methods. Thus, SmEdA results should be compared in the future to those predicted with other mid-frequency methods as well as to measurements to assess the ultimate scope of this approach.
Nevertheless, it can be said in general that SmEdA is an interesting alternative to the well established numerical methods SEA and FEM, because it combines advantages of the two. On the one hand, total energies of subsystems for whole frequency bands can be predicted by SmEdA quite easily and fast like in SEA. On the other hand, it is also possible to create energy distributions like with FEM. Another advantage of SmEdA is also that only a part of the complete computation has to be repeated by changing parameters like the excitation or the damping.

Bibliography

[1] G. Pavic, Noise sources and virtual noise synthesis, in: Proceedings of Inter-noise 2008, Shanghai.

[2] A. Moorhouse, Virtual acoustic prototypes: listening to machines that don't exist, in: Proceedings of Acoustics 2005, Busselton.

[3] B. Troclet, B. Hiverniau, M. Ichchou, L. Jezequel, K. Kayvantash, T. Bekkour, J. Mouillet, A. Gallet, FEM/SEA hybrid method for predicting mid and high frequency structure-borne transmission, Open Acoustic Journal 2 (2009) 45–60.

[4] R. Ohayon, C. Soize, Structural Acoustics and Vibration: Mechanical Models, Variational Formulations and Discretization, Academic Press, 1998.

[5] A. J. Keane, W. G. Price (Eds.), Statistical Energy Analysis: An overview with applications in structural dynamics, Cambridge University Press, 1994.

[6] L. Maxit, J.-L. Guyader, Estimation of the SEA coupling loss factors using a dual formulation and FEM modal information, part I: theory, Journal of Sound and Vibration 239(5) (2001) 907–930.

[7] R. H. Lyon, R. G. DeJong, Theory and application of statistical energy analysis, Butterworth-Heinemann, 2nd edn., 1995.

[8] T. Scharton, R. Lyon, Power Flow and Energy Sharing in Random Vibration, Journal of the Acoustical Society of America 43 (6) (1968) 1332–1343.

[9] E. Ungar, Statistical energy analysis of vibrating systems, Tech. Rep. AFFDL-TR-66-52, US Air Force, 1966.

[10] J. Woodhouse, An approach to the theoretical background of statistical energy analysis applied to structural vibration, Journal of the Acoustical Society of America 69 (6) (1981) 1695–1709.

[11] R. S. Langley, A general derivation of the statistical energy analysis equations for coupled dynamic systems, Journal of Sound and Vibration 135 (3) (1989) 499–608.

[12] F. J. Fahy, W. G. Price (Eds.), IUTAM Symposium on Statistical Energy Analysis, Kluwer Academic Publishers, 1999.

[13] R. Craik, I. Bosmans, C. Cabos, K. Heron, E. Sarradj, J. Steel, G. Vermeir, Structural transmission at line junctions: a benchmarking exercise, Journal of Sound and Vibration 272 (2004) 1086–1096.

[14] K. Renji, P. S. Nair, S. Narayanan, Non-resonant response using statistical energy analysis, Journal of Sound and Vibration 241(2) (2001) 253–270.

[15] K. De Langhe, P. Sas, Statistical analysis of the power injection method, Journal of the Acoustical Society of America 100 (1) (1996) 294–303.

[16] L. Gagliardini, L. Houillon, G. Borello, L. Petrinelli, Virtual SEA - FEM-based modeling of mid-frequency structure-borne noise, Sound and Vibration 39 (2005) 22–28.

[17] A. Le Bot, V. Cotoni, Validity diagrams of statistical energy analysis, Journal of Sound and Vibration 329 (2010) 221–235.

[18] R. Langley, V. Cotoni, Response variance prediction in the statistical energy analysis of built-up systems, Journal of the Acoustical Society of America 115 (2) (2004) 706–718.

[19] M. Chargin, O. Gartmeier, A finite element procedure for calculating fluid-structure interaction using MSC/Nastran, Tech. Rep. NASA Technical Memorandum 102857, NASA (National Aeronautics and Space Adminstration), 1990.

[20] F. Fahy, P. Gardonio, Sound and structural vibration : radiation, transmission and response, Elsevier Academic Press, 2nd edn., 2007.

[21] R. S. Langley, P. G. Bremner, A hybrid method for the vibration analysis of complex structural-acoustic systems, Journal of the Acoustical Society of America 105 (3) (1999) 1657–1671.

[22] P. J. Shorter, R. S. Langley, Vibro-acoustic analysis of complex systems, Journal of Sound and Vibration 288 (2005) 669–699.

[23] V. Cotoni, P. Shorter, Numerical and experimental validation of a hybrid finite element-statistical energy analysis method, Journal of the Acoustical Society of America 122 (1) (2007) 259–270.

[24] W. Desmet, A wave based prediction technique for coupled vibro-acoustic analysis, Ph.D. thesis, K.U. Leuven, 1998.

[25] P. Ladeveze, H. Riou, Calculation of medium-frequency vibrations over a wide frequency range, Computer Methods in Applied Mechanics and Engineering 194 (2005) 3167–3191.

[26] P. Rouch, P. Ladeveze, The variational theory of complex rays: a predictive tool for medium-frequency vibrations, Computer methods in applied mechanics and engineering 192 (2003) 3301–3315.

[27] R. Kovalevsky, P. Ladevèze, H. Riou, On some enhancement of the VTCR for mid-frequency acoustics and vibrations, in: Proceedings of ISMA 2010, Leuven.

[28] W. Desmet, O. Atak, B. Bergen, E. Deckers, S. Jonckheere, J. Lee, A. Maressa, B. Pluymers, B. Van Genechten, K. Vergote, Assessment report on WBM, Tech. Rep., ITN Mid-Frequency, project website http://www.mid-frequency.org, 2011.

[29] K. Vergote, B. Van Genechten, D. Vandepitte, W. Desmet, On the analysis of vibro-acoustic systems in the mid-frequency range using a hybrid deterministic-statistical approach, Computers and Structures 89 (2011) 868–877.

[30] O. Giannini, A. Carcaterra, A. Sestieri, High frequency vibration analysis by the complex envelope vectorization, Journal of the Acoustical Society of America 121 (6) (2007) 3472–2483.

[31] A. Carcaterra, A. Sestieri, Complex envelope displacement analysis: a quasi-static approach to vibrations, Journal of Sound and Vibration 201 (2) (1997) 205–233.

[32] L. Maxit, Extension et reformulation du modèle SEA par la prise en compte de la répartition des énergies modales, Ph.D. thesis, INSA Lyon, 2000.

[33] R. Lyon, G. Maidanik, Power Flow between Linearly Coupled Oscillators, Journal of the Acoustical Society of America 34 (5) (1962) 623–639.

[34] R. Stelzer, N. Totaro, G. Pavic, J. Guyader, Prediction of Transmission Loss using an improved SEA Method, in: Proceedings of CFA 2010, Lyon.

[35] R. Stelzer, N. Totaro, G. Pavic, J. Guyader, L. Maxit, Non resonant contribution and energy distributions using Statistical modal Energy distribution Analysis (SmEdA), in: Proceedings of ISMA 2010, Leuven.

[36] N. Totaro, J.-L. Guyader, extension of SmEdA method to estimate energy repartition into SEA subsystems, in: Proceedings of ISMA 2008, Leuven.

[37] N. Totaro, C. Dodard, J.-L. Guyader, SEA coupling loss factors of complex vibro-acoustic systems, Journal of Vibration and Acoustics 131 (2009) 041009–4.

[38] L. Cremer, M. Heckl, B. Petersson, Structure-Borne Sound, Springer, 3rd edn., 2005.

[39] F. Mechel (Ed.), Formulas of Acoustics, Springer-Verlag, Berlin, Heidelberg 2002.

[40] R. Stelzer, N. Totaro, G. Pavic, J.-L. Guyader, Assessment report on SmEdA, Tech. Rep., ITN Mid-Frequency, project website http://www.mid-frequency.org, 2011.

[41] Dodard, Simulation des Transferts Energétiques en Vibro-Acoustique et Recherche des Energies Locales par Méthode SmEdA, Master's thesis, INSA Lyon, 2006.

[42] R. Stelzer, Calculation of the sound transmission loss of anisotropic thin plates with dissipative boundary conditions, Master's thesis, University of Stuttgart / Fraunhofer-Institut of building physics, 2009.

[43] R. Stelzer, N. Totaro, G. Pavic, J. Guyader, Improved modal energy analysis for industrial problems, in: Proceedings of ICSV 18, 2011 (Rio de Janeiro).

[44] F. Fahy, Foundations of Engineering Acoustics, Elsevier Academic Press, 2005.

[45] T. H. Fronk, K. C. Womack, K. D. Ellis, L. W. Finlinson, Finite element modelling of damping in constrained layer composite structures induced by inplane loads using ADINA, Computers and Structures 56 (1995) 357–363.

[46] H. Koruk, K. Y. Sanliturk, Assesment of the complex eigenvalue and the modal strain energy methods for damping predictions, in: Proceedings of ICSV 18, 2011 (Rio de Janeiro).

[47] P. Fischer, M. Engelbrechtsmüller, Local damping effects in acoustic analysis of large FE engine structures, in: Proceedings of ISMA 25, 2000 (Leuven).

[48] A. Hufenbach, D. Blanchet, M. Gude, M. Dannemann, F. Kolbe, Integrated vibro-acoustic calculation procedure of composite structures using coupled finite and boundary element method, in: Proceedings of ISMA 2010, Leuven.

[49] M. Möser, Technische Akustik, Springer, 7th edn., 2007.

[50] L. Maxit, J.-L. Guyader, Extension of SEA model to subsystems with non-uniform modal energy distribution, Journal of Sound and Vibration 265 (2003) 337–358.

[51] N. Totaro, J.-L. Guyader, Structure/ cavity coupling using Statistical Energy Analysis: Coupling Loss Factors and energy maps into subsystems, in: Proceeedings of Acoustics 08, Paris.

[52] N. Totaro, L. Maxit, J.-L. Guyader, Post-traitement et analyse énergétiques de résultats eléments finis, in: Proceedings of CFA 2010, Lyon.

[53] M. Heckl, The tenth Sir Richard Farey memorial lecture: Sound transmission in buildings, Journal of Sound and Vibration 77(2) (1981) 165–189.

[54] A. C. Nilsson, Reduction Index and boundary conditions for a wall between two rectangular rooms, part I: theoretical results, Acustica 26 (1972) 1–18.

[55] A. Dijckmans, G. Vermeir, Application of the wave based prediction technique to building acoustical problems, in: Proceedings of ISMA 2010, Leuven.

[56] T. Bravo, S. J. Elliott, Variability of low frequency sound transmission measurements, Journal of the Acoustical Society of America 115 (6) (2004) 2986–2997.

[57] J. Rayleigh, The theory of sound, vol. 2, Dover Publications, 1945.

[58] R. Berger, Über die Schalldurchlässigkeit, Ph.D. thesis, Königlich Technische Hochschule zu München, 1911.

[59] L. Maxit, N. Totaro, J.-L. Guyader, Investigation of the damping effect on the energy response of a structure-cavity system in the case of a heavy fluid, in: Proceeedings of 20th International Congress on Acoustics, 2010 (Sydney).

[60] R. Haberkern, On how to Obtain Diffuse Field Sound Transmission Loss from Cremers Thin Plate Transmission Coefficient Formula, acta acustica 87 (2001) 542–551.

[61] A. Berry, J.-L. Guyader, J. Nicolas, A general formulation for the sound radiation from rectangular baffled plates with arbitrary boundary conditions, Journal of the Acoustical Society of America 88(6) (1990) 2792 – 2802.

[62] A. Berry, A new formulation for the vibrations and sound radiation of fluid-loaded plates with elastic boundary conditions, Journal of the Acoustical Society of America 96(2) (1994) 889 –901.

[63] R. Woodcock, J. Nicolas, A generalized model for predicting the sound transmission properties of generally orthotropic plates with arbitrary boundary conditions, Journal of the Acoustical Society of America 97(2) (1995) 1099–1112.

[64] M. J. Crocker (Ed.), Handbook of Noise and Vibration control, Wiley, 2007.

[65] G. B. Warburton, The vibration of rectangular plates, Proc. Inst. Mech. Eng. Scr. A 168 (1954) 371–384.

[66] S. M. Dickinson, The buckling and frequency of flexural vibration of rectengular isotropic and orthotropic plates using Rayleigh´s method, Journal of Sound and Vibration 61(1) (1978) 1–8.

[67] M. C. Bhattacharya, R. W. Guy, M. J. Crocker, Coincidence effect with sound waves in a finite plate, Journal of Sound and Vibration 18 (2) (1971) 157–169.

[68] A. Dijckmans, Wave based calculation methods for sound-structre interaction: Applications to sound insulation and sound radiation of composite walls and floors, Ph.D. thesis, KU Leuven, 2011.

[69] M. C. Bhattacharya, R. W. Guy, The influence of the maesuring facility on the measured sound insulating property of a panel, Acustica 26 (1972) 344–348.

[70] G. Pavic, The role of damping on energy and power in vibrating systems, Journal of Sound and Vibration 281 (2005) 45–71.

[71] R. Stelzer, N. Totaro, G. Pavic, J.-L. Guyader, Application of SmEdA to systems with high mode densities, in: Proceedings of NOVEM 2012, Sorrento.

Part II.

Publications

6. Paper I: Prediction of Transmission Loss using an improved SEA Method

Contents

Published in the Proceedings of "10ème Congrès Français d'Acoustique" (CFA 2010), Lyon, France, April 12-16, 2010

Prediction of Transmission Loss using an improved SEA Method

Rainer Stelzer[1], Nicolas Totaro[1], Goran Pavic[1], Jean-Louis Guyader[1]
[1] *INSA Lyon Laboratoire Vibrations et Acoustique, 25 Bis Avenue Jean Capelle Bâtiment St. Exupéry, 69621 Villeurbanne Cedex*
rainer.stelzer@insa-lyon.fr

Abstract
Statistical energy analysis (SEA) is a well-known method, which can be also used for prediction of transmission loss. The difficulty in this method is to estimate the coupling loss factors, which are needed to calculate the energy transfer between the subsystems. It has been shown in previous articles on examples for structure-to-structure and structure-to-cavity coupling, that the statistical modal energy distribution analysis (SmEdA) is a convenient method for calculating this coupling loss factors. This approach relies on a dual modal formulation to describe vibrations of coupled subsystems. However, the original SmEdA formulation takes into account only the resonant modes related to a frequency band. That is the reason for developing an improved approach on the basis of SmEdA in the framework of the Marie Curie project "MID-FREQUENCY". This improved method integrates the non resonant modes in the calculation. The application possibilities and the advantages of the new extended version of SmEdA are demonstrated on the example of transmission loss of a plate between two finite cavities. The principal advantages are that transmission loss can be predicted for non-diffuse sound fields and for different boundary conditions.

1. Introduction

The well-know transmission loss R is used to characterize the physical process of the transmission of acoustic power through a partition. It is defined with the transmission factor τ as follows [1]:

$$R = 10\lg\left(\frac{1}{\tau}\right). \tag{1}$$

The transmission factor τ itself is the ratio of the power P_t transmitted through the partition and the incident power P_i.

$$\tau = \frac{P_t}{P_i} \tag{2}$$

The search for equations for τ depending on the parameters of the incident waves and the partition is a quite old field of research. The first one was the still very popular and often used so called "mass law"

$$R = 10\lg\left[1+\left(\frac{\omega m\cos\vartheta}{2\rho c}\right)^2\right] \tag{3}$$

It describes the relation between the mass per area m, the angular frequency ω, the density ρ and the speed of sound c of the fluid, the angle of incidence ϑ and the transmission loss R. The basic acoustic equations for this law were formulated by Rayleigh and it was experimentally verified amongst others by Berger. The further development of this physical law was the formula of Cremer for thin infinite plates. He included the influence of the bending stiffness B on the transmission loss using the plate equation of Kirchhoff.

$$R_C = 10\lg\left[1+\left(\omega m - B\omega^3\frac{\sin^4\vartheta}{c^4}\right)^2\left(\frac{\cos\vartheta}{2\rho c}\right)^2\right] \tag{4}$$

In the following years till this day many other transmission loss models have been developed. For that purpose it exists more or less four different ways to handle the transmission problem. The first one is the wave approach, which was also used for the mass law and the formula of Cremer. Here it is tried to find exact analytical solutions of the wave equations and so to predict the transmission loss. Such approaches has been established for example for finite plates by Heckl [1] or for finite plate and finite cavities by Nilsson [2] and by Josse and Lamure [3]. But because of the involved assumptions and simplifications these are only useful for special cases and provide only rough estimates. The second way is to solve the transmission problem with a numerical method. This is in principle possible for all cases, even for complex geometries. Sakuma and Oshima [4], for example, developed a computational procedure for a finite plate with arbitrary elastic boundary conditions between two semi-infinite rooms with FEM. The third procedure is to use a variational approach. This is in principle a very general formulation of the transmission problem, but only applicable to simple geometries, like a rectangular plate. The variational approach was used for example by Gaglardini, Roland and Guyader [5] (finite systems) and by Woodcock [6] (finite plate) to develop transmission loss models. The fourth way is to calculate the transmission loss with the statistical energy analysis (SEA), like Lyon and DeJong [7] or Renji, Nair and Narayanan [8] have done it. SEA is a quite easy and fast method, because only a linear power balance equation system (one equation for each subsystem) must be solved. But the problem of this model is the description of the cavity-plate-cavity coupling. In addition SEA is generally only dedicated for high frequencies and diffuse sound fields. A description of it is given in the following chapter. All in all there are still a lot of problems to calculate the transmission loss of more or less realistic cases. At the moment

no calculation method exists, that can be used without restrictions for different geometries of cavities and plates, for different boundary conditions and for non diffuse sound fields. The calculation method for the transmission loss with the statistical modal energy distribution analysis (SmEdA), presented in this paper, can in principle handle these restrictions. SmEdA, which was developed by Maxit and Guyader [9], is a mixture of the other already described approaches. The basic equation system is the same as the one of SEA and it needs a functional basis, namely the eigenmodes of the subsystems, which can be calculated by one of the other methods. The latter represents a critical point of this prediction procedure, because the mode density increases with rising frequency and with rising size of the subsystems and so does the computation time.

2. Theory

2.1. Classical Statistical Energy Analysis

The statistical energy analysis is a well-known energy based method. The development of it started in the early 1960s with the works about coupled oscillators by Lyon and Smith [7]. The fundamental equation of this method is the power balance for each subsystem (for example an oscillator). This means, that all the power Π^i, which is input to a subsystem i, must be dissipated (Π^i_{dis}) in this subsystem or must be transmitted into another connected subsystem (Π^i_{ex}).

$$\Pi^i = \Pi^i_{dis} + \Pi^i_{ex} \tag{5}$$

Lyon has found out that this power exchange Π^i_{ex} between two coupled subsystems is proportional to the difference of their total time-averaged energies. Also the total energy is linked via the subsystem damping loss factor η_i to the dissipation power Π^i_{dis}. So it can be written

$$\Pi^i = \omega_c \eta_i E_i + \omega_c \eta_{ij}(E_i - E_j) \tag{6}$$

where ω_c is the central angular frequency of the frequency band and η_{ij} is the coupling loss factor. Moreover, the coupling loss factors of two coupled subsystems are interrelated through the reciprocity relation

$$n_i \eta_{ij} = n_j \eta_{ji} \tag{7}$$

with the modal densities n_i and n_j of subsystems i and j. All in all the energies of the subsystems are calculated with a linear equation system at a given power input. So SEA is principally an easy calculation method, but one problem is the estimation of the coupling loss factors. Also it produces only global results for the average energy of each subsystem without any further detailed informations, like the distribution of these energies. One way to predict the coupling loss factors for the transmission loss calculation of a finite plate between two finite cavities is described by Lyon and DeJong [7]. They divided the process of transmission into two parts, the non resonant and the resonant transmission. The first is more or less an extended version of the mass law for a diffuse sound field and is characterized by the coupling loss factor η_{12} for the direct coupling between the two cavities.

$$\eta_{12} = \beta_c I_{12} \frac{c_1}{f k_1^2 V_1} \frac{\tau_{12,\infty}(0)}{2 - \tau_{12,\infty}(0)} \tag{8}$$

with the transmission coefficient $\tau_{12,\infty}(0)$ for normal incidence, the correction factor β_c for the case of low modal overlap, the frequency f, the correction factor I_{12} for diffuse sound field and the sound velocity c_1, the wavenumber k_1 and the volume V_1 of the cavity one. The second

part of transmission in the model of Lyon and DeJong, the resonant transmission through the resonant modes of the plate, is represented by an indirect coupling factor η_{p2}. This is related to the plate radiation efficiency σ_{rad} as follows:

$$\eta_{p2} = \frac{\rho_1 c_1}{\omega \rho_p h_p} \sigma_{rad} \tag{9}$$

where ρ_1 and c_1 are the density and the sound velocity of cavity one, ρ_p and h_p are the density and the thickness of the plate and ω is the angular frequency. Finally the basic power balance equation system of SEA reads [8]:

$$\begin{pmatrix} \Pi_1 \\ 0 \\ 0 \end{pmatrix} = A \begin{pmatrix} E_1 \\ E_p \\ E_2 \end{pmatrix} \tag{10}$$

with

$$A = \begin{pmatrix} \eta_1 + \eta_{1p} + \eta_{12} & -\eta_{p1} & -\eta_{21} \\ -\eta_{1p} & \eta_2 + \eta_{p1} + \eta_{p2} & -\eta_{2p} \\ -\eta_{12} & -\eta_{p2} & \eta_2 + \eta_{2p} + \eta_{21} \end{pmatrix}$$

At equal fluids in the both cavities η_{p2} is equal to η_{p1}. The rest of the coupling factors can be obtained from the reciprocity relation (equation (7)). The transmission factor can be then calculated with the estimated energies using the following equation, [10]:

$$\tau = \frac{p_2^2 A_2}{p_1^2 S} \tag{11}$$

where p_2 and p_1 are the effective values of the pressures in cavity one and two, A_2 is the equivalent absorption area of cavity two and S the surface of the plate. The pressure and the equivalent absorption area in a cavity i are given by [11, 8]:

$$p_i^2 = \frac{\rho_i c_i^2 E_i}{V_i} \tag{12}$$

and

$$A_i = \frac{4 \eta_i \omega_c V_i}{c_i} \tag{13}$$

where ρ_i, c_i and V_i are the density, the sound velocity and the volume of cavity i and ω_c is the central frequency of the excited frequency band. To sum up, contrary to the mass law and the formula of Cremer this formulation does not neglect the influence of the cavity parameters, size and damping, and takes into account the finite size of the plate.

2.2. Statistical modal Energy distribution Analysis

The statistical modal energy distribution analysis (SmEdA) is based on the dual formulation of two gyroscopic coupled oscillators [9]. Under the assumption of a white noise excitation the modal coupling loss factor reads:

$$\beta_{pq}^{12} = \frac{(W_{pq}^{12})^2}{M_p^1 M_q^2 (\omega_q^2)^2} \left[\frac{\eta_p^1 \omega_p^1 (\omega_q^2)^2 + \eta_q^2 \omega_q^2 (\omega_p^1)^2}{d} \right] \tag{14}$$

with

$$d = \quad (\eta_p^1\omega_p^1 + \eta_q^2\omega_q^2)(\eta_p^1\omega_p^1(\omega_q^2)^2 + \eta_q^2\omega_q^2(\omega_p^1)^2) \\ +((\omega_p^1)^2 - (\omega_q^2)^2)^2$$

where W_{pq}^{12} is the interaction modal work and where M_p^1, M_q^2, η_1, η_2, ω_1 and ω_2 are the modal masses, the damping factors and the eigenfrequencies of the p-th and q-th mode of the subsystems 1 and 2. The coupling loss factors of classical SEA can be calculated then on condition of modal equipartition of energy [12] with the following formulas:

$$\eta_{12} = \frac{1}{p_{max}\omega_c}\sum_{p=1}^{p_{max}}\sum_{q=1}^{q_{max}}\beta_{pq}^{12} \tag{15}$$

$$\eta_{21} = \frac{1}{q_{max}\omega_c}\sum_{p=1}^{p_{max}}\sum_{q=1}^{q_{max}}\beta_{pq}^{12} \tag{16}$$

where p_{max} and q_{max} are the numbers of resonant modes relative to the excited frequency band with the central frequency ω_c. It was shown by some authors, for example by Maxit and Guyader [13] for structure-structure coupling or by Totaro, Dodard and Guyader [12] for structure-cavity coupling, that the coupling factors computed by SmEdA agree well with these obtained by other approaches. Moreover, the energies of the different subsystems can be also calculated directly using β_{pq}^{12} and a power balance equation system with one equation for each mode instead of one for each subsystem like in SEA.

$$\Pi_p^1 = \eta_p^1\omega_p^1E_p^1 + \sum_{q=1}^{q_{max}}\beta_{pq}^{12}(E_p^1 - E_q^2) \tag{17}$$

A main drawback of this original SmEdA approach is that because of the assumption of white noise excitation only resonant modes in an excited frequency band are taken into account. But the influence of non resonant modes can be not neglected in some cases, for example in the case of highly damped systems. To find a solution for this problem it is necessary to have a closer lock to the original derivation of the method for the case of a cavity-plate coupling. In SmEdA the coupled system is split into a clamped cavity and free plate on the coupling surface to describe the coupling between the pressure in the cavity and the plate velocity. This is the same as the assumption ”blocked pressure” in other transmission loss models, where it is assumed that the move of the plate is negligible for the calculation of the surface pressure and the plate is then excited by the resultant force. But of course for the evaluation of the kinetic energy of the cavity and the potential energy of the plate the boundary conditions must be respected. These conditions are the equality of the velocities $\dot{y}_i^b$ and the equality of the products of the stress tensors σ_{rs}^{ib} and normal vectors n_s^i at the coupling surface.

$$\dot{y}_1^b = \dot{y}_2^b \tag{18}$$

$$\sigma_{rs}^{1b}n_s^1 = \sigma_{rs}^{2b}n_s^2 \tag{19}$$

The latter is not the case in the original SmEdA formulation. Finally the coupled system is defined with four equations, the two coupled differential equations of original SmEdA and the two boundary conditions, but there are only two variables. Such overdetermined systems have in general no exact solution and it is difficult to find an approximate solution. Through trial

and error it was found out that the mass law and the formula of Cremer, equations (3) and (4), can be derived analytically with the original coupling factor β_{pq}^{12}, equation (14), and the power balance, equation (17). So β_{pq}^{12} seems to be also the general coupling factor for any coupling of two modes, non resonant and resonant ones, because the coupling in the formula of Cremer is arbitrary and no assumption of white noise is needed. Perhaps this works, because β_{pq}^{12} can be also interpreted as the average coupling loss factor between two modes of all possible single-frequency excitations from zero to infinity. Altogether because of these reasons the non resonant modes are also taken into account in an extended SmEdA approach using β_{pq}^{12}, whereas the excitation still remains in a frequency band only. Finally the obtained energies, the geometrical data and the damping factors of the cavities need only to be inserted in equation (11) to get the transmission factor and so the transmission loss. This transmission loss depends on the same parameters as the one obtained by the SEA approach.

3. Comparison of the approaches

3.1. System under study

To compare the results for the transmission loss of the different calculation methods we consider a basic configuration of a rectangular plate between two parallelepipedic cavities as presented in Figure 1 and Table 1.

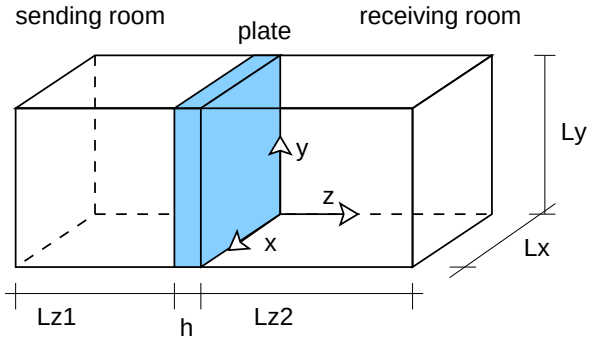

Figure 1.: Sketch of the system

	plate	**sending room**	**receiving room**
$Lx \times Ly \times Lz(h)\ (m)$	$1.2 \times 0.9 \times 0.004$	$1.2 \times 0.9 \times 0.7$	$1.2 \times 0.9 \times 1$
$\rho\ (kg/m^3)$	7820	1.2	1.2
$c\ (m/s)$		340	340
η	0.01	0.01	0.01
$E\ (MPa)$	210		
ν	0.3		

Table 1.: Characteristics of the subsystems

In the present case the eigenmodes and eigenfrequencies can be calculated quite easily analytically. The shapes p_{qrs} of the eigenmodes and the eigenfrequencies ω_{qrs} for the cavities are given by [10]

$$p_{qrs} = \cos\left(\frac{q\pi x}{L_x}\right)\cos\left(\frac{r\pi y}{L_y}\right)\cos\left(\frac{s\pi z}{L_z}\right) \tag{20}$$

and

$$\omega_{qrs} = c\sqrt{\left(\frac{q\pi}{L_x}\right)^2 + \left(\frac{r\pi}{L_y}\right)^2 + \left(\frac{s\pi}{L_z}\right)^2} \tag{21}$$

For the plate there is the possibility to choose between different boundary conditions. We take for our study the simply supported and the free boundary condition. The eigenfrequencies ω^s_{mn} and the modes W^s_{mn} of the simply supported boundary condition are

$$\omega^s_{mn} = \pi^2\left[\left(\frac{m}{L_x}\right)^2 + \left(\frac{n}{L_y}\right)^2\right]\sqrt{\frac{B}{m}} \tag{22}$$

and

$$W^s_{mn} = \sin\left(\frac{m\pi x}{L_x}\right)\sin\left(\frac{n\pi y}{L_y}\right) \tag{23}$$

with the mass per area m and the bending stiffness B of the plate.

3.2. Transmission Loss

3.2.1. Simply supported plate

At first before we compare the results from the SmEdA approach with those of other models, it is necessary to compare the different possibilities of calculations with SmEdA. So the next two Figures (2 and 3) show the results of transmission loss for different plate damping factors η_2 calculated with

- SEA with SmEdA estimated couplings factors (SmEdA SEA CLF; equations (6), (15) and (16))
- SmEdA direct only with resonant modes (SmEdA resonant; equations (14) and (17))
- SmEdA direct with resonant and non resonant modes (SmEdA non resonant; equations (14) and (17)).

For the last approach the number of modes, that are taken into account, is enlarged until the changes in the transmission loss get small, for example smaller than 1 dB. In our case at the plate damping 0.1 it is necessary to take into account all the modes of the not excited subsystems from 600 Hz below to 300 Hz above the frequency band (band width: 400 Hz). The non resonant modes of the excited systems, which are also not excited, do not matter.

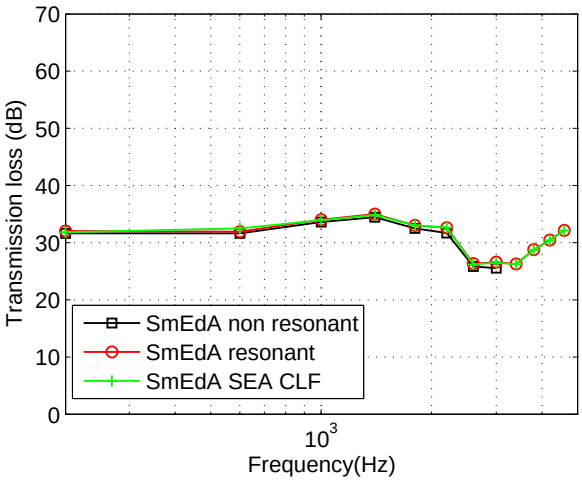

Figure 2.: Transmission loss of the different SmEdA models at $\eta_2 = 0.001$

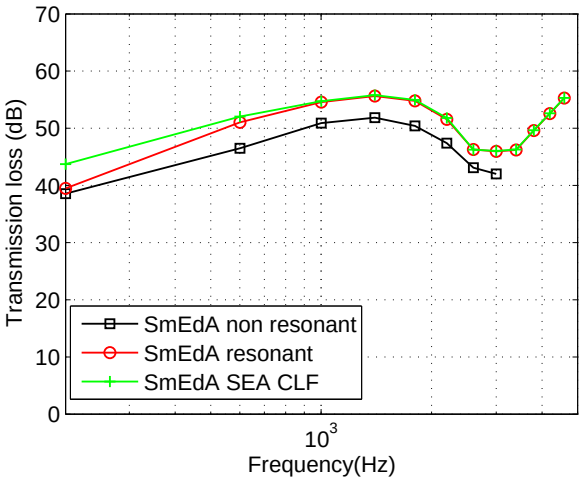

Figure 3.: Transmission loss of the different SmEdA models at $\eta_2 = 0.1$

All in all Figures 2 and 3 demonstrate that the case with the simply supported boundaries of the plate is at low damping governed by the resonant modes for the whole frequency range while the non resonant modes play a role only at quite high damping. Furthermore between the SEA calculation with SmEdA coupling factors and SmEdA direct only with resonant modes there is only a difference at low frequencies, because the assumption of modal equipartition of energy (see equation (7)) is generally not valid for low modal densities [14]. Because of these facts only the SmEdA direct calculation without non resonant modes is given in the following figures, except in the case of high damping, where the non resonant modes are needed. Figures 4 to 6 show now for three damping factors η_2 of the plate the different transmission losses predicted with the mass law for normal incidence, the formula of Cremer for a diffuse sound field, the SEA model of Lyon and DeJong and the SmEdA approach.

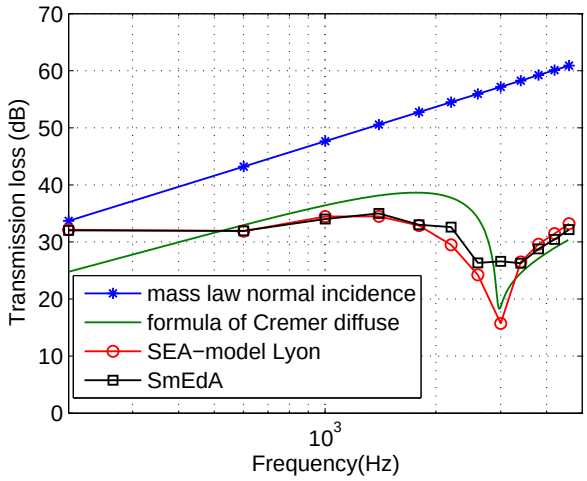

Figure 4.: Transmission loss of the different models at $\eta_2 = 0.001$

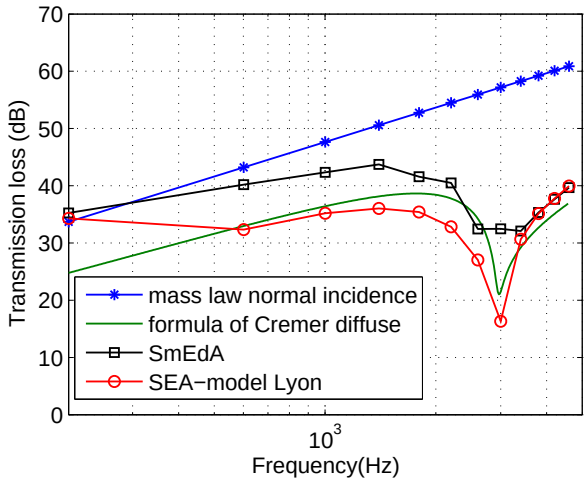

Figure 5.: Transmission loss of the different models at $\eta_2 = 0.01$

By looking at the results of the different models it attracts attention that both, the SmEdA and SEA prediction, are sensitive below the critical frequency to a change of the damping, unlike the formula of Cremer. The main reason for this is that the dissipation of energy of the vibrating plate modes rises with increasing damping, because the coupling factors change only a little. Above the critical frequency the dependency of the transmission loss on the plate damping is then equal for these three models. This difference between the formula of Cremer and the SmEdA approach does not come from different descriptions of the transmission mechanism. Under the same assumptions as for the formula of Cremer (diffuse sound field, infinite plate, etc.) the transmission loss predicted with SmEdA is analytically given by

$$R = 10 \lg \left[1 + S \left(\frac{\cos \vartheta}{2\rho c} \right)^2 \right] \tag{24}$$

with

$$S = \left(\omega m - \omega^3 B \frac{\sin^4 \vartheta}{c^4} \right)^2 + mB\eta^2 \omega^4 \frac{\sin^4 \vartheta}{c^4}$$

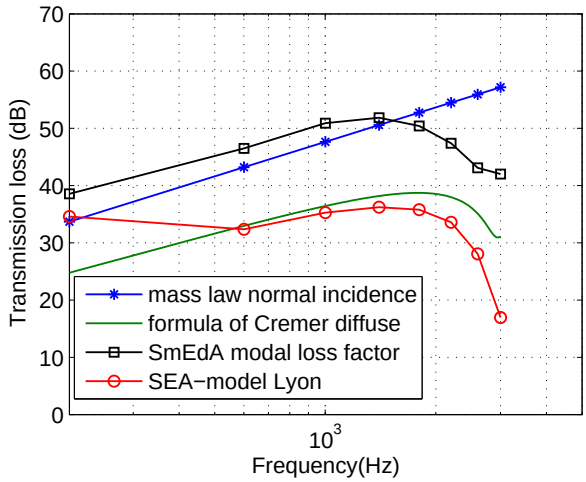

Figure 6.: Transmission loss of the different models at $\eta_2 = 0.1$

This formulation is compared to the original formula of Cremer (equation (4)) in Figure 7 for our configuration and a diffuse sound field (average over all possible incident directions). The damping in this original formula is taken into account via the usual assumption of a complex bending stiffness $\hat{B} = B(1 - i\eta_2)$.

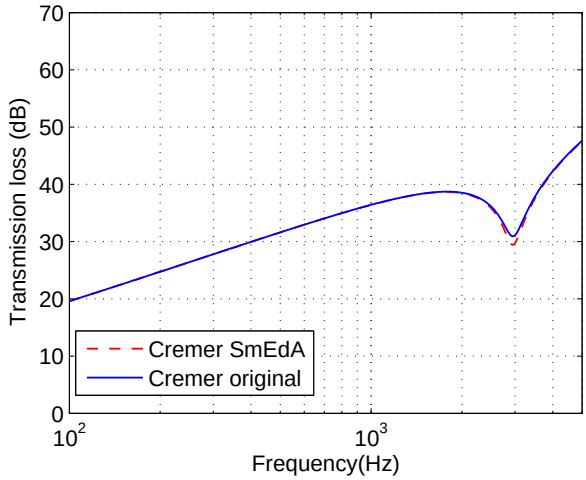

Figure 7.: Transmission loss of the infinite models from Cremer and SmEdA at $\eta_2 = 0.1$

It could be seen, there is only a small difference at the critical frequency between the two formulations. To sum up, this means that the transmission loss of a small system, where we have a small plate and no diffuse field at lower frequencies, is quite different than the one of a big or infinite one below the critical frequency but stays equal above it.

3.2.2. Free plate

As a second example for a plate boundary, the free boundary condition was chosen. In Figure 8 the calculation possibilities of SmEdA with and without non resonant modes and the formula of Cremer are compared. In this case the plate is 1 cm thick and not 4 mm as in the calculations for the simply supported plate.

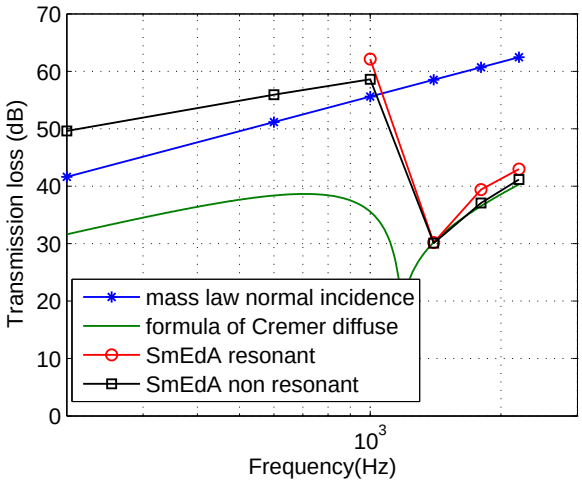

Figure 8.: Transmission loss of the different models at $\eta_2 = 0.01$

Using the original SmEdA calculation, i.e. only with resonant modes, the transmission loss becomes infinite below the critical frequency. This means that all modal works between the resonant modes are zero. Thus it is necessary to take into account below the critical frequency all the modes from zero Hz to the upper limit of the frequency band, because the energy transfer proceeds only through the non resonant modes. This shows, that the configuration with a free boundary condition has a non resonant behaviour below the critical frequency and a more or less resonant above it. In comparison to the formula of Cremer the transmission loss calculated with SmEdA is much higher. One reason for this is the small number of energy transporting combinations of plate and cavity modes. In addition to this no diffuse sound field exists in such a small system with lots of modes, which could excite the plate better.

4. Conclusion

As it is shown on the previous examples, the presented new method to estimate the transmission loss with SmEdA is an interesting alternative to the other existing prediction models, especially in the frequency range below the critical frequency and for small systems with non diffuse fields. Furthermore this method demonstrates that the transmission loss can be smaller or much higher in this frequency range than the one predicted by the infinite models. Another important advantage is the very general formulation of the transmission problem. So not only the presented cases of a simply supported and a free plate between to finite cavities can be handled but also cases with arbitrary plate boundaries and complex geometries. Also it would be, for example, possible to predict the transmission loss with SmEdA for window assemblies, where the plate is smaller than the corresponding walls of the cavities. The only limits are the estimation of the modes and the computation time growing with a rising number of modes, which are taken into account.

5. Acknowledgment

The authors gratefully acknowledge the ITN Marie Curie project GA-214909 ”MID-FREQUENCY - CAE Methodologies for Mid-Frequency Analysis in Vibration and Acoustics”.

Bibliography

[1] M. Heckl, The tenth Sir Richard Farey memorial lecture: Sound transmission in buildings, Journal of Sound and Vibration 77(2) (1981) 165–189.

[2] A. C. Nilsson, Reduction Index and boundary conditions for a wall between two rectangular rooms, part I: theoretical results, Acustica 26 (1972) 1–18.

[3] R. Josse, C. Lamure, Transmission du son par une paroi simple, Acustica 14 (1964) 266–280.

[4] T. Sakuma, T. Oshima, Numerical Analysis of Sound Transmission Loss of Glass Pane - On the Treatment of Edge Damping, in: Proceedings of Inter-noise 2008, Shanghai.

[5] L. Gagliardini, J. Roland, J.-L. Guyader, The use of a functional basis to calculate acoustic transmission between rooms, Journal of Sound and Vibration 145(3) (1991) 457–478.

[6] R. Woodcock, J. Nicolas, A generalized model for predicting the sound transmission properties of generally orthotropic plates with arbitrary boundary conditions, Journal of the Acoustical Society of America 97(2) (1995) 1099–1112.

[7] R. H. Lyon, R. G. DeJong, Theory and application of statistical energy analysis, Butterworth-Heinemann, 2nd edn., 1995.

[8] K. Renji, P. S. Nair, S. Narayanan, Non-resonant response using statistical energy analysis, Journal of Sound and Vibration 241(2) (2001) 253–270.

[9] L. Maxit, J.-L. Guyader, Estimation of the SEA coupling loss factors using a dual formulation and FEM modal information, part I: theory, Journal of Sound and Vibration 239(5) (2001) 907–930.

[10] M. Möser, Technische Akustik, Springer, 7th edn., 2007.

[11] M. Bruneau, Fundamentals of acoustics, ISTE, 2006.

[12] N. Totaro, C. Dodard, J.-L. Guyader, SEA coupling loss factors of complex vibro-acoustic systems, Journal of Vibration and Acoustics 131 (2009) 041009–4.

[13] L. Maxit, J.-L. Guyader, Estimation of the SEA coupling loss factors using a dual formuulation and FEM modal information, part II: numerical applications, Journal of Sound and Vibration 239(5) (2001) 931–948.

[14] A. Le Bot, V. Cotoni, Validity diagrams of statistical energy analysis, Journal of Sound and Vibration 329 (2010) 221–235.

7. Paper II: Non resonant contribution and energy distributions using Statistical modal Energy distribution Analysis (SmEdA)

Contents

Published in the Proceedings of International Conference on Noise and Vibration Engineering (ISMA 2010), Leuven, Belgium, September 20-22, 2010

Non resonant contribution and energy distributions using Statistical modal Energy distribution Analysis (SmEdA)

Rainer Stelzer[1], Nicolas Totaro[1], Goran Pavic[1], Jean-Louis Guyader[1], Laurent Maxit[1]
[1] *INSA Lyon Laboratoire Vibrations et Acoustique, 25 Bis Avenue Jean Capelle Bâtiment St. Exupéry, 69621 Villeurbanne Cedex*
rainer.stelzer@insa-lyon.fr

Abstract
Statistical modal energy distribution analysis (SmEdA) is a method to compute modal energies in coupled subsystems. This approach relies on the basic statistical energy analysis (SEA) relations and on a dual modal formulation to describe responses of coupled subsystems. In contrast to the classical SEA it describes not the global coupling between the subsystems but the coupling between each mode of different subsystems. This has the advantage, that it is possible to estimate in a post-processing step the energy distributions of the subsystems with the calculated modal energies. The SmEdA approach is intended to be further improved within the framework of the Marie Curie project ”MID-FREQUENCY” on two points. The first is to include the cross modal terms, which are neglected in previous works, in the calculation of energy distributions. These terms are important for coherent sound fields, for example that of a plate excited by only one point force. The second point is to take into account also non resonant modes relating to an excited frequency band, which are especially important for highly damped systems, because this is not done in the original formulation of SmEdA. The application possibilities and the advantages of the improved approach are demonstrated on the example of a point force excited plate between two finite cavities.

1. Introduction

The most well-known energy based method is the Statistical Energy Analysis. The development of it started in the early 1960s with the works about coupled oscillators by Lyon and Smith [1]. The fundamental equation of this method is the power balance for each subsystem (for example an oscillator). This means, that all the power Π^i, which is input to a subsystem i, must be dissipated (Π^i_{dis}) in this subsystem or must be transmitted into another connected subsystem (Π^i_{ex}).

$$\Pi^i = \Pi^i_{dis} + \Pi^i_{ex} \tag{1}$$

Lyon has found out that this power exchange Π^i_{ex} between two coupled subsystems is proportional to the difference of their total time-averaged energies. Also the total energy is linked via the subsystem damping loss factor η_i to the dissipation power Π^i_{dis}. So it can be written

$$\Pi^i = \omega_c \eta_i E_i + \omega_c \eta_{ij}(E_i - E_j) \tag{2}$$

where ω_c is the central angular frequency of the frequency band and η_{ij} is the coupling loss factor. Moreover, the coupling loss factors of two coupled subsystems are interrelated through the reciprocity relation

$$n_i \eta_{ij} = n_j \eta_{ji} \tag{3}$$

with the modal densities n_i and n_j of subsystems i and j. All in all the energies of the subsystems are calculated with a linear equation system at a prescribed power input. So SEA is principally an easy calculation method, but the main question is how to determine the coupling loss factors. For this purpose there are a lot of estimation methods. Some classical prediction formulas for point, line and area coupling are given for example by Lyon and DeJong [1]. Also the Power Injected Method (PIM) is often used experimentally or numerically with Finite Element software [2, 3]. Another possibility to calculate the coupling loss factors is to use the Statistical modal Energy distribution Analysis (SmEdA), which was developed at first only for this purpose by Maxit and Guyader [4]. The advantages of SmEdA in comparison to other methods at the prediction of coupling loss factors have been already demonstrated, for example on the applications for structure-structure coupling [5] and for structure-cavity coupling [3]. But SmEdA is not only a method for the prediction of SEA coupling loss factors, but also a fully independent energy method, as it was shown by Totaro and Guyader [2, 6]. The main difference between SmEdA and SEA is that SmEdA describes the coupling between all the single modes of the different subsystems and not only between the entire subsystems like in SEA. For this reason it is necessary to calculate the eigenmodes and eigenfrequencies, for example with the Finite Element Method (FEM), to get the basic input information for SmEdA. This cause the advantage in comparison to SEA that it is contrary to SEA possible to handle the case of a point force excitation and to evaluate by a post-processing the energy distributions of the subsystems. Also SmEdA can be used at lower frequencies than SEA. On the other hand, the computation cost is of course higher with SmEdA. One of the problems of both energy methods, original SmEdA and SEA, is the fact, that only resonant modes relating to a frequency band can be taken into account. Yet the influence of non resonant modes is important in some cases, for example for highly damped systems. For this reason this article presents an extended version of SmEdA with a non resonant contribution. The second topic of the article is the estimation of energy distributions in modal description with the calculated modal energies from SmEdA. Here it is shown, how to handle the cross modal terms, which have been neglected in previous works [2, 6, 7], because this terms are very important for coherent sound fields. One important example for such a sound field is the often treated technical case of a single point force excitation.

2. Statistical modal Energy distribution Analysis

The statistical modal energy distribution analysis (SmEdA) is based on the dual formulation of two gyroscopic coupled oscillators [4]. The time-averaged power flow P_{12} between these two oscillators is directly proportional to the difference of their time-averaged energies E_1 and E_2. The proportionality factor is the so called coupling factor β.

$$P_{12} = \beta(E_1 - E_2) \tag{4}$$

The velocities $\dot{y}_1$ and $\dot{y}_2$ and displacements y_1 and y_2 of the two oscillators 1 and 2, that are needed to calculate the energies and the power flow and so β, are definable through solving the following coupled differential equation system:

$$\begin{aligned} \ddot{y}_1(t) + \Delta_1\dot{y}_1(t) + \omega_1^2 y_1(t) - \sqrt{M_1^{-1}M_2}\gamma\dot{y}_2(t) &= F_1(t) \\ \ddot{y}_2(t) + \Delta_2\dot{y}_2(t) + \omega_2^2 y_2(t) + \sqrt{M_2^{-1}M_1}\gamma\dot{y}_1(t) &= F_1(t) \end{aligned} \tag{5}$$

where $\Delta_i = \omega_i\eta_i$ is the damping coefficient and γ is the gyroscopic coupling factor. Under the assumption of a white noise excitation, represented through $F_1(t)$ and $F_2(t)$ (harmonic time dependence: $e^{-i\omega t}$), β is given by

$$\beta = \frac{\gamma^2\left(\eta_1\omega_1\omega_2^2 + \eta_2\omega_2\omega_1^2\right)}{(\omega_1^2 - \omega_2^2)^2 + (\eta_1\omega_1 + \eta_2\omega_2)(\eta_1\omega_1\omega_2^2 + \eta_2\omega_2\omega_1^2)} \tag{6}$$

where η_1 and η_2 are the damping factors and ω_1 and ω_2 are the eigenfrequencies of the oscillators. A detailed derivation of this equation can be found for example in [1]. This principle was formulated more arbitrarily and extended to coupled vibrating continuous systems by Maxit and Guyader [4]. They assumed, that the coupling between each mode of different subsystems is equal to the coupling between two oscillators, if one system is uncoupled a blocked system and the other is uncoupled a free system on the coupling area. This is for example the case for a cavity-structure coupling. So the first is characterized with stress or pressure mode shapes p_p^1 and the second with displacement mode shapes W_q^2. In this way the modal coupling coefficient γ_{pq}^{12}, equivalent to the gyroscopic coupling factor γ in equation (5), is deduced.

$$\gamma_{pq}^{12} = \frac{1}{\sqrt{(\omega_p^1)^2 M_p^1 M_q^2}} \int_S p_p^1 W_q^2 \, dS = \frac{W_{pq}^{12}}{\sqrt{(\omega_p^1)^2 M_p^1 M_q^2}} \tag{7}$$

where W_{pq}^{12}, the integral over the coupling area S of the product of the mode shapes, is the interaction modal work and where M_p^1 and M_q^2 are the modal masses of the p-th and q-th mode of the subsystems 1 and 2. Finally, under the assumption of a white noise excitation the modal coupling loss factor reads:

$$\beta_{pq}^{12} = \frac{(W_{pq}^{12})^2}{M_p^1 M_q^2 (\omega_q^2)^2}\left[\frac{\eta_p^1\omega_p^1(\omega_q^2)^2 + \eta_q^2\omega_q^2(\omega_p^1)^2}{((\omega_p^1)^2 - (\omega_q^2)^2)^2 + (\eta_p^1\omega_p^1 + \eta_q^2\omega_q^2)(\eta_p^1\omega_p^1(\omega_q^2)^2 + \eta_q^2\omega_q^2(\omega_p^1)^2)}\right] \tag{8}$$

where η_1, η_2, ω_1 and ω_2 are the modal masses, the damping factors and the eigenfrequencies of the p-th and q-th mode of the subsystems 1 and 2. The coupling loss factors of classical SEA

can be calculated then on condition of modal equipartition of energy [3] with the following formulas:

$$\eta_{12} = \frac{1}{p_{max}\omega_c} \sum_{p=1}^{p_{max}} \sum_{q=1}^{q_{max}} \beta_{pq}^{12} \tag{9}$$

$$\eta_{21} = \frac{1}{q_{max}\omega_c} \sum_{p=1}^{p_{max}} \sum_{q=1}^{q_{max}} \beta_{pq}^{12} \tag{10}$$

where p_{max} and q_{max} are the numbers of resonant modes relative to the excited frequency band with the central frequency ω_c. Moreover, the energies of the different subsystems can be also calculated directly using β_{pq}^{12} and a power balance equation system with one equation for each mode instead of one for each subsystem like in SEA, equation (2).

$$\Pi_p^1 = \eta_p^1 \omega_p^1 E_p^1 + \sum_{q=1}^{q_{max}} \beta_{pq}^{12} (E_p^1 - E_q^2) \tag{11}$$

The whole energy of a subsystem is then the sum of all modal energies of this subsystem (see chapter 3). A main drawback of this original SmEdA approach is that because of the assumption of a white noise excitation only resonant modes in an excited frequency band are taken into account. But the influence of non resonant modes can not be neglected in some cases, for example in the case of highly damped systems. To find a solution for this problem it is necessary to have a closer lock to the original derivation of the method for the case of a cavity-plate coupling. In SmEdA the coupled system is split into a clamped cavity and a free plate on the coupling surface to describe the coupling between the pressure in the cavity and the plate velocity. This is the same as the assumption "blocked pressure" in some transmission loss models, where it is assumed that the move of the plate is negligible for the calculation of the surface pressure and the plate is then excited by the resultant force. But of course for the evaluation of the kinetic energy of the cavity and the potential energy of the plate the boundary conditions must be respected. These conditions are the equality of the velocities $\dot{y}_i^b$ and the equality of the products of the stress tensors σ_{rs}^{ib} and normal vectors n_s^i at the coupling surface.

$$\dot{y}_1^b = \dot{y}_2^b \tag{12}$$

$$\sigma_{rs}^{1b} n_s^1 = \sigma_{rs}^{2b} n_s^2 \tag{13}$$

The latter is not the case in the original SmEdA formulation. Finally the coupled system is defined with four equations, the two coupled differential equations of original SmEdA (equation (5)) and the two boundary conditions, but there are only two variables. Such overdetermined systems have in general no exact solution and it is difficult to find an approximate solution. Through trial and error it was found out that the mass law and the formula of Cremer

$$R_C = 10 \lg \left[1 + \left(\omega m - B\omega^3 \frac{\sin^4 \vartheta}{c^4} \right)^2 \left(\frac{\cos \vartheta}{2\rho c} \right)^2 \right] \tag{14}$$

can be derived analytically with the original coupling factor β_{pq}^{12}, equation (8), and the power balance, equation (11), [8]. So β_{pq}^{12} seems to be also the general coupling factor for any coupling of two modes, non resonant and resonant ones, because the coupling in the formula of Cremer is arbitrary and no assumption of white noise is needed. Perhaps this works, because β_{pq}^{12} can be also interpreted in the sense of the original formulation as the average coupling loss factor

between two modes of all possible single-frequency excitations from zero to infinity. Altogether because of these reasons the coupling between a non resonant and a non resonant, a resonant and a non resonant and a resonant and a resonant mode can be described now using the same formula for β_{pq}^{12}, equation (8). For example this allows to make calculations for a point force excitation at only one frequency. This means that the point force excites more or less all the modes of one subsystem at the excitation frequency and then the modes of the excited subsystem can be coupled to all modes of the other subsystem.

3. Energy and energy distributions in modal description

The SmEdA approach provides the modal information, shape and total energy, of every mode (look at the previous chapter) and so it should be in principle possible to compute the energy density distributions of every subsystem by a post-processing step. This is the topic of the present chapter.
The kinetic energy density e_n^c and the potential energy density e_n^p of every mode n are defined as follows [7]:

$$e_n^c = \frac{1}{4} M_n \dot{u}_n^2 = \frac{1}{4} M_n (\bar{\dot{u}}_n)^2 \Phi_n^2 \tag{15}$$

$$e_n^p = \frac{1}{4} K_n u_n^2 = \frac{1}{4} K_n \bar{u}_n^2 \Phi_n^2 \tag{16}$$

where u_n and $\dot{u}_n$ are the displacement and the velocity of the mode n, $\bar{\dot{u}}_n$ and $\bar{u}_n$ are the amplitudes of the displacement and the velocity, M and K are the modal mass and the modal stiffness and Φ_n is the shape of the mode n. The sum of the kinetic and the potential energy densities gives the required total modal energy density e_n^i of the subsystem i.

$$e_n^i = e_n^c + e_n^p = \frac{1}{4} M_n (\bar{\dot{u}}_n)^2 \Phi_n^2 + \frac{1}{4} K_n \bar{u}_n^2 \Phi_n^2 = R_n \Phi_n^2 \tag{17}$$

The integral over the area A of this e_n^i is on the other hand the known modal energy E_n, which can be computed for example with SmEdA.

$$E_n = \int_A e_n^i \, dA = R_n \int_A \Phi_n^2 \, dA = R_n N_n \tag{18}$$

where N_n is the norm of the mode [9]. Thus it is possible to define the at first unknown factor R_n and so the total modal energy density e_n^i finally reads:

$$e_n^i = \frac{E_n}{N_n} \Phi_n^2 \tag{19}$$

To predict the energy density e^i of a whole subsystem i from these of every mode previous works [2, 6, 7] assume that all kind of cross modal terms can be neglected and so e^i is just the sum of all total modal energy densities of this subsystem.

$$e^i = \sum_n e_n^i \tag{20}$$

But Totaro and Guyader [2] have shown that this is for example not a good assumption for a broadband point force excited plate with a high damping coupled to a cavity. The problem of such a case of excitation at one single point is that the resultant sound field is coherent [10, 11, 12].

3.1. Excitation at a single frequency

In arbitrary for all kind of sound fields the superposition principle can be used for the quadratic value of the total pressure p^2 or the total velocity v^2 of a subsystem [13] and so it can be written for example for the total quadratic pressure

$$p^2 = \left(\sum_n p_n\right)^2 = p_1^2 + p_2^2 + p_3^2 + \ldots + 2\Re(p_1 p_2^*) + 2\Re(p_1 p_3^*) + \ldots = \sum_m p_m^2 + 2\sum_m \sum_{n=m+1} \Re(p_m p_n^*) \tag{21}$$

where p_n is the complex modal pressure of the mode n and * denotes complex conjugate. In analogy to this fact the total energy density e^i of a subsystem i for a single frequency excitation can be exactly defined as follows, because the energy is proportional to the quadratic pressure:

$$e^i = \left[\sum_n \sqrt{e_n^i}\right]^2 = e_1^i + e_2^i + e_3^i + \ldots + 2\sqrt{e_1^i e_2^i} + 2\sqrt{e_1^i e_3^i} + \ldots = \underbrace{\sum_m e_m^i}_{=D} + \underbrace{2\sum_m \sum_{n=m+1} \sqrt{e_m^i e_n^i}}_{=B} \tag{22}$$

The differences to the previous equation (20) is only the additional factor B, which describes the influence of the cross modal terms on the energy density. This factor B becomes zero for incoherent sound fields [13], that means that every excited mode is independent from the others and that the excited modes are uncorrelated. The total energy of a subsystem is then the integral over the area A of e^i.

$$E^i = \int_A e^i \, dA = \int_A D \, dA + \int_A B \, dA \tag{23}$$

Herein the integral over the area of B is due to the orthogonality of the mode shapes Φ_n always zero [3, 10] and so it follows that the total energy of a subsystem i is always the sum of all the modal energies.

$$E^i = \int_A D \, dA = \sum_n E_n^i \tag{24}$$

In the next step equation (19) is inserted in the term B to have a closer look at it.

$$\begin{aligned} B = 2\sum_m \sum_{n=m+1} \sqrt{\frac{E_m}{N_m}\Phi_m^2 \frac{E_n}{N_n}\Phi_n^2} &= 2\sum_m \sum_{n=m+1} \left[(\pm\Phi_m)(\pm\Phi_n)\sqrt{\frac{E_m}{N_m}\frac{E_n}{N_n}}\right] \\ &= 2\sum_m \sum_{n=m+1} \left[S_{mn}\Phi_m\Phi_n\sqrt{\frac{E_m}{N_m}\frac{E_n}{N_n}}\right] \end{aligned} \tag{25}$$

The problem of this equation is, that it is necessary to define the sign S_{nm}, plus or minus, of the mode shapes. But there is no information about it in the previous calculations from SmEdA, because an energy method, which works at last only with quadratic values of the shapes, does not need it. At a look at equations (21) and (22), it can be seen that the searched sign for every amplitude of every corresponding term must be the same as the analogous one of the other equation. From this it follows that

$$S_{mn} = sign(\hat{p}_m \hat{p}_n^*) = sign(\hat{v}_m \hat{v}_n^*) \tag{26}$$

where $\hat{}$ denotes the amplitude. These modal pressure or modal velocity amplitudes can be approximated using analytic solutions for the excited uncoupled subsystems.
As examples to demonstrate this procedure, an arbitrary excited structure and a cavity, which is

excited at the boundary by a vibrating structure, are chosen. The velocity in modal description of an arbitrary excited plate is given by [14]

$$v = \sum_n v_n = \sum_n \frac{\Phi_n}{M_n\left(\omega_n^2 - \omega^2 + d_n\right)} \int_A i\omega p_{ex} \Phi_n \, dA \tag{27}$$

where ω_n is the eigenfrequency of the mode n, ω is the excitation frequency, p_{ex} is the excitation pressure and d_n is the modal damping factor. For the modal damping factor d_n it is possible to use structural damping,

$$d_n^s = i\eta_p \omega_n^2 \tag{28}$$

or viscous damping,

$$d_n^v = i\eta_p \omega_n \omega \tag{29}$$

where η_p is the damping factor of the plate. All in all the sign S_{nm}^p for an excited plate then reads:

$$S_{mn}^p = sign(v_m v_n^*) = sign\left(\left\{ \left[\omega_m^2 - \omega^2\right] \left[\omega_n^2 - \omega^2\right] - d_m d_n \right\} \int_A p_{ex} \Phi_m \, dA \int_A p_{ex} \Phi_n \, dA \right) \tag{30}$$

For the special case of an excitation at only one point, which has the coordinates x_e and y_e, equation (30) becomes

$$S_{mn}^p = sign\left(\left\{ \left[\omega_m^2 - \omega^2\right] \left[\omega_n^2 - \omega^2\right] - d_m d_n \right\} \Phi_m(x_e, y_e) \Phi_n(x_e, y_e) \right) \tag{31}$$

The pressure p^c of the other example, the cavity excited by a vibrating structure, is described with modal pressures p_r^c as follows [9]:

$$p^c = \sum_r p_r^c = \sum_r \left[\Phi_r^c \left(-\rho_c \omega^2 \sum_s \frac{a_s^p W_{rs}}{N_r (k^2 - k_r^2)} \right) \right] \tag{32}$$

where W_{rs} is the interaction modal work (see chapter 2), N_r is the norm of the mode r with the mode shape Φ_r^c and ρ_c is the density of the fluid in the cavity. The modal amplitude a_s^p of the s-th mode of the structure is given by

$$a_s^p = \frac{1}{M_n\left(\omega_n^2 - \omega^2 + d_n\right)} \int_A p_{ex} \Phi_n \, dA \tag{33}$$

and the wave numbers k and k_r are defined as

$$k = \frac{\omega}{c_0 (1 + i\eta_c)} \tag{34}$$

and

$$k_r = \frac{\omega_n}{c_0} \tag{35}$$

where c_0 and η_c are the sound velocity and the damping factor of the cavity. Finally the sign S_{mn}^c for the cavity excited by a vibrating structure is calculated again with equation (26). It must be pointed out at this that equation (32) uses another definition for the damping in the cavity than the SmEdA approach. For a damping $\eta_c \ll 1$ the relation between η_c and the damping η_s of SmEdA is given by [9]

$$\eta_c \approx \frac{\eta_s}{2} \tag{36}$$

3.2. Broadband excitation

Next the whole formulation for the energy density e^i for a single frequency excitation must be extended for a broadband excitation. For this purpose the superposition principle can be used to describe the searched solution for the frequency band $\Delta\omega$ as a sum of solutions for discrete frequency steps ω_f.

$$\begin{aligned} e^i(\Delta\omega) = \sum_f e^i(\omega_f) &= e^i_m(\omega_1) + e^i_m(\omega_2) + \ldots + 2\sqrt{e^i_m(\omega_1)e^i_n(\omega_1)} + 2\sqrt{e^i_m(\omega_2)e^i_n(\omega_2)} + \ldots \\ &= \sum_m \sum_f e^i_m(\omega_f) + 2\sum_m \sum_{n=m+1} \sum_f \sqrt{e^i_m(\omega_f)e^i_n(\omega_f)} \\ &= \sum_m e^i_m(\Delta\omega) + \underbrace{2\sum_m \sum_{n=m+1} \sum_f \sqrt{e^i_m(\omega_f)e^i_n(\omega_f)}}_{=B_{\Delta\omega}} \end{aligned} \tag{37}$$

On the other hand the resultant modal energies from the SmEdA calculation are values for the whole frequency band $\Delta\omega$ and so the total energy density must have the following form (S: SmEdA):

$$e^i_S(\Delta\omega) = \sum_m e^i_m(\Delta\omega) + \underbrace{2\sum_m \sum_{n=m+1} \sqrt{e^i_m(\Delta\omega)e^i_n(\Delta\omega)}}_{=B^S_{\Delta\omega}} \tag{38}$$

For an incoherent sound field, where $B_{\Delta\omega}$ and $B^S_{\Delta\omega}$ are zero, the two equations (37) and (38) are equal and again the same as equation (20). Also the total energy of a whole subsystems i is always again just the sum of all modal energies like in equation (24). But for a coherent sound field there is the problem that the factor $B^S_{\Delta\omega}$ does not agree with the exact factor $B_{\Delta\omega}$. This fact shows that for a broadband excitation not only the informations for the sign of the shape functions (see chapter 3.1) can get lost at an energy method like SmEdA but also the information how much energy get every mode at every excitation frequency. The information about the last is important for coherent sound fields, because $B_{\Delta\omega}$ describes in this way the interaction between the excited modes. So the size of the sum over the frequencies step for one pair of modes in equation (37) is a synonym for the size of the influence on each other. Normally such a sum can be only big in general, when the difference between the eigenfrequencies of two modes is small, because then the amount of the energies of the both modes can be quite big at the excitation frequencies near their eigenfrequencies. There are now two possibilities to solve this problem of the broadband excitation for SmEdA. The first one is to calculate the modal energies also with SmEdA for many discrete frequency steps, but then the calculation cost grows immense. The second and less computation time intensive one is to make only one SmEdA calculation for the whole frequency band and to define a correction factor C_{mn} for each pair of modes. This correction factor is defined as follows so that the difference between the product of the energies for a frequency band of equation (38) and the midmost sum of equation (37) is equalized:

$$C_{mn} = \frac{\sum_f \sqrt{e^i_m(\omega_f)e^i_n(\omega_f)}}{\sqrt{e^i_m(\Delta\omega)e^i_n(\Delta\omega)}} \tag{39}$$

From this and equation (37) it follows for the total energy density e^i of a subsystem i under a broadband excitation that

$$e^i(\Delta\omega) = \sum_m e^i_m(\Delta\omega) + 2\sum_m \sum_{n=m+1} C_{mn}\sqrt{e^i_m(\Delta\omega)e^i_n(\Delta\omega)} \tag{40}$$

At last C_{mn} is nothing else than a kind of correlation factor for every pair of modes, which describes the relationship between them at a broadband excitation. Through insertion of equation (19) in equation (39) C_{mn} becomes then a relation of modal energies

$$C_{mn} = \frac{\sum_f S_{mn}(\omega_f)(\Phi_m)(\Phi_n)\sqrt{\frac{E_m(\omega_f)}{N_m}\frac{E_n(\omega_f)}{N_n}}}{(\Phi_m)(\Phi_n)\sqrt{\frac{E_m(\Delta\omega)}{N_m}\frac{E_n(\Delta\omega)}{N_n}}} = \frac{\sum_f S_{mn}(\omega_f)\sqrt{E_m(\omega_f)E_n(\omega_f)}}{\sqrt{E_m(\Delta\omega)E_n(\Delta\omega)}} \tag{41}$$

Next it is possible to make the approximation that the pairs of modal energies E_m for single frequency excitations and for a broadband excitation have the same relation to each other as the corresponding modal input powers Π_m, because the modal input powers of a subsystem are proportional to the modal energies of this subsystem and are except the modal energies the only factors, which depend on the frequency in the linear equation system of SmEdA (see chapter 2).

$$C_{mn} = \frac{\sum_f S_{mn}(\omega_f)\sqrt{\Pi_m(\omega_f)\Pi_n(\omega_f)}}{\sqrt{\Pi_m(\Delta\omega)\Pi_n(\Delta\omega)}} \tag{42}$$

At last it can be also assumed that the frequency band is divided into infinite frequency steps and the input power $\Pi_n(\Delta\omega)$ for the whole frequency band can be expressed with the integral over the frequency band of the modal input power Π_m for a single frequency. Finally C_{mn} is then given by

$$C_{mn} = \frac{\sum_{f=1}^{\infty} S_{mn}(\omega_f)\sqrt{\Pi_m(\omega_f)\Pi_n(\omega_f)}}{\sqrt{\int_{\Delta\omega}\Pi_m(\omega)\,d\omega\int_{\Delta\omega}\Pi_n(\omega)\,d\omega}} = \frac{\int_{\Delta\omega} S_{mn}(\omega)\sqrt{\Pi_m(\omega)\Pi_n(\omega)}\,d\omega}{\sqrt{\int_{\Delta\omega}\Pi_m(\omega)\,d\omega\int_{\Delta\omega}\Pi_n(\omega)\,d\omega}} \tag{43}$$

where $S_{mn}(\omega_f)$ is defined by equation (26). The modal input powers Π_m can be calculated with the modal pressure $p_m(A)$ and the modal velocity $v_r(A)$ of the respective subsystem on the excited area A using the following formula:

$$\Pi_m = \frac{1}{2}\int_A \Re[p_m(A)v_r^*(A)]\,dA = \frac{1}{2}\int_A \frac{\Re[p_m(A)p_m^*(A)]}{Z}\,dA = \frac{1}{2}\int_A Z\,\Re[v_r(A)v_r^*(A)]\,dA \tag{44}$$

where Z is the impedance of the material or fluid. For the two examples from the last chapter, the excited structure and the cavity excited by a structure, equation (27) for the velocity of the structure and equation (32) for the pressure in the cavity can be used. So, for example, the factor C^p_{mn} of the structure reads as follows for the special case of a point force excitation:

$$C^p_{mn} = \frac{\int_{\Delta\omega} S^p_{mn}\sqrt{\frac{\omega^4}{\left[(\omega_m^2-\omega^2)^2-d_m^2\right]\left[(\omega_n^2-\omega^2)^2-d_n^2\right]}}\,d\omega}{\sqrt{\int_{\Delta\omega}\frac{\omega^2}{(\omega_m^2-\omega^2)^2-d_m^2}\,d\omega\int_{\Delta\omega}\frac{\omega^2}{(\omega_n^2-\omega^2)^2-d_n^2}\,d\omega}} \tag{45}$$

where S_{mn}^{p} and d_m respectively d_n are defined by the equations (31), (28) and (29).

4. Results

4.1. System under study

To demonstrate the advantages of the extended SmEdA aprroach with the non resonant contribution and to show the application possibilities of the post-processing method for the energy distributions we consider a basic example configuration of a simply supported rectangular plate between two parallelepipedic cavities as presented in Figure 1 and Table 1.

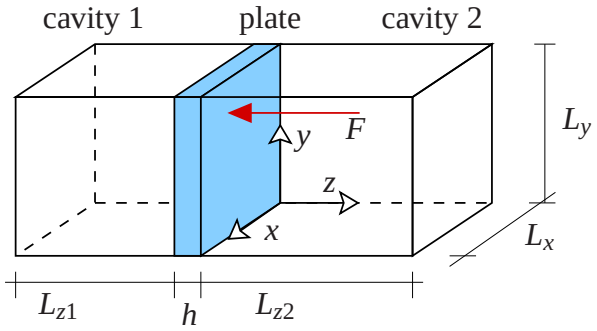

Figure 1.: Sketch of the system

	plate	**cavity 1**	**cavity 2**
$L_x \times L_y \times L_z(h)$ (m)	$1.2 \times 0.9 \times 0.004$	$1.2 \times 0.9 \times 0.7$	$1.2 \times 0.9 \times 1$
ρ (kg/m^3)	7820	1.2	1.2
c (m/s)		340	340
η	0.01	0.01	0.01
E (MPa)	210		
ν	0.3		

Table 1.: Characteristics of the subsystems

The plate is excited with a point force ($[F] = 1N$) at one point, which has the coordinates $x_e = 0.211765$ and $y_e = 0.189474$, and the coincidence frequency of the plate is 2933 Hz. In the present case the necessary eigenmodes and eigenfrequencies for SmEdA can be calculated quite easily analytically. The eigenmodes p_{qrs} and the eigenfrequencies ω_{qrs} of the cavities are given by [15]

$$p_{qrs} = \cos\left(\frac{q\pi x}{L_x}\right)\cos\left(\frac{r\pi y}{L_y}\right)\cos\left(\frac{s\pi z}{L_z}\right); \quad q,r,s = 0,1,2,3,\ldots \tag{46}$$

and

$$\omega_{qrs} = c\sqrt{\left(\frac{q\pi}{L_x}\right)^2 + \left(\frac{r\pi}{L_y}\right)^2 + \left(\frac{s\pi}{L_z}\right)^2} \tag{47}$$

The eigenfrequencies ω_{mn}^s and the modes W_{mn}^s of the simply supported plate are

$$\omega_{mn}^s = \pi^2 \left[\left(\frac{m}{L_x} \right)^2 + \left(\frac{n}{L_y} \right)^2 \right] \sqrt{\frac{B}{m}}; \quad m,n = 1,2,3,\ldots \tag{48}$$

and

$$W_{mn}^s = \sin\left(\frac{m\pi x}{L_x} \right) \sin\left(\frac{n\pi y}{L_y} \right) \tag{49}$$

with the mass per area m and the bending stiffness B of the plate.

4.2. Energy

In the Figures 2 to 4 the results for the total energies of the different subsystems calculated with SmEdA are compared for three 200 Hz frequency bands with these predicted with a standard direct FEM calculation. With SmEdA there are the follwing three calculation possibilities as it is shown in chapter 2:

- SEA with couplings factors estimated by SmEdA (SmEdA SEA CLF; equations (2), (9) and (10))
- SmEdA direct only with resonant modes (SmEdA resonant; equations (8) and (11))
- SmEdA direct with resonant and non resonant modes (SmEdA non resonant; equations (8) and (11)).

For the last approach the number of modes, that are taken into account, is enlarged until the changes in the values of the energies get small enough, for example smaller than 0.1 dB at an increase of the frequency range by 300 Hz. In our case (see chapter 4.1) at the plate damping $\eta_p = 0.1$ it is for example necessary at an excitation in the frequency band from 600 Hz to 800 Hz to take into account all the modes from 0 Hz to 1500 Hz above the frequency band. At low plate damping, for example $\eta_p = 0.01$, the results for the excited plate of all these different calculations are more or less the same and equal to these obtained by FEM. Also for the energy in the non directly excited cavities it is not so important, if non resonant modes are taken into account or not. But at a higher damping, $\eta_p = 0.1$, it is really necessary to take into account also non resonant modes, especially for the cavities, because otherwise we get a difference of 5 dB and more in comparison to the FEM results. The energy values predicted with resonant and non resonant modes agree then well with these of the FEM calculation.

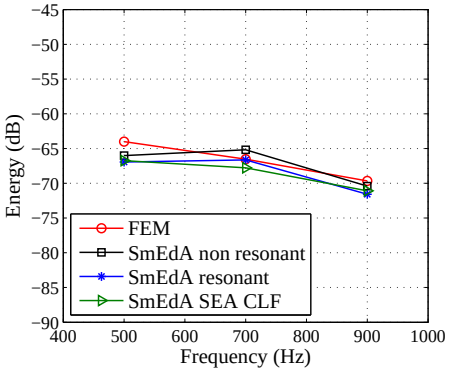

2.1: Energy in cavity 1 ($\eta_2 = 0.01$)

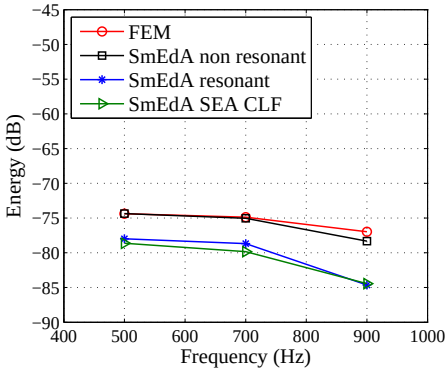

2.2: Energy in cavity 1 ($\eta_2 = 0.1$)

Figure 2.: Energy in cavity 1 at different plate damping factors η_2

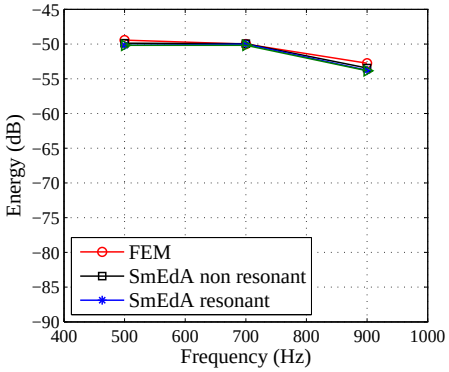

3.1: Energy of the plate ($\eta_2 = 0.01$)

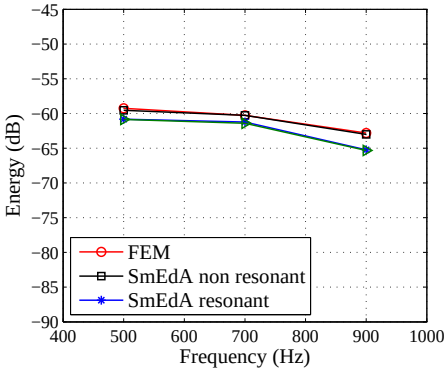

3.2: Energy of the plate ($\eta_2 = 0.1$)

Figure 3.: Energy of the plate at different plate damping factors η_2

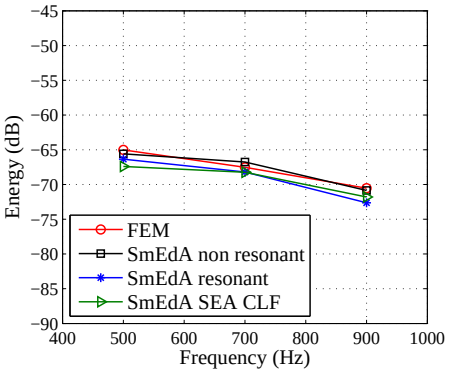

4.1: Energy in cavity 2 ($\eta_2 = 0.01$)

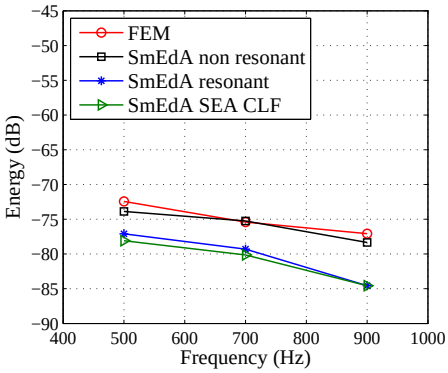

4.2: Energy in cavity 2 ($\eta_2 = 0.1$)

Figure 4.: Energy in cavity 2 at different plate damping factors η_2

4.3. Energy distributions

In this chapter examples for total energy density distributions of the new SmEdA post-processing procedure, which is described in chapter 3, are compared to these obtained fully analytically and by classical FEM. For an analytical solution equations (27) and (32) are used, because they are indeed only solutions for an uncoupled plate and a system for one plate and one cavity, but this should make not a big difference for our case with a light fluid. Also we want to have a look, how big is the discrepancy, if the cross modal terms are neglected for the energy distributions (SmEdA diagonal) like in previous works.

4.3.1. Single frequency excitation

Figures 5 and 6 and show the total energy densities distributions of the plate for two different damping factors calculated by FEM, analytically and by the SmEdA post-processing procedure with and without cross modal terms. The plate is herein excited with the point force only at 600 Hz. At the higher plate damping, $\eta_p = 0.1$ (Figure 5), the energy density distributions in absolute values (J/m^2) of the different models are quite the same except the one without the cross modal terms. A little problem at high damping, which can not be seen in this figure, is that the energy density predicted by SmEdA can be a little bit negative in areas of very small values, if the number of modes, which are taken into account, are not high enough.

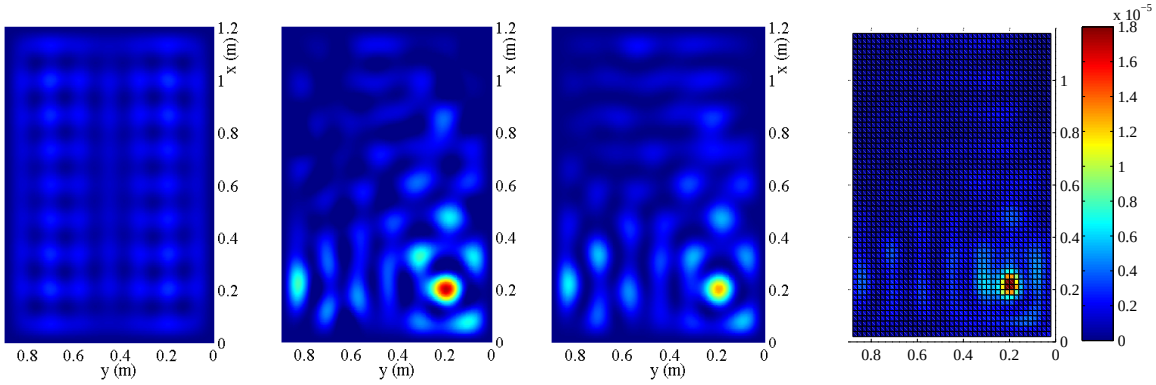

5.1: SmEdA diagonal 5.2: SmEdA 5.3: analytic 5.4: FEM

Figure 5.: Energy density distribution of the plate(frequency: 600Hz; plate damping: $\eta_2 = 0.1$)

Also at a lower damping, $\eta_p = 0.01$ (Figure 6), the SmEdA post-processing procedure with the cross modal terms agree well again with the analytic solution. Due the quite rough mesh the FEM energy density distribution is here not so exact and the values are a little bit lower than these of SmEdA and the analytical method, which work with exact functions and not with discrete points. To get also such a good detailed energy density distribution with FEM it is necessary to take a very fine mesh as it is shown in Figure 7 for an uncoupled plate. But one problem is then, that the value at the excitation point is overestimated by FEM. For the whole energy of the plate a finer mesh is not necessary, because the change is only plus minus 0.5 dB. Another important point at Figures 5 and 6 is that they demonstrate that the cross modal terms are always essential to get good results for the energy density distributions in the case of a single frequency point force excitation. So this means that the sound field is very coherent here.

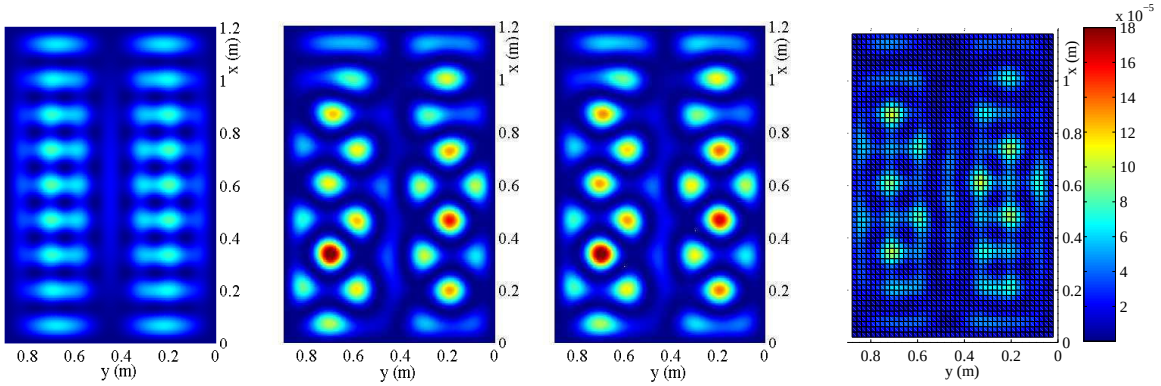

6.1: SmEdA diagonal 6.2: SmEdA 6.3: analytic 6.4: FEM

Figure 6.: Energy density distribution of the plate(frequency: 600Hz; plate damping: $\eta_2 = 0.01$)

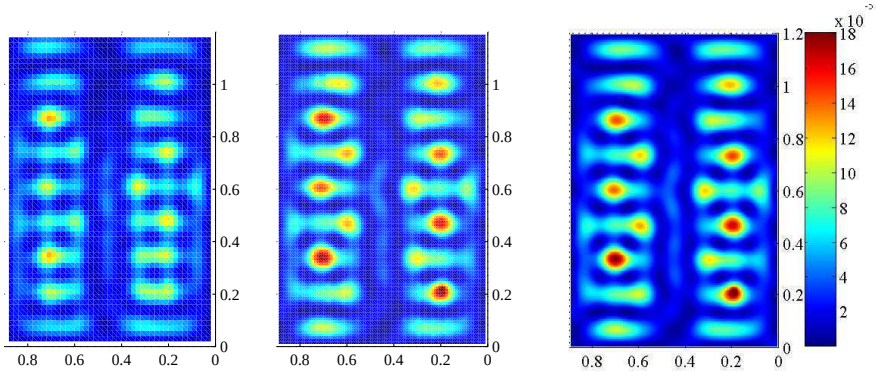

7.1: 1938 elements 7.2: 7752 elements 7.3: 31008 elements

Figure 7.: Energy density distribution of a uncoupled plate at different FEM meshes (frequency: 600Hz; plate damping: $\eta_2 = 0.01$)

4.3.2. Broadband excitation

At a broadband excitation we get at a high plate damping, $\eta_p = 0.1$ (Figure 8), again a similar shape for the energy density distribution of the plate as for the single frequency excitation (see chapter 4.3.1). The solutions of the different models except SmEdA without the cross modal terms (SmEdA diagonal) are more or less equal. But at lower plate damping , $\eta_p = 0.01$ (Figure 9), the sound field on the plate becomes more symmetric and the estimation without the cross modal terms is here relatively good. This effect at the broadband excitation comes from the spectral averaging and depends on the bandwidth and the damping [12]. That means for example that the sound field becomes more and more incoherent with a decreasing damping and so also the influence of the cross modal terms declines.

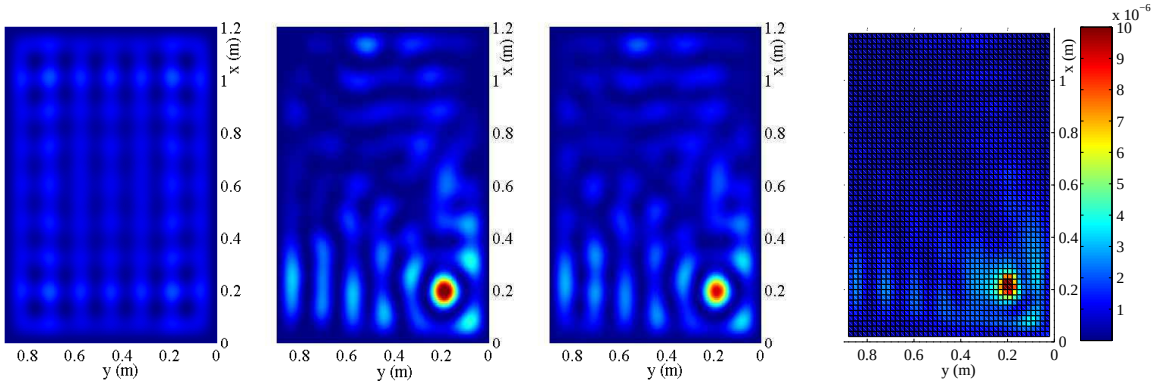

8.1: SmEdA diagonal 8.2: SmEdA 8.3: analytic 8.4: FEM

Figure 8.: Energy density distribution of the plate (frequency band: 600-800 Hz; plate damping: $\eta_2 = 0.1$)

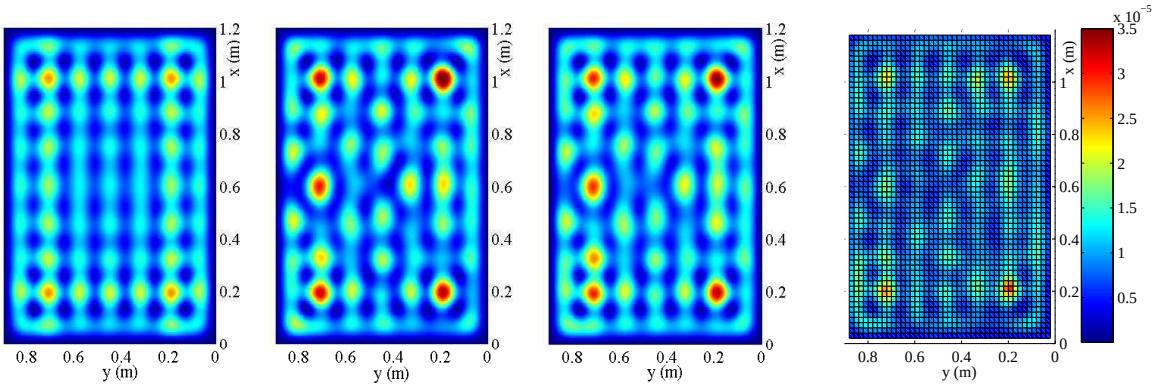

9.1: SmEdA diagonal 9.2: SmEdA 9.3: analytic 9.4: FEM

Figure 9.: Energy density distribution of the plate (frequency band: 600-800 Hz; plate damping: $\eta_2 = 0.01$)

Finally we want to have a look at the energy density distributions (J/m^3) in cavity 1. So Figure 10 shows the energy density distribution at $z = -0.3624$ and at a damping of $\eta = 0.01$ in all the subsystems. Here it plays in contrast to the directly excited plate a big role, how much modes are taken into account for the SmEdA and the analytic calculation, because there is a quite big difference between the results only with the resonant modes (Figures 10.1, 10.2 and 10.3) and these with non resonant modes (Figures 10.5, 10.6 and 10.7). The energy distributions calculated with resonant and non resonant modes agree then quite well with the one predicted by FEM. But of course due to the rough mesh and so on there are the same discrepancies compared to FEM (Figures 8.4, 9.4 and 10.4) as described in chapter 4.3.1. Also the values of the analytic approach are in general bigger, because the underlying formula is only for a system of one plate and one cavity and not for two cavities like in our case. Finally, these energy density distributions of the cavity points out that the sound field is here not a diffuse one, in which the energy would have been the same in every point in the cavity.

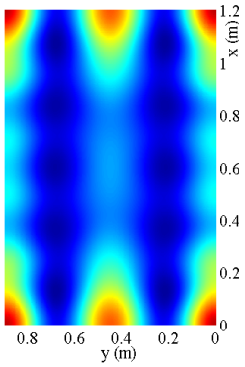

10.1: SmEdA diagonal resonant

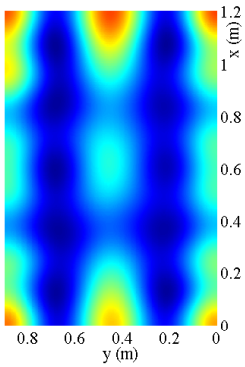

10.2: SmEdA resonant

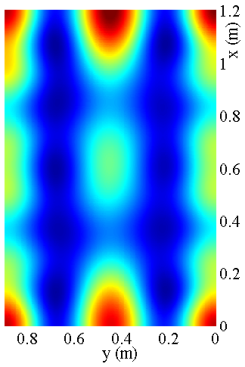

10.3: analytic resonant

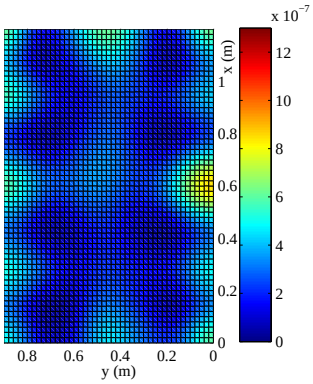

10.4: FEM

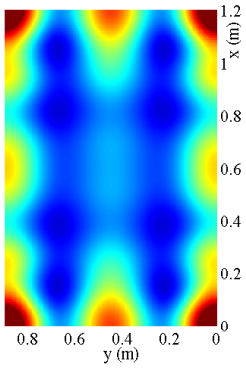

10.5: SmEdA diagonal non resonant

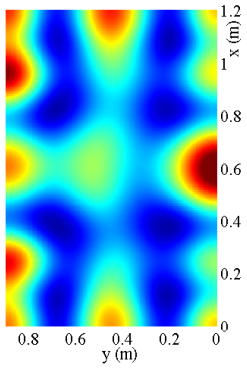

10.6: SmEdA non resonant

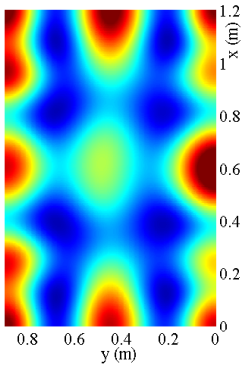

10.7: analytic non resonant

Figure 10.: Energy density distribution in the cavity at $z = -0.3624$ (frequency band: 600-800 Hz; damping: $\eta_2 = 0.01$)

5. Conclusion

As it is shown in the previous examples, it is possible to calculate using the non resonant contribution all cases in the whole frequency range, below and above the critical frequency. So it is possible to predict for example the energies of highly damped systems and even of systems, which are excited only at one single frequency. Also the new developed post-precessing method for coherent energy density distributions works well in comparison to other models. All in all this two improvements offer big advantages compared to SEA, which can predict only energy values of whole subsystems. The advantages in comparison to FEM are that the eigenmodes must be computed for SmEdA, for example with FEM, only once and then only a part or the whole SmEdA procedure must be recalculated, if the excitation or the damping is changed. Using FEM, in contrast, the whole calculation for a coupled system must be always repeated, if one parameter is changed. Furthermore only one simple linear equation system must be solved in SmEdA for a whole frequency band and not complete independent calculations for a lot of frequency steps like in FEM. So SmEdA can save time dramatically. To sum up, SmEdA is because of these arguments a good alternative to other methods, like FEM and SEA, especially if one is interested in average values for a frequency band but wants to have also a detailed energy mapping.

6. Acknowledgment

The authors gratefully acknowledge the ITN Marie Curie project GA-214909 ”MID-FREQUENCY - CAE Methodologies for Mid-Frequency Analysis in Vibration and Acoustics”.

Bibliography

[1] R. H. Lyon, R. G. DeJong, Theory and application of statistical energy analysis, Butterworth-Heinemann, 2nd edn., 1995.

[2] N. Totaro, J.-L. Guyader, Structure/ cavity coupling using Statistical Energy Analysis: Coupling Loss Factors and energy maps into subsystems, in: Proceeedings of Acoustics 08, Paris.

[3] N. Totaro, C. Dodard, J.-L. Guyader, SEA coupling loss factors of complex vibro-acoustic systems, Journal of Vibration and Acoustics 131 (2009) 041009–4.

[4] L. Maxit, J.-L. Guyader, Estimation of the SEA coupling loss factors using a dual formulation and FEM modal information, part I: theory, Journal of Sound and Vibration 239(5) (2001) 907–930.

[5] L. Maxit, J.-L. Guyader, Estimation of the SEA coupling loss factors using a dual formuulation and FEM modal information, part II: numerical applications, J. Sound Vib. 239(5) (2001) 931–948.

[6] N. Totaro, J.-L. Guyader, extension of SmEdA method to estimate energy repartition into SEA subsystems, in: Proceedings of ISMA 2008, Leuven.

[7] N. Totaro, L. Maxit, J.-L. Guyader, Post-traitement et analyse énergétiques de résultats eléments finis, in: Proceedings of CFA 2010, Lyon.

[8] R. Stelzer, N. Totaro, G. Pavic, J. Guyader, Prediction of Transmission Loss using an improved SEA Method, in: Proceedings of CFA 2010, Lyon.

[9] Dodard, Simulation des Transferts Energétiques en Vibro-Acoustique et Recherche des Energies Locales par Méthode SmEdA, Master’s thesis, INSA Lyon, 2006.

[10] W. T. Chu, Eigenmode analysis of the interference patterns in reveberant sound fields, Journal of the Acoustical Society of America 68 (1) (1980) 184–190.

[11] W. Chu, Comments on the coherent and incoherent nature of a reverberent sound fields, Journal of the Acoustical Society of America 69 (6) (1981) 1710–1715.

[12] F. Jacobsen, T. Roisin, The coherence of reveberant sound fields, Journal of the Acoustical Society of America 68 (1) (2000) 184–190.

[13] E. Hering, R. Martin, M. Stohrer, Physik für Ingenieure, Springer, 10th edn., 2007.

[14] L. Cremer, M. Heckl, B. Petersson, Structure-Borne Sound, Springer, 3rd edn., 2005.

[15] M. Möser, Technische Akustik, Springer, 7th edn., 2007.

8. Paper III: Improved modal Energy Analysis for industrial problems

Contents

Published in the Proceedings of 18th Congress on Sound and Vibration (ICSV18), Rio de Janeiro, Brazil, July 10-14, 2011

Improved modal Energy Analysis for industrial problems

Rainer Stelzer[1], Nicolas Totaro[1], Goran Pavic[1], Jean-Louis Guyader[1]
[1] *INSA Lyon Laboratoire Vibrations et Acoustique, 25 Bis Avenue Jean Capelle Bâtiment St. Exupéry, 69621 Villeurbanne Cedex*
rainer.stelzer@insa-lyon.fr

Abstract
The most popular methods for the analysis of vibro-acoustic systems are the finite element method (FEM) and the statistical energy analysis (SEA). To close the gap in the mid frequency range between FEM and SEA and to overcome their drawbacks, the statistical modal energy distribution analysis (SmEdA) was developed. Contrary to SEA, all the modes of different subsystems are coupled to each other and not only whole subsystems. The newly developed version of SmEdA, described herewith, can handle coupling between all the modes, resonant and non resonant ones, and not only between resonant modes like the classical SmEdA. Using a suitable post-processing, SmEdA enables the calculation of energy distributions. Up to now, such a post-processing and the improved SmEdA were only tested and validated on simple academic cases. In the present paper, an application of these methods to real industrial systems is demonstrated on an example of a double-deck train.

1. Introduction

Two classical calculations methods in vibro-acoustics are the finite element method (FEM) and the statistical energy analysis (SEA). The finite element method solves in general a problem, which is described by one or more differential equations, for discrete geometrical points. An overview and details about FEM can be found in many books like [1]. The number of mesh points has to become larger if the frequency increases and so does the computation time. Thus, FEM is in general an effective computation method only for lower frequencies. Another disadvantage of this method is that a lot of calculation steps are necessary to get frequency band averaged values, which are often required in practical applications. The second often used method, the statistical energy analysis, is an energy based approach. That means that the basic equation for each subsystem i is the following power balance equation:

$$\Pi^i = \Pi^i_{dis} + \Pi^i_{ex} \tag{1}$$

where Π^i is the input power, Π^i_{dis} is the dissipated power and Π^i_{ex} is the transmitted power into connected subsystems. The dissipated power Π^i_{dis} is proportional to the total energy E_i of system i and Π^i_{ex} is proportional to the difference of the total energies between the concerned subsystem and the connected subsystems [2]. The proportionality factors in these relations are the damping loss factor η_i and the coupling loss factor η_{ij}. Hence, the power balance, equation (1), reads:

$$\Pi^i = \omega_c \eta_i E_i + \omega_c \eta_{ij}(E_i - E_j) \tag{2}$$

where ω_c is the central frequency of an excited frequency band. All in all, only a system of linear equations with one equation for each subsystem has to be solved to get global total energy values for each subsystem. But SEA is in general only valid at high frequencies, because the mode density has to be high in a frequency band. Details about the validity of SEA are described for example in [3]. Another deficiency amongst others is that SEA outputs only the global energy values but no information about the distributions of these (see for example [4]).
To close the gap in the mid-frequency range between the low frequency method FEM and the high frequency method SEA many different methods have been already developed and are still developed. Examples are the hybrid FEM/SEA method [5], the wave based method [6], the Variational Theory of complex Rays (VTCR) [7] and the statistical modal energy distribution analysis (SmEdA) which is the topic of this article. This method is an energy based one like SEA, but uses the coupling of pairs of modes from different subsystems and not only coupling between different subsystems. That has the advantage that SmEdA can be used in principal in the whole frequency range. In the original SmEdA [8] it was only possible to take into account the coupling between resonant modes relating to an excited frequency band. Because of the importance of non resonant modes in many acoustical problems like highly damped systems the SmEdA method has been extended so that couplings between all modes, resonant and non resonant ones, can be taken into account [9, 10]. Furthermore, a post-processing method has been developed to obtain energy distributions with the modal energies predicted with SmEdA [10]. In the articles [9] and [10], simple academic examples were presented to demonstrate the possibilities and advantages of this post-processing method and the improved SmEdA.
To illustrate how the new methods can be used for real complex industrial structures, a computation of a part of a double-deck train is presented at the end of this article. First, an introduction to SmEdA and the post-processing method for energy distributions is given. The latter is extended in this article – compared to that of [10]– to kinetic and potential energy distributions of three-dimensional structures.

2. Statistical modal Energy distribution Analysis

The eigenmodes and einfrequencies of subsystems, which can be calculated for example with FEM, provides the basis of SmEdA. The coupling between these modes is characterised in SmEdA with a dual formulation of two gyroscopic coupled oscillators [8], which are described by the following coupled differential equations:

$$\begin{aligned} \ddot{y}_1(t) + \Delta_1 \dot{y}_1(t) + \omega_1^2 y_1(t) - \sqrt{M_1^{-1} M_2}\,\gamma \dot{y}_2(t) &= F_1(t) \\ \ddot{y}_2(t) + \Delta_2 \dot{y}_2(t) + \omega_2^2 y_2(t) + \sqrt{M_2^{-1} M_1}\,\gamma \dot{y}_1(t) &= F_2(t) \end{aligned} \tag{3}$$

where $\Delta_i = \omega_i \eta_i$ is the damping coefficient with the eigenfrequency ω_i and the damping factor η_i, γ is the gyroscopic coupling factor and M_1, M_2, y_1 and y_2 are the masses and displacements of the oscillators one and two. This is a good analogous mechanical model for example for coupling between pressure modes p_p^1 of a fluid filled cavity and displacement bending modes W_q^2 of a structure. Furthermore, the exchanged power P_{12} between two modes respectively two oscillators is – similar to SEA, equation (1) – proportional to the difference of their energies.

$$P_{12} = \beta_{12}(E_1 - E_2) \tag{4}$$

where β_{12} is the modal coupling loss factor. The gyroscopic coupling γ for two coupled modes is given by, [8],

$$\gamma = \frac{1}{\sqrt{(\omega_p^1)^2 M_p^1 M_q^2}} \int_S p_p^1 W_q^2 \, dS = \frac{W_{pq}^{12}}{\sqrt{(\omega_p^1)^2 M_p^1 M_q^2}} \tag{5}$$

Finally, the modal coupling loss factor β_{12} follows from equations (3) to (5):

$$\beta_{pq}^{12} = \frac{(W_{pq}^{12})^2}{M_p^1 M_q^2 (\omega_q^2)^2} \left[\frac{\eta_p^1 \omega_p^1 (\omega_q^2)^2 + \eta_q^2 \omega_q^2 (\omega_p^1)^2}{((\omega_p^1)^2 - (\omega_q^2)^2)^2 + (\eta_p^1 \omega_p^1 + \eta_q^2 \omega_q^2)(\eta_p^1 \omega_p^1 (\omega_q^2)^2 + \eta_q^2 \omega_q^2 (\omega_p^1)^2)} \right] \tag{6}$$

where W_{pq}^{12} is the interaction modal work and where M_p^1, M_q^2, ω_p^1 and ω_q^2 are the modal masses and the eigenfrequencies of the p-th and q-th mode of the subsystems one and two. In [9] and [10] it has been shown that this modal coupling loss factor describes the coupling between every pair of two modes of different subsystems and not only between resonant ones like it was demonstrated by Maxit and Guyader [8]. With β_{12} the energy of every mode is calculated using a power balance equation system like in SEA, equation (2), but with one equation for every mode and not only with one for every subsystem.

$$\Pi_p^1 = \eta_p^1 \omega_p^1 E_p^1 + \sum_{q=1}^{q_{max}} \beta_{pq}^{12} (E_p^1 - E_q^2) \tag{7}$$

The sum of all these modal energies of a subsystem i gives the whole energy E^i of a subsystem i [11, 10].

$$E^i = \sum_n E_n^i \tag{8}$$

3. Energy distribution

3.1. Energy distribution of a single mode

It has been shown in [11] and [10] that the relation between the total energy distribution e_n^t of a mode n and the total energy E_n of this mode is given exact for a cavity and approximative for a structure by

$$e_n^t = \frac{E_n}{N_n}\Phi_n^2 \tag{9}$$

where N_n and Φ_n are the norm and the shape function of the mode n. To get also equations for the distributions of the kinetic and the potential energy, e_n^k and e_n^p, of a mode as a function of E_n it is necessary to characterise the relation between the kinetic energy E_n^k and the potential energy E_n^p, which are [2]

$$E_n^p = \frac{1}{2}K_n y^2 \tag{10}$$

$$E_n^k = \frac{1}{2}M_n \dot{y}^2 = \frac{1}{2}M_n \omega^2 y^2 \tag{11}$$

where y is the time averaged displacement of a mode, ω is the excitation frequency and K_n and M_n are the modal stiffness and the modal mass. Thus, it follows with the quadratic modal eigenfrequency

$$\omega_n^2 = \frac{K_n}{M_n} \tag{12}$$

for the relation between E_n^p and E_n^k

$$\frac{E_n^p}{E_n^k} = \frac{K_n y^2}{M_n \omega^2 y^2} = \frac{\omega_n^2}{\omega^2} \tag{13}$$

The relations between the total modal energy E_n and the modal potential energy E_n^p respectively the modal kinetic energy E_n^k are consequently given by

$$E_n = E_n^p + E_n^k = E_n^p \left(1 + \frac{\omega^2}{\omega_n^2}\right) \tag{14}$$

$$E_n = E_n^p + E_n^k = E_n^k \left(1 + \frac{\omega_n^2}{\omega^2}\right) \tag{15}$$

Finally, the energy distributions e_n^p and e_n^k can be written as follows using the stiffness and the mass matrix, K and M, like in [12]:

$$e_n^p = E_n^p \frac{\left(\Phi_n^Q\right)^T K \Phi_n}{K_n} = \frac{E_n \left(\Phi_n^Q\right)^T K \Phi_n}{\left(1 + \frac{\omega^2}{\omega_n^2}\right) K_n} \tag{16}$$

$$e_n^k = E_n^k \frac{\left(\Phi_n^Q\right)^T M \Phi_n}{M_n} = \frac{E_n \left(\Phi_n^Q\right)^T M \Phi_n}{\left(1 + \frac{\omega_n^2}{\omega^2}\right) M_n} \tag{17}$$

where e_n^p is again only approximative, $\left(\Phi_n^Q\right)^T$ is the transpose of the shape function vector of the mode n at a point Q and Φ_n is here the complete shape function vector for all points Q. For a broadband excitation ω is approximately the central frequency of the excited band.

3.2. Energy distributions of whole subsystems

3.2.1. Theory

The energy distribution of a subsystem is given for a broadband excitation as a function of the modal energy distributions defined in chapter 3.1 as follows, [10]:

$$e^i(\Delta\omega) = \sum_m e^i_m(\Delta\omega) + 2\sum_m \sum_{n=m+1} C_{mn}\sqrt{e^i_m(\Delta\omega)e^i_n(\Delta\omega)} \tag{18}$$

where $e^i(\Delta\omega)$ is the total, kinetic or potential energy distribution of a whole broadband excitation with the bandwidth $\Delta\omega$. The factor C_{mn} of equation (18) is a correction factor to describe the correlation between two modes and is given by

$$C_{mn} = \frac{\int_{\Delta\omega} S_{mn}S^{(2)}_{mn}\sqrt{\Pi_m(\omega)\Pi_n(\omega)}\,d\omega}{\sqrt{\int_{\Delta\omega}\Pi_m(\omega)\,d\omega\int_{\Delta\omega}\Pi_n(\omega)\,d\omega}} \tag{19}$$

This correction is necessary, because information, which are important to identify the spatial and the frequency correlation of modes, get lost using frequency band averaged energies. The spatial correlation is characterised by the factors S_{mn} and $S^{(2)}_{mn}$. S_{mn} compares the signs of the amplitudes of two modes, which depend on the given excitation, and can be approximated using analytic solutions for the amplitude of the velocity $\hat{v}$ or of the pressure $\hat{p}$ of uncoupled systems as follows [10]:

$$S_{mn} = sign(\hat{p}_m\hat{p}^*_n) = sign(\hat{v}_m\hat{v}^*_n) \tag{20}$$

The other factor, $S^{(2)}_{mn}$, describes the relation between the modes at a point Q and is for the kinetic and the potential energy distributions, equations (16) and (17), equal to the cosine of the angle α between two modal shape vectors at Q (only the translational degrees of freedom are used here!).

$$S^{(2)}_{mn} = \cos\alpha = \frac{\Phi^Q_m\Phi^Q_n}{\left|\Phi^Q_m\right|\left|\Phi^Q_n\right|} \tag{21}$$

For the total energy distribution, equation (9), $S^{(2)}_{mn}$ is 1, because the shape functions Φ_n can be extracted from the root of the second term of equation (18). The second type of correlation, the frequency correlation, is described with the power inputs $\Pi_m(\omega)$ and $\Pi_n(\omega)$ in the modes m and n. They can be again approximated with analytic solutions for the velocity or the pressure of uncoupled systems like for equation (20) as follows using the impedance Z of a structure or a fluid, [10]:

$$\Pi_m = \frac{1}{2}\int_A \Re[p_m(A)v^*_r(A)]\,dA = \frac{1}{2}\int_A \frac{\Re[p_m(A)p^*_m(A)]}{Z}\,dA = \frac{1}{2}\int_A Z\,\Re[v_r(A)v^*_r(A)]\,dA \tag{22}$$

3.2.2. Example: Correction factor for a point force excited structure

The velocity v in modal description of an arbitrary excited and uncoupled structure is given as a sum over the modal velocities v_n [13].

$$v = \sum_n v_n = \sum_n \frac{\Phi_n}{M_n(\omega^2_n - \omega^2 + i\eta_s\omega_n\omega)}\int_A i\omega p_{ex}\Phi_n\,dA \tag{23}$$

where η_s and ω_n are the damping factor and the n-th eigenfrequency of the structure and p_{ex} and A are the excitation pressure and the excited area. Thus, it follows for the correction factor C_{mn}, equation (19), of a structure excited with a point force at a point P using equation (22):

$$C_{mn} = \frac{\int_{\Delta\omega} S_{mn} S_{mn}^{(2)} \sqrt{\frac{\omega^4}{\left[(\omega_m^2-\omega^2)^2+(\eta_s\omega_m\omega)^2\right]\left[(\omega_n^2-\omega^2)^2+(\eta_s\omega_n\omega)^2\right]}}\, d\omega}{\sqrt{\int_{\Delta\omega} \frac{\omega^2}{(\omega_m^2-\omega^2)^2+(\eta_s\omega_m\omega)^2}\, d\omega \int_{\Delta\omega} \frac{\omega^2}{(\omega_n^2-\omega^2)^2+(\eta_s\omega_n\omega)^2}\, d\omega}} \tag{24}$$

with

$$S_{mn} = sign\left(\left\{\left[\omega_m^2-\omega^2\right]\left[\omega_n^2-\omega^2\right]+\eta_s\omega_m\omega_n\omega^2\right\}\Phi_m(P)\Phi_n(P)\right) \tag{25}$$

4. Example

4.1. System under study

In the following a section of a double-deck train (Figure 2) is chosen as an industrial example of use to demonstrate the application possibilities of the extended SmEdA approach and the post-processing method for energy distributions described in chapters 2 and 3. The section of the train is simulated as a simple supported structure coupled to two cavities. The structure consists of many different components (windows, stiffnessers, ...) and is excited with 8 point forces at the bottom between 280 and 355 Hz. The number of degrees of freedom and the number of modes in different frequency ranges of these three subsystems are presented in Table 1.

Table 1.: Degrees of freedoms and number of modes of the subsystems

	structure	**lower cavity**	**upper cavity**
degrees of freedom	334920	56699	54079
number of modes			
0 - 280 Hz	120	42	24
280 - 355 Hz	72	30	24
355 - 600 Hz	235	222	178
600 - 1000 Hz	648	850	715

4.2. Energies of the subsystems

The energies of the three subsystems calculated with SmEdA and FEM are compared in Table 2. For SmEdA all the modes between 0 and 600 Hz are taken into account and not only those in the excited frequency band (280-355Hz), because the contribution of the non resonant modes to the total energies is high, especially for the upper cavity. This is illustrated with the energy ratios of the modes (modal energy divided by the total energy of the corresponding subsystem) between 0 and 1000 Hz in Figure 1. The resonant modes store only 78%, 62% and 28% of the energy of the structure, the lower cavity and the upper cavity respectively. Figure 1 also shows that the most of the energy is stored only in a few modes. All in all, the result for the energies of the structure and the lower cavity of SmEdA are very good compared to these of

FEM (see Table 2). There is only an essential difference for the energy in the upper cavity. But this is the subsytem that is not directly connected to the excition area and its energy is very small compared to other energies. Thus, maybe the error of the direct FEM calculation is also relativly high.

Table 2.: Comparison of the total energies of the subsystems calculated with SmEdA and FEM

total energy [**dB**]	**SmEdA**	**FEM**	**difference** [**dB**]
structure	-56.8	-56.2	0.6
lower cavity	-67.4	-65.7	1.7
upper cavity	-81.1	-86.7	5.6

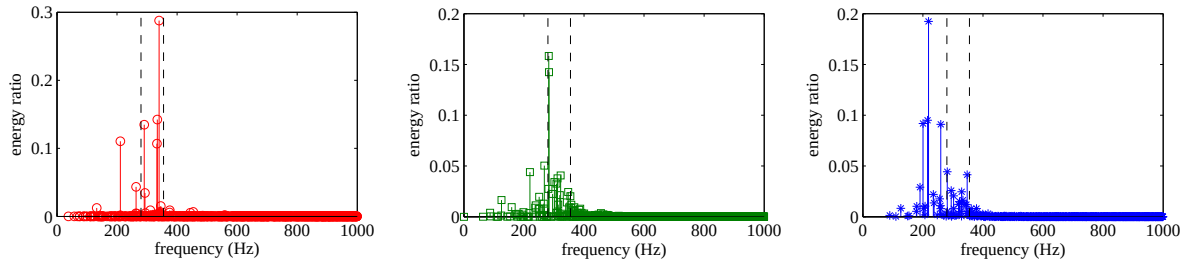

1.1: structure 1.2: lower cavity 1.3: upper cavity

Figure 1.: Energy ratios of the modes (frequency area between the dashed lines: excited frequency band)

4.3. Energy distributions of the subsystems

The kinetic energy distribution of the structure and the total energy distributions of the central sections of the cavities are presented as examples in Figures 2 to 3. The kinetic energy distribution of the structure predicted with the the post-precessing method of SmEdA (see chapter 3) is quite similar to that calculated with FEM. In contrast, there are more discrepancies between the energy distributions for the lower (Figure 4) and the upper cavity (Figure 3) predicted with the post-precessing method and FEM. One reason is certainly that the total energies of the cavities obtained by SmEdA and FEM are differ more than the total energies of the structure (see Table 2) and so do the energy distributions. The problem of the energy distributions of the cavities predicted from the modal energies with the post-processing method is that these converge quite slowly against a stable solution. This is demonstrated by comparing Figures 4 and 3, where in Figures 3.1 and 4.1 all the modes from 0 to 600 Hz and in Figures 3.2 and 4.2 all the modes from 0 to 1000 Hz have been used for calculation. Especially for the lower cavity (Figure 4), the change of the energy distribution is enormous when using more modes, although the energies of these modes are negligible for the calculation of the total energies as demonstrated in Figure 1. Therefore, it is difficult to say how much modes are necessary to get a good stable solution for the energy distributions of the cavities.

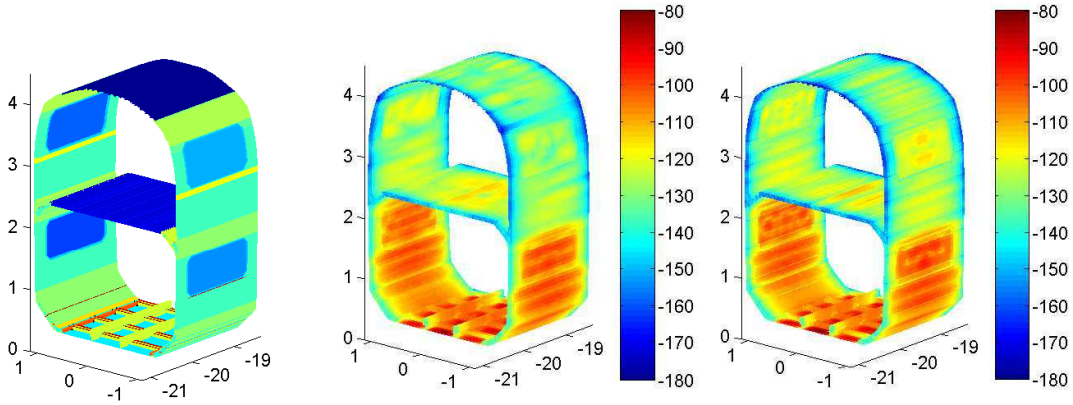

2.1: model of the train (one colour for each property)

2.2: SmEdA (using all modes from 0 to 600 Hz)

2.3: FEM

Figure 2.: Model and kinetic energy distribution [dB] using SmEdA and FEM of the train structure

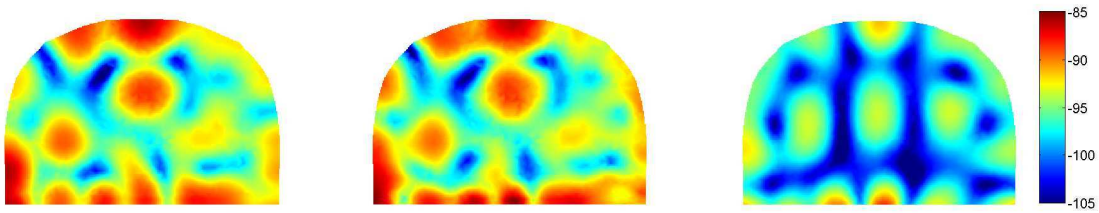

3.1: SmEdA (using all modes from 0 to 600 Hz)

3.2: SmEdA (using all modes from 0 to 1000 Hz)

3.3: FEM

Figure 3.: Energy distribution [dB] of the central section of the upper cavity using SmEdA and FEM

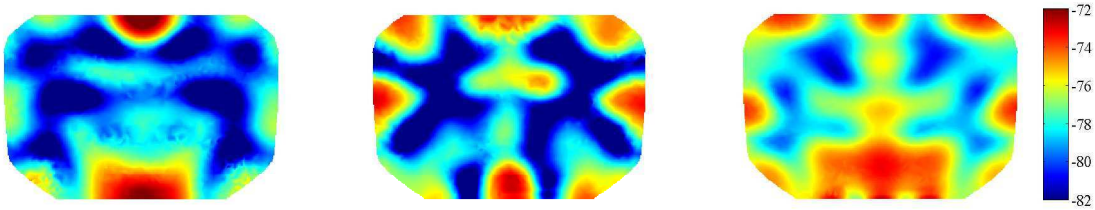

4.1: SmEdA (using all modes from 0 to 600 Hz)

4.2: SmEdA (using all modes from 0 to 1000 Hz)

4.3: FEM

Figure 4.: Energy distribution [dB] of the central section of the lower cavity using SmEdA and FEM

5. Conclusion

As it is demonstrated on the example of a part of a double-deck train, SmEdA could be an alternative to the existing methods for vibro-acoustic calculations of real industrial problems. An advantage of SmEdA is in this connection that the predictions of total energies is quite fast and easy and energy distributions can be generated after this main calculation in a post-processing applied only to interested areas. In contrast, FEM is in general more time-consuming, because

the distributions of whole systems must be calculated to get the total values. And for SEA, which outputs also total energies, a post-precessing to get energy distributions is not possible, because of the missing modal information. But the article shows also that there are two points, which must be investigated in detail in the future research. The first point is to identify the reasons for the differences between FEM and SmEdA results, which occur in a few cases. The other one is the quite slow convergence of the post-processing method for energy distributions of cavities.

6. Acknowledgment

The authors gratefully acknowledge the ITN Marie Curie project GA-214909 ”MID-FREQUENCY - CAE Methodologies for Mid-Frequency Analysis in Vibration and Acoustics”.

Bibliography

[1] S. Marburg, B. Nolte (Eds.), Computational Acoustics of Noise Propagation in Fluids - Finite and Boundary Element Methods, Springer, 2008.

[2] R. H. Lyon, R. G. DeJong, Theory and application of statistical energy analysis, Butterworth-Heinemann, 2nd edn., 1995.

[3] A. Le Bot, V. Cotoni, Validity diagrams of statistical energy analysis, J. Sound Vib. 329 (2010) 221–235.

[4] A. J. Keane, W. G. Price (Eds.), Statistical Energy Analysis: An overview with applications in structural dynamics, Cambridge University Press, 1994.

[5] P. J. Shorter, R. S. Langley, Vibro-acoustic analysis of complex systems, Journal of Sound and Vibration 288 (2005) 669–699.

[6] W. Desmet, A wave based prediction technique for coupled vibro-acoustic analysis, Ph.D. thesis, K.U. Leuven, 1998.

[7] P. Rouch, P. Ladeveze, The variational theory of complex rays: a predictive tool for medium-frequency vibrations, Computer methods in applied mechanics and engineering 192 (2003) 3301–3315.

[8] L. Maxit, J.-L. Guyader, Estimation of the SEA coupling loss factors using a dual formulation and FEM modal information, part I: theory, Journal of Sound and Vibration 239(5) (2001) 907–930.

[9] R. Stelzer, N. Totaro, G. Pavic, J. Guyader, Prediction of Transmission Loss using an improved SEA Method, in: Proceedings of CFA 2010, Lyon.

[10] R. Stelzer, N. Totaro, G. Pavic, J. Guyader, L. Maxit, Non resonant contribution and energy distributions using Statistical modal Energy distribution Analysis (SmEdA), in: Proceedings of ISMA 2010, Leuven.

[11] N. Totaro, C. Dodard, J.-L. Guyader, SEA coupling loss factors of complex vibro-acoustic systems, Journal of Vibration and Acoustics 131 (2009) 041009–4.

[12] N. Totaro, L. Maxit, J.-L. Guyader, Post-traitement et analyse énergétiques de résultats eléments finis, in: Proceedings of CFA 2010, Lyon.

[13] L. Cremer, M. Heckl, B. Petersson, Structure-Borne Sound, Springer, 3rd edn., 2005.

9. Paper IV: Assessment report on SmEdA

EUROPEAN COMMISSION
RESEARCH EXECUTIVE AGENCY

“MID-FREQUENCY”

7th FRAMEWORK PROGRAMME
Marie Curie Initial Training Network (ITN)
Grant Agreement 214909

D21
Assessment report on SmEdA

Deliverable no.	D21
Dissemination level	Public
Work Package	WP2
Author(s)	Rainer Stelzer
Co-author(s)	Nicolas Totaro, Goran Pavic, Jean-Louis Guyader
Status (F: final, D: draft)	F (15.09.2011)
File Name	D21_assessmentreport_SmEdA.pdf
Project Start Date and Duration	October 1st, 2008 - September 30, 2012

Contents

1. Executive summary

The most popular methods for the analysis in vibro-acoustics are the finite element method (FEM) and the statistical energy analysis (SEA). FEM is used for the low frequency range, because the computational cost increases strongly with rising frequency. Another disadvantage of this method is that a lot of calculations for single frequencies steps are necessary to get average values over frequency bands, which are often used in practical applications. The second method, the statistical energy analysis, is an energy based approach for high frequencies, which outputs global energy values for each subsystem without any information about the distributions of these energies.
To close the gap in the mid frequency range between FEM and SEA and to overcome their described drawbacks, the statistical modal energy distribution analysis (SmEdA) is developed since more than 10 years. This method is based on the principle of the energy conversation like SEA but describes contrary to SEA the power exchange between subsystems with couplings between the modes of these subsystems and not only with couplings between whole subsystems. SmEdA is further developed in the framework of “Mid-Frequency” with a focus on the coupling between fluid filled cavities and structures. Due to that this method can handle couplings between all modes, resonant and non resonant ones relating to an excited frequency band, and not only between resonant modes like in previous works. Furthermore, a post-processing method has been developed to obtain energy distributions using the modal energies predicted with SmEdA. This extended version of SmEdA can be used in the whole frequency range and is also principally not statistical. Thus, it is maybe better to call this method modal energy distribution analysis (MEDA).
This deliverable gives first an overview over the recent version of SmEdA and the related post-processing for the prediction of energy distributions. In a second part the application possibilities and advantages of these methods are demonstrated on some examples. At last, the report shows also some recent enhancements and a perspective on the future research.

2. Basic concepts

2.1. Statistical modal Energy distribution Analysis

2.1.1. Coupling between modes

The basis of the energy based method SmEdA are the eigenmodes and eigenfrequencies which have to be calculated first of all for example analytically for easy subsystems or with FEM. To describe the coupling between these modes of different subsystems the analogous mechanical model of two coupled gyroscopic oscillators is used. Maxit and Guyader [1] have demonstrated that this oscillator coupling is equal to the coupling between two modes, if one system is uncoupled a blocked system and the other is uncoupled a free system on the coupling area. This is for example the case for a cavity-structure coupling. In this way the well established research results for coupled oscillators, which can be found for example in [2], [3], [4] or [5], were used as a basis to define a coupling factor for two coupled modes. Therefore, the coupling factor β_{pq}^{12} between a mode p of a system one and a mode q of a system two was deduced in [6] as

$$\beta_{pq}^{12} = \frac{(W_{pq}^{12})^2}{M_p^1 M_q^2 (\omega_q^2)^2} \left[\frac{\eta_p^1 \omega_p^1 (\omega_q^2)^2 + \eta_q^2 \omega_q^2 (\omega_p^1)^2}{((\omega_p^1)^2 - (\omega_q^2)^2)^2 + (\eta_p^1 \omega_p^1 + \eta_q^2 \omega_q^2)(\eta_p^1 \omega_p^1 (\omega_q^2)^2 + \eta_q^2 \omega_q^2 (\omega_p^1)^2)} \right] \quad (1)$$

with the interaction modal work

$$W_{pq}^{12} = \int_S \Phi_p^1(S) \Phi_q^2(S)\, dS \quad (2)$$

where S is the coupling area and M_p^1, M_q^2, η_p^1, η_q^2, ω_p^1, ω_q^2, Φ_p^1 and Φ_q^2 are respectively the modal masses, the modal damping factors, the eigenfrequencies and the mode shapes of the p-th and the q-th mode of the subsystems one and two. In [7], [8] and [9] it has been shown that this modal coupling loss factor describes the coupling between every pair of two modes of different subsystems (see Figure 1) and not only between resonant ones like it was demonstrated by Maxit [6]. Because of that it is even possible to make calculations with SmEdA for single frequency excitations and for highly damped structures (see [8]).

2.1.2. Power input

Another quantity, which is necessary for the later calculation of the energies of the subsystems is the external power input in each mode for example from a point force on a structure or from a monopole in a fluid filled cavity. For an excited structure the following equation for this modal power input Π_m can be used:

$$\Pi_m = \frac{1}{2} \int_A \Re[p_{ex}(A) v_m^*(A)]\, dA \quad (3)$$

where $p_{ex}(A)$ is an external pressure acting on a area A and * denotes the conjugate complex of a quantity. The modal velocity $v_m(A)$ on the excitation area A of a structure under an arbitrary excitation is given for an uncoupled system in [10] by

$$v_m(A) = \frac{\Phi_m(A)}{M_n(\omega_m^2 - \omega^2 + i\eta_s \omega_m \omega)} \int_A i\omega p_{ex} \Phi_m(A)\, dA \quad (4)$$

where ω_m is the eigenfrequency of the mode m, $\Phi_m(A)$ is the mode shape of the mode m at the excitation area A, ω is the excitation frequency and η_s is the modal damping factor. The power

input for a mode of a fluid filled cavity is defined similar to (3) as follows:

$$\Pi_m = \frac{1}{2}\Re[p_m(x_q)Q^*]\,dA \tag{5}$$

or

$$\Pi_m = \frac{1}{2}\int_A \frac{\Re[p_m(A)p_m^*(A)]}{Z}\,dA \tag{6}$$

where Q is the the volume source strength of a point monopole [11] and Z is the impedance of the fluid. In the case of a monopole excitation, equation (5), the modal pressure $p_m(x_q)$ at the location x_q of the monopole is given in [11] by

$$p_m(x_q) = i\omega\rho_f Q\frac{\Phi_m^2(x_q)}{N_m(k^2-k_m^2)} \tag{7}$$

where $\Phi_m(x_q)$ is the mode shape of the mode m at the excitation point x_q, ρ_f is the density of the fluid and N_m is the norm of a mode m. The wave numbers k_m and k, which includes damping using a complex sound velocity [10], are given by

$$k_m = \frac{\omega_m}{c_f} \tag{8}$$

and

$$k = \frac{\omega}{c_f(1+i\eta_f)} \tag{9}$$

where c_f is the sound velocity of the fluid. The relation between this damping factor η_f of the fluid and a damping factor η_e, which is defined in a complex modulus of elasticity $D = \overline{D}(1+i\eta_e)$ and normally used in SmEdA and FEM calculations, is given for a small damping (4% error for $\eta_e = 0.5$ [10]) by

$$\eta_f = \frac{\eta_e}{2} \tag{10}$$

Furthermore, η_f can be linked to the absorption on the boundary surfaces and can be expressed for the case of equipartition of the absorption as [12]

$$\eta_f = \frac{A_s c_f}{4\omega V_f} \tag{11}$$

where A_s and V_f are the equivalent absorption area and the volume of a fluid filled cavity. For the other possible excitation of a fluid filled cavity, the excitation via a vibrating boundary structure, equation (6) is used. The modal pressure $p_m(A)$ at the excitation area A reads here [11]:

$$p_m(A) = -\rho_f\omega^2\Phi_m\sum_s \frac{a_s W_{ms}}{N_m(k^2-k_m^2)} \tag{12}$$

where W_{rs} is the interaction modal work, equation (2). The modal amplitude a_s of the s-th mode of the structure is the amplitude of the velocity $v_m(A)$ from equation (4).

2.1.3. Energies of subsystems

To calculate first the modal energies and then the total energies of total subsystems a power balance equation system is used like in SEA, but with one equation for each mode instead of one for each subsystem. This means, that all the input power Π^i_m (see previous chapter) of a mode m of a subsystem i must be dissipated ($\Pi^i_{dis,m}$) in this mode or must be transmitted into other connected modes of other subsystems ($\Pi^i_{ex,m}$).

$$\Pi^i_m = \Pi^i_{dis,m} + \Pi^i_{ex,m} \tag{13}$$

Using the modal coupling factor β^{12}_{pq}, equation (1), the power balance equation system reads in terms of the modal energies E^1_p and E^2_q of a system one and two [1]:

$$\Pi^1_p = \eta^i_p \omega^1_p E^1_p + \sum_{q=1}^{q_{max}} \beta^{12}_{pq}(E^1_p - E^2_q) \tag{14}$$

The sum of all these modal energies of a subsystem i gives the whole energy E^i of a subsystem i [13, 8].

$$E^i = \sum_n E^i_n \tag{15}$$

If only resonant modes are taken into account, it is also possible to calculate the SEA coupling loss factors η_{ij} on condition of modal equipartition of energy and to make a classical SEA calculation. Those factors η_{ij} result from the modal coupling loss factors [13] as follows:

$$\eta_{12} = \frac{1}{p_{max}\omega_c} \sum_{p=1}^{p_{max}} \sum_{q=1}^{q_{max}} \beta^{12}_{pq} \tag{16}$$

$$\eta_{21} = \frac{1}{q_{max}\omega_c} \sum_{p=1}^{p_{max}} \sum_{q=1}^{q_{max}} \beta^{12}_{pq} \tag{17}$$

where p_{max} and q_{max} are the number of resonant modes relating to an excited frequency band with the central frequency ω_c.

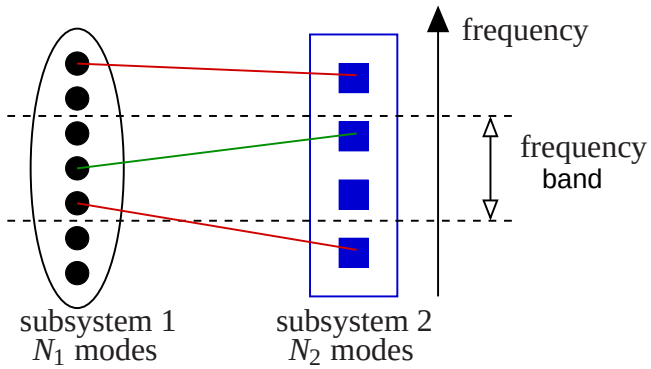

Figure 1.: Resonant and non resonant modes and their different coupling possibilities

2.2. Energy distributions

2.2.1. Energy distribution of a single mode

To characterise the energy distribution of a single mode there are the following equations from [14] and [15] for the total energy density distribution e_n^t, the kinetic energy density e_n^k and the potential energy distribution e_n^p as functions of the modal energy E_n.

$$e_n^t = \frac{E_n}{N_n}\Phi_n^2 \tag{18}$$

$$e_n^p(Q) = E_n^p \frac{\left(\Phi_n^Q\right)^T M\Phi_n}{M_n} = \frac{E_n\left(\Phi_n^Q\right)^T M\Phi_n}{\left(1+\frac{\omega^2}{\omega_n^2}\right)M_n} \tag{19}$$

$$e_n^k(Q) = E_n^k \frac{\left(\Phi_n^Q\right)^T K\Phi_n}{K_n} = \frac{E_n\left(\Phi_n^Q\right)^T K\Phi_n}{\left(1+\frac{\omega_n^2}{\omega^2}\right)K_n} \tag{20}$$

where ^{T} denotes the transpose of a vector, Φ_n^Q is the mode shape of the mode n at a point Q, M and K are the stiffness and the mass matrix and Φ_n, N_n, M_n and K_n are respectively the mode shape, the norm, the modal mass and the modal stiffness of a mode n. The excitation frequency ω can be approximated for calculations with non resonant modes for the case of an excited frequency band as the central frequency ω_c of this frequency band. The equations (18) and (20) are only approximate formulas for structures, because the deformation of a structure can not be defined for single points like these equations make it with the energies but only for areas. In contrast, the kinetic energy can be given for single points when a diagonal mass matrix is used, because that defines a mass for each single point of a mesh. To get a correct solution for the potential energy of a structure it is necessary to use instead of the stiffness matrix K the element stiffness matrix K_e like it is done in FEM programs [16]

$$e_n^p = \frac{1}{2}u^T K_e u \tag{21}$$

where u is the displacement of the structure. Thus, it results for the potential energy distribution as a function of the modal energy similar to equation (20)

$$e_n^p = E_n^p \frac{\left(\Phi_n^R\right)^T K_e \Phi_n^R}{K_n} = \frac{E_n E_{n,R}^s}{\left(1+\frac{\omega_n^2}{\omega^2}\right)E_n^s} \tag{22}$$

where Φ_n^R is the modal vector of an element R of the mode n. Instead of calculating directly with the element stiffness matrix it is easier– if for example the FEM program Nastran is used– to work with the element modal strain energies $E_{m,R}^s$ and the total modal strain energy E_n^s of a mode n like it is shown in equation (22). For a fluid filled cavity equation (18) is applied. This equation gives here an exact result for the energy density distribution, because the pressure in a cavity is defined for single points and the energy density e^t at a point is so given by [17]:

$$e^t = \frac{p_i^2}{2\rho_f c_f^2} \tag{23}$$

where p_i is the pressure at a point i and ρ_f and c_f are the density and the sound velocity of the fluid.

2.2.2. Energy distributions of whole subsystems

The energy distribution of a whole subsystem for an arbitrary excitation has been derived in [8] from a superposition principle as a function of the modal energy distributions of the previous chapter as

$$e^i(\Delta\omega) = \sum_m e^i_m(\Delta\omega) + 2\sum_m \sum_{n=m+1} C_{mn}\sqrt{e^i_m(\Delta\omega)e^i_n(\Delta\omega)} \tag{24}$$

where $e^i(\Delta\omega)$ is the total, kinetic or potential energy distribution of a whole broadband excitation with the bandwidth $\Delta\omega$. The correction factor C_{mn} describes the correlation between two modes and can be written as [15]

$$C_{mn} = \frac{\int_{\Delta\omega} S_{mn}S^d_{mn}\sqrt{\Pi_m(\omega)\Pi_n(\omega)}\,d\omega}{\sqrt{\int_{\Delta\omega}\Pi_m(\omega)\,d\omega\int_{\Delta\omega}\Pi_n(\omega)\,d\omega}} \tag{25}$$

This correction is necessary, because some information, which is important to identify the spatial and the frequency correlation of modes, get lost using frequency band averaged energies. The spatial correlation is characterised by the factors S_{mn} and S^d_{mn}. S_{mn} compares the signs of the amplitudes of two modes, which depend on the given excitation, and can be approximated using analytic solutions for the amplitudes of the velocities $\hat{v}$ or of the pressures $\hat{p}$ of uncoupled systems (see equations (4), (7) and (12)) as follows [8]:

$$S_{mn} = sign(\hat{p}_m\hat{p}^*_n) = sign(\hat{v}_m\hat{v}^*_n) \tag{26}$$

The other factor, S^d_{mn}, describes the relation between the modes at a point Q and is for the kinetic and the potential energy distributions, equations (19), (20) and (22), equal to the cosine of the angle α between two modal shape vectors at Q (only the translational degrees of freedom are used here!) [15].

$$S^d_{mn} = \cos\alpha = \frac{\Phi^Q_m\Phi^Q_n}{\left|\Phi^Q_m\right|\left|\Phi^Q_n\right|} \tag{27}$$

For the total energy distribution, equation (18), S^d_{mn} is 1, because the shape functions Φ_n can be extracted from the root of the second term of equation (24). The second type of correlation, the frequency correlation, is described with the power inputs $\Pi_m(\omega)$ and $\Pi_n(\omega)$ in the modes m and n, which are given in section 2.1.2. In this way the correction factor C_{mn}, equation (24), can be for example written for a structure excited with a point force at a point Q as

$$C_{mn} = \frac{\int_{\Delta\omega} S_{mn}S^{(2)}_{mn}\sqrt{\dfrac{\omega^4}{\left[\left(\omega^2_m-\omega^2\right)^2+\left(\eta_s\omega_m\omega\right)^2\right]\left[\left(\omega^2_n-\omega^2\right)^2+\left(\eta_s\omega_n\omega\right)^2\right]}}\,d\omega}{\sqrt{\int_{\Delta\omega}\dfrac{\omega^2}{\left(\omega^2_m-\omega^2\right)^2+\left(\eta_s\omega_m\omega\right)^2}\,d\omega\int_{\Delta\omega}\dfrac{\omega^2}{\left(\omega^2_n-\omega^2\right)^2+\left(\eta_s\omega_n\omega\right)^2}\,d\omega}} \tag{28}$$

with

$$S_{mn} = sign\left(\left\{\left[\omega^2_m-\omega^2\right]\left[\omega^2_n-\omega^2\right]+\eta_s\omega_m\omega_n\omega^2\right\}\Phi_m(Q)\Phi_n(Q)\right) \tag{29}$$

3. Performance illustrations

3.1. Plate-cavity system

The first example, which is presented in this deliverable to demonstrate the application possibilities of the SmEdA approach and the post-processing method for the energy distributions, is a system of a point force excited rectangular plate coupled to a parallelepipedic cavity (see Figure 2). The plate is excited with a point force ($[F] = 1N$) between 600 and 800 Hz at one point, which has the coordinates $x_e = 0.211765$ and $y_e = 0.189474$. The characteristics of the plate and the cavity are presented in Table 1. Contrary to [8], only a system with one cavity is used here and the modes for the following calculation examples are predicted with FEM and not analytically.

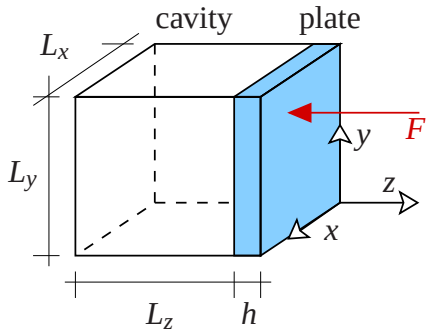

Figure 2.: Sketch of the point force excited system

	plate	**cavity**
$L_x \times L_y \times L_z(h)\ (m)$	$1.2 \times 0.9 \times 0.004$	$1.2 \times 0.9 \times 0.7$
$\rho\ (kg/m^3)$	7820	1.2
$c\ (m/s)$		340
η	0.01	0.01
$E\ (MPa)$	210	
ν	0.3	

Table 1.: Characteristics of the subsystems

3.1.1. Energies of the subsystems

In the Figures 3 and 4 the results for the total energies of the different subsystems calculated with SmEdA are compared for three 200 Hz frequency bands with those predicted with a standard direct FEM calculation. For the SmEdA calculation the results with (SmEdA non resonant) and without (SmEdA resonant) non resonant modes are shown in these figures to illustrate the influence of the non resonant modes for different plate damping factors. For the prediction with non resonant modes all the modes between 0 and 1500 Hz are taken into account here. There are 342 cavity modes and 121 plate modes in this frequency range (see table 2). For the lower plate damping, $\eta_p = 0.01$, these non resonant modes play for the plate energy and even for the energy in the cavity a quite small role like Figures 3.1 and 4.1 demonstrate. But for the case of the higher plate damping, $\eta_p = 0.1$ (see Figures 3.2 and 4.2), it is important especially for the non directly excited cavity to take into account non resonant modes, otherwise the difference to the FEM calculation is up to 8 dB. All in all, the energy values predicted with SmEdA using non resonant modes agree well with those of the FEM calculation. Only for the highest frequency band it would be necessary to increase the number of modes for the calculation of the cavity energy – as it was done in [8]– to get a more exact result for the cavity.

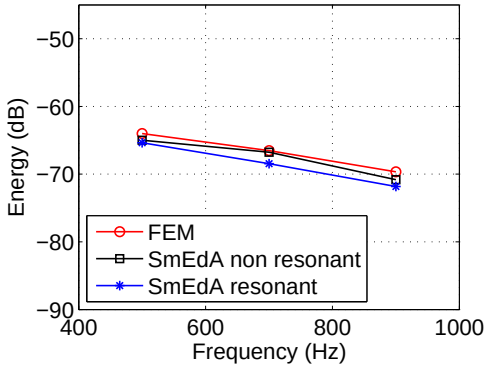

3.1: Energy in the cavity ($\eta_p = 0.01$)

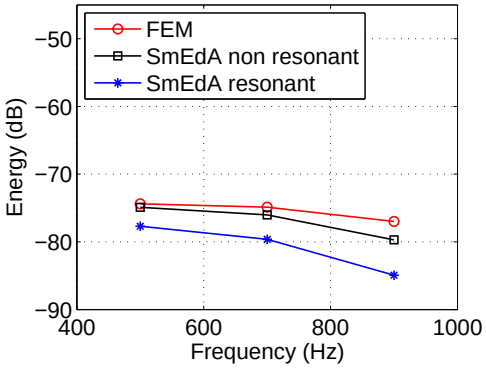

3.2: Energy in the cavity ($\eta_p = 0.1$)

Figure 3.: Energy in the cavity at different plate damping factors η_p

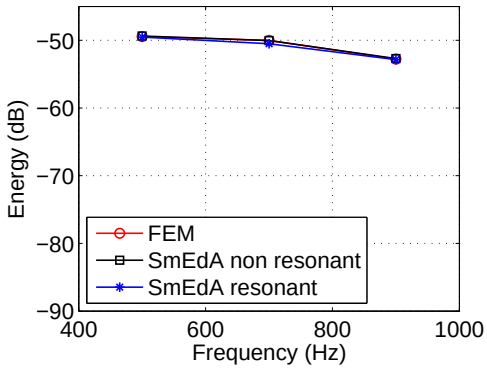

4.1: Energy of the plate ($\eta_p = 0.01$)

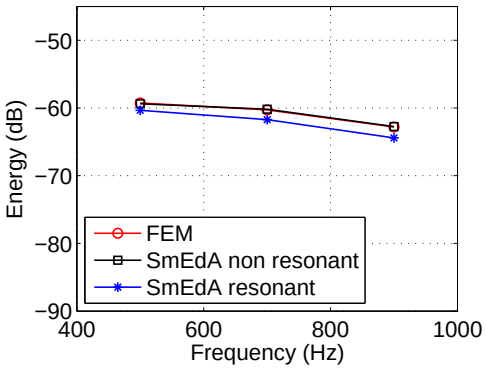

4.2: Energy of the plate ($\eta_p = 0.1$)

Figure 4.: Energy of the plate at different plate damping factors η_p

	plate	**cavity**
degrees of freedom	12168	62868
number of modes		
0 - 400 Hz	28	12
400 - 600 Hz	16	21
600 - 800 Hz	16	34
800 - 1000 Hz	19	51
1000 - 1500 Hz	42	224

Table 2.: Degrees of freedoms and number of modes of the plate and the cavity

3.1.2. Energy distributions of the subsystems

Next, the kinetic and potential energy distributions of the plate calculated with SmEdA and the post-processing from section 2.2 are compared for the excited frequency band from 600 to 800 Hz in Figures 5 to 8 for the plate damping factors $\eta_p = 0.01$ and $\eta_p = 0.01$ to those predicted with FEM. For this purpose the modal energy results of the SmEdA calculation are taken, which use all the modes between 0 and 1500 Hz (see previous section). These comparison demonstrates that even energy distributions with a concentration of energy at one area around the excitation can be obtained well with the modal energies calculated with SmEdA and the used post-processing method. As Figures 6.1, 6.2, 8.1 and 8.2 moreover show, it is necessary to use equation (22) for the modal potential energy distribution in the calculation process instead of the approximative one, (20), to get a good result for the potential energy distribution at the boundary.

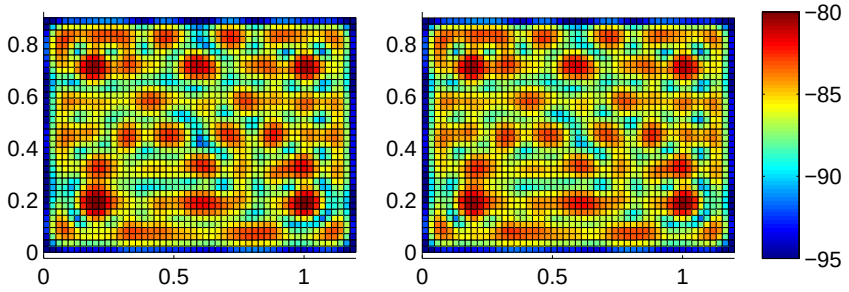

5.1: SmEdA 5.2: FEM

Figure 5.: Kinetic energy distribution of the plate (plate damping $\eta_p = 0.01$)

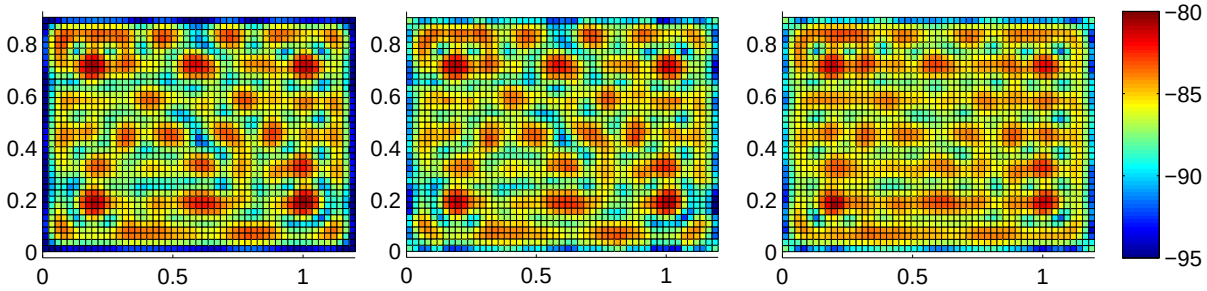

6.1: SmEdA using equation (20) 6.2: SmEdA using equation (22) 6.3: FEM

Figure 6.: Potential energy distribution of the plate (plate damping $\eta_p = 0.01$)

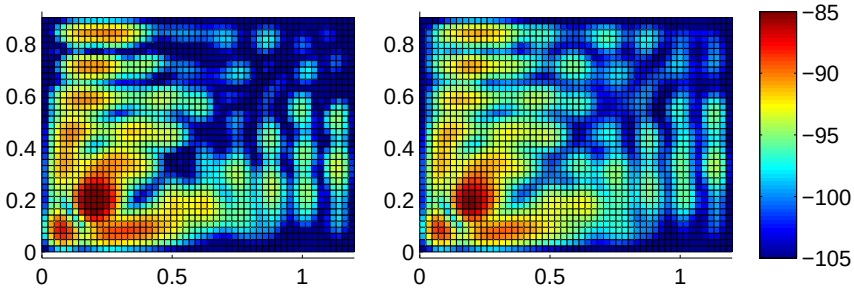

7.1: SmEdA 7.2: FEM

Figure 7.: Kinetic energy distribution of the plate (plate damping $\eta_p = 0.1$)

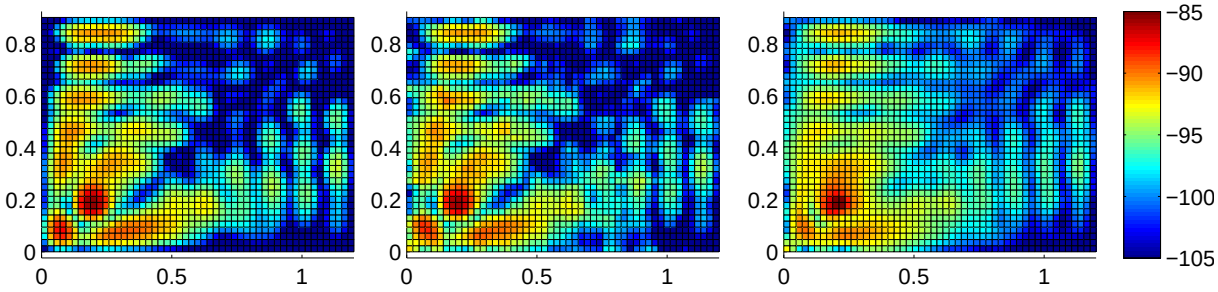

8.1: SmEdA using equation (20) 8.2: SmEdA using equation (22) 8.3: FEM

Figure 8.: Potential energy distribution of the plate (plate damping $\eta_p = 0.1$)

Finally, also the energy density distribution in the mid of the cavity at $z = -0.3624$ predicted with SmEdA and FEM is given in Figure 9 for the case of the plate damping $\eta_p = 0.01$ and the excited frequency band from 600 to 800 Hz. The result for this energy density distribution of the post-processing method using SmEdA results agrees again –like the energy distributions for the plate – well with those of FEM.

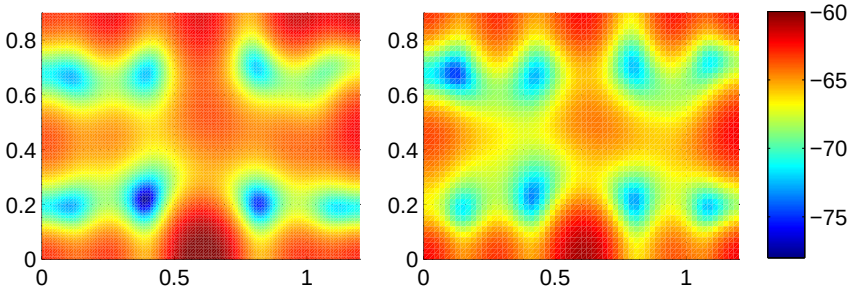

9.1: SmEdA 9.2: FEM

Figure 9.: Energy density distribution in the cavity at $z = -0.3624$ (plate damping $\eta_p = 0.01$)

3.2. Transmission loss

The next example of the performance illustration is quite similar to the first one (see Figure 2) but with one cavity on both sides of the plate (see Figure 10) and with an excitation in an edge of a cavity (sending cavity) with a monopole source. This excitation is more or less equal to an equal power input in all the resonant modes like it was done in [7]. The transmission loss of such a small system calculated by SmEdA is compared in the following sections to the infinite models, the mass law and the formula of Cremer, and a standard FEM calculation. The coincidence frequency of the plate is 2933 Hz. The other characteristics of the subsystems are given in Table 3.

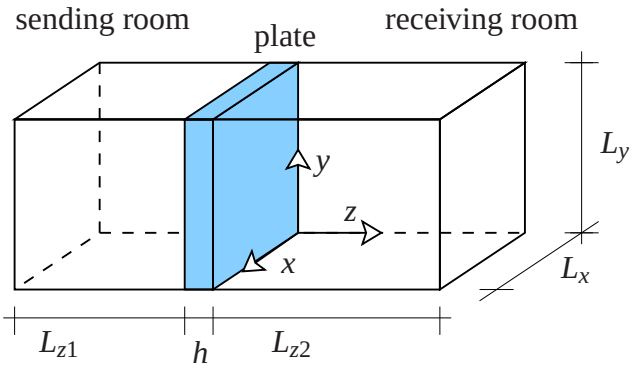

Figure 10.: Sketch of the cavity-plate-cavity system

	plate	**sending room**	**receiving room**
$L_x \times L_y \times L_z(h)\ (m)$	$1.2 \times 0.9 \times 0.004$	$1.2 \times 0.9 \times 0.7$	$1.2 \times 0.9 \times 1$
$\rho\ (kg/m^3)$	7820	1.2	1.2
$c\ (m/s)$		340	340
η	0.01	0.01	0.01
$E\ (MPa)$	210		
ν	0.3		

Table 3.: Characteristics of the subsystems

In the present case the necessary eigenmodes and eigenfrequencies for SmEdA can be calculated quite easily analytically. The eigenmodes p_{qrs} and the eigenfrequencies ω_{qrs} of the cavities are given by [18]

$$p_{qrs} = \cos\left(\frac{q\pi x}{L_x}\right)\cos\left(\frac{r\pi y}{L_y}\right)\cos\left(\frac{s\pi z}{L_z}\right); \quad q,r,s = 0,1,2,3,\ldots \tag{30}$$

and

$$\omega_{qrs} = c\sqrt{\left(\frac{q\pi}{L_x}\right)^2 + \left(\frac{r\pi}{L_y}\right)^2 + \left(\frac{s\pi}{L_z}\right)^2} \tag{31}$$

The eigenfrequencies ω^s_{mn} and the modes W^s_{mn} of the simply supported plate are

$$\omega^s_{mn} = \pi^2\left[\left(\frac{m}{L_x}\right)^2 + \left(\frac{n}{L_y}\right)^2\right]\sqrt{\frac{B}{m}}; \quad m,n = 1,2,3,\ldots \tag{32}$$

and

$$W_{mn}^{s} = \sin\left(\frac{m\pi x}{L_x}\right)\sin\left(\frac{n\pi y}{L_y}\right) \tag{33}$$

with the mass per area m and the bending stiffness B of the plate.

3.2.1. Comparison to the infinite transmission loss models

Like it was demonstrated in section 3.1.1 the interaction between a small simple supported plate and a cavity is dominated for low plate damping by the relation of the resonant modes and the influence of the non resonant modes relating to an excited frequency band grows with an increasing damping. This behaviour appears also in the case of the transmission loss of such a system, because there is only a significant difference in the transmission loss between SmEdA with (SmEdA non resonant) and without non resonant modes (SmEdA resonant) at the plate damping $\eta_p = 0.1$ (see Figures 11 to 13). The transmission loss graphs in these figures were calculated for excited frequency bands with a bandwidth of 400 Hz and for the calculations with non resonant modes all the modes from 800 Hz below to 200 Hz above the respective frequency band were used. In comparison of these results for the transmission loss predicted with SmEdA to the infinite transmission loss model, the formula of Cremer, it attracts attention that the SmEdA results are contrary to the formula of Cremer sensitive below the critical frequency to a change of the damping. The reason for this is that the incident power on an infinite plate is transmitted below the critical frequency only by the non resonant modes, on which the damping has no influence, and not by resonant modes like it is the case at a small simple supported plate. In [7] it is demonstrated that these different behaviour depends not only on the size of the plate but for example also on the boundary condition, because the transmission loss of a free plate is also fully dominated by the non resonant modes below the critical frequency. Another difference between an infinite and a small finite system is that the mode densities of a small plate and of a small cavity (see Figure 2) are much smaller than those of infinite systems, which are infinity. Because of that the interaction between the different subsystems is in general maybe worser for finite systems at a given frequency if resonance effects plays there not a role. Hence, the transmission loss of the highly damped small plate (Figure 11) is much bigger than those of the formula of Cremer, because the resonant effects are more or less suppressed.

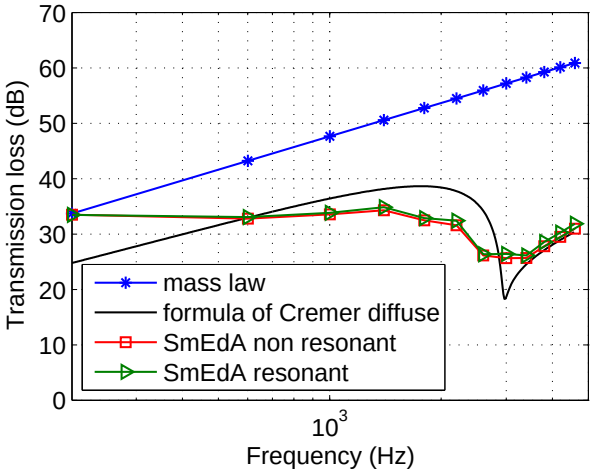

Figure 11.: Transmission loss for plate damping $\eta_p = 0.001$ (frequency band width: 400 Hz)

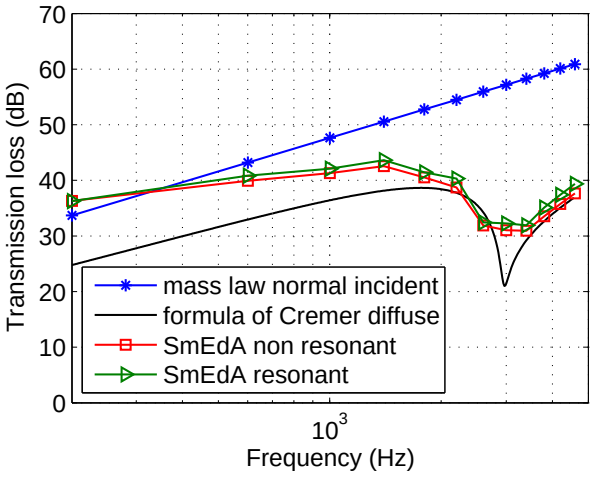

Figure 12.: Transmission loss for plate damping $\eta_p = 0.01$ (frequency band width: 400 Hz)

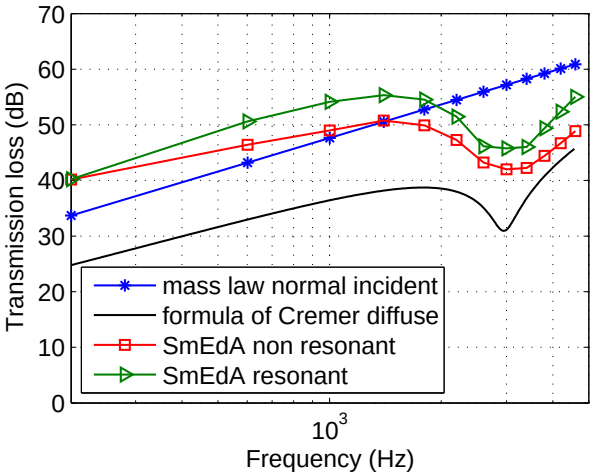

Figure 13.: Transmission loss for plate damping $\eta_p = 0.1$ (frequency band width: 400 Hz)

To demonstrate that all these described effects are not influenced of possible different descriptions of the transmission mechanism of the formula of Cremer and of the SmEdA approach and to validate the SmEdA transmission loss model, the formula of Cremer was derived analytically with the SmEdA formalism [9]. Under the same assumptions as for the formula of Cremer (free sound fields on both sides of the plate, infinite plate, etc.) the transmission loss predicted with SmEdA is given by

$$R_s = 10\lg\left[1+\left(\frac{\cos\vartheta}{2\rho c}\right)^2\left\{\left(\omega m-\omega^3 B\frac{\sin^4\vartheta}{c^4}\right)^2+mB\eta^2\omega^4\frac{\sin^4\vartheta}{c^4}\right\}\right] \tag{34}$$

where ϑ is angle of incidence, B, η and m are the bending stiffness, the damping and the mass per area of the plate and c and ρ are the density and the speed of sound of the fluid. Compared to the original formula of Cremer (equation (35)), in which the damping is taken into account via the usual assumption of a complex bending stiffness $\hat{B} = B(1-i\eta)$, only the damping term of equation (34) is different.

$$R_c = 10\lg\left[1+\left(\frac{\cos\vartheta}{2\rho c}\right)^2\left\{\left(\omega m-\omega^3 B\frac{\sin^4\vartheta}{c^4}\right)^2+B^2\eta^2\omega^6\frac{\sin^8\vartheta}{c^8}\right\}\right] \tag{35}$$

But a graphical comparison in Figure 14 of this two equations for a diffuse incident sound (average over all the angles of incidence) shows that this makes only a small difference at the critical frequency.

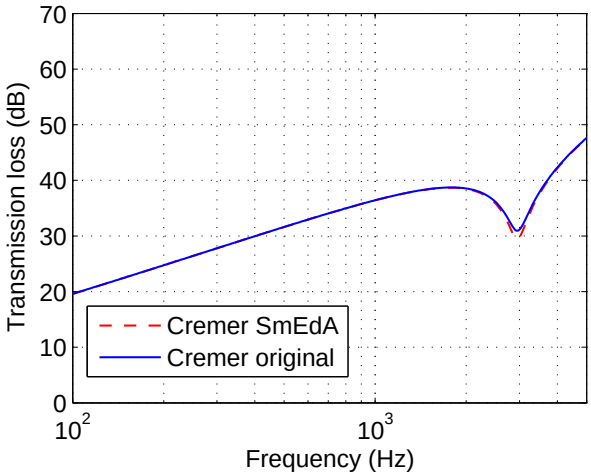

Figure 14.: Transmission loss of the infinite models from Cremer and SmEdA (plate damping $\eta_p = 0.1$)

3.2.2. Comparison to FEM

To compare the transmission loss calculation with SmEdA and with FEM the transmission loss for the plate damping factors $\eta_p = 0.01$ and $\eta_p = 0.001$ is illustrated in Figure 15. The bandwidth of the excited frequency is here 200 Hz. This Figure shows that contrary to the transmissions losses predicted with SmEdA (only resonant modes are used) those calculated with FEM are less sensitive to a change of the plate damping and always higher in the investigated frequency range than the transmission loss of the mass law/ formula of Cremer.

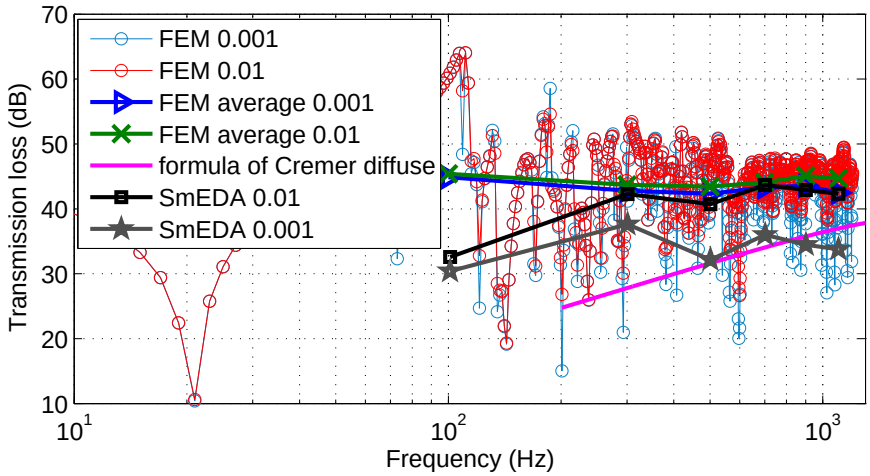

Figure 15.: Comparison of the transmission loss for different plate damping factors η_p calculated with SmEdA and FEM

To investigate where this difference come from the FEM formulation must be discussed. In FEM a coupled fluid-structure system is normally described with two coupled differential equation system as follows [19]:

$$\begin{bmatrix} M_s & 0 \\ -C^T & M_f \end{bmatrix} \begin{bmatrix} \ddot{U} \\ \ddot{P} \end{bmatrix} + \begin{bmatrix} D_s & 0 \\ 0 & D_f \end{bmatrix} \begin{bmatrix} \dot{U} \\ \dot{P} \end{bmatrix} + \begin{bmatrix} K_s & C \\ 0 & K_f \end{bmatrix} \begin{bmatrix} U \\ P \end{bmatrix} = \begin{bmatrix} L_s \\ L_f \end{bmatrix} \tag{36}$$

where U is the displacement of the structure, P is the pressure in the fluid and M_s, M_f, D_s, D_f, K_s, K_f, L_s and L_f are respectively the mass, the damping and stiffness matrices and the external force vectors of the structure and the fluid. One important assumption of this formulation is that the boundary surface of the cavity are considered as rigid and a vibrated boundary is handled like a source at these rigid boundaries [20]. In this way the formulation, which describes finally the interaction between bending modes of a structure and modes of a cavity, does not respect the boundary conditions of the equality of the velocities on the surface. That means in the modal description that the summation of all modes converge against the correct surface pressure but leads to wrong normal velocities on the boundaries [20]. This is maybe not a problem for a system which consists of one structure and one fluid filled cavity. But to get a complete and correct description of coupled fluid-structure problems it is necessary to respect the velocity boundary condition, like it is also written in [11]. In contrast, this problem with this boundary condition is taken into account in SmEdA (see [7, 8, 9]). All in all, because of these facts the mistake, which is made by a such FEM calculation, is big for a transmission loss problem and thus this FEM formulation seems not to be convenient for systems with more than two subsystems.

3.3. Double-deck train

In the following a section of a double-deck train (Figure 16) is chosen as an industrial example of use to demonstrate the application possibilities of the SmEdA approach and the post-processing method for energy distributions (see chapter 2) also on a real complex industrial case. The section of the train is simulated as a simple supported structure coupled to two cavities. The structure consists of many different components (windows, stiffnessers, ...) and is excited with 8 point forces at the bottom between 280 and 355 Hz. The number of degrees of freedom and the number of modes in different frequency ranges of these three subsystems are presented in Table 4.

	structure	**lower cavity**	**upper cavity**
degrees of freedom	334920	56699	54079
number of modes			
0 - 280 Hz	120	42	24
280 - 355 Hz	72	30	24
355 - 600 Hz	235	222	178
600 - 1000 Hz	648	850	715

Table 4.: Degrees of freedoms and number of modes of the subsystems

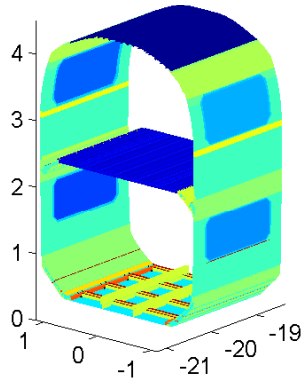

Figure 16.: Model of the train (one colour for each property)

3.3.1. Energies of the subsystems

The energies of the three subsystems calculated with SmEdA and FEM are compared in Table 5. For SmEdA all the modes between 0 and 1000 Hz are taken into account and not only those in the excited frequency band (280-355 Hz), because the contribution of the non resonant modes to the total energies is high, especially for the upper cavity. This is illustrated with the energy ratios of the modes (modal energy divided by the total energy of the corresponding subsystem) between 0 and 1000 Hz in Figure 17. The resonant modes store only 78%, 62% and 28% of the energy of the structure, the lower cavity and the upper cavity respectively. Figure 17 also shows that the most of the energy is stored only in a few modes. All in all, the result for the energies of the structure and the lower cavity of SmEdA are good compared to those of FEM (see Table 4). There is only an essential difference for the energy in the upper cavity. This is maybe a mistake of the used FEM formalism because that does not respect all the boundary conditions as it is described in section 3.2.2.

total energy [**dB**]	**SmEdA**	**FEM**	**difference** [**dB**]
structure	-56.8	-56.2	0.6
lower cavity	-67.4	-65.7	1.7
upper cavity	-81.1	-86.7	5.6

Table 5.: Comparison of the total energies of the subsystems calculated with SmEdA and FEM

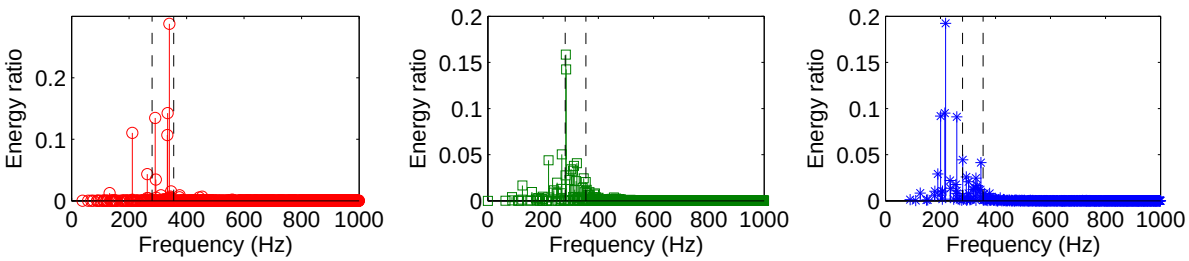

17.1: structure 17.2: lower cavity 17.3: upper cavity

Figure 17.: Energy ratios of the modes (frequency area between the dashed lines: excited frequency band)

3.3.2. Energy distributions of the subsystems

The kinetic energy distribution and the potential energy distribution of the structure predicted with the post-precessing method of SmEdA (see section 2.2) using equations (19) and (22) are quite similar to that calculated with FEM. If the approximate formula for the modal energy distribution, equation (20), is used to describe the potential energy (Figure 19.1), the differences are but quite big especially at the boundaries.

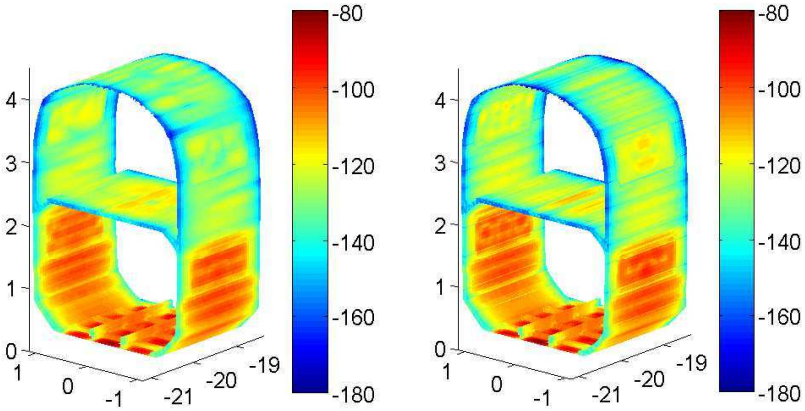

18.1: SmEdA (using all modes from 0 to 600 Hz)

18.2: FEM

Figure 18.: Kinetic energy distribution [dB] of the train structure calculated with SmEdA and FEM

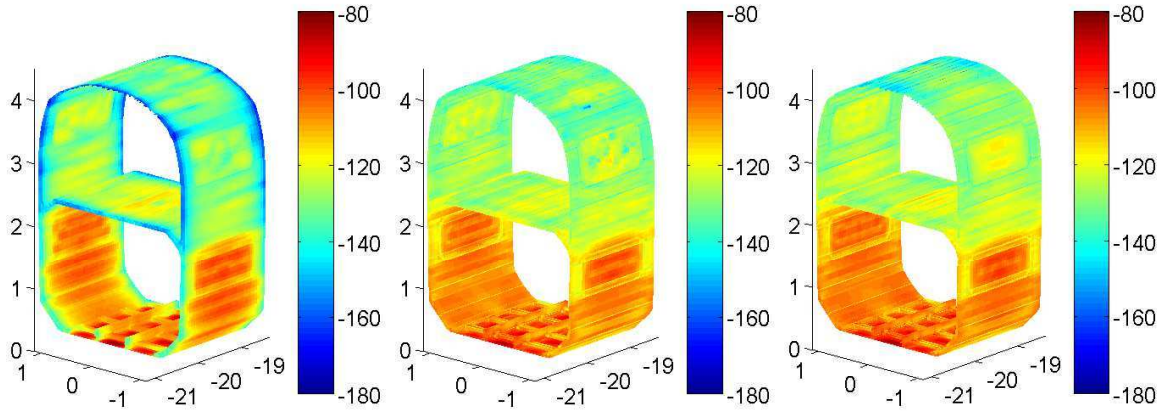

19.1: SmEdA using equation (20)

19.2: SmEdA using equation (22)

19.3: FEM

Figure 19.: Potential energy distribution [dB] of the train structure calculated with SmEdA and FEM

In contrast, there are more discrepancies between the energy distributions for the lower (Figure 20) and the upper cavity (Figure 21) predicted with the post-precessing method and FEM. One reason is certainly that the total energies of the cavities obtained by SmEdA and FEM are differ more than the total energies of the structure (see Table 5) and so do the energy distributions. The problem of the energy distributions of the cavities predicted from the modal energies with the post-processing method is that these converge quite slowly against a stable solution. This is demonstrated by comparing Figures 20 and 21, where in Figures 20.1 and 21.1 all the

modes from 0 to 600 Hz and in Figures 20.2 and 21.2 all the modes from 0 to 1000 Hz have been used for the calculation. Especially for the lower cavity (Figure 21), the change of the energy distribution is enormous when using more modes, although the energies of these modes are negligible for the calculation of the total energies as demonstrated in Figure 17. Therefore, it is difficult to say how much modes are necessary to get a good stable solution for the energy distributions of the cavities.

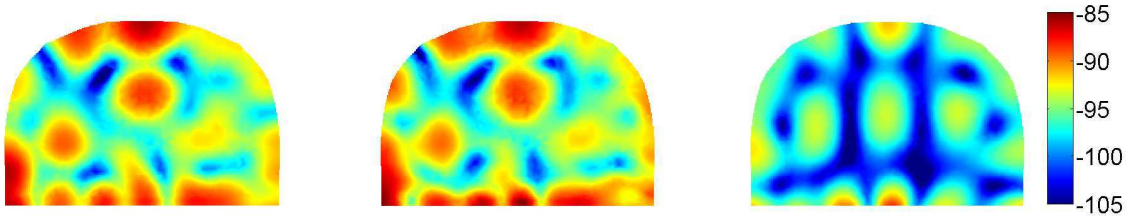

20.1: SmEdA (using all modes from 0 to 600 Hz) 20.2: SmEdA (using all modes from 0 to 1000 Hz) 20.3: FEM

Figure 20.: Energy distribution [dB] of the central section of the upper cavity calculated with SmEdA and FEM

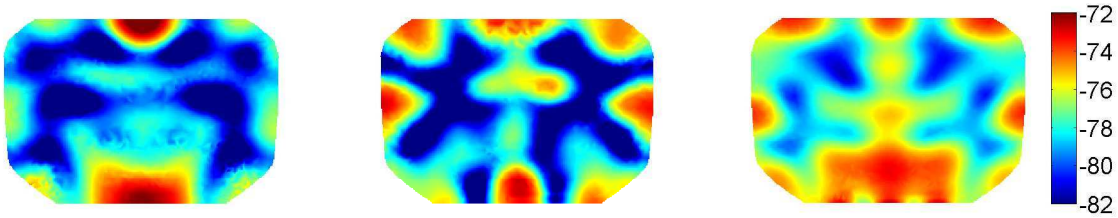

21.1: SmEdA (using all modes from 0 to 600 Hz) 21.2: SmEdA (using all modes from 0 to 1000 Hz) 21.3: FEM

Figure 21.: Energy distribution [dB] of the central section of the lower cavity calculated with SmEdA and FEM

4. Recent enhancements and future research in SmEdA

One of the next steps in the future research is the validation of the SmEdA approach with some of the validation cases, which are defined in the deliverables D8 and D12 of the project "Mid-Frequency". Another part of the future research will be the further development of the recent enhancements in the area of reduction of computational cost. This is an important research topic to handle systems with high mode densities, because the computational cost grows with an increasing number of modes. Two ideas to reach this aim are presented in combination with first easy applications on the transmission loss problem in the following section. Furthermore, in many real problems the damping is not uniformly distributed and thus it will be necessary to investigate in the future how localised damping can be taken into account in SmEdA. Two methods from the literature, which can be used for this purpose, are described shortly in section 4.2.

4.1. Reduction of computational cost

4.1.1. Approximate modes

In the case of huge fluid filled cavities it costs a lot of computational time to predict the huge number of eigenmodes and eiegenfrequencies. To solve this problem a method is developed, which approximate the eigenfrequencies and the shapes of the eigenmodes. For the former the following approximate formula for the mode density n [11] is used as a basis

$$n = \frac{k^2 V_f}{2\pi^2 c_f} \tag{37}$$

where k is the wavenumber and c_f and V_f are the sound velocity and the volume of the fluid. From this equation it follows for the number of modes N in a frequency range via integration over ω

$$N = \int_{\omega_1}^{\omega_2} \frac{k^2 V_f}{2\pi^2 c_f} d\omega \tag{38}$$

Under the assumption that a frequency is an eigenfrequency ω_m, for which under the condition of $\omega_1 = 0$ the number N of the modes is an integer, it results from equation (38)

$$\omega_m = \sqrt[3]{\frac{6\pi^2 c_f^3 m}{V_f}} \tag{39}$$

where m is a positive integer. The approximation of the second part of the eigensystem, the shapes of the eigenmodes, bases upon the idea that every mode can be linked to an angle of incidence of an incident wave. Thus, it follows that there is a minimal possible on the surface of a structure projected wavelength λ_{min}^m for each eigenfrequency ω_m, which corresponds to an incidence parallel to a boundary surface (angle of incidence is 90°). This wavelength λ_{min}^m is given by

$$\lambda_{min}^m = \frac{2\pi c}{\omega_m \sin 90^\circ} = \frac{2\pi c}{\omega_m} \tag{40}$$

Because of that the wavelength λ_m^s of a mode shape on a surface of a coupled structure can takes values between this minimum and infinity (equates to normal incidence of a wave) and can be approximated as follows for each eigenfrequency using a uniformly distributed random angle of incidence ϑ:

$$\lambda_m^s = \frac{2\pi c}{\omega_m \sin \vartheta} \geq \lambda_{min}^m \tag{41}$$

In addition to get a complete description of a mode shape Φ_m^s on a boundary surface relating to a coordinate system it is necessary to define the direction of incidence with an angle φ (see Figure 22) and the phase shift δ.These values can be also characterised as uniformly distributed random numbers, which can take values between zero and 2π. All in all, this random method to get approximate modes works theoretically exact for infinite cavities, because in this case an infinite number of modes exists at every frequency and the angle and the direction of incidence and the phase shift are uniformly distributed. At lower mode densities of real cavities this leads to an error for the eigensystems, but this error becomes smaller for increasing dimensions.

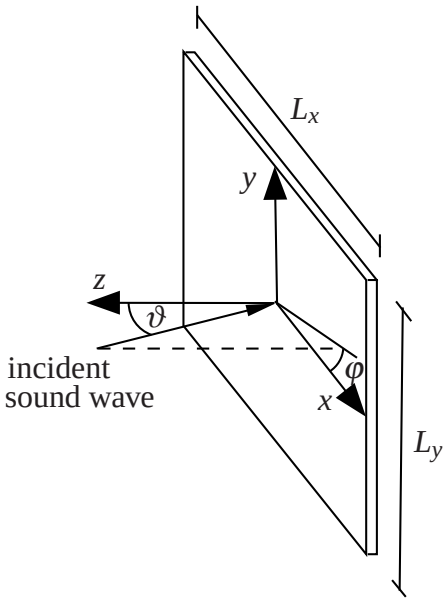

Figure 22.: Sound incident on a boundary surface

In a first example these so approximated eigensystems are used for the calculation of the transmission loss of the small cavity-plate-cavity system from section 3.2. In this case the approximate mode shapes Φ_m^s on the surface of the plate are given by

$$\Phi_m^s = \cos\left(\frac{2\pi x}{\lambda_{m,x}^s} + \delta\right)\cos\left(\frac{2\pi y}{\lambda_{m,y}^s} + \delta\right) = \cos\left(k_f x \sin\vartheta\cos\varphi + \delta\right)\cos\left(k_f y \sin\vartheta\sin\varphi + \delta\right) \tag{42}$$

where k_f is the wavenumber of the fluid and $\lambda_{m,x}^s$ and $\lambda_{m,x}^s$ are the approximate wavelength in the directions of x and y. The so obtained transmission loss is illustrated in Figure 23 for the plate damping factors $\eta_p = 0.01$ and $\eta_p = 0.001$. Using a random phase shift δ gives here in general a huge error below the critical frequency. On the other hand, for a constant $\delta = 0$ the difference in comparison to the exact SmEdA calculation becomes much smaller below the critical frequency. The reason for this phenomena is that the phase shift of the modes of a finite cavity is as a consequence of the boundary condition constant like the formula for cavity modes, equation (30), shows, but at higher frequencies, where the wavelengths are small in comparison to the dimensions of the cavity the influence of the boundary condition becomes less important. All in all, with such a approximate method it is possible to reach even for a small system a quiet good approximation of the transmission loss above the first 400 Hz frequency band, although the modes are very roughly estimated and the numbers of modes are quite small in the frequency bands (see Table 6).

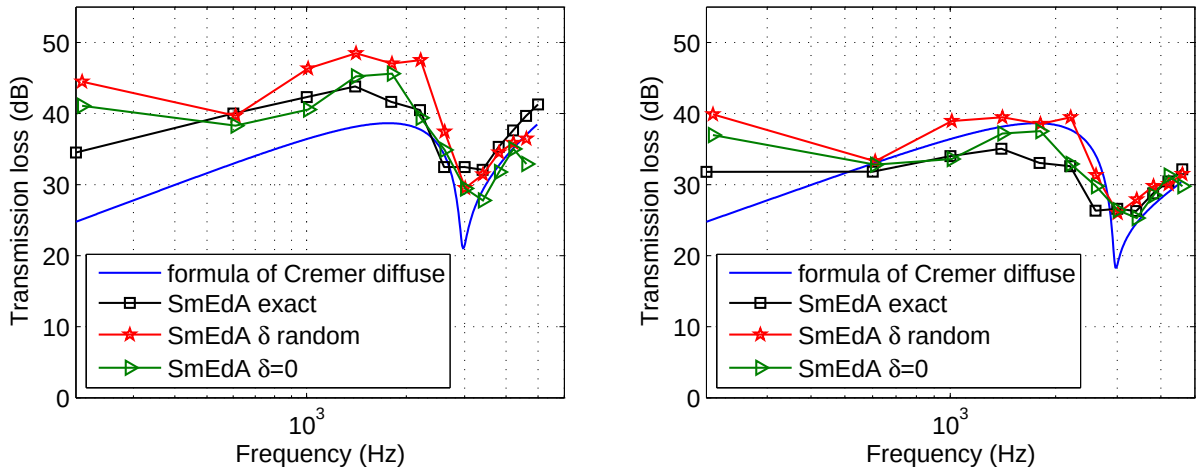

23.1: $\eta_p = 0.01$ 23.2: $\eta_p = 0.001$

Figure 23.: Transmission loss for different plate damping factors η_p predicted with approximate modes

frequency band	**number of modes**			
	sending cavity		receiving cavity	
	exact	approximate	exact	approximate
10 - 410 Hz	11	5	15	7
410 - 810 Hz	55	37	74	54
810 - 1210 Hz	125	100	180	142
1210 - 1610 Hz	237	194	321	277
1610 - 2010 Hz	373	318	517	454
2010 - 2410 Hz	517	473	740	677
2410 - 2810 Hz	741	660	1038	942
2810 - 3210 Hz	951	877	1340	1254
3210 - 3610 Hz	1213	1126	1724	1607
3610 - 4010 Hz	1514	1405	2133	2007
4010 - 4410 Hz	1810	1715	2589	2450
4410 - 4810 Hz	2183	2056	3079	2937

Table 6.: Exact and approximate number of modes in the different frequency bands

4.1.2. Mixed power balance equation systems

Another possibility to reduce the computational cost is to use mixed power balance equation systems. That means that one power balance equation is used for one whole system and power balance equations for each mode for another connected subsystem (see equation (14)). But because of the necessary condition of energy equipartition of the modal energies (see section 2.1.3) it is only possible to take into account resonant modes for the system, which is represented only with one power balance equation. The coupling loss factor for this system is equal to the SEA one and is predicted using equation (16). Finally, a mixed power balance equation system

for two connected subsystems reads [21]:

$$\begin{aligned} P^1 &= \omega_c \left(\eta^1 + \eta_{12}\right) E^1 - E_m^2 \sum_n \beta_{nm}^{12} \\ P_m^2 &= \left(\eta_m^2 \omega_m^2 + \sum_n \beta_{nm}^{12}\right) E_m^2 - \frac{E^1}{n} \sum_n \beta_{nm} \end{aligned} \tag{43}$$

where β_{nm}^{12} is modal coupling loss factor, equation (1), η_{12} is the SEA couplling loss factor, equation (16), ω_m^2, η_m^2, P_m^2 and E_m^2 are the eigenfrequency, the damping factor, the input power and the modal energy of the mode m of subsystem two, ω_c is the central frequency of the excited frequency band, n is the number of modes of subsystem one in the excited frequency band and η^1, P^1 and E^1 are the damping factor, the input power and the energy of the whole subsystem one. Such a mixed power balance equation system can be applied for example for the calculation of the transmission loss, because the non resonant modes can be neglected in general for the sending room. In this way this transmission loss case can be described with one power balance equation for the sending cavity and with power balance equations for each mode of the receiving cavity and of the structure in between the cavities. To demonstrate that this works the transmission loss of the small cavity-plate-cavity system of section 3.2 is given for the plate damping $\eta_p = 0.1$ in the following figure. Here, the transmission loss graphs are calculated with SmEdA including non resonant modes once using a full power balance equation system (one equation for each mode of each subsystem) and once using the described mixed power balance equation system.

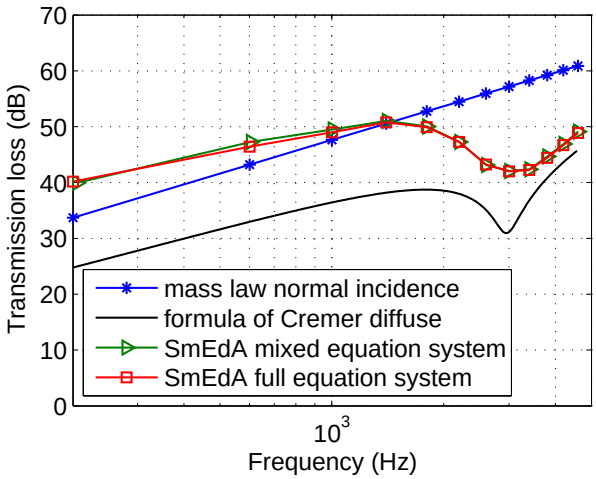

Figure 24.: Transmission loss calculated with a mixed power balance equation system (plate damping $\eta_p = 0.1$)

4.2. Localised damping

To describe a localised damping in modal methods, like SmEdA, it is necessary to define an unique damping factor for each single mode, because the assumption of one equal damping factor for all the modes as used in section 2.1.2 is only valid for uniformly distributed damping. These modal factors can be calculated for example for structures using a strain energy method [22, 23] or a complex eigenvalue method [23, 24, 25]. The strain energy method is used for multi-layered structures or structures with added damping materials in some areas. Here it is

assumed that the damping factor η_d of the damping material is much bigger than those of the other component, for example steel. The modal damping factor for a mode n is given by

$$\eta_n = \frac{\eta_d E^s_{d,n}}{E^s_n} \tag{44}$$

where E^s_n is the total modal strain energy of mode n and $E^s_{d,n}$ is the modal strain energy of mode n contained in the area of the damping material. The other method, the complex eigenvalue method, is applied to arbitrary structures like vehicle components [24]. To get a damping factor for each mode, the complex eigenvalue problem of a damped system, which is described by the following equation, is solved first in this method.

$$M\ddot{y} + D\dot{y} + Ky = F \tag{45}$$

where y is the displacement, F is the excitation force vector and M, K and D are the mass, the stiffness and the damping matrix. The modal damping factors η_m can be calculated from the real and the imaginary part of the complex eigenvalues λ_m as follows [24]:

$$\eta_m = \frac{|\Re(\lambda_m)|}{|\Im(\lambda_m)|} \tag{46}$$

Such a complex eigenvalue method can be maybe also used for cavities, which have not uniformly distributed damping on the boundaries.

5. Conclusion

This deliverable demonstrates after the explanation of the basic concepts (section 2) on some examples (section 3) that SmEdA is a good alternative method for the calculation of coupled cavity-structure problems. One advantage of SmEdA in comparison to FEM is the faster prediction of total energies of subsystems for broad band excitations, because after the calculation of eigensystems only one linear power equation system has to be solved for one frequency band using SmEdA instead of coupled differential equations for a lot of single frequency steps. Moreover, it is also possible to predict energy distributions of the subsystems with the presented post-processing method (see section 2.2) and not only total energies as is the case with SEA. But one problem of SmEdA is that the computation time increases for example with rising frequency like in FEM, because the mode density especially of cavities increase and so does the time for the prediction of the eigensystems and for the SmEdA calculation procedure. Therefore, the development of methods, which reduce the computational cost, has been started (see section 4). Other future research topics will be the handling of localised damping in connection with SmEdA and further application possibilities.

Bibliography

[1] L. Maxit, J.-L. Guyader, Estimation of the SEA coupling loss factors using a dual formulation and FEM modal information, part I: theory, Journal of Sound and Vibration 239(5) (2001) 907–930.

[2] T. Scharton, R. Lyon, Power Flow and Energy Sharing in Random Vibration, Journal of the Acoustical Society of America 43 (6) (1968) 1332–1343.

[3] E. Ungar, Statistical energy analysis of vibrating systems, Tech. Rep. AFFDL-TR-66-52, US Air Force, 1966.

[4] J. Woodhouse, An approach to the theoretical background of statistical energy analysis applied to structural vibration, Journal of the Acoustical Society of America 69 (6) (1981) 1695–1709.

[5] R. H. Lyon, R. G. DeJong, Theory and application of statistical energy analysis, Butterworth-Heinemann, 2nd edn., 1995.

[6] L. Maxit, Extension et reformulation du modèle SEA par la prise en compte de la répartition des énergies modales, Ph.D. thesis, INSA Lyon, 2000.

[7] R. Stelzer, N. Totaro, G. Pavic, J. Guyader, Prediction of Transmission Loss using an improved SEA Method, in: Proceedings of CFA 2010, Lyon.

[8] R. Stelzer, N. Totaro, G. Pavic, J. Guyader, L. Maxit, Non resonant contribution and energy distributions using Statistical modal Energy distribution Analysis (SmEdA), in: Proceedings of ISMA 2010, Leuven.

[9] R. Stelzer, N. Totaro, G. Pavic, J.-L. Guyader, Non resonant modes and Transmission Loss using Statistical modal Energy distribution Analysis (SmEdA), article in preparation, 2011.

[10] L. Cremer, M. Heckl, B. Petersson, Structure-Borne Sound, Springer, 3rd edn., 2005.

[11] F. Fahy, Foundations of Engineering Acoustics, Elsevier, 2005.

[12] K. Renji, P. S. Nair, S. Narayanan, Non-resonant response using statistical energy analysis, Journal of Sound and Vibration 241(2) (2001) 253–270.

[13] N. Totaro, C. Dodard, J.-L. Guyader, SEA coupling loss factors of complex vibro-acoustic systems, Journal of Vibration and Acoustics 131 (2009) 041009–4.

[14] N. Totaro, L. Maxit, J.-L. Guyader, Post-traitement et analyse énergétiques de résultats eléments finis, in: Proceedings of CFA 2010, Lyon.

[15] R. Stelzer, N. Totaro, G. Pavic, J. Guyader, Improved modal energy analysis for industrial problems, in: Proceedings of ICSV 18, 2011 (Rio de Janeiro).

[16] MSC-Software-Corporation, MSC.Nastran 2001: Quick reference Guide, 2000.

[17] M. Bruneau, Fundamentals of acoustics, ISTE, 2006.

[18] M. Möser, Technische Akustik, Springer, 7th edn., 2007.

[19] M. Chargin, O. Gartmeier, A finite element procedure for calculating fluid-structure interaction using MSC/Nastran, Tech. Rep. NASA Technical Memorandum 102857, NASA (National Aeronautics and Space Adminstration), 1990.

[20] F. J. Fahy, Sound and structural vibration : radiation, transmission and response, Elsevier/Acad. Press Amsterdam, 2nd edn., 2007.

[21] L. Maxit, J.-L. Guyader, Extension of SEA model to subsystems with non-uniform modal energy distribution, Journal of Sound and Vibration 265 (2003) 337–358.

[22] T. H. Fronk, K. C. Womack, K. D. Ellis, L. W. Finlinson, Finite element modelling of damping in constrained layer composite structures induced by inplane loads using ADINA, Computers and Structures 56 (1995) 357–363.

[23] H. Koruk, K. Y. Sanliturk, Assesment of the complex eigenvalue and the modal strain energy methods for damping predictions, in: Proceedings of ICSV 18, 2011 (Rio de Janeiro).

[24] P. Fischer, M. Engelbrechtsmüller, Local damping effects in acoustic analysis of large FE engine structures, in: Proceedings of ISMA 25, 2000 (Leuven).

[25] A. Hufenbach, D. Blanchet, M. Gude, M. Dannemann, F. Kolbe, Integrated vibro-acoustic calculation procedure of composite structures using coupled finite and boundary element method, in: Proceedings of ISMA 2010, Leuven.

10. Paper V: Application of SmEdA to systems with high mode densities

Contents

Published in the Proceedings of Conference “Noise and Vibration: Emerging methods” (NOVEM 2012), Sorrento, Italy, April 1-4, 2011

Application of SmEdA to systems with high mode densities

Rainer Stelzer[1], Nicolas Totaro[1], Goran Pavic[1], Jean-Louis Guyader[1]
[1] *INSA Lyon Laboratoire Vibrations et Acoustique, 25 Bis Avenue Jean Capelle Bâtiment St. Exupéry, 69621 Villeurbanne Cedex*
rainer.stelzer@insa-lyon.fr

Abstract
The statistical modal energy distribution analysis (SmEdA) has been developed to bridge the gap in the mid frequency range between the finite element method (FEM) and the statistical energy analysis (SEA). SmEdA requires a solution of the eigenvalue problem for each subsystem. But it can be very time consuming to compute the modal parameters of a subsystem in some cases, for example that of a large cavity. Also, the information about the mode shapes in the whole space is not necessary, if one is interested only in total energies of subsystems. Because of these reasons a method to approximate eigensystems only at the coupling surface between to subsystems is developed. Another possibility to reduce the computation cost for systems with high mode densities is to use a hybrid SEA/SmEdA method, which was presented in a previous article about SmEdA in connection with structure-structure coupling. In the present paper, the new method to approximate eigensystems and the hybrid SEA/SmEdA method are presented. The application possibilities of them are demonstrated on cavity-structure systems.

1. Introduction

The most popular methods for the analysis of vibro-acoustic systems are the finite element method (FEM) for the low frequency range and the statistical energy analysis (SEA) for the high frequency range. To close the gap in the mid frequency range between FEM and SEA, the statistical modal energy distribution analysis (SmEdA) was developed by Maxit and Guyader [1, 2] to create an energy based method which can be used at lower frequencies than SEA. This aim was reached by using a coupling between the modes of different subsystems instead of the coupling of complete subsystems like in SEA. In this way the key SEA constraint, that of equipartition of modal energies, is removed. But on the other hand SmEdA uses still the principle of conservation of energy like SEA. That means in the case of SEA that the basic equation for each subsystem i is the following power balance equation:

$$\Pi^i = \Pi^i_{dis} + \Pi^i_{ex} \tag{1}$$

where Π^i is the input power, Π^i_{dis} is the dissipated power and Π^i_{ex} is the transmitted power into connected subsystems. The dissipated power Π^i_{dis} is proportional to the total energy E_i of a system i and Π^i_{ex} is proportional to the difference of the total energies between the concerned subsystem and the connected subsystems [3]. The proportionality factors in these relations are the damping loss factor η_i and the coupling loss factor η_{ij}. Hence, the power balance, equation (1), reads:

$$\Pi^i = \omega_c \eta_i E_i + \omega_c \eta_{ij}(E_i - E_j) \tag{2}$$

where ω_c is the central frequency of an excited frequency band. How this energy principle is used in SmEdA for each mode is explained in detail in the next chapter of this article. Moreover, this chapter gives an overview over the recent extended version of SmEdA for cavity-structure coupled systems, which takes into account also non resonant modes contrary to the original SmEdA [1, 2]. The non resonant modes play for example an important role for highly damped systems. In previous articles [4, 5, 6], the advantages in comparison to FEM and SEA and the application possibilities of the extended SmEdA approach have been demonstrated on both simple academic and industrial cavity-structure problems. But one problem of SmEdA is that the computational cost grows with increasing mode densities, because each mode is described with one power balance equation and so the linear equation system increases, which has to be solved. This is especially a problem for cavities, where the mode density increases strongly with a rising frequency. If only the resonant modes are necessary to get a good result, this problem can be solved by using SEA with coupling loss factors predicted from the modal coupling factors of SmEdA as described in [7]. In other cases it may be possible to find some subsystems, which can be handled as SEA subsystems using only resonant modes, and to apply a hybrid SEA/SmEdA method. Such a technique, which was used first by Maxit and Guyader [8] in combination with structure-structure coupling, is presented and used for structure-cavity coupling in this article. Another problem is that the eigensystems, basis of SmEdA, are calculated normally with FEM, because the computational cost of such a calculation is in the case of high mode densities also quite high and increases with a rising frequency because of the need of a finer mesh. Furthermore, a cavity is sometimes ill defined and so the exact shape of it, which is necessary for a FEM calculation, is not known. Because of these reasons a new method, described in this article, has been developed to approximate eigensystems of cavities. After the presentation of this method and of the hybrid SmEdA/SEA method, the advantages and application possibilities of the two methods are demonstrated using the examples of transmission loss calculation, which are discussed in detail in [4], [9] and [10].

2. Statistical modal Energy distribution Analysis

It was demonstrated by Maxit [2] that the coupling between two modes of different subsystems can be described as an gyroscopic coupling between two oscillators, if one subsystem can be considered as blocked on the coupling area and another as free. This is for example possible in the case of a cavity-structure coupling, where the vibrations in the cavity can be described with blocked eigenmodes and those in the structure with in vacuo modes. The same analogy is also used for structure-structure coupling, for example in [2] and [8], but this article is only about SmEdA for cavity-structure couplings. The advantage of this analogy to coupled oscillators is that the well established results for coupled oscillators from for example [11], [12], [13] or [3] can be used. One important result, which was the start of the development of SEA, is the description of the coupled problem with one coupled energy conservation equation for each oscillator. In this way, a first energy based analogous mechanical model consisting of gyroscopic coupled oscillators (see Figure 2) was developed by Maxit and Guyader for the real problem of coupled subsystems (see Figure 1). Here, each mode of a subsystem is represented by one oscillator whose mass is equal to the respective modal mass. The coupling between two oscillators is described with a coupling factor β_{pq}^{12} as a function of the mode parameters as follows, [1]:

$$\beta_{pq}^{12} = \frac{(W_{pq}^{12})^2}{M_p^1 M_q^2 (\omega_q^2)^2} \left[\frac{\eta_p^1 \omega_p^1 (\omega_q^2)^2 + \eta_q^2 \omega_q^2 (\omega_p^1)^2}{((\omega_p^1)^2 - (\omega_q^2)^2)^2 + (\eta_p^1 \omega_p^1 + \eta_q^2 \omega_q^2)(\eta_p^1 \omega_p^1 (\omega_q^2)^2 + \eta_q^2 \omega_q^2 (\omega_p^1)^2)} \right] \tag{3}$$

where M_p^1, M_q^2, ω_p^1 and ω_q^2 are the modal masses and the eigenfrequencies of the p-th and q-th mode of the subsystems one and two. The interaction modal work W_{pq}^{12} is the integral over the coupling area S of the product of the mode shapes p_p^1 and W_q^2 of the p-th and q-th mode of the subsystems one and two:

$$W_{pq}^{12} \int_S p_p^1 W_q^2 \, dS \tag{4}$$

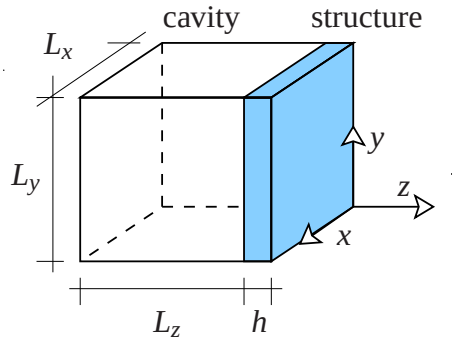

Figure 1.: System in reality: A cavity coupled to a structure

The problem of this first analogous model is that only resonant modes relating to an excited frequency band can be taken into account, because a white noise excitation is assumed for the derivation of the coupling factor like in the classical theory of coupled oscillaors [3]. Also, the boundary conditions between a cavity and a structure, for example the equality of the normal velocities, are not respected and thus it was necessary to extend this analogous model. In [10] it has been demonstrated using the formula of Cremer (transmission loss of an infinite plate) as reference, that the boundary conditions between the real subsystems can be respected in the

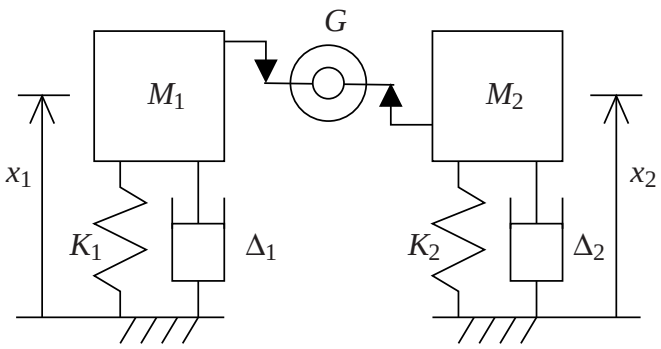

Figure 2.: Analogous mechanical model: Two gyroscopic coupled oscillators

analogous mechanical model with the response of the oscillators frequency averaged from zero to infinity. In this way, the coupling factors between all the oscillators, which represent resonant or non resonant modes, are equal to β_{pq}^{12} of equation (3). Because of this average response the kinetic and potential energies of all oscillators are also always equal and so they are only equal to those of the respective modes in the case of resonant excited modes. But the total energy of an oscillator and its respective mode is of course always equal. The advantage of these equality of the potential and kinetic energies for the oscillator is, that the real coupled cavity-structure system can be represented with a power balance equation system as a function of total energies like in SEA, equation (2), but with one equation for each mode and not only with one for each subsystem.

$$\Pi_p^1 = \eta_p^1 \omega_p^1 E_p^1 + \sum_{q=1}^{q_{max}} \beta_{pq}^{12} (E_p^1 - E_q^2) \tag{5}$$

where Π_p^1 is the power input in the p-th mode of the subsystem one. The sum of all these total modal energies, respectively energies of oscillators, of a subsystem i gives the whole energy E^i of a subsystem i [7, 5].

$$E^i = \sum_n E_n^i \tag{6}$$

3. Hybrid SEA/SmEdA methods

In the following it is shown how the SmEdA approach can be combined with SEA. If only resonant modes are necessary to be taken into account for the different subsystems, the SEA coupling loss factors η_{ij} can be calculated on condition of modal equipartition of energy from the modal coupling loss factors (equation (3)) like in [7] as follows:

$$\eta_{12} = \frac{1}{p_{max}\omega_c} \sum_{p=1}^{p_{max}} \sum_{q=1}^{q_{max}} \beta_{pq}^{12} \tag{7}$$

$$\eta_{21} = \frac{1}{q_{max}\omega_c} \sum_{p=1}^{p_{max}} \sum_{q=1}^{q_{max}} \beta_{pq}^{12} \tag{8}$$

where p_{max} and q_{max} are the number of resonant modes relating to an excited frequency band with the central frequency ω_c. Using equations (7) and (8), it is possible to make a classical SEA calculation, equation (2). This reduces the computational cost dramatically, because the linear power balance equation system, which has to be solved, consist here only of one equation for each subsystem instead of a lot of equations for modes in the case of a SmEdA calculation. In

[4] and [5] it has been demonstrated yet that this procedure produces good results in comparison to a usal SmEdA calculation if only resonant modes are necessary and the non resonant modes do not play a role. If only a part of the subsystems can be described with resonant modes only, there is also the possibility to generate a hybrid SEA/SmEdA power balance equation system to reduce the computational cost. For example a mixed power balance equation system for two connected subsystems reads, [8]:

$$\begin{aligned} P^1 &= \omega_c \left(\eta^1 + \eta_{12}\right) E^1 - E_m^2 \sum_n \beta_{nm}^{12} \\ P_m^2 &= \left(\eta_m^2 \omega_m^2 + \sum_n \beta_{nm}^{12}\right) E_m^2 - \frac{E^1}{n} \sum_n \beta_{nm} \end{aligned} \tag{9}$$

where ω_m^2, η_m^2, P_m^2 and E_m^2 are the eigenfrequency, the damping factor, the input power and the modal energy of the mode m of subsystem two, ω_c is the central frequency of the excited frequency band, n is the number of modes of subsystem one in the excited frequency band and η^1, P^1, and E^1 are the damping factor, the input power and the energy of the entire subsystem one.

4. Approximate modes

To predict approximatively the eigensystems of fluid filled cavities two approximations, one for the eigenfrequencies and one for the mode shapes, are necessary. From the literature, for example [14], it is known that the mode density n is approximately given by

$$n = \frac{k^2 V_f}{2\pi^2 c_f} \tag{10}$$

where k is the wavenumber and c_f and V_f are the sound velocity of the fluid and the volume of the cavity. Thus, the number of modes N in a frequency range, ω_1 to ω_2, fellows from integration over ω

$$N = \int_{\omega_1}^{\omega_2} \frac{k^2 V_f}{2\pi^2 c_f} d\omega \tag{11}$$

Under the assumption that ω_1 is zero and that a frequency is an eigenfrequency, for which the number N of the modes is an integer, the eigenfrequencies ω_m can be approximated as follows using equation (11):

$$\omega_m = \sqrt[3]{\frac{6\pi^2 c_f^3 m}{V_f}} \tag{12}$$

where m is a positive integer. For the approximation of the shapes of the eigenmodes, it can be assumed that the shape of a cavity mode at the coupling surface is approximately equal to the distribution of the pressure on a structure of an incident sound wave. The frequencies of these waves are assumed to be equal to the approximate eigenfrequencies ω_m of the modes. In this way, the wavelength λ_m^s of a mode shape on a surface is equal to the on the surface projected wavelength (trace wavelength) of the corresponding sound wave. Therefore, it results that

$$\lambda_m^s = \frac{2\pi c}{\omega_m \sin\vartheta} \tag{13}$$

where ϑ is the angle of incidence of an incident wave (see Figure 3). The trace wavelength becomes minimal for an incidence parallel to a boundary surface (angle of incidence is 90°).

$$\lambda_{min}^{m} = \frac{2\pi c}{\omega_m \sin 90^\circ} = \frac{2\pi c}{\omega_m} \tag{14}$$

Thus, the wavelength λ_m^s of a mode shape on a surface of a coupled structure can takes values between this minimum and infinity (normal incidence). In addition to get a complete description of a mode shape Φ_m^s on a boundary surface relating to a coordinate system it is necessary to define also the direction of incidence with an azimuthal angle φ (see Figure 3) and the phase shift δ. For example, in the case of a plane structure the approximate mode shapes Φ_m^s on the surface can be thus written as

$$\Phi_m^s = \cos\left(\frac{2\pi x}{\lambda_{m,x}^s} + \delta\right) \cos\left(\frac{2\pi y}{\lambda_{m,y}^s} + \delta\right) = \cos\left(k_f x \sin\vartheta \cos\varphi + \delta\right) \cos\left(k_f y \sin\vartheta \sin\varphi + \delta\right) \tag{15}$$

where k_f is the wavenumber of the fluid and $\lambda_{m,x}^s$ and $\lambda_{m,x}^s$ are the approximate wavelength in the directions of x and y. All these values, φ, δ and ϑ can be characterised as uniformly distributed random numbers, which can take values between zero and 2π respectively $\pi/2$ for ϑ. The mode shapes approximated in this way are theoretically exact for infinite cavities, because in this case an infinite number of modes exists at every frequency and all the incidence parameters are uniformly distributed. At lower mode densities of real cavities this leads to an error for the eigensystems, but this error becomes in general smaller with increasing dimensions. All in all, these approximate eigenfrequencies, equation (12), and these approximate mode shapes on a coupling surface, equations (13) and (15), are a sufficient description of eigensystems for the use in connection with SmEdA, because only the mode shapes on the coupling surfaces and the eigenfrequancies are necessary to calculate the modal coupling factors, equation (3). But there is no information in this way about the mode shapes of a cavity in the rest of the volume.

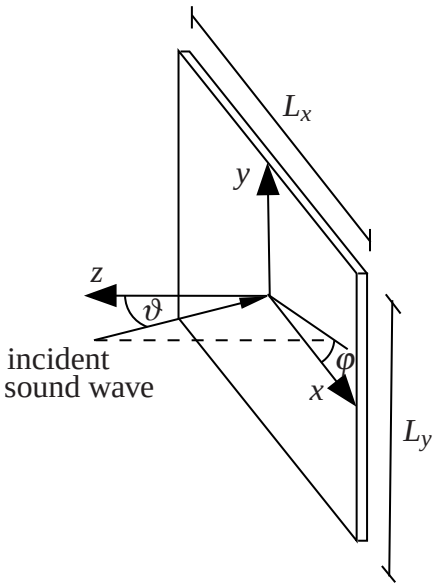

Figure 3.: Sound incident on a boundary surface

5. Example

5.1. System under study

To demonstrate the advantages and the application possibilities of the hybrid SEA/SmEdA methods and of SmEdA with approximate eigensystems, a basic example configuration of a simply supported rectangular plate between two parallelepipedic cavities as presented in Figure 4 and Table 1 is chosen. This system is excited in a corner of one of the cavities (sending room) with a monopole source. The coincidence frequency of the plate is 2933 Hz. The exact eigenmodes and eigenfrequencies for the SmEdA calculations are calculated in the present case analytically. The eigenmodes p_{qrs} and the eigenfrequencies ω_{qrs} of the cavities are given by [15]

$$p_{qrs} = \cos\left(\frac{q\pi x}{L_x}\right)\cos\left(\frac{r\pi y}{L_y}\right)\cos\left(\frac{s\pi z}{L_z}\right); \quad q,r,s = 0,1,2,3,\ldots \tag{16}$$

and

$$\omega_{qrs} = c\sqrt{\left(\frac{q\pi}{L_x}\right)^2 + \left(\frac{r\pi}{L_y}\right)^2 + \left(\frac{s\pi}{L_z}\right)^2} \tag{17}$$

The eigenfrequencies ω^s_{mn} and the modes W^s_{mn} of the simply supported plate are

$$\omega^s_{mn} = \pi^2\left[\left(\frac{m}{L_x}\right)^2 + \left(\frac{n}{L_y}\right)^2\right]\sqrt{\frac{B}{m}}; \quad m,n = 1,2,3,\ldots \tag{18}$$

and

$$W^s_{mn} = \sin\left(\frac{m\pi x}{L_x}\right)\sin\left(\frac{n\pi y}{L_y}\right) \tag{19}$$

with the mass per area m and the bending stiffness B of the plate.

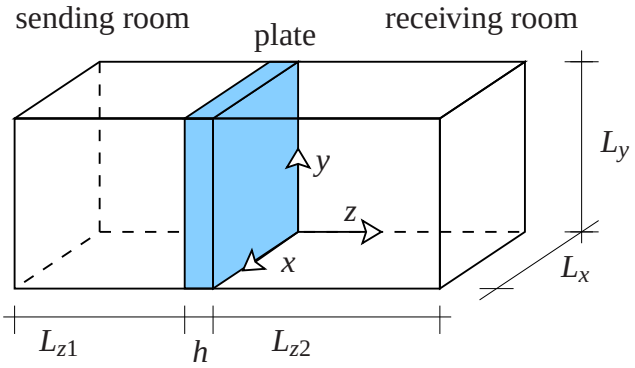

Figure 4.: Sketch of the cavity-plate-cavity system

	plate	sending room	receiving room
$L_x \times L_y \times L_z(h)\ (m)$	$1.2 \times 0.9 \times 0.004$	$1.2 \times 0.9 \times 0.7$	$1.2 \times 0.9 \times 1$
$\rho\ (kg/m^3)$	7820	1.2	1.2
$c\ (m/s)$		340	340
η	0.01	0.01	0.01
$E\ (MPa)$	210		
ν	0.3		

Table 1.: Characteristics of the subsystems

5.2. Transmission Loss calculation using hybrid SEA/SmEdA methods

As demonstrated in [4] and [9], it is necessary to take into account non resonant modes to calculate the transmission loss of the chosen example system, Figure 4, if the damping factor η_p of the plate is high (see Figures 5 and 6). Therefore, only for a low plate damping it is possible to reduce the computational cost using a complete SEA calculation with coupling loss factors predicted from SmEdA as described in chapter 3. But in this case the so calculated transmission loss (line "SEA SmEdA" in Figure 5) agrees well with those of the usual SmEdA calculation. The only difference between the results of the two methods exists at very low frequencies because of the low modal densities [4].

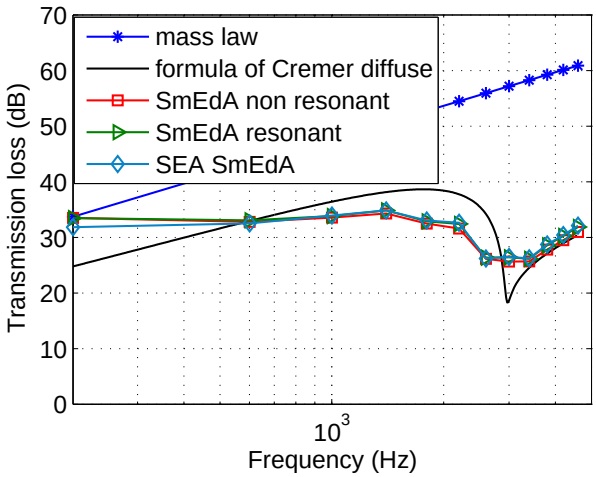

Figure 5.: Transmission loss for a plate damping $\eta_p = 0.001$ (frequency band width: 400 Hz; graph "SmEdA non resonant": resonant and non resonant modes are used for the calculation)

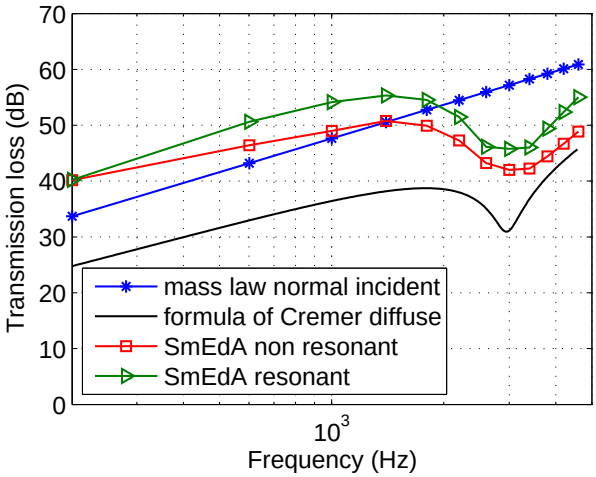

Figure 6.: Transmission loss for a plate damping $\eta_p = 0.1$ (frequency band width: 400 Hz; graph "SmEdA non resonant": resonant and non resonant modes are used for the calculation)

To reduce the computational cost also for the case of a high plate damping a hybrid SEA/SmEdA calculation, equation (9), can be used. Here, the sending room can be represented with one SEA-like equation, because the excitation with a monopole in a corner is more or less equal to an equal nonzero power input in all the resonant modes only [9]. Thus, if the other two subsystems are described with power balance equations for resonant and non resonant modes, the transmission loss predicted with such a hybrid method (line "SEA/SmEdA 1 cavity" in Figure 7) is as expected almost equal to the one calculated with a full SmEdA approach. Next, the computational cost is reduced further using SEA-like equations for the two cavities for the calculation of the transmission loss (line "SEA/SmEdA 2 cavities" in Figure 7). But the difference in comparison to a complete SmEdA calculation becomes here quite large like for the calculation without non resonant modes in Figure 6. Thus, only the sending room can be described with one SEA-like power balance equation in this example, because non resonant modes have to be taken into account for the other cavity (receiving room).

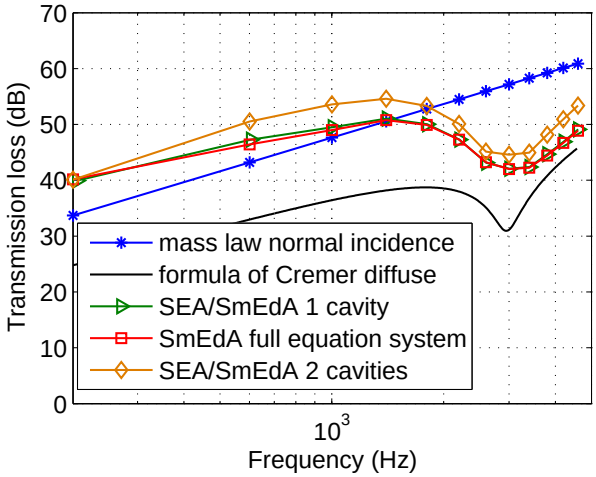

Figure 7.: Transmission loss calculated with a mixed power balance equation system (plate damping $\eta_p = 0.1$)

5.3. Transmission Loss calculation using approximate modes

Next, the transmission losses obtained with approximate eigensystems (see chapter 4) for the two cavities are compared in Figures 8 and 9 to those predicted with exact analytic eigensystems, equations (16) and (17). As it is not possible to handle localised point excitations with approximate modes as these are only defined on the coupling surface (see chapter 4), only all the resonant modes have equal nonzero power input, what is nearly the same as with the excitation at one corner [9]. Using a random phase shift δ gives here in general a huge error for the transmission loss below the critical frequency. On the contrary, for a constant $\delta = 0$ the difference in comparison to the exact SmEdA calculation becomes much smaller below the critical frequency. The reason for this effect is that the phase shift of the modes of a finite cavity is as a consequence of the boundary condition constant like the formula for cavity modes, equation (16), shows. But at higher frequencies, where the wavelengths are small in comparison to the dimensions of the cavity the influence of the boundary condition becomes less important.

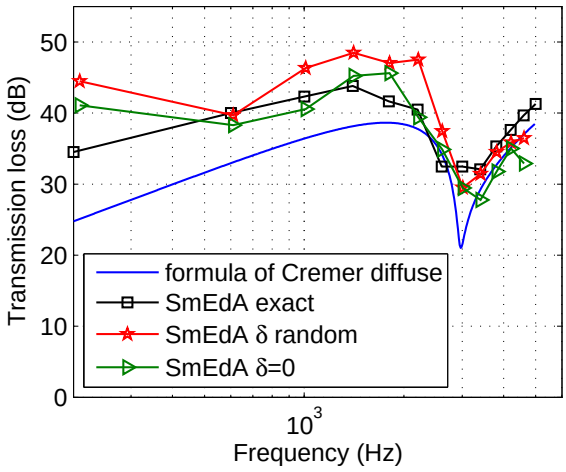

Figure 8.: Transmission loss for a plate damping factor $\eta_p = 0.01$ predicted with approximate modes

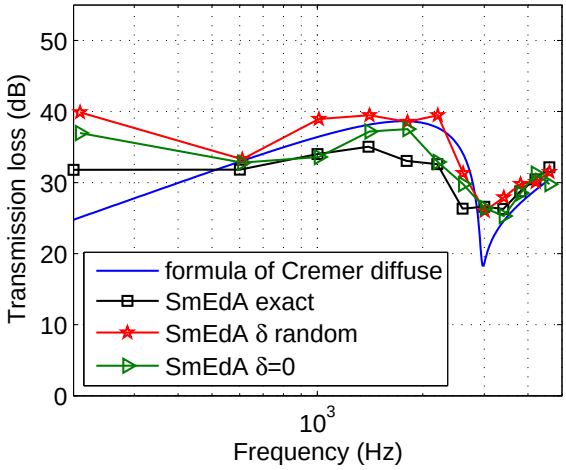

Figure 9.: Transmission loss for a plate damping factor $\eta_p = 0.001$ predicted with approximate modes

Another problem of the approximate method as described in chapter 4 is that the angle of incidence ϑ is assumed to be uniformly distributed, because especially in the case of small cavities different directions of incidence can be dominant in cavities, which have the same volume. If for example L_z (see Figure 4) is much larger than L_x and L_y, the waves normal to the plate and with small angles of incidence would be dominant. But all in all, with such an approximate method it is possible to reach even for a small system a quite good approximation of the transmission loss above the first 400 Hz frequency band, although the modes are very roughly estimated and the numbers of modes are quite small in different frequency bands (see Table 2).

frequency band	**number of modes**			
	sending cavity		receiving cavity	
	exact	approximate	exact	approximate
10 - 410 Hz	11	5	15	7
410 - 810 Hz	55	37	74	54
810 - 1210 Hz	125	100	180	142
1210 - 1610 Hz	237	194	321	277
1610 - 2010 Hz	373	318	517	454
2010 - 2410 Hz	517	473	740	677
2410 - 2810 Hz	741	660	1038	942
2810 - 3210 Hz	951	877	1340	1254
3210 - 3610 Hz	1213	1126	1724	1607
3610 - 4010 Hz	1514	1405	2133	2007
4010 - 4410 Hz	1810	1715	2589	2450
4410 - 4810 Hz	2183	2056	3079	2937

Table 2.: Exact and approximate number of modes in the different frequency bands

6. Conclusion

As demonstrated on the examples of the transmission loss calculations in the previous chapter, hybrid SEA/SmEdA methods can be successfully applied under some conditions and can reduce so the computational cost. But one problem is that it has to be identified first if it is sufficient to use only resonant modes for a subsystems and thus to describe this subsystem with a SEA-like power balance equation. At this, also the connected subsystems and their characteristics, for example the damping, can play a role especially for non direct excited subsystems, like the sending room of the presented example. Thus, it can be quite difficult to decide a priori if non resonant modes are necessary to be taken into account or not. Other problems are typical SEA ones. So it is not possible to respect the differences between different point excitations in a SEA-like subsystem. Also, there is no information about the distribution of the energy in such a subsystem. The other in this article presented method, the new method to approximate modes for ill defined systems or systems with high mode densities, has been tested here for the first time but on a quite small system with low mode densities. Although this method is designed for systems with high mode densities because of the assumption of uniformly distributions of the mode shape describing values, the predicted transmission losses are so far quite good. Thus, it seems to be a good method to describe ill defined systems and to reduce the computational cost,

maybe also in combination with the hybrid SEA/SmEdA methods, for systems with high mode densities, because no time consuming calculation of the eigensystems with FEM is needed. But to get more exact results with this method also for small systems, it is necessary to research in the future different distributions for the directions of incidence and the phase shift, which are used to define the mode shape on the coupling surface. Another problem is, that similar to SEA no localised external excitations can be handled with these approximate mode shape because of their definition only on the coupling surfaces.

7. Acknowledgment

The authors gratefully acknowledge the ITN Marie Curie project GA-214909 ”MID-FREQUENCY - CAE Methodologies for Mid-Frequency Analysis in Vibration and Acoustics”.

Bibliography

[1] L. Maxit, J.-L. Guyader, Estimation of the SEA coupling loss factors using a dual formulation and FEM modal information, part I: theory, Journal of Sound and Vibration 239(5) (2001) 907–930.

[2] L. Maxit, Extension et reformulation du modèle SEA par la prise en compte de la répartition des énergies modales, Ph.D. thesis, INSA Lyon, 2000.

[3] R. H. Lyon, R. G. DeJong, Theory and application of statistical energy analysis, Butterworth-Heinemann, 2nd edn., 1995.

[4] R. Stelzer, N. Totaro, G. Pavic, J. Guyader, Prediction of Transmission Loss using an improved SEA Method, in: Proceedings of CFA 2010, Lyon.

[5] R. Stelzer, N. Totaro, G. Pavic, J. Guyader, L. Maxit, Non resonant contribution and energy distributions using Statistical modal Energy distribution Analysis (SmEdA), in: Proceedings of ISMA 2010, Leuven.

[6] R. Stelzer, N. Totaro, G. Pavic, J. Guyader, Improved modal energy analysis for industrial problems, in: Proceedings of ICSV 18, 2011 (Rio de Janeiro).

[7] N. Totaro, C. Dodard, J.-L. Guyader, SEA coupling loss factors of complex vibro-acoustic systems, Journal of Vibration and Acoustics 131 (2009) 041009–4.

[8] L. Maxit, J.-L. Guyader, Extension of SEA model to subsystems with non-uniform modal energy distribution, Journal of Sound and Vibration 265 (2003) 337–358.

[9] R. Stelzer, N. Totaro, G. Pavic, J.-L. Guyader, Assessment report on SmEdA, Tech. Rep., ITN Mid-Frequency, project website http://www.mid-frequency.org, 2011.

[10] R. Stelzer, N. Totaro, G. Pavic, J.-L. Guyader, Non resonant modes and Transmission Loss using Statistical modal Energy distribution Analysis (SmEdA), article in preparation, 2011.

[11] T. Scharton, R. Lyon, Power Flow and Energy Sharing in Random Vibration, Journal of the Acoustical Society of America 43 (6) (1968) 1332–1343.

[12] E. Ungar, Statistical energy analysis of vibrating systems, Tech. Rep. AFFDL-TR-66-52, US Air Force, 1966.

[13] J. Woodhouse, An approach to the theoretical background of statistical energy analysis applied to structural vibration, Journal of the Acoustical Society of America 69 (6) (1981) 1695–1709.

[14] F. Fahy, Foundations of Engineering Acoustics, Elsevier, 2005.

[15] M. Möser, Technische Akustik, Springer, 7th edn., 2007.

11. Paper VI: Non resonant modes and Transmission Loss using Statistical modal Energy distribution Analysis (SmEdA)

Contents

article in preparation for submission

Non resonant modes and Transmission Loss using Statistical modal Energy distribution Analysis (SmEdA)

Rainer Stelzer[1], Nicolas Totaro[1], Goran Pavic[1], Jean-Louis Guyader[1]
[1] *INSA Lyon Laboratoire Vibrations et Acoustique, 25 Bis Avenue Jean Capelle Bâtiment St. Exupéry, 69621 Villeurbanne Cedex*
rainer.stelzer@insa-lyon.fr

Abstract
The Statistical Modal Energy Distribution Analysis (SmEdA) has been conceived to close the mid-frequency gap between the widely used low-frequency FEM and high-frequency SEA. Unlike SEA which couples the entire sub-systems, SmEdA uses the coupling between individual modes of subsystems. The original SmEdA formulation is limited to coupling between resonant modes only. This makes it for example less applicable to highly damped systems. A novel version of SmEdA is presented in the paper, extended to non resonant modes. The advantages of the new method are demonstrated by modelling the transmission loss of a flat panel inserted between two cavities. One principal advantage is, that contrary to other methods, which assume often a diffuse sound field, SmEdA can predict the transmission loss of partitions in between cavities with non-diffuse sound fields.

1. Introduction

1.1. Transmission Loss

Different approaches have been in use for vibro-acoustic calculations: – analytical, variational, finite element and energy methods. One important application of these approaches is the prediction of transmission loss through a partition. Several transmission loss models have been developed over the past century. The transmission loss characterises the physical process of the transmission of the acoustical power through a partition with the transmission factor τ, the ratio between the transmitted power P_t and the incident power P_i. In this way, the transmission loss R in decibel is defined as follows [1]:

$$R = 10\lg\left(\frac{1}{\tau}\right) = 10\lg\left(\frac{P_i}{P_t}\right) \tag{1}$$

The earliest and simplest transmission loss model is the mass law:

$$R_M = 10\lg\left[1+\left(\frac{\omega m\cos\vartheta}{2\rho c}\right)^2\right] \tag{2}$$

which assumes a rigid partition between two free sound fields. Equation (2) shows that the transmission loss depends on the mass of a partition (m: mass per area), the angle frequency ω, the density ρ of the fluid, the speed of sound c of the fluid and the angular of incidence ϑ. The theoretical background of this law was first formulated by Rayleigh [2] and experimentally verified amongst others by Berger [3]. The next development was made by Cremer. He replaced the model of a rigid partition by the Kirchhoff plate model to account for the plate deformation. Assuming an infinite plate Cremer obtained an expression of the transmission loss which not only depends on the plate mass but also on its bending stiffness B:

$$R_C = 10\lg\left[1+\left(\omega m - B\omega^3\frac{\sin^4\vartheta}{c^4}\right)^2\left(\frac{\cos\vartheta}{2\rho c}\right)^2\right] \tag{3}$$

The additional dependence on stiffness yields the so-called coincidence effect: a resonance phenomenon which appears when the wavelength of a free plate bending wave matches the wavelength of an incident sound wave projected onto the plate (trace wavelength). The lowest frequency allowing the coincidence is the so-called critical frequency:

$$f_c = \frac{c^2}{2\pi}\sqrt{\frac{m}{B}}\,. \tag{4}$$

Due to the simplicity of the formula of Cremer and its good approximation of the principal tendency of transmission loss, especially above the critical frequency, this formula is still often used. Other analytical solutions were searched and formulated later for more complex and realistic configurations like for finite plates by Heckl [1] or for finite plates between finite cavities by Nilsson [4] and by Josse and Lamure [5]. But these models are only rough estimates due to multiple involved assumptions. This has prompted creation of other models to predict the transmission loss using variational, finite element and energy methods. The first one, the variational approach, was used for example by Woodcock and Nicolas [6] for finite plates or by Gagliardini, Roland and Guyader [7] for a finite plate between two finite cavities. The drawback of these models is that the functional basis of a complete system, which satisfies the geometrical

boundary conditions, can be found only for simple geometries like a rectangular plate. However, there is also a newer variational approach, the wave based method, that overcomes this obstacle by using the functional basis only for parts of simple geometry. One application of this approach was demonstrated by Dijckmans and Vermeir [8] for the transmission loss of a real cavity-plate-cavity system. Another group of calculation tools are the finite element method (FEM) and the boundary element method (BEM). For example Sakumaa, Egawa and Yasuda [9] used a combination of FEM and BEM to predict the transmission loss of finite plates in between diffuse sound fields. The main difficulty of these methods is the rapid increase of the computation cost with rising frequency and with increasing size of the system. Finally, there are the energy methods, the statistical energy analysis (SEA) and the statistical modal energy distribution analysis (SmEdA), which is the topic of this article. These two methods are based on the principle of the balance of energy for each subsystem, like a cavity or a plate, and describe the coupling between subsystems with one or more coupling factors. In contrast to the other calculation methods the energy methods output energies rather than pressures, velocities or displacements.
The original formulations of energy methods can take into account only resonant modes related to an excited frequency band. But non resonant modes are important for example for highly damped systems, narrow band excitations or some boundary conditions. In SEA applied to transmission problem, this is solved by using a non physical direct coupling factor between two cavities. The present paper describes how to handle this non resonant modes in a new extended version of SmEdA.

1.2. Statistical energy analysis

The statistical energy analysis is the most popular energy based method. The development of it started in the early 1960s with the works over coupled oscillators from Lyon and Smith [10]. The fundamental equation of this method is the power balance for each subsystem (for example an oscillator). This means, that all the power Π^i, which is input in a subsystem i, is dissipated (Π^i_{dis}) in this subsystem or transmitted into another connected subsystem (Π^i_{ex}).

$$\Pi^i = \Pi^i_{dis} + \Pi^i_{ex} \tag{5}$$

It has been found out, that the power exchange Π^i_{ex} between two coupled subsystems is proportional to the difference of their total time-averaged energies. The total energy of a subsystem E_i is linked over the subsystem damping loss factor η_i to the dissipation power Π^i_{dis}. Thus, it can be written

$$\Pi^i = \omega_c \eta_i E_i + \omega_c \eta_{ij}(E_i - E_j) \tag{6}$$

where ω_c is the central angular frequency of the frequency band and η_{ij} is the coupling loss factor. Moreover, the coupling loss factors of two coupled subsystems are interrelated through the reciprocity relation

$$n_i \eta_{ij} = n_j \eta_{ji} \tag{7}$$

with the modal densities n_i and n_j of subsystems i and j. All in all, the energies of subsystems at a given power input are calculated with a linear set of equations. Thus, SEA is principally an easy calculation method, but the key problem is the estimation of the coupling loss factors. These coupling factors can be predicted for the transmission loss calculation of a finite plate in between two finite cavities using for example the method of Renji, Nair and Narayanan [11] or that of Lyon and DeJong [10]. In [10] the process of transmission is divided into two paths, the non resonant and the resonant transmission. The first is more or less an extended version of the

mass law and is characterized by the coupling loss factor η_{12} for the direct coupling between the two cavities under the assumption of diffuse sound fields.

$$\eta_{12} = \beta_c I_{12} \frac{c_1}{f k_1^2 V_1} \frac{\tau_{12,\infty}(0)}{2 - \tau_{12,\infty}(0)} \tag{8}$$

with the transmission coefficient $\tau_{12,\infty}(0)$ for normal incidence, the correction factor β_c for the case of low modal overlap, the frequency f, the correction factor I_{12} for diffuse sound field and the sound velocity c_1, the wavenumber k_1 and the volume V_1 of the cavity one. The factors β_c, I_{12} and $\tau_{12,\infty}(0)$ are explained in appendix C. The second path of transmission, the resonant transmission through the resonant modes of the plate, is represented by the indirect coupling factor η_{p2}. This factor is related to the plate radiation efficiency σ_{rad} as follows:

$$\eta_{p2} = \frac{\rho_1 c_1}{2\pi f \rho_p h_p} \sigma_{rad} \tag{9}$$

where ρ_1 and c_1 are the density and the sound velocity of cavity one, ρ_p and h_p are the density and the thickness of the plate and ω is the angular frequency. For a simple supported thin plate and light fluids in the cavities the radiation efficiency is approximately given by, [10],

$$\sigma_{rad} = \frac{2k_1^2 L_s}{\pi A_p k_p^3 \left(1 + \frac{\pi k_1^2}{2k_p^2}\right)} + \frac{1}{\sqrt{\left(\frac{k_p^2}{k_1^2} - 1\right)^2 \left(\frac{\pi k_p^4}{k_1^4} + 1\right)^2 + \frac{2\pi}{k_p \sqrt{A_p}}}} \tag{10}$$

with the length of the edge L_s, the plate area A_p and the wavenumbers k_p and k_1 of the plate respectively of the cavity. Finally, the basic power balance equation system of SEA reads [11]:

$$\begin{pmatrix} \Pi_1 \\ 0 \\ 0 \end{pmatrix} = \begin{pmatrix} \eta_1 + \eta_{1p} + \eta_{12} & -\eta_{p1} & -\eta_{21} \\ -\eta_{1p} & \eta_2 + \eta_{p1} + \eta_{p2} & -\eta_{2p} \\ -\eta_{12} & -\eta_{p2} & \eta_2 + \eta_{2p} + \eta_{21} \end{pmatrix} \begin{pmatrix} E_1 \\ E_p \\ E_2 \end{pmatrix} \tag{11}$$

Using these energies of the subsystems estimated in this way the transmission loss is calculated with the formulas for finite cavity-plate-cavity systems given in appendix A. To sum up, contrary to the mass law and the formula of Cremer the present formulation does not neglect the influence of the cavity size and damping and takes into account the finite size of the plate.

2. Coupling between two oscillators

The statistical modal energy distribution analysis (SmEdA) was developed by Maxit and Guyader [12] to extend the frequency range to lower frequencies, where energy based methods like SEA cannot be used. The description of coupling in SmEdA is based on the dual formulation of two gyroscopic coupled oscillators (Figure 1).

2.1. Resonant excited oscillators

The behaviour of gyroscopic coupled oscillators is described by the following coupled differential equations:

$$\begin{aligned} \ddot{y}_1(t) + \Delta_1 \dot{y}_1(t) + \omega_1^2 y_1(t) - \sqrt{M_1^{-1} M_2}\, \gamma \dot{y}_2(t) &= F_1(t) \\ \ddot{y}_2(t) + \Delta_2 \dot{y}_2(t) + \omega_2^2 y_2(t) + \sqrt{M_2^{-1} M_1}\, \gamma \dot{y}_1(t) &= F_2(t) \end{aligned} \tag{12}$$

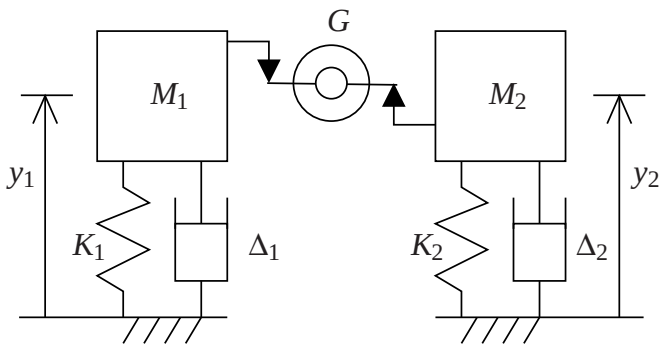

Figure 1.: Two oscillators coupled by a gyroscopic element

where $\Delta_i = \omega_i \eta_i$ is the damping coefficient, γ is the gyroscopic coupling factor and M_1 and M_2 are the masses of the oscillators. It was shown that under a white noise excitation the time-averaged power flow P_{12} between the oscillators is directly proportional to the difference of their time-averaged energies E_1 and E_2 [13].

$$P_{12} = \beta (E_1 - E_2) \tag{13}$$

where β is the coupling factor. Furthermore, P_{12}, E_1 and E_1 can be expressed in terms of the time-averaged velocities $\langle \dot{y}_i \rangle$ of the oscillators [10] as follows :

$$\begin{aligned} E_1 &= \tfrac{1}{2} M_1 \left\langle \dot{y}_1^2 \right\rangle \\ E_2 &= \tfrac{1}{2} M_2 \left\langle \dot{y}_2^2 \right\rangle \\ P_{12} &= \tfrac{1}{2} \Re \left(\gamma \sqrt{M_1 M_2} \left\langle \dot{y}_1 \dot{y}_2 \right\rangle \right) \end{aligned} \tag{14}$$

These velocities are calculated for harmonic forces $F_i(t)$ using equation (12). Therefore, for uncorrelated forces $F_i(t)$ the velocity terms can be written in the following form [14, 10] (*: complex conjugate):

$$\begin{aligned} \left\langle \dot{y}_1^2 \right\rangle &= \int S_{l_1} \omega^2 \left| H_{11} \right|^2 d\omega + \int S_{l_2} \omega^2 \left| H_{12} \right|^2 d\omega \\ \left\langle \dot{y}_2^2 \right\rangle &= \int S_{l_2} \omega^2 \left| H_{22} \right|^2 d\omega + \int S_{l_1} \omega^2 \left| H_{21} \right|^2 d\omega \\ \left\langle \dot{y}_1 \dot{y}_2 \right\rangle &= \int S_{l_1} \omega^2 H_{11} H_{21}^* \, d\omega + \int S_{l_2} \omega^2 H_{12} H_{22}^* \, d\omega \end{aligned} \tag{15}$$

with the complex frequency response functions

$$\begin{aligned} H_{11} &= \frac{-\omega^2 + i\omega\Delta_2 + \omega_2^2}{M_1 D} \\ H_{22} &= \frac{-\omega^2 + i\omega\Delta_1 + \omega_1^2}{M_2 D} \\ H_{12} &= \frac{i\omega\gamma}{D\sqrt{M_1 M_2}} \\ H_{21} &= \frac{-i\omega\gamma}{D\sqrt{M_1 M_2}} \end{aligned} \tag{16}$$

and

$$D = \omega^4 - i\omega^3 (\Delta_1 + \Delta_2) - \omega^2 \left(\omega_1^2 + \omega_2^2 + \Delta_1 \Delta_2 + \gamma^2 \right) + i\omega \left(\Delta_1 \omega_2^2 + \Delta_2 \omega_1^2 \right) + \omega_1^2 \omega_2^2 \tag{17}$$

Under the assumption of a white noise excitation, the spectra S_i of the forces F_i are given by

$$S_i(\omega) = \text{const.} \neq 0 \tag{18}$$

in the whole frequency range. Finally, equations (13) to (18) yield:

$$\beta = \frac{\gamma^2 \left(\eta_1 \omega_1 \omega_2^2 + \eta_2 \omega_2 \omega_1^2\right)}{(\omega_1^2 - \omega_2^2)^2 + (\eta_1 \omega_1 + \eta_2 \omega_2)(\eta_1 \omega_1 (\omega_2)^2 + \eta_2 \omega_2 (\omega_1)^2)} \tag{19}$$

where η_1 and η_2 are the damping factors and ω_1 and ω_2 are the eigenfrequencies of the oscillators.

2.2. Non resonant excited oscillators

The principle stating that the exchanged power of connected systems is proportional to the difference of the energies of these systems is a quite general concept which can be used not only for oscillators excited with a with a white noise, equation (13). Such an example is given by Lyon and DeJong [10]. They used two connected fluid filled containers as an analogous model for two coupled subsystems. In the case of two oscillators excited with the same single frequency ω the relation between the kinetic energies and the exchanged power can be generally described using the following equations for the difference of the kinetic energies E_i^k of two oscillators and the exchanged power P_{12}.

$$2(E_1^k - E_2^k) = \frac{1}{2}\omega^2 \left(M_1 \left\langle y_1^2 \right\rangle - M_2 \left\langle y_2^2 \right\rangle\right) \tag{20}$$

$$P_{12} = \frac{1}{2}\omega^2 \gamma \sqrt{M_1 M_2}\, \Re\left(\langle y_1 y_2 \rangle\right) \tag{21}$$

Solving equation (20) for ω^2 and insertion of the result in equation (21) gives:

$$P_{12} = 2\alpha \left(E_1^k - E_2^k\right) \tag{22}$$

The factor α is given for two uncorrelated forces with equal single excitation frequencies using equations (15) and (16) by

$$\alpha = \frac{M_1 M_2 \gamma^2 \omega^2 \left(S_2 M_1 \Delta_1 - S_1 M_2 \Delta_2\right)}{S_2 M_2 M_1^2 \left(\omega^4 - 2\omega^2 \omega_1^2 + \omega_1^4 + \omega^2 \Delta_1^2 - \omega^2 \gamma^2\right) - S_1 M_1 M_2^2 \left(\omega^4 - 2\omega^2 \omega_2^2 + \omega_2^4 + \omega^2 \Delta_2^2 - \omega^2 \gamma^2\right)} \tag{23}$$

The factor α is symmetric ($\alpha_{12} = \alpha_{21}$) and thus the exchanged power is really proportional to the difference of the kinetic energies, because the symmetry is a necessary and sufficient condition for the proportionality [15]. Therefore, an arbitrary power balance equation system for oscillators can be written – similar to this of SEA, equation (6) – as a function of the kinetic energies of coupled oscillators.

$$\Pi^i = 2\omega_i \eta_i E_{kin,i} + 2\alpha (E_{kin,i} - E_{kin,j}) \tag{24}$$

3. SmEdA

3.1. Original formulation of SmEdA

The coupling between two oscillators was formulated more arbitrarily than in SEA and extended to continuous vibrating systems. It has been demonstrated in [12], that the coupling between any two modes of different subsystems is equal to the coupling between two oscillators, if across the coupling area one system is taken as blocked and the other as free. This is for example the case of a cavity-structure coupling. The cavity subsystem is characterized here with pressure mode shapes p_p^1 and the structure with displacement mode shapes W_q^2. In this way, the modal coupling coefficient γ_{pq}^{12}, equivalent to the gyroscopic coupling factor γ in equation (25), is deduced.

$$\gamma_{pq}^{12} = \frac{1}{\sqrt{(\omega_p^1)^2 M_p^1 M_q^2}} \int_S p_p^1 W_q^2 \, dS = \frac{W_{pq}^{12}}{\sqrt{(\omega_p^1)^2 M_p^1 M_q^2}} \tag{25}$$

where W_{pq}^{12}, the integral over the coupling area S of the product of the mode shapes, is the interaction modal work and where M_p^1 and M_q^2 are the modal masses of the p-th and q-th mode of the subsystems 1 and 2. Finally, again under the assumption of a white noise excitation, the modal coupling loss factor reads:

$$\beta_{pq}^{12} = \frac{(W_{pq}^{12})^2}{M_p^1 M_q^2 (\omega_q^2)^2} \left[\frac{\eta_p^1 \omega_p^1 (\omega_q^2)^2 + \eta_q^2 \omega_q^2 (\omega_p^1)^2}{((\omega_p^1)^2 - (\omega_q^2)^2)^2 + (\eta_p^1 \omega_p^1 + \eta_q^2 \omega_q^2)(\eta_p^1 \omega_p^1 (\omega_q^2)^2 + \eta_q^2 \omega_q^2 (\omega_p^1)^2)} \right] \tag{26}$$

The modal energies of the different subsystems can be calculated directly with β_{ij} with a system power balance equations. One equation for each mode is used here instead of one equation per subsystem like in SEA.

$$\Pi_p^1 = \eta_p^1 \omega_p^1 E_p^1 + \sum_{q=1}^{q_{max}} \beta_{pq}^{12} (E_p^1 - E_q^2) \tag{27}$$

The entire energy of a subsystem is the sum of all modal energies of this subsystem [16, 17] and the transmission loss can be calculated using equations (43) to (45) from A. Moreover, the coupling loss factors of classical SEA can be calculated with the modal coupling loss factors on condition of modal equipartition of energy [17] with the following formulae:

$$\eta_{12} = \frac{1}{p_{max} \omega_c} \sum_{p=1}^{p_{max}} \sum_{q=1}^{q_{max}} \beta_{pq}^{12} \tag{28}$$

$$\eta_{21} = \frac{1}{q_{max} \omega_c} \sum_{p=1}^{p_{max}} \sum_{q=1}^{q_{max}} \beta_{pq}^{12} \tag{29}$$

where p_{max} and q_{max} are the number of resonant modes relating to an excited frequency band with the central frequency ω_c. It was shown by some authors, for example by Maxit and Guyader [18] for structure-structure coupling or by Totaro, Dodard and Guyader [17] for structure-cavity coupling, that the SEA coupling factors computed by SmEdA agree well with these obtained by other approaches.

3.2. Extended version for structure-cavity coupling including non resonant modes

A main drawback of the original SmEdA approach is that only resonant modes in an excited frequency band are taken into account in view of the assumption of a white noise excitation. However, the influence of non resonant modes can not be neglected in some cases, for example for highly damped systems. To find a solution involving non-resonant modes for the cavity-structure coupling it is necessary to have a closer look at the original derivation of the method. In SmEdA the coupled system is split into a blocked cavity and a free structure on the coupling surface to describe the coupling between the pressure in the cavity and the structure velocity. This is equivalent to the "blocked pressure" assumption which is often used, for example in [6] or [19], where it is assumed that the motion of the plate is negligible for the calculation of the surface pressure and the plate is then excited by the resultant force. However, the calculation of e.g. the transmission loss or the sound radiation requires that the boundary conditions are respected. This is not the case in the original SmEdA formulation. The boundary conditions are the equality of the velocities $\dot{y}_i^b$ and the equality of the products of the stress tensors σ_{rs}^{ib} and normal vectors n_s^i at the coupling surface.

$$\dot{y}_1^b = \dot{y}_2^b \tag{30}$$

$$\sigma_{rs}^{1b} n_s^1 = \sigma_{rs}^{2b} n_s^2 \tag{31}$$

Finally, the coupled system is defined in this way with four equations, the two coupled differential equations of original SmEdA, equation (12), and the two boundary conditions. On the other hand, only two variables are involved. Such an overdetermined system has in general no exact solution and it is difficult to find an approximate solution. Because of this problem an exact analytic solution for the fluid-structure interaction, the formula of Cremer (equation (3)), is used here as a reference to find and to validate an analogous mechanical model consisting of two gyroscopic coupled oscillators. This model describes the coupling between bending waves of an infinite plate and waves of free sound fields which can be considered as modes of an infinite plate and of semi-infinite cavities. Here, there is not only coupling between resonant modes but also between other combinations with non resonant modes. Therefore, different possible coupling factors can be tested in the following if they can describe also couplings with non resonant modes.

3.2.1. Infinite transmission loss models expressed with power balance equations

The coupling in the formula of Cremer concerns one incident wave, respectively one mode, one plate mode and one transmitted wave. That means this case is described under inclusion of chapter 3.2 by three power balance equations with only one nonzero power input.

$$\begin{aligned} P_1 &= 2\eta_1\omega_1 E_{kin,1} + 2\beta_{12}\left(E_{kin,1} - E_{kin,2}\right) \\ P_2 = 0 &= 2\eta_2\omega_2 E_{kin,2} + 2\beta_{21}\left(E_{kin,2} - E_{kin,1}\right) + \beta_{23}\left(E_{kin,2} - E_{kin,3}\right) \\ P_3 = 0 &= 2\eta_3\omega_3 E_{kin,3} + 2\beta_{32}\left(E_{kin,3} - E_{kin,2}\right) \end{aligned} \tag{32}$$

where the indices 1, 2 and 3 identify the sending room, the plate and the receiving room. From this equation system it follows for $E_{kin,3}$:

$$E_{kin,3} = \frac{\beta_{32}\beta_{21}E_1}{(\eta_2\omega_2 + \beta_{21} + \beta_{23})\left[\eta_3\omega_3 + \beta_{32}\left(1 - \frac{\beta_{23}}{(\eta_2\omega_2 + \beta_{21} + \beta_{23})}\right)\right]} \tag{33}$$

Also, it is assumed that $\eta_3 = \eta_1 = 0$ for the infinite models and consequently, it results from equations (1) and (33) for the transmission factor

$$\frac{1}{\tau} = \frac{E_{kin,1}}{E_{kin,3}} = 1 + \frac{\eta_2 \omega_2}{\beta_{12}} \tag{34}$$

Here, the kinetic energies can be used to calculate the transmission loss, because the same modes are excited in the two cavities and so the relations between the total energies and the kinetic energies are equal.

3.2.2. Comparison to the formula of Cremer without damping

From the power balance equation system (32) it can be inferred that a coupling factor β_{12}^t with a coupling between one resonant excited cavity mode ($\omega = \omega_1$, $S_1(\omega_1) \neq 0$) and one plate mode, which is excited only by this cavity mode ($S_2(\omega) = 0$), could be a correct description of the coupling. The test modal coupling loss factor β_{12}^t can be then obtained from equation (23), which is a solution for gyroscopic coupled oscillators not subjected to any additional conditions,

$$\beta_{12}^t = \frac{\gamma^2 \omega_1^2 \Delta_2}{\left(\omega_2^2 - \omega_1^2\right)^2 + \omega_1^2 \Delta_2^2 - \omega_1^2 \gamma^2} \tag{35}$$

Upon inserting β_{12}^t in equation (34), using the formulae given in appendices D and E and assuming $\eta_2 = 0$ one gets:

$$\frac{1}{\tau} = \frac{\left(\omega_2^2 - \omega_1^2\right)^2}{\gamma^2 \omega_1^2} = \left(\frac{\cos\vartheta}{2\rho_1 c_1}\right)^2 \left[\omega_1 m - \omega_1^3 B \left(\frac{\sin\vartheta}{c_1}\right)^4\right]^2 \tag{36}$$

This result matches well equations (2) and (3) if the influence of the factor "+1" can be neglected. But this is not the searched exact result of the formula of Cremer and so β_{12}^t is also not a general coupling factor. Next, the original β_{pq}^{12} (equation (26)) is tested in the same way. Here the obtained result is an exact one, i.e. the searched transmission factor.

$$\frac{1}{\tau} = 1 + \frac{\left(\omega_2^2 - \omega_1^2\right)^2}{\gamma^2 \omega_1^2} = 1 + \left(\frac{\cos\vartheta}{2\rho_1 c_1}\right)^2 \left[\omega_1 m - \omega_1^3 B \left(\frac{\sin\vartheta}{c_1}\right)^4\right]^2 \tag{37}$$

To get β_{pq}^{12} a white noise excitation is assumed rather than a single frequency excitation like in the case of the infinite models. This means that there must be a second way to get an integration from zero to infinity in equations (15). This other way is to calculate the averages of the velocity/displacement terms for all possible single frequency excitations from zero to infinity. For example $\langle \dot{y}_1^2 \rangle$ is then given by

$$\langle \dot{y}_1^2 \rangle = \frac{1}{\Delta\omega} \left(\int_0^\infty S_{l_1} \omega^2 \left|H_{11}\right|^2 d\omega + \int_0^\infty S_{l_2} \omega^2 \left|H_{12}\right|^2 d\omega \right) \tag{38}$$

The factor $\frac{1}{\Delta\omega}$ is canceled out using equations (13) and (14) to calculate β and so the result is a kind of averaged coupling factor which is equal to that in equation (26).

3.2.3. Comparison to the formula of Cremer with damping

Normally a complex stiffness $\hat{B} = B(1 - i\eta_c)$ is applied in the formula of Cremer (equation (3)) to take into account the plate damping whereby the transmission loss reads:

$$R_c = 10\lg\left[1 + \left(\frac{\cos\vartheta}{2\rho_1 c_1}\right)^2 \left\{\left(\omega_1 m - \omega_1^3 B\frac{\sin^4\vartheta}{c_1^4}\right)^2 + B^2\eta_c^2\omega_1^6\frac{\sin^8\vartheta}{c_1^8}\right\}\right] \tag{39}$$

This assumption is not necessary for SmEdA because of the dependence of the balance equation system on the plate damping. Therefore, the formula of Cremer can be written as follows using SmEdA and the coupling factor β_{pq}^{12} (equation (26)), which describes correctly the case without damping (previous chapter):

$$R_s = 10\lg\left[1 + \left(\frac{\cos\vartheta}{2\rho_1 c_1}\right)^2 \left\{\left(\omega_1 m - \omega_1^3 B\frac{\sin^4\vartheta}{c_1^4}\right)^2 + mB\eta_2^2\omega^4\frac{\sin^4\vartheta}{c_1^4}\right\}\right] \tag{40}$$

In the case of the two eigenfrequencies ω_1 and ω_2 being equal the transmission loss equation is equal to that of Cremer, because equation (40) can be then transformed as follows using equation (66):

$$\begin{aligned} R_s &= 10\lg\left[1 + \left(\frac{\cos\vartheta}{2\rho_1 c_1}\right)^2 \left\{\left(\omega_1 m - \omega_1^3 B\frac{\sin^4\vartheta}{c_1^4}\right)^2 + \frac{\omega_2^2}{\omega_1^2}mB\eta_2^2\omega^4\frac{\sin^4\vartheta}{c_1^4}\right\}\right] \\ &= 10\lg\left[1 + \left(\frac{\cos\vartheta}{2\rho_1 c_1}\right)^2 \left\{\left(\omega_1 m - \omega_1^3 B\frac{\sin^4\vartheta}{c_1^4}\right)^2 + B^2\eta_c^2\omega_1^6\frac{\sin^8\vartheta}{c_1^8}\right\}\right] = R_c \end{aligned} \tag{41}$$

In contrast, the damping parts of the two transmission loss equations are not equal for two coupled modes of different eigenfrequencies. But this mismath is of little importance, because below the critical frequency, where the difference between ω_1 and ω_2 is large, the transmission loss of the formula of Cremer is independent from the damping [20] and the coupling factor, equation (26), is only dominated by the freqèuency difference. Moreover, Figure 2 shows for an example of a steel plate in between a diffuse sound field (average over all incident angles), that the transmission losses of equations (39) and (40) are equal for the whole considered frequency band. The small difference at the critical frequency between the two transmission loss values appears only because of an error in the numerical integration over the incident angle ϑ.

3.2.4. Conclusion from the comparisons with the formula of Cremer

The comparisons with the formula of Cremer in the previous sections demonstrate that the coupling between two oscillators, which represent two modes in the analogous mechanical model, is described by β_{pq}^{12} (equation (26)). The coupling depends on the modes shapes, the modal masses, the modal damping factors and the eigenfrequencies but not on the excitation frequency. This implies that β_{pq}^{12} of the original formulation is the general coupling factor in the analogous mechanical model to describe every possible combination of coupling of resonant and non resonant modes. Another consequence of this resulting coupling factor β_{pq}^{12} is that the responses of the coupled oscillators become averaged (see equation (38)) and similar to those under white noise excitation. This makes the kinetic energies of the oscillators are always equal to the potential energies like in the case of the white noise excitation [13] resulting in no difference between oscillators, which represent resonant modes, and those, which represent

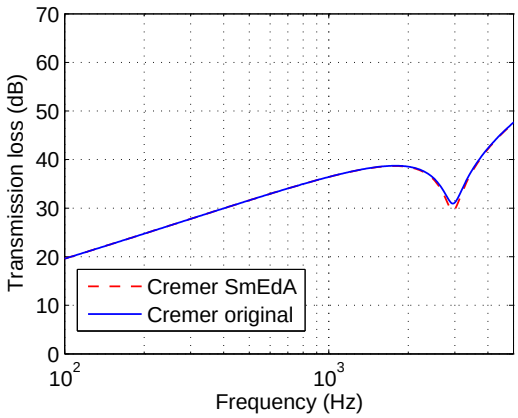

Figure 2.: Transmission loss of the infinite models from Cremer and SmEdA at $\eta_2 = 0.1$

non resonant modes. Thus the real coupled structure-cavity system can be represented by an analogous mechanical model of gyroscopically coupled oscillators, where the coupling factors at any frequency equals the coupling factor resulting from the averaged responses and where the kinetic and the potential energy of each oscillator are equal. This may lead to wrong results in the kinetic and potential energies of the oscillators in comparison to the real system but to the right results for the total energies and the transmission loss. As a consequence, the power balance equation system, equation (24), can be written for this special case of coupled oscillators as a function of total energies instead of kinetic energies. The resulting equation system is equal to the one of the original formulation of SmEdA, equation (27). Regarding the damping it is assumed that the original damping factors of the real cavity-structure system can be used, because the error made by this assumption is negligible (see previous chapter). SmEdA becomes in this way a quasi-deterministic method close to FEM or to a variational approach. The only statistical aspect is that external excitations of different subsystems have to be uncorrelated, because this is assumed in equation (15). Furthermore, the novel extended SmEdA approach can be even applied to cases with a singly frequency excitation.

4. Example

In the previous chapter the new extended SmEdA approach including non resonant modes is derived and validated using the transmission loss case of an infinite plate. To investigate the behaviour of small systems and to compare SmEdA with other calculation methods the example of a simply supported rectangular plate in between two parallelepipedic cavities is chosen, Figure 3. The parameters of this assembly are given in Table 1. The system is excited in a first case by a point force on the plate and in a second case by a monopole source at an edge of the sending room. The modes and eigenfrequencies in the present case can be calculated analytically as shown in appendix B.

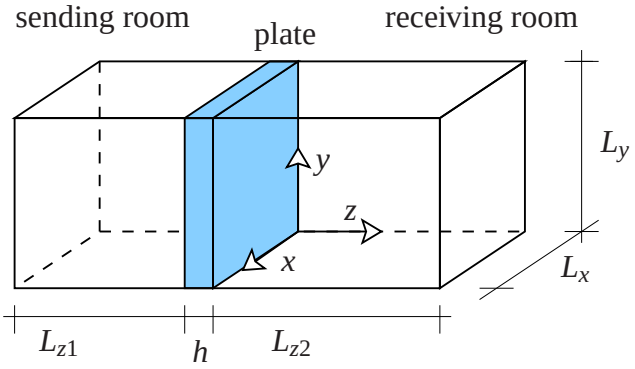

Figure 3.: Sketch of the cavity-plate-cavity system

	plate	**sending room**	**receiving room**
$L_x \times L_y \times L_z(h)\ (m)$	$1.2 \times 0.9 \times 0.004$	$1.2 \times 0.9 \times 0.7$	$1.2 \times 0.9 \times 1$
$\rho\ (kg/m^3)$	7820	1.2	1.2
$c\ (m/s)$		340	340
η	0.01	0.01	0.01
$E\ (MPa)$	210		
ν	0.3		

Table 1.: Characteristics of the subsystems

4.1. Plate excited by a point force

The cavity-plate-cavity system (see Figure 3) is first excited by a point force on the plate (excitation point: $x_e = 0.211765$ and $y_e = 0.189474$). The plate excitation splits the system into two separate cavity-plate systems in which the interaction between the cavities is negligible. As shown in Figures 4 to 6 the energies of the different subsystems calculated with SmEdA and FEM are equal in this case. These figures demonstrated that it is necessary to take into account non resonant modes for a high plate damping $\eta_p = 0.1$, line "SmEdA non resonant". Here, all the modes from 0 Hz to 1500 Hz above the 200 Hz wide excited frequency bands are used for the calculation with non resonant modes. The point force exciton case validates the new extended SmEdA formulation as a correct method for the calculation of energies of coupled subsystems.

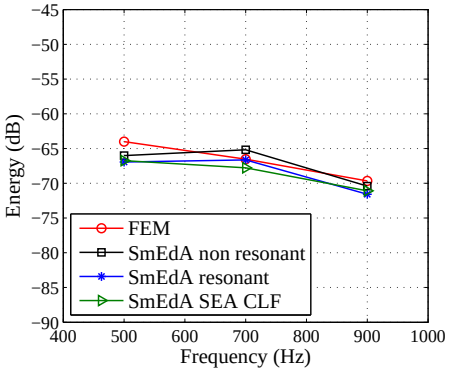

4.1: Energy in cavity 1 ($\eta_p = 0.01$)

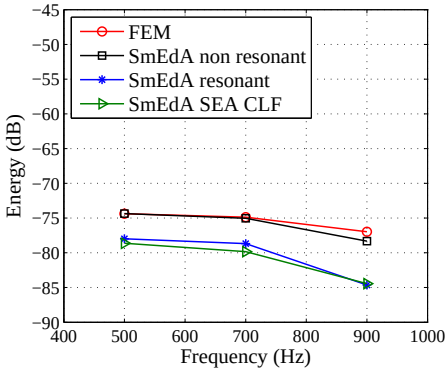

4.2: Energy in cavity 1 ($\eta_p = 0.1$)

Figure 4.: Energy in cavity 1 at different plate damping factors η_p

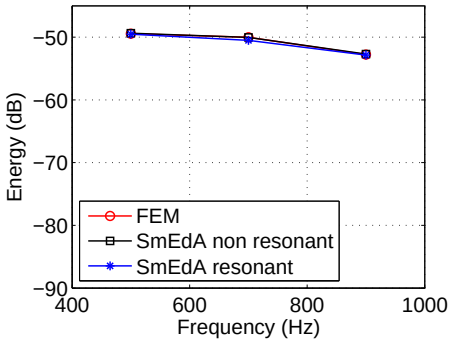

5.1: Energy of the plate ($\eta_p = 0.01$)

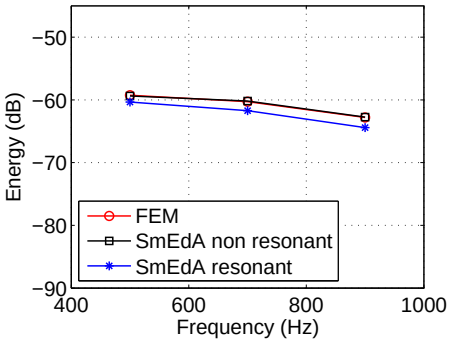

5.2: Energy of the plate ($\eta_p = 0.1$)

Figure 5.: Energy of the plate at different plate damping factors η_p

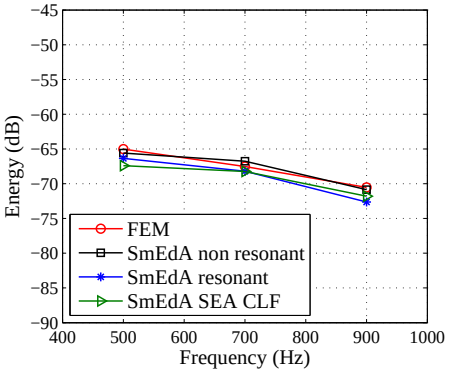

6.1: Energy in cavity 2 ($\eta_p = 0.01$)

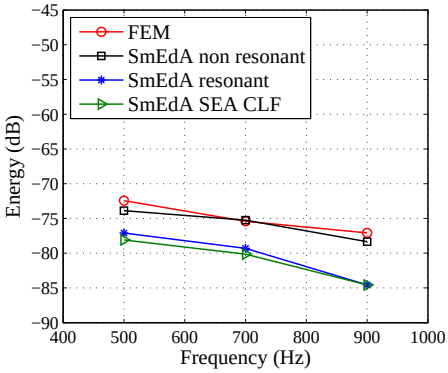

6.2: Energy in cavity 2 ($\eta_p = 0.1$)

Figure 6.: Energy in cavity 2 at different plate damping factors η_p

4.2. Transmission loss of small systems

4.2.1. Comparison to the infinite transmission loss model

For low plate damping the interaction between a small simply supported plate and a cavity is dominated by the resonant modes as shown in Figures 7 to 9. The influence of the non resonant modes grows with an increasing damping. At the plate damping $\eta_p = 0.1$, the difference in the transmission loss obtained with (line “SmEdA non resonant”) and without non resonant

modes (line “SmEdA resonant”) becomes significant. The transmission loss in these figures was calculated for excited frequency bands with a bandwidth of 400 Hz. The calculations with non resonant modes comprise the modes in the frequency range from 800 Hz below to 200 Hz above the respective excited frequency band. In comparison of these results for the transmission loss predicted with SmEdA to the infinite transmission loss model, formula of Cremer, under the assumption of a diffuse field it attracts attention that the SmEdA results are below the critical frequency sensitive to a change of the damping contrary to the formula of Cremer. The reason for this is that the incident power on an infinite plate is transmitted below the critical frequency only by the non resonant modes, on which the damping has no influence, and not by resonant modes like it in the case of a small simply supported plate. In [21] it has been demonstrated that these different behaviour depends not only on the size of the plate but for example also on the boundary conditions, because the transmission loss of a free plate is also fully dominated by the non resonant modes below the critical frequency. Another difference between an infinite and a small finite system is that the mode densities of a small plate and of a small cavity are much lower than those of infinite systems, which are infinity. Because of that the interaction between the different subsystems is in general maybe worser for finite systems at a given frequency if resonance effects plays there not a role. Hence, the transmission loss of the highly damped small plate (Figure 7) is much higher than the one of the formula of Cremer, because the resonant effects are globally suppressed.

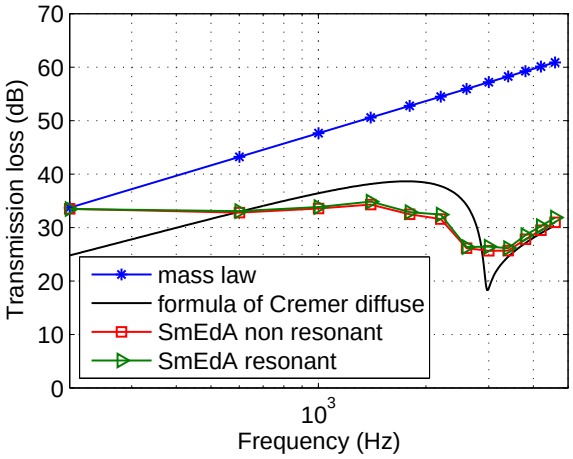

Figure 7.: Transmission loss for plate damping $\eta_p = 0.001$ (frequency band width: 400 Hz)

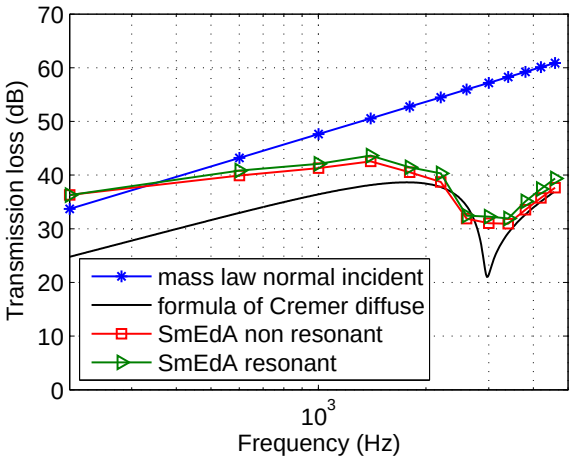

Figure 8.: Transmission loss for plate damping $\eta_p = 0.01$ (frequency band width: 400 Hz)

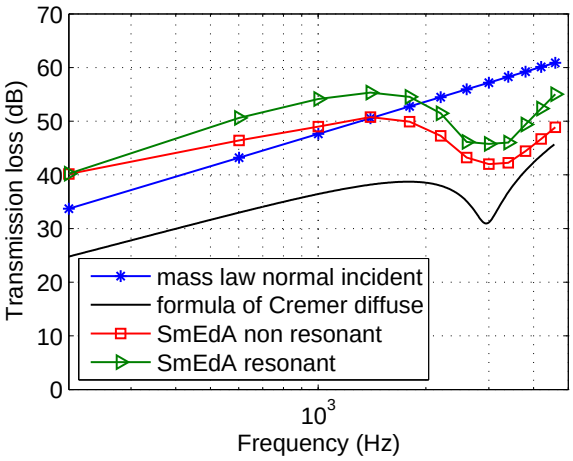

Figure 9.: Transmission loss for plate damping $\eta_p = 0.1$ (frequency band width: 400 Hz)

4.2.2. Comparison to SEA

By looking at the transmission losses predicted with SEA, Figures 10 to 12, using the coupling loss factors described in chapter 1.2 one notices that below the critical frequency these depend on the damping like those predicted with SmEdA, but less strongly. Moreover, the transmission loss is much higher at low frequencies than that of the formula of Cremer, because the used SEA coupling factors respect only partly the low modal overlap at low frequencies (see C). But the transmission loss obtained with SEA is globally more similar to the one of the formula of Cremer than to the one predicted with SmEdA. This is a consequence of the assumption that the sound field is diffuse. However the sound field of such small cavities becomes diffuse only at quite high frequencies. Thus, the SEA coupling factors do not respect all the assumptions relative to small finite systems.

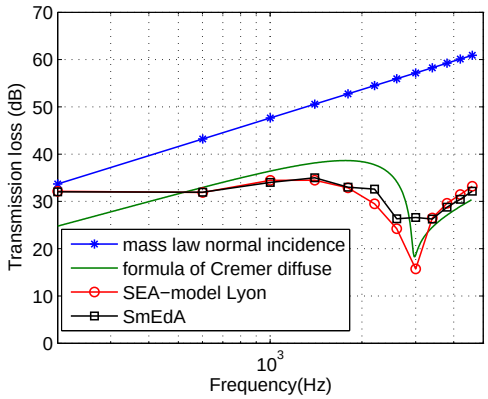

Figure 10.: Transmission loss calculated with different methods (plate damping $\eta_p = 0.001$)

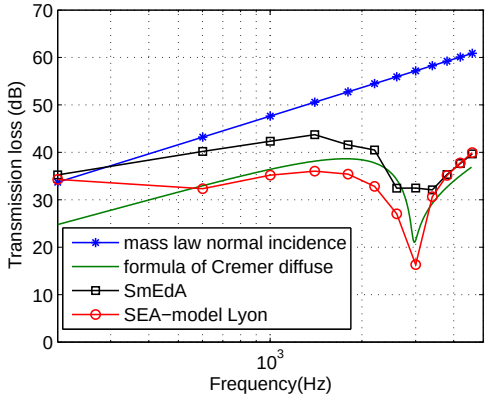

Figure 11.: Transmission loss calculated with different methods (plate damping$\eta_p = 0.01$)

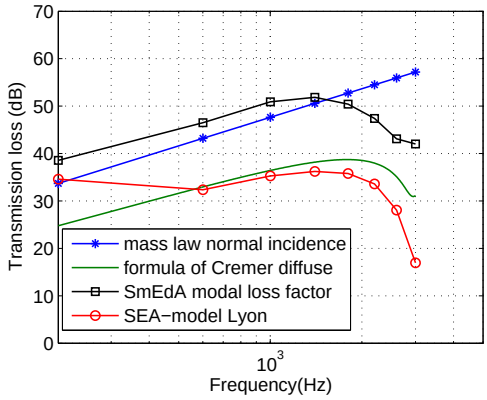

Figure 12.: Transmission loss calculated with different methods (plate damping $\eta_p = 0.1$)

4.2.3. Comparison to FEM

To compare the transmission loss calculation obtained with SmEdA and with FEM the computation was done using the plate damping factors $\eta_p = 0.01$ and $\eta_p = 0.001$, Figure 13. The bandwidth of the excited frequency band is here 200 Hz. The Figure shows that contrary to the

transmissions losses predicted with SmEdA (only resonant modes are used) those calculated with FEM are less sensitive to a change of the plate damping. Moreover the FEM results are always higher in the investigated frequency range than the transmission loss of the mass law/ formula of Cremer. To find out where the difference comes from the FEM formulation needs to be discussed.

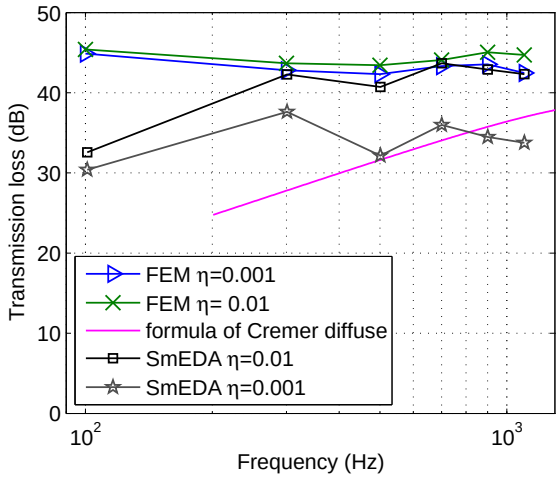

Figure 13.: Comparison of the transmission loss for different plate damping factors η_p calculated with SmEdA and FEM (frequency band width: 200 Hz)

In FEM a coupled fluid-structure system is described with a system of two coupled differential equation – similar to the equations for the coupled oscillators, equation (12) – as follows [22]:

$$\begin{bmatrix} M_s & 0 \\ -C^T & M_f \end{bmatrix} \begin{bmatrix} \ddot{U} \\ \ddot{P} \end{bmatrix} + \begin{bmatrix} D_s & 0 \\ 0 & D_f \end{bmatrix} \begin{bmatrix} \dot{U} \\ \dot{P} \end{bmatrix} + \begin{bmatrix} K_s & C \\ 0 & K_f \end{bmatrix} \begin{bmatrix} U \\ P \end{bmatrix} = \begin{bmatrix} L_s \\ L_f \end{bmatrix} \tag{42}$$

Here U is the displacement of the structure, P is the pressure in the fluid and M_s, M_f, D_s, D_f, K_s, K_f, L_s and L_f are respectively the mass, the damping and stiffness matrices and the external force vectors of the structure and the fluid. One important assumption of this formulation is that the boundary surface of the cavity is considered as rigid and a vibrating boundary is modelled as a source distributed across a rigid boundary [23]. In this way, the formulation, which describes finally the interaction between bending modes of a structure and modes of a cavity, does not respect the boundary conditions of the equality of the velocities on the surface. This means that the mode summation converges to the correct surface pressure but produces a wrong normal velocity on the boundaries [23]. On the contrary, the velocity boundary condition is taken into account in SmEdA (see chapter 3.2). Such a discrepancy may not be a problem for a system which consists of one structure and one fluid filled cavity as shown in chapter 4.1. This is also the configuration for that the FEM formulation, equation (42), was developed [23]. Yet a complete and correct description of coupled fluid-structure problems has to respect the velocity boundary condition [24]. The comparison of SmEdA and FEM for the two cases of excitation, monopole and point force excitation, demonstrates that the influence of the boundary condition may be small in the case of two coupled subsystems but huge in the case of three coupled subsystems. Therefore, the FEM formulation seems to be a convenient method only in the case of two coupled subsystem, for which it was developed.

5. Conclusion

As shown in the previous examples for the transmission loss, the new extended SmEdA approach is an interesting alternative to the existing prediction models for vibro-acoustic systems, especially in the frequency range below the critical frequency and for small systems with non diffuse sound fields. Furthermore, this method demonstrates that the transmission loss can be smaller or much higher below the critical frequency for finite systems than the one predicted by the often used infinite models, mass law and formula of Cremer. Another important advantage of the extended approach is that contrary to the applicable FEM formulation SmEdA respects the boundary conditions between subsystems and thus becomes useful for cases which consist of more than two subsystems. Moreover, only one linear system of equations, equation (27), has to be solved in SmEdA to get a result for a whole frequency band. This stands in strong contrast with FEM which requires independent calculations for a lot of frequency steps. But on the other hand FEM is needed to calculate first the eigenmodes and eigenfrequencies of the subsystems, as analytic solutions exist only for simple cases. This also one reason for the increasing of the computional time with the frequency, because the number of FEM elements have to increase to predict modes at higher frequencies and so does the computational time. The second reason for this problem is that also the linear systems of power balance equations, equation (27), increase with the frequency because the mode density especially of cavities rise and so does the number of modes. To sum up, SmEdA is now a numerical model that can be used in the whole frequency range also for problems in which non resonant modes are necessary like for highly damped systems or for narrow band excitations. Moreover, SmEdA can be used not only for cases with simple geometries like in this article but also for real industrial applications with complex geometries.

6. Acknowledgment

The authors gratefully acknowledge the ITN Marie Curie project GA-214909 “MID-FREQUENCY - CAE Methodologies for Mid-Frequency Analysis in Vibration and Acoustics”.

Appendix

A. Transmission factor for a finite cavity-structure-cavity system

The transmission factor for finite cavity-structure-cavity system is , [25],

$$\tau = \frac{p_2^2 A_2}{p_1^2 S} \tag{43}$$

where p_2 and p_1 are the effective values of the pressures in cavity one and two, A_2 is the equivalent absorption area of cavity two and S the surface of the plate. The pressure and the equivalent absorption area in a cavity i are given by [26, 11]

$$p_i^2 = \frac{\rho_i c_i^2 E_i}{V_i} \tag{44}$$

and

$$A_i = \frac{4\eta_i \omega_c V_i}{c_i} \tag{45}$$

where ρ_i, c_i and V_i are the density, the sound velocity and the volume of a cavity i and ω_c is the central frequency of the excited frequency band.

B. Modes and Eigenfrequancies of finite plates and cavities

The eigenmodes p_{qrs} and eigenfrequencies ω_{qrs} of parallelepipedic cavities are given by [25]

$$p_{qrs} = \cos\left(\frac{q\pi x}{L_x}\right)\cos\left(\frac{r\pi y}{L_y}\right)\cos\left(\frac{s\pi z}{L_z}\right); \quad q,r,s = 0,1,2,3,\ldots \tag{46}$$

and

$$\omega_{qrs} = c\sqrt{\left(\frac{q\pi}{L_x}\right)^2 + \left(\frac{r\pi}{L_y}\right)^2 + \left(\frac{s\pi}{L_z}\right)^2} \tag{47}$$

The eigenfrequencies ω^s_{mn} and the modes W^s_{mn} of a simply supported plate are

$$\omega^s_{mn} = \pi^2\left[\left(\frac{m}{L_x}\right)^2 + \left(\frac{n}{L_y}\right)^2\right]\sqrt{\frac{B}{m}}; \quad m,n = 1,2,3,\ldots \tag{48}$$

and

$$W^s_{mn} = \sin\left(\frac{m\pi x}{L_x}\right)\sin\left(\frac{n\pi y}{L_y}\right) \tag{49}$$

with the mass per area m and the bending stiffness B of the plate.

C. Factors of the direct coupling factor of Lyon and DeJong

The correction factor β_c for the the case of low modal overlap is specified by

$$\beta_c = \frac{1}{\left\{1 + \left[\frac{1}{2\pi\left(\beta_{1,net} + \beta_{2,net}\right)}\right]^8\right\}^{1/4}} \tag{50}$$

with the net effective modal overlap factor

$$\beta_{i,net} = \frac{\pi c_{gl}}{f\eta_{i,net}k_i^2 V_i} \tag{51}$$

where $\eta_{i,net}$ is the net effective loss factor. The latter is in a first approximation equal to the damping loss factor η_i of the cavity i. The factor I_{12} is approximately given by

$$I_{12} = \frac{2k_1^2 A_p}{\pi\left[\left(1 - \frac{k_1^2}{k_p^2}\right)^2\left(1 + \frac{k_1^2}{\pi k_p^2}\right)^2 + 8\tau_{12,\infty}(0)\sqrt{1 + \frac{2\pi f\eta_p\rho_p h_p}{2\rho_1 c_1}}\right]} \tag{52}$$

and the normal incidence transmission coefficient is

$$\tau_{12,\infty}(0) = \frac{4\rho_1^2 c_1^2}{\left|2\rho_1 c_1 + i2\pi f\rho_p h_p\right|^2} \tag{53}$$

where A_p, ρ_p, h_p, η_p and k_p are the area, the density, the thickness, the damping factor and the wave number of the plate and where ρ_1 and c_1 are the the density and the sound velocity of cavity 1.

D. Modes and modal works of infinite plates and cavities

The mode of the plate W_2 and the cavities p_1 and p_3 can be described under the assumption of an infinite plate arbitrarily with sine or cosine functions. But since the modal work, equation (25), is only nonzero for in phase modes the mode shapes are determined as follows (see also [1]):

$$p_1 = p_3 = \cos\left(\frac{m\pi x}{L_x}\right)\cos\left(\frac{n\pi y}{L_y}\right)\cos\left(\frac{q\pi z}{L_z}\right); \quad m,n,q = 0,1,2,3,\ldots \tag{54}$$

$$W_2 = \cos\left(\frac{r\pi x}{L_x}\right)\cos\left(\frac{s\pi y}{L_y}\right); \quad r,s = 0,1,2,3,\ldots \tag{55}$$

The corresponding modal masses are given by

$$M_1 = M_3 = \frac{2^{\delta_{mnq}}}{8}\left(\frac{L_x L_y L_z}{\rho_1 c_1^2 \omega_1^2}\right) \tag{56}$$

$$M_2 = \int_{V_2} \rho_2 W_2 \, dV_2 = \frac{2^{\delta_{rs}}}{4} L_x L_y h \rho_2 \tag{57}$$

where L_x, L_y and L_z are the lengths of the cavities in the direction of the three dimension and h and V_2 are the thickness and the volume of the plate. For the modal work W^{12} it follows using equations (25), (54) and (55):

$$W^{12} = \int_S p_i(S) W_2 \, dS = \begin{cases} 0 & \text{for } \frac{r}{L_x} \neq \frac{m}{L_x} \text{ or } \frac{s}{L_y} \neq \frac{n}{L_y} \\ \frac{L_x L_y}{4} & \text{for } \frac{r}{L_x} = \frac{m}{L_x} \text{ and } \frac{s}{L_y} = \frac{n}{L_y} \\ L_x L_y & \text{for } r = m = s = n = 0 \end{cases} \tag{58}$$

The missing information on the depth L_z in equation (56) is derived from Newton's third law, which is used in the original derivations of the mass law and the formula of Cremer. Assuming the hypothesis "blocked pressure" this law reads as follows :

$$\rho_2 h a_p = p_e + p_r = 2p_e \tag{59}$$

where p_e and p_r are the pressures of the incident and the reflected wave and a_p is acceleration of the plate. The pressure p_e can be written as

$$p_e = \rho_1 L_e a_e \tag{60}$$

with a length L_e and a acceleration a_e in the direction of the incident wave. The relations between a_p and a_e and between L_e and the depth L_z in the z-direction are given by

$$a_e = \frac{a_p}{\cos\vartheta} \tag{61}$$

$$L_e = \frac{L_z}{\cos\vartheta} \tag{62}$$

where ϑ is the incident angle (see Figure 14). It follows therefore through insertion of equations (60) to (62) in equation (59):

$$L_z = h\left(\cos\vartheta\right)^2 \frac{\rho_2}{2\rho_1} \tag{63}$$

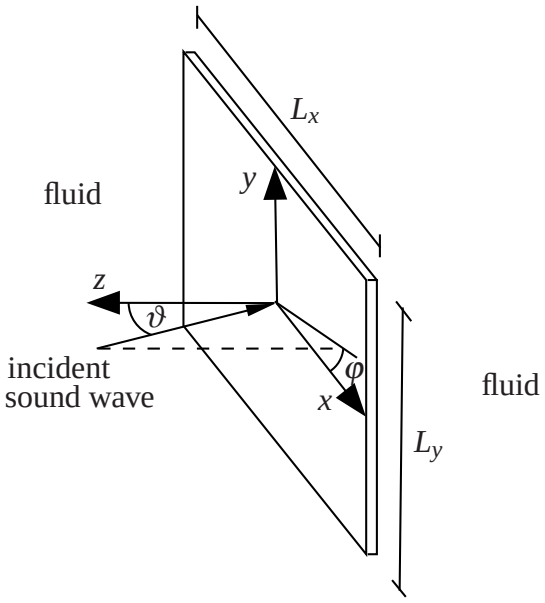

Figure 14.: Sketch of the transmission problem

E. Relation between the bending wave frequency and the frequency of the incident wave

The bending wavelength of the plate is described as fellows [27]:

$$\lambda_B = \frac{2\pi}{\sqrt{\omega_2}} \sqrt[4]{\frac{B}{m_2}} \tag{64}$$

In the infinite models only the bending wave with the wavelength of the incident wavelength λ_e projected on the plate is excited. This means that

$$\lambda_B = \frac{\lambda_e}{\sin\vartheta} = \frac{2\pi c_1}{\omega_1 \sin\vartheta} \tag{65}$$

From these two equations it follows for the relation between the free bending wave frequency and the frequency of the incident wave:

$$\omega_2 = \omega_1^2 \left(\frac{\sin\vartheta}{c_1}\right)^2 \sqrt{\frac{B}{m_2}} \tag{66}$$

Bibliography

[1] M. Heckl, The tenth Sir Richard Farey memorial lecture: Sound transmission in buildings, Journal of Sound and Vibration 77(2) (1981) 165–189.

[2] J. Rayleigh, The theory of sound, vol. 2, Dover Publications, 1945.

[3] R. Berger, Über die Schalldurchlässigkeit, Ph.D. thesis, Königlich Technische Hochschule zu München, 1911.

[4] A. C. Nilsson, Reduction Index and boundary conditions for a wall between two rectangular rooms, part I: theoretical results, Acustica 26 (1972) 1–18.

[5] R. Josse, C. Lamure, Transmission du son par une paroi simple, Acustica 14 (1964) 266–280.

[6] R. Woodcock, J. Nicolas, A generalized model for predicting the sound transmission properties of generally orthotropic plates with arbitrary boundary conditions, Journal of the Acoustical Society of America 97(2) (1995) 1099–1112.

[7] L. Gagliardini, J. Roland, J.-L. Guyader, The use of a functional basis to calculate acoustic transmission between rooms, Journal of Sound and Vibration 145(3) (1991) 457–478.

[8] A. Dijckmans, G. Vermeir, Application of the wave based prediction technique to building acoustical problems, in: Proceedings of ISMA 2010, Leuven.

[9] T. Sakuma, T. Oshima, Numerical Analysis of Sound Transmission Loss of Glass Pane - On the Treatment of Edge Damping, in: Proceedings of Inter-noise 2008, Shanghai.

[10] R. H. Lyon, R. G. DeJong, Theory and application of statistical energy analysis, Butterworth-Heinemann, 2nd edn., 1995.

[11] K. Renji, P. S. Nair, S. Narayanan, Non-resonant response using statistical energy analysis, Journal of Sound and Vibration 241(2) (2001) 253–270.

[12] L. Maxit, J.-L. Guyader, Estimation of the SEA coupling loss factors using a dual formulation and FEM modal information, part I: theory, Journal of Sound and Vibration 239(5) (2001) 907–930.

[13] T. Scharton, R. Lyon, Power Flow and Energy Sharing in Random Vibration, Journal of the Acoustical Society of America 43 (6) (1968) 1332–1343.

[14] E. Ungar, Statistical energy analysis of vibrating systems, Tech. Rep. AFFDL-TR-66-52, US Air Force, 1966.

[15] J. Woodhouse, An approach to the theoretical background of statistical energy analysis applied to structural vibration, Journal of the Acoustical Society of America 69 (6) (1981) 1695–1709.

[16] N. Totaro, J.-L. Guyader, extension of SmEdA method to estimate energy repartition into SEA subsystems, in: Proceedings of ISMA 2008, Leuven.

[17] N. Totaro, C. Dodard, J.-L. Guyader, SEA coupling loss factors of complex vibro-acoustic systems, Journal of Vibration and Acoustics 131 (2009) 041009–4.

[18] L. Maxit, J.-L. Guyader, Estimation of the SEA coupling loss factors using a dual formuulation and FEM modal information, part II: numerical applications, Journal of Sound and Vibration 239(5) (2001) 931–948.

[19] M. J. Crocker (Ed.), Handbook of Noise and Vibration control, Wiley, 2007.

[20] R. Haberkern, On how to Obtain Diffuse Field Sound Transmission Loss from Cremers Thin Plate Transmission Coefficient Formula, acta acustica 87 (2001) 542–551.

[21] R. Stelzer, N. Totaro, G. Pavic, J. Guyader, Prediction of Transmission Loss using an improved SEA Method, in: Proceedings of CFA 2010, Lyon.

[22] M. Chargin, O. Gartmeier, A finite element procedure for calculating fluid-structure interaction using MSC/Nastran, Tech. Rep. NASA Technical Memorandum 102857, NASA (National Aeronautics and Space Adminstration), 1990.

[23] F. Fahy, P. Gardonio, Sound and structural vibration : radiation, transmission and response, Elsevier Academic Press, 2nd edn., 2007.

[24] F. Fahy, Foundations of Engineering Acoustics, Elsevier Academic Press, 2005.

[25] M. Möser, Technische Akustik, Springer, 7th edn., 2007.

[26] M. Bruneau, Fundamentals of acoustics, ISTE, 2006.

[27] F. Mechel (Ed.), Formulas of Acoustics, Springer-Verlag, Berlin, Heidelberg 2002.

FOLIO ADMINISTRATIF

THESE SOUTENUE DEVANT L'INSTITUT NATIONAL DES SCIENCES APPLIQUEES DE LYON

NOM : Stelzer
(avec précision du nom de jeune fille, le cas échéant)

DATE de SOUTENANCE : 07/06/2012

Prénoms : Rainer Michael

TITRE :

Une méthode énergétique pour les systèmes vibro-acoustiques couplés
An energy based method for coupled vibro-acoustic systems

NATURE : Doctorat

Numéro d'ordre : AAAAISALXXXX

Ecole doctorale : Mécanique, Energétique, Génie Civil, Acoustique (MEGA)

Spécialité : Acoustique

RESUME :

Ce mémoire de thèse présente le développement de la méthode «statistical modal energy distribution analysis (SmEdA)» pour des systèmes vibro-acoustiques couplés. Cette méthode de calcul est basée sur le bilan énergétique dans des sous-systèmes fermés couplés, comme une structure ou une cavité. L'interaction entre de tels systèmes est décrite par des couplages entre les modes. La version initiale de SmEdA prend en compte seulement les modes qui ont une fréquence propre dans le bande d'excitation. Le travail présenté ici étudie l'effet des modes non résonants sur la réponse et identifie les cas dans lesquels un tel effet devient important. L'introduction des modes non résonants permet d'utiliser la méthode SmEdA dans des cas d'applications plus larges. En outre, une nouvelle méthode de post-traitement a été développée pour calculer des distributions d'énergie dans les sous-systèmes. Finalement, une nouvelle méthode d'approximation pour la prise en compte des modes de systèmes de grandes dimensions ou mal définis a été formulée. Toutes ces méthodes ont été comparées avec d'autres méthodes de calcul via des exemples académiques et industriels. Ainsi, la nouvelle version de SmEdA incluant le post-traitement pour obtenir des distributions d'énergie a été validé et les avantages et possibilités d'applications sont montrés.
This dissertation presents the further development of the statistical modal energy distribution analysis (SmEdA) for vibro-acoustic coupled problems. This prediction method is based on the energy balance in bounded coupled subsystems, like a structure or a cavity. The interaction between such subsystems is described by mode-to-mode coupling. The original SmEdA formulation takes into account only the modes having the eigenfrequencies within the excitation band. The present work investigates the effect of non resonant modes to the response and identifies cases in which such an effect becomes important. The inclusion of non resonant modes has thus resulted in a new SmEdA formulation which can be used in extended applications. Furthermore, a new post-processing method has been developed to predict energy distribution within subsystems. Finally a novel approximation method for handling modes of huge or ill-defined systems has been formulated. All these methods have been compared to other prediction methods via academic and industrial examples. In this way, the extended SmEdA approach including the post-processing for energy distribution has been validated and its advantages and application possibilities have been demonstrated.

MOTS-CLES :

SmEdA, méthode énergétique, systèmes vibro-acoustiques couplés, distribution d'énergie, systèmes mal définies, méthode modal
SmEdA, energy based method, coupled vibro-acoustic systems, energy distribution, ill-defined system, modal approach

Laboratoire (s) de recherche: Laboratoire Vibrations Acoustique

Directeur de thèse:

Goran PAVIC (Directeur de thèse), Nicolas TOTARO (Co-Directeur de thèse)

Président de jury :

Composition du jury :

Goran PAVIC (Professeur), INSA de Lyon, Directeur de thèse
Nicolas TOTARO (Maître de Conférences), INSA de Lyon, Co-Directeur de thèse
Robin LANGLEY (Professeur), University of Cambridge, Rapporteur
Ennes SARRADJ (Professeur) TU Cottbus, Rapporteur
Herve RIOU (Maître de Conférences), LMT Cachan, Examinateur
Michael THIVANT, Vibratec, Examinateur